Kensaku Mori *Editor*

The Olfactory System

From Odor Molecules to Motivational Behaviors

Springer

The Olfactory System

Kensaku Mori
Editor

The Olfactory System

From Odor Molecules to Motivational Behaviors

Springer

Editor
Kensaku Mori
Department of Physiology
The University of Tokyo
Tokyo, Japan

ISBN 978-4-431-54375-6 ISBN 978-4-431-54376-3 (eBook)
DOI 10.1007/978-4-431-54376-3
Springer Tokyo Heidelberg New York Dordrecht London

Library of Congress Control Number: 2014938039

Printed on acid-free paper

Springer is part of Springer Science+Business Media (www.springer.com)

Preface

Olfaction, the sense of smell, plays a key role in the daily life of humans and animals. Its functions include selecting palatable and nutritious foods and rejecting spoiled foods, avoiding dangerous predators or poisonous gases, searching for a mate, and engaging in a variety of social interactions. The olfactory system of the vertebrate brain contains neuronal circuits that translate external odor information into appropriate behavioral responses. One of the most basic functions of the brain is to perceive and evaluate sensory information obtained from the external world to induce adequate motivational and behavioral responses. Thus, exploring the basic functional logic of the neuronal circuits in the olfactory system appears to be crucial in understanding the workings of the complex neuronal circuits of the brain, particularly those in the cerebral cortex.

Olfactory sensory neurons project axons directly to the telencephalon, the most rostral segment of the embryonic brain that gives rise to the cerebral cortex. Given that the cerebral cortex is the most prominently evolved structure in the human brain, the olfactory system has long been considered critical to an understanding of the cerebral cortex. When I began my study of the olfactory system 39 years ago, few researchers in Japan had selected the central olfactory system as a major area of investigation. Although olfactory research was a minor field at that time, I was encouraged by the words of senior researchers who predicted the importance of olfactory research in understanding the workings of the human brain. For example, Sir Wilfred Le Gros Clark, a professor of anatomy at Oxford who was interested in human evolution, mentioned in the Ferrier Lecture that

> There are certain reasons why the study of the olfactory connections offers particularly favourable opportunities for the study of the neural basis of sensory discrimination in general.—I should perhaps emphasize that the olfactory bulb, in which the olfactory nerve fibers terminate, is developmentally an extension forward of the cerebral hemisphere, and is taken to be an expression of the fact that, from the evolutional point of view, the cerebral hemispheres were initially developed in the vertebrate series in relation to the olfactory sense (Le Gros Clark 1957).

These words convinced me that studies of the olfactory system are relevant to important questions of the brain and mind.

Despite the numerous important findings of the pioneers of olfactory research, progress was relatively slow and the number of researchers was small compared with those engaged in research into the visual, auditory, and somatic sensory systems. Triggered by discovery of the odorant receptor gene family by Linda Buck and Richard Axel in 1991, however, understanding of the basic biological mechanisms of the olfactory system has advanced enormously in the last two decades. The first objective of this book is to summarize recent advances in understanding of the mammalian and fish olfactory systems, with particular regard to the basic neurobiological mechanisms of neuronal circuit function in the olfactory system. Fortunately, several researchers working in or around the Tokyo area of Japan—Hitoshi Sakano, Kazushige Touhara, Yoshihiro Yoshihara, and Masahiro Yamaguchi—have collaborated on workshops on the olfactory system, which included a guest speaker, Noam Sobel. I took this opportunity to ask each of them to write a chapter of this book to describe recent developments in olfactory research for the coming generation of scientists: undergraduates, graduate students, and postdoctoral researchers in the fields of neuroscience, neurobiology, chemical senses, food and nutritional sciences, medical science, sensory psychology, and behavioral sciences.

We humans enjoy the flavor of delicious foods, as well as wonderful music and beautiful scenery. To understand the neural mechanisms by which we enjoy this world, an essential part of our daily life, studying the neuronal basis of flavor perception in the olfactory and gustatory system, that of music perception in the auditory system, and that of fine art perception in the visual system would appear to be good and valuable ideas. Despite rapid progress in understanding the olfactory system, however, it remains unclear how odor information is processed at levels beyond the olfactory bulb, which include many areas of the olfactory cortex, olfactory tubercle, amygdala, entorhinal cortex, and orbitofrontal cortex. Indeed, it is only recently that we have begun to understand the brain mechanism for flavor perception (Shepherd 2012). Much current research on the olfactory system is focused on the functional logic at these higher centers of the olfactory system, and I predict that progress in understanding the olfactory system will soon accelerate at an even greater pace. The second purpose of this book is to provide perspectives on future directions in olfactory system research to next-generation scientists. As knowledge of higher olfactory centers advances, we might even come to understand the secret of how our brain allows us to enjoy foods and wine.

Tokyo, Japan Kensaku Mori

References

Le Gros Clark WE (1957) Inquiries into the anatomical basis of olfactory discrimination. Proc R Soc Lond B Biol Sci 146(924):299–319

Shepherd GM (2012) Neurogastronomy. Columbia University Press, New York

Contents

Chapter 1
Unique Characteristics of the Olfactory System

Kensaku Mori and Hiroyuki Manabe

Abstract The olfactory system in the brain plays key roles in the daily lives of humans and animals. This chapter briefly sketches the recent rapid progress in understanding the structure and function of the olfactory system and some unsolved important questions regarding this system. Olfactory perception occurs in discrete respirations (sniffs), and this chapter underscores the intimate relationship between the function of the olfactory system and the sniff rhythm. In addition, this chapter provides basic knowledge about the unique characteristics of the olfactory neural circuits, starting from olfactory sensory neurons in the nose through the olfactory bulb and olfactory cortex up to the orbitofrontal cortex and olfactory tubercle.

Keywords Exhalation • Inhalation • Motivational behaviors • Odor molecules • Odorant receptor • Olfactory bulb • Olfactory cortex • Orbitofrontal cortex • Sniff rhythm

1.1 From Odor Molecules to Behavioral Responses

One of the basic functions of the human brain is to process sensory information about the external world. This processing is done with reference to one's internal state to choose and evaluate salient objects so that one can express appropriate emotional, motivational, and behavioral responses. It is therefore natural for olfactory system researchers to ask "What is the neuronal circuit logic of the olfactory system that enables humans and animals to translate external odor information to necessary behavioral outputs?" However, understanding this translation

K. Mori (✉) • H. Manabe
Department of Physiology, Graduate School of Medicine, The University of Tokyo, Bunkyo-ku, Tokyo 118-0033, Japan
e-mail: moriken@m.u-tokyo.ac.jp; hmanabe@m.u-tokyo.ac.jp

K. Mori (ed.), *The Olfactory System: From Odor Molecules to Motivational Behaviors*,
DOI 10.1007/978-4-431-54376-3_1,

(or understanding the input–output relationship) is no easy task. The difficulty originates from the tremendous diversity of odors in the world. It is estimated that the human nose can detect and discriminate more than 400,000 volatile compounds (odor molecules or odorants), each having a distinct molecular structure. Further, single objects emit a multitude of odor molecules—an apple, for example, emits an object-specific combination of more than 100 different odor molecules. The number of possible input patterns of odorants to the nose is beyond count. How does the olfactory system cope with these tremendously diverse input patterns, composed of an astronomically diverse range of odorant combinations?

As we discuss here, the discovery of the odorant receptor gene family by Linda Buck and Richard Axel (Buck and Axel 1991) triggered elucidation of the key logic of odorant coding (a type of combinatorial coding) at the level of the odorant receptors, olfactory sensory neurons in the nose, and glomeruli in the olfactory bulb. Before the identification of this key logic, relating each of the "innumerable odors" to each of the "large variety of percepts and behavioral responses" was considered almost impossible. However, the finding of the key logic encouraged us to speculate whether it might in fact be possible to relate any of "approximately 390 human odorant receptors" to any of "a large variety of percepts and behavioral responses."

The difficulty also originates from the diversity and complexity of percepts, motivational behaviors, and emotional behaviors. For example, while the detection of food odor may lead to food search behaviors followed by eating, the expression of these behaviors is also dependent on internal states such as hungriness and thirstiness. In response to predator odors, a good strategy for rodents is to escape from the danger, but there are numerous behavioral patterns for escape, including the fight or flight choice. Odors or pheromones from the opposite sex may lead to a variety of behavioral responses (Wyatt 2009), whereas distinct conspecific odors induce diverse social behaviors (Doty 1986). Furthermore, humans and mammals can learn to associate any neutral odorant with a reward or punishment, such that the odor can induce specific attractive or aversive behavior based on previous experience.

One possible strategy for the "odorant receptor input–behavioral output" translation is to form simple reflex-like neuronal connections (or so-called zombie-like connections) between olfactory sensory neurons in the nose and the motor circuits responsible for specific behavioral output. The spinal cord, brainstem, and midbrain contain a rich variety of reflex pathways (or short-circuit pathways) that connect somatosensory, gustatory, auditory, and visual inputs to motor outputs. In striking contrast, the olfactory system is unique among the five sensory systems in that it does not have direct connections with these regions and lacks simple reflex-like pathways. All axons of olfactory sensory neurons synapse with neurons in the olfactory bulb, which is developmentally an expansion forward of the cerebral cortex. In other words, olfactory sensory neurons directly connect with cerebral cortex networks.

Furthermore, the olfactory bulb and olfactory cortex lie in the telencephalic segment of the brain, which includes the neocortex, paleocortex, and basal ganglia.

Understanding the logic of olfactory sensory input–behavioral output translation therefore requires elucidation of the cortical and basal ganglia circuit mechanism. The discovery of odorant receptors led to rapid progress during the past two decades in understanding the mechanism of odorant coding at the level of odorant receptors, olfactory sensory neurons, and glomeruli in the olfactory bulb (Axel 1995; Buck and Axel 1991; Mori et al. 1999). Nevertheless, the question of how olfactory codes at the level of the glomeruli in the olfactory bulb are read by the olfactory cortex and higher association areas to translate the coded olfactory information into appropriate behavioral outputs remains largely unknown. We still lack an understanding of the functional logic of neuronal circuits in the olfactory cortex and higher association areas, and extensive exploration of the olfactory cortex and higher association areas in the paleocortex, neocortex, and basal ganglia has only recently begun. This new focus on these regions predicts rapid near-term progress in understanding the key logic of the neuronal circuits that translate the olfactory inputs to emotional, motivational, and behavioral output.

After providing an overall characterization of the structure and function of the olfactory system in Chap. 1, Kazushige Touhara summarizes in Chap. 2 recent progress in the state of knowledge about chemosensory signals, receptors, olfactory network, and behavioral outputs, and provides prospects for future progress and questions to be solved. Hitoshi Sakano describes his group's remarkable findings in the molecular and cellular mechanisms of olfactory map formation by olfactory sensory axons on the glomeruli in the olfactory bulb in Chap. 3. The structure and function of olfactory maps in the mammalian olfactory bulb is briefly described in Chap. 4. Although this book mostly describes the olfactory system of land mammals, there is also rapid growth in understanding the zebrafish olfactory system, which has become one of the most useful and important model organism in neurobiology. Yoshihiro Yoshihara describes the zebrafish olfactory system in Chap. 5. Masahiro Yamaguchi focuses on inhibitory interneurons in the olfactory bulb and discusses the functional roles of adult-born granule cell inhibitory interneurons in Chap. 6. Shin Nagayama, Kei Igarashi, Hiroyuki Manabe, and Kensaku Mori discuss how odor signals are conveyed from the olfactory bulb to the olfactory cortex in Chap. 7, focusing on parallel tufted cell and mitral cell pathways. Chapter 8 proposes possible structural and functional organization of the piriform cortex, olfactory tubercle, and orbitofrontal cortex. Finally, Noam Sobel summarizes olfactory system neurobiology and perception in humans in Chapter 9.

1.2 Sniff Rhythm and Olfaction

Although it is controversial whether perception in general relies on discrete processing epochs, it is agreed that conscious olfactory perception occurs in discrete respirations (or sniffs) (Kepecs et al. 2006; Mainland and Sobel 2006; VanRullen and Koch 2003). Sniff rhythm appears to be a conductor orchestrating the mode of information processing globally across a wide variety of members

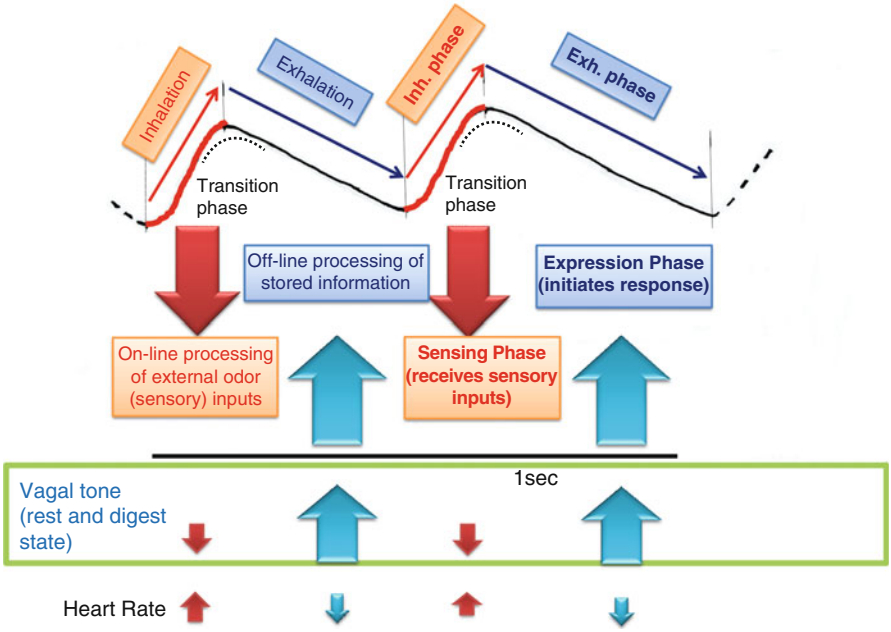

Fig. 1.1 Inhalation–exhalation sniff cycles. The *topmost trace* indicates the sniff rhythm of a rat (during awake resting) recorded with a thermocouple placed in the nasal cavity. *Upward swing of trace* indicates inhalation. *Broken line* indicates the phase of transition from inhalation to exhalation (*Exh.*). *Large* and *small arrows* below the respiration monitor illustrate possible functional state of the central olfactory system, the autonomic parasympathetic nervous system, and heart rate

(areas) of the central olfactory system. In land mammals, each respiration cycle consists of an inhalation phase followed by an exhalation phase (Fig. 1.1). During the inhalation phase, odorants in the external world are drawn, together with air, into the nasal cavity and thus activate olfactory sensory neurons in the nose.

Although it takes time for inhaled odorants to reach and then activate olfactory sensory neurons, the response of these neurons starts at the rising phase of the inhalation, continues during the rest of the inhalation phase, and then declines during the exhalation phase (Wachowiak 2011; Wilson and Sullivan 1999). This observation suggests that external odor input is processed on-line in the central olfactory system mostly during the inhalation phase, including the transition phase from inhalation to exhalation (Fig. 1.1). In this scenario, the inhalation phase is the time window for the central olfactory system to "explore" the external odor information. Because autonomic parasympathetic nervous system activity (so-called vagal tone) decreases during the inhalation phase, on-line processing of external odor inputs is associated with a decrease in parasympathetic activity and an increase in heart rate (Fig. 1.1).

In contrast, during the exhalation phase, particularly the latter part of a long exhalation, the central olfactory system is temporarily isolated from the external

odor world and processes olfactory information off-line. In parallel, parasympathetic nervous system activity increases during the exhalation phase, resulting in a decrease in heart rate. Because parasympathetic activity is thought to represent the "rest and digest" state of the body, we speculate that the exhalation phase is associated with the "rest and digest" state of the central olfactory system. We further speculate that the inhalation–exhalation sequence of a sniff cycle not only determines the timing of external odor information sampling but also regulates the mode of information processing in the central olfactory system. The inhalation phase might be a "sensing phase," specialized in the receipt of external sensory input, and the exhalation phase might be an "expression phase," specialized in the processing of stored information to initiate appropriate behavioral responses.

The working of the neuronal networks in the central olfactory system, particularly the information processing mode, therefore appears to depend heavily on the sniff cycle and rhythm. This is the case during wakefulness, especially during fast sniffs, in which animals actively explore the external odor world. However, during sleep states with slow respiration, the central olfactory system, particularly the olfactory cortex and higher association areas, is largely isolated from the external odor world by behavioral state-dependent sensory gating (Murakami et al. 2005). The information processing rhythm in the central olfactory system during sleep states is, if present, thus largely independent of the respiration rhythm.

In humans and animals, respiration rhythm varies precisely according to behavioral state, and each sniff rhythm has distinct behavioral correlates (Homma and Masaoka 2008; Manabe and Mori 2013). Figure 1.2 and Table 1.1 summarize the distinct sniff (or respiration) patterns that are induced during different behavioral states. The sniff rhythm in Fig. 1.2 was recorded with a thermocouple placed in the nasal cavity of a freely behaving rat. In addition, the sniff rhythm-paced neuronal activity in the olfactory system was monitored by recording local field potentials in the deep layer (granule cell layer) of the olfactory bulb, the first information processing center in the central olfactory system. The tight coupling between sniff rhythm and neuronal activity in the olfactory system underscores the critical importance of monitoring sniff cycles in analyzing the functional properties of the neuronal circuits in the olfactory system of freely behaving animals.

During walking, running, and exploratory movements, rats make a series of small, brief, and rapid sniffs at the theta frequency range (6–10 Hz) (Fig. 1.2a). The local field potential in the olfactory bulb shows nested gamma oscillations superimposed on the sniff-paced oscillations of the theta frequency range. Here, we focus on the sniff-paced theta oscillations, leaving discussion of the gamma oscillations for Chap. 7. During the movement state, local field potentials in the hippocampus (or hippocampal EEG) are known to show theta oscillations (6–12 Hz). Because this hippocampal theta oscillation during the movement state is called the "translation-movement theta oscillation" (t-theta) (O'Keefe 2007), we call the theta sniffs "translation-movement theta sniffs" (t-theta sniffs).

When rats are immobile, showing no translation movement, but are in exploratory behavior with arousal and attention state, they show also a train of small, brief, and rapid sniffs of theta frequency range (3–8 Hz) followed by one or a few sniffs with a

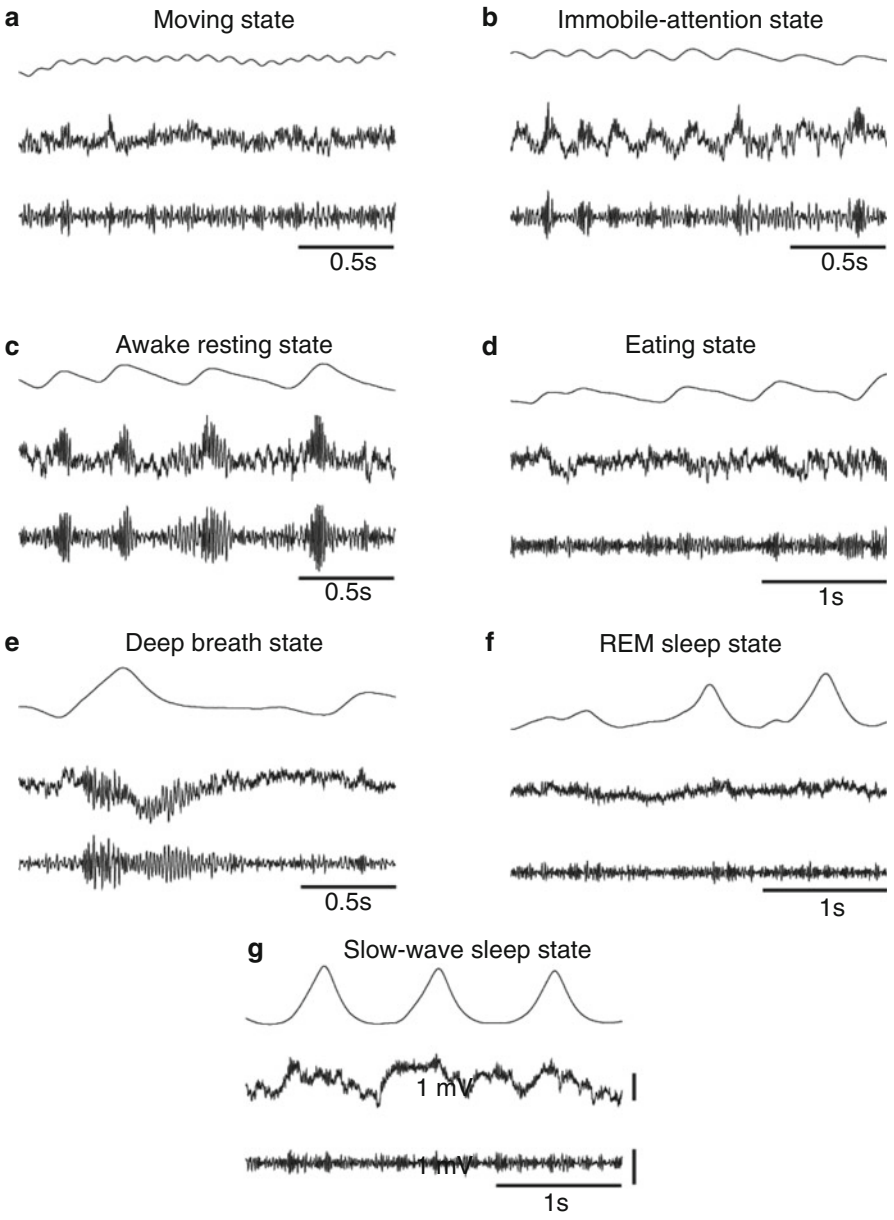

Fig. 1.2 Each sniff rhythm has distinct behavioral correlates. Simultaneous recordings of respiration rhythm (*topmost traces*; upward swing indicates inhalation), local field potential in the granule cell layer of the olfactory bulb (*middle traces*), and gamma oscillations of the local field potential (bandpass filtered, 30–140 Hz; *bottom traces*) during moving (**a**), during immobile-attentional state (**b**), during awake resting (**c**), during eating (**d**), during deep breath (**e**), during REM sleep (**f**), and during slow-wave sleep (**g**)

Table 1.1 Behavioral correlates of sniff rhythm

	Wakefulness					Sleep	
Behavioral state	Translation-movement state	Immobile-attention or arousal state	Awake resting state	Eating state	Deep breath state	REM sleep state	Slow-wave sleep state
Typical behavior	Walking, running, exploratory movement	Arousal, attention	Quiet sitting, grooming	Eating, drinking	Deep breath	Rapid eye movement, whisker movement	No movement
Respiratory (sniff) pattern	t-theta sniff (Fig. 1.2a)	a-theta sniff (Fig. 1.2b)	Resting slow sniff (Fig. 1.2c)	Eating slow sniff	Deep sniff	Irregular respiration (Fig. 1.2f)	Regular slow respiration (Fig. 1.2g)
Hippocampal EEG	t-theta oscillation	a-theta oscillation	LIA with SPW/ripples	LIA with SPW/ripples	LIA during exhalation phase	REM-theta oscillation	LIA with SPW/ripples

relatively long exhalation phase (Fig. 1.2b). During the theta frequency sniffs, rats show synchronization between sniff and whisking (rapid movements of vibrissae), with vibrissae protraction during the brief inhalation and vibrissae retraction during the brief exhalation (Welker 1964). Local field potential in the olfactory bulb shows the sniff rhythm-paced theta oscillatory activity with superimposed nested gamma oscillations. During this behavioral state, hippocampal EEG shows theta oscillations (4–9 Hz), which are called "immobile attention-related theta oscillations" (a-theta). Accordingly, the theta sniffs during this behavioral state can be classified as "attention-related theta sniffs" (a-theta sniffs).

When rats are in the awake resting state sitting quietly, they show a slow low-frequency sniff pattern (~2.5 Hz on average), with a sniff cycle consisting of a slow inhalation followed by a longer exhalation. The longer exhalation phase may reflect the dominance of the "rest and digest" state of the olfactory system. Local field potential in the olfactory bulb exhibits sniff rhythm-paced slow oscillations with superimposed nested gamma oscillations (Fig. 1.2c). In contrast, the hippocampal EEG typically shows large irregular amplitude activity (LIA) with sharp wave/ripple events, which are thought not to be driven by external sensory inputs but to be generated internally based on memory traces stored during preceding movement or exploratory behavior (Buzsaki 2006).

Eating foods is a typical daily olfactory behavior, and rats show slow low-frequency sniffs with a relatively long exhalation phase during eating and drinking (Fig. 1.2d). During the exhalation phase, rats sometimes stop respiration for a short period, which may correspond to the respiration-absent period for swallowing (swallowing apnea). The long exhalation phase of the eating slow sniff is a unique time window in which the central olfactory system receives strong retronasal odor stimulation from foods in the mouth (Gautam and Verhagen 2012). Hippocampal EEG exhibits LIA with sharp wave/ripple events during this behavioral state.

If you breathe slowly and deeply, your mind becomes calm. Rats also sometimes show slow and deep breathing with an extremely long exhalation phase or apnea phase, as exemplified in Fig. 1.2e. In synchrony with the large inhalation, the olfactory bulb shows prominent gamma oscillations superimposed on a large slow potential. Rich oscillatory activity also appears during the exhalation phase, in which the olfactory bulb does not receive direct olfactory sensory inputs. The hippocampal EEG shows LIA with sharp waves/ripples during the exhalation phase, but these events are typically absent during the inhalation phase (Manabe 2008).

During a sleep episode, rats show several cycles of slow-wave sleep and rapid eye movement (REM) sleep. They show very regular slow respiration of large amplitude during the slow-wave sleep state, but strikingly irregular respirations with a wide variety of amplitude during REM sleep. During these sleep states, the olfactory bulb does not show sniff-paced oscillations of local field potential. During slow-wave sleep states, the olfactory bulb shows slow irregular waves, but their occurrence is largely independent of respiration rhythms. The hippocampal EEG

shows characteristic theta oscillations during REM sleep (REM-theta) and LIA with sharp waves/ripples during slow-wave sleep.

In this way, as each hippocampal EEG pattern has distinct behavioral correlates, so also does each sniff rhythm. Researchers with rich experience in studying rat olfactory behavior tell us that they can correctly guess the behavioral state of the rat by monitoring the sniff pattern, even without direct observation of the rat's behavior. Furthermore, the sniff rhythm depends on motivational state and the type of motor activity. If the information processing rhythm in the central olfactory system of a rat occurs in synchrony with its sniff rhythm, what is the function of this rhythm in olfactory information processing? And if sniff rhythm is a key to olfactory information processing, what types of information are processed at different phases of a sniff cycle?

As already stated, each sniff cycle consists of an inhalation phase (on-line phase) followed by an exhalation phase (off-line phase). Figure 1.2 shows that several types of nested oscillatory activity occur sequentially in the olfactory bulb at fixed phases of an inhalation–exhalation sniff cycle. The nested gamma oscillations during the inhalation phase (including those that occur just after the end of inhalation) are thought to reflect neuronal activities that are induced directly by the odor inhalation. As shown in Fig. 1.2, however, a large amount of nested oscillatory activities in the olfactory bulb sometimes also occurs during the subsequent long-exhalation phase or off-line "rest and digest" phase. Such nested oscillatory activities occur also in the olfactory cortex and higher olfactory centers during the long exhalation phase up to the initial part of the next inhalation, in which the central olfactory system is nearly disengaged from the external odor world (see Chap. 8).

Odor information is conveyed from the olfactory bulb to the olfactory cortex via two types of projection neurons, tufted cells and mitral cells (see Chap. 7). A sniff cycle can be divided into an inhalation phase and exhalation phase (Fig. 1.1). At which phase of the sniff cycle do tufted cells and mitral cells send odor information to the olfactory cortex? Recent studies by Igarashi et al. (2012) and Fukunaga et al. (2012) indicate that tufted cells and mitral cells send odor information at different phases of the respiration cycle. During the inhalation phase, including the inhalation–exhalation transition phase (on-line "exploratory" phase), a subset of tufted cells start to respond with spike discharges at the rising phase of inhalation, which is followed by the later-onset burst discharges of many mitral cells during the inhalation–exhalation transition phase (see Chap. 7). The initial on-line processing of odor inputs by tufted cells during the inhalation phase might mediate initial fast responses or initial detection of an inhaled odor. The later-onset on-line processing by mitral cells might be important for later integration processes in the olfactory cortex (see Chaps. 7 and 8).

It should be noted that many mitral cells also show burst discharges during the later part of the exhalation phase. Why do many mitral cells show spike discharges during the exhalation phase? What is the functional role of the neuronal activities of the central olfactory system during the off-line "rest and digest" phase? Olfactory researchers have no clear answers to these questions. One can only speculate that

during the exhalation phase the central olfactory system is engaged in off-line processing of odor information that is stored during the preceding inhalation phase. The off-line processing of odor information might be used to initiate adequate behavioral outputs. In addition, off-line processing might also be important in inducing specific emotional and motivational states in the brain. Furthermore, the olfactory system processes retronasal odor inputs from foods in the mouth during the off-line exhalation period, presumably for the evaluation of foods. Off-line processing is discussed in more detail in Chap. 8.

Once you detect rhythms in music, you anticipate subsequent tones in the next rhythmic cycle. From this, we further speculate that once humans or animals detect the sniff rhythm (or once the cerebral neocortex actively elicits the sniff rhythm), off-line processing might be used in anticipating particular types of odor inputs during subsequent inhalation. Monitoring the respiration cycle provides a unique opportunity to differentiate neuronal activities in the on-line processing of odor inputs from those in off-line processing, which occur at distinct time windows.

In all sensory systems, including the olfactory system, distinction between on-line processing and off-line processing also occurs over a much longer time scale, that is, on-line processing during wakefulness and off-line processing during sleep. In the olfactory system, on-line processing during inhalation and off-line processing during exhalation occur alternatively throughout the period of wakefulness. During sleep, in contrast, off-line processing may continually occur irrespective of respiration rhythm, as described in Chap. 8. In other words, there are at least three distinct time windows for information processing in the central olfactory system: during wakefulness, there is a constant alternation of on-line processing of odor inputs at the inhalation phase and off-line processing of olfactory information at the exhalation phase, whereas continuous off-line processing occurs during sleep.

Sensory neuroscience has been markedly successful in advancing knowledge of neuronal circuit mechanisms in the on-line processing of sensory inputs. In contrast, progress in understanding the mechanisms of off-line processing of sensory information is relatively slow. Future studies of the central olfactory system will substantially contribute to advancing our knowledge of this latter point.

1.3 Unique Characteristics of Olfactory Pathways

In this section, we briefly review the characteristic structural organization of the central olfactory pathways in the brain, starting from the olfactory sensory neurons in the olfactory epithelium of the nose (Fig. 1.3). Olfactory information from the external world is carried in a vast variety of odorants, small volatile compounds with a molecular mass less than 300 Da. Odorants are drawn into the nasal cavity during the inhalation phase of the respiration. They are received by odorant receptors expressed on the cilial surface membrane of olfactory sensory neurons (Buck and Axel 1991).

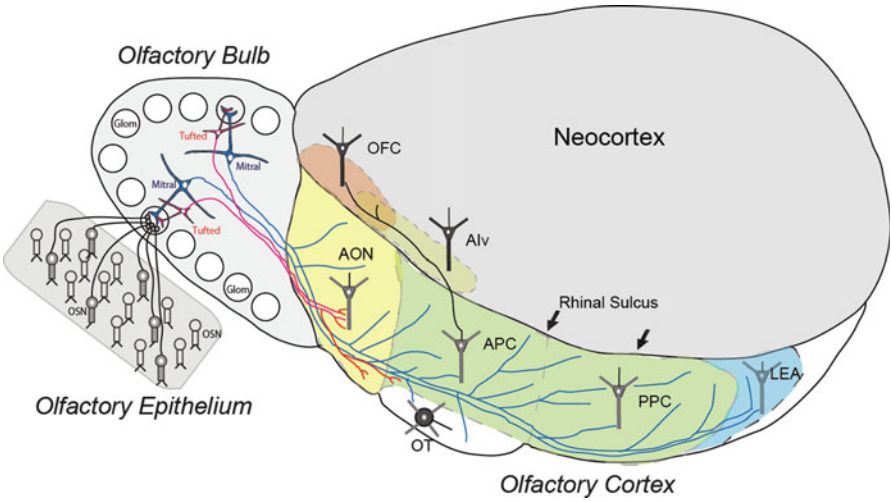

Fig. 1.3 Olfactory pathways to the orbitofrontal cortex in rodents. A schematic diagram of the lateral view of the rodent brain illustrates the neuronal pathways from olfactory sensory neurons through the olfactory bulb and olfactory cortex to the orbitofrontal cortex. *AIv* ventral agranular insular cortex, *AON* anterior olfactory nucleus, *APC* anterior piriform cortex, *Glom* glomerulus, *LEA* lateral entorhinal cortex, *OFC* orbitofrontal cortex, *OSN* olfactory sensory neuron, *OT* olfactory tubercle, *PPC* posterior piriform cortex. Axons of tufted cells are shown by *red*; those of mitral cells are shown by *blue*. (Modified from Mori et al. 2013)

In the mouse olfactory system, each olfactory sensory neuron expresses only one type of functional odorant receptor among a repertoire of more than 1,000 different odorant receptor types, a phenomenon called the "one cell–one receptor" rule. Each olfactory sensory neuron projects a single axon (olfactory axon) to a single glomerulus in the olfactory bulb, which has approximately 1,800 glomeruli spatially arranged around its surface (Fig. 1.3). Axons of numerous olfactory sensory neurons expressing the same type of odorant receptor converge onto two target glomeruli located at fixed positions in the olfactory bulb (see Chap. 3). Each glomerulus therefore represents a single type of odorant receptor (the "one glomerulus—one receptor" rule).

Within each glomerulus of the olfactory bulb, olfactory axons form excitatory synaptic connections on the terminal tufts of primary dendrites of two types of projection neurons, tufted cells and mitral cells (Figs. 1.3 and 1.4). Because of the one glomerulus—one receptor rule, all the olfactory axons and all the sister tufted and mitral cells that project to a single glomerulus form a functional module (glomerular module or glomerular unit) that represents a single type of odorant receptor (Mori and Sakano 2011; Shepherd et al. 2004). For information on the synaptic organization of the olfactory bulb, we refer readers to Shepherd et al. (2004).

The olfactory cortex is defined as those areas that receive direct synaptic input from projection neurons in the olfactory bulb (Fig. 1.5) (Neville and Haberly 2004; Price 1985; Wilson and Sullivan 2011). Individual mitral cells have large cell bodies in the mitral cell layer and send axons in a dispersed manner to virtually

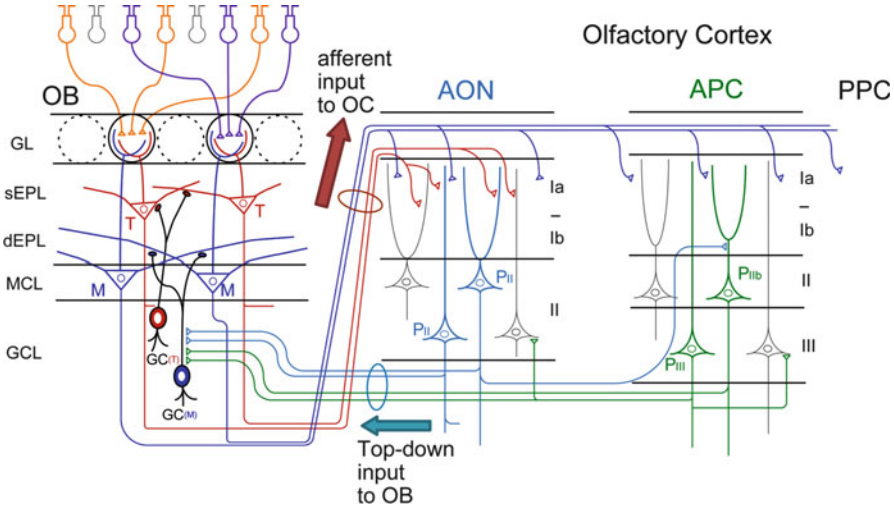

Fig. 1.4 Schematic diagram of the neuronal circuit of the olfactory system shows connectivity of olfactory sensory neurons in the olfactory epithelium (*upper left*), projection neurons and local interneurons in the olfactory bulb (*OB*), and pyramidal cells in the anterior olfactory nucleus (*AON*) and anterior piriform cortex. *GL* glomerular layer, *sEPL* superficial part of the external plexiform layer, *dEPL* deep part of the external plexiform layer, *MCL* mitral cell layer, *GCL* granule cell layer, *T* tufted cell, *M* mitral cell, *GC*(*T*) tufted cell-targeting granule cell, *GC*(*M*) mitral cell-targeting granule cell, *PII* pyramidal cell in layer II of the AON, *PIIb* pyramidal cell in layer IIb of the APC, *PIII* pyramidal cell in layer III of the APC, *PPC* posterior piriform cortex. (Modified from Yamaguchi et al. 2013)

all areas of the olfactory cortex, including the piriform cortex (anterior and posterior piriform cortex), areas in the olfactory peduncle (anterior olfactory nucleus, tenia tecta, and dorsal peduncular cortex), olfactory tubercle, cortical amygdaloid nuclei (nucleus of the lateral olfactory tract, anterior cortical amygdaloid nucleus and posterolateral cortical amygdaloid nucleus), and lateral entorhinal area (Figs. 1.4, 1.5, and 1.6) (Haberly and Price 1977; Igarashi et al. 2012; Luskin and Price 1983; Neville and Haberly 2004; Shipley and Ennis 1996). Tufted cells have smaller cell bodies that are distributed in the external plexiform layer (EPL). Each tufted cell projects axons selectively to focal targets in the olfactory peduncle areas, the rostroventral part of the anterior piriform cortex, and rostrolateral parts of the olfactory tubercle (see Chap. 7).

Except for the olfactory tubercle, all areas of the olfactory cortex have a pyramidal cell-based cortical organization (Figs. 1.4 and 1.6) (Neville and Haberly 2004). Each of these areas has a relatively simple cortical structure, typically with three distinct layers (I, II, and III). Axons of olfactory bulb projection neurons (afferent input) form excitatory synaptic connections (in layer Ia) on the apical dendrites of layer II and layer III pyramidal cells (Figs. 1.4 and 1.6). The pyramidal cells send association fibers to form excitatory synapses on neurons in the same area and in other areas of the olfactory cortex and higher association areas. In the

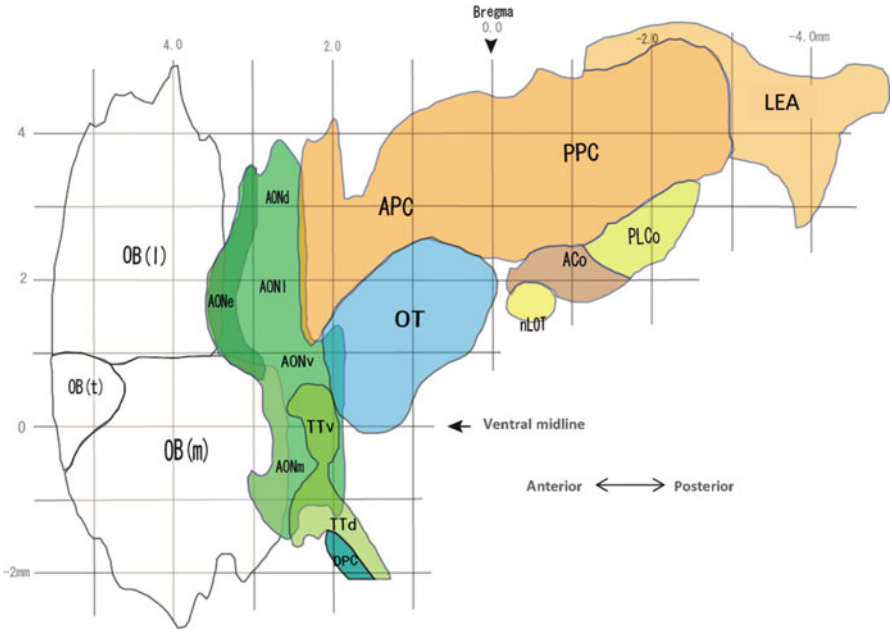

Fig. 1.5 Unrolled flattened map of olfactory bulb (*OB*) and olfactory cortex (*ventral view*). The unrolled map of the olfactory cortex was reconstructed based on the coronal sections of the mouse brain shown in Paxinos and Franklin (2001); that of the olfactory bulb was reconstructed by OCAM-labeled coronal sections shown in Nagao et al. (2000). *OB*(*l*) lateral map of the olfactory bulb, *OB*(*m*) medial map of the olfactory bulb, *OB*(*t*) tongue-like region of the olfactory bulb, *AONe* anterior olfactory nucleus pars externa, *AONd* dorsal part of the AON, *AONl* lateral part of the AON, *AONv* ventral part of the AON, *AONm* medial part of the AON, *TTv* ventral tenia tecta, *TTd* dorsal tenia tecta, *DPC* dorsal peduncular cortex, *APC* anterior piriform cortex, *OT* olfactory tubercle, *nLOT* nucleus of lateral olfactory tract, *ACo* anterior cortical amygdaloid nucleus, *PLCo* posterolateral cortical amygdaloid nucleus, *PPC* posterior piriform cortex, *LEA* lateral entorhinal area. Different areas of the olfactory cortex are shown by different colors

afferent pathways (Figs. 1.4 and 1.6), direct afferent input from the olfactory bulb terminates in layer Ia of the piriform cortex, whereas association fiber inputs terminate mainly in layer Ib (Neville and Haberly 2004). Pyramidal cells in layers II and III of the anterior olfactory nucleus and anterior piriform cortex also massively project collateral axons of the association fibers to the olfactory bulb, and thus form top-down feedback pathways (Fig. 1.4).

Figure 1.7 illustrates the major olfactory afferent pathways from the piriform cortex to the neocortex. Pyramidal cells in layer II of the anterior piriform cortex (APC) project axons to the orbitofrontal cortex (OFC), which includes the ventrolateral orbital cortex (VLO) and lateral orbital cortex (LO). These pyramidal cells also project axons to the ventral agranular insular cortex (AIv) of the neocortex. The projection from the APC to the OFC/AIv is composed of two parallel pathways (Ekstand et al. 2001): pyramidal cells in the ventral part of the APC (APCv) project axons to the VLO, and those in the dorsal APC (APCd) send axons to the LO and AIv.

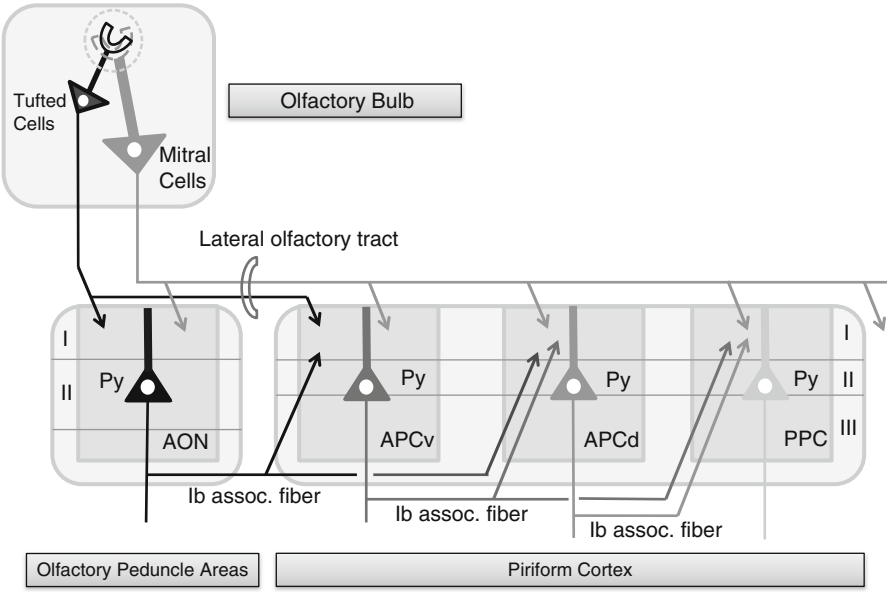

Fig. 1.6 Olfactory afferent pathways from the olfactory bulb through the anterior olfactory nucleus to the three subdivisions of the piriform cortex. Tufted cell axons and mitral cell axons form two types of direct afferent pathways from the olfactory bulb and terminate in the superficial part of layer I (layer Ia) of the olfactory cortex. *AON* anterior olfactory nucleus, *APCv* ventral subdivision of the anterior piriform cortex (APC), *APCd* dorsal subdivision of the APC, *PPC* posterior piriform cortex. Ib association fiber afferent pathways (*Ib assoc. fiber*) are also shown by *arrows* that terminate in the deep part of layer I (layer Ib). *Py* pyramidal cell; *I*, *II*, and *III* indicate layers I, II, and III, respectively, of the olfactory cortex

The olfactory pathway to the OFC/AIv is unique in that the orbitofrontal cortex is only three synapses (olfactory bulb, APC, and OFC synapses) distant from olfactory sensory neurons. However, in addition to the direct projection from the APC to OFC/AIv, indirect transthalamic pathways are also present (Fig. 1.7). The APCd projects axons to the endopiriform nucleus (En), which projects axons to the mediodorsal nucleus (MD) of the thalamus. Thalamocortical neurons in the MD project axons to the LO and AIv. The APCv connects with the pre-endopiriform nucleus (pEn), which projects axons to the submedius nucleus (SM) of the thalamus. Thalamocortical neurons in the SM send axons to the VLO.

The direct projection from the piriform cortex to the neocortex shows broad topographical organization (Figs. 1.7 and 1.8) (Ekstand et al. 2001; Ray and Price 1992). The APCv projects to the VLO, the most rostral target area of the neocortex. The APCd directly sends axons to the LO and AIv. Pyramidal cells in the posterior piriform cortex (PPC) project axons to the AIv and posterior agranular insular cortex (AIp). The OFC in turn projects axons back to layer III of the piriform cortex. This top-down projection also shows broad topography, as shown in Fig. 1.7

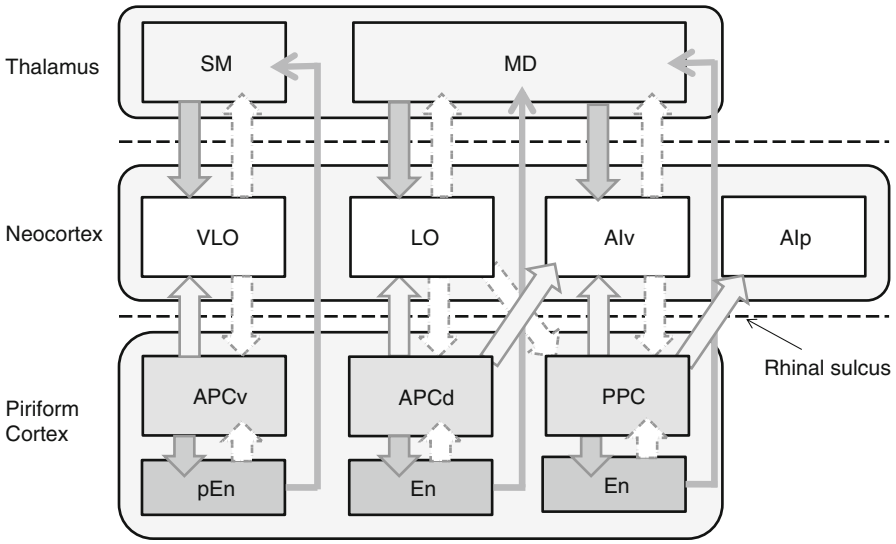

Fig. 1.7 Direct and transthalamic pathways from the three subdivisions of the piriform cortex to the neocortex. Ventral subdivision of the anterior piriform cortex (*APCv*), dorsal subdivision of the anterior piriform cortex (*APCd*), and posterior piriform cortex (*PPC*) form distinct pathways to the neocortex. *VLO* ventrolateral orbital cortex, *LO* lateral orbital cortex, *AIv* ventral agranular insular cortex, *AIp* posterior agranular insular cortex, *SM* submedius nucleus of thalamus, *MD* mediodorsal nucleus of thalamus, *pEn* pre-endopiriform nucleus, *En* endopiriform nucleus. *Solid arrows* indicate afferent axonal connections; *broken arrows* show top-down connections

(Illig 2005). The lateral entorhinal cortex has reciprocal connections with the perirhinal cortex (Fig. 1.8) (Amaral and Lavenex 2007).

The olfactory cortex is a key structure that sends olfactory sensory information not only to the neocortex but also to other higher association areas (Fig. 1.8). For example, the lateral entorhinal cortex sends axons to the hippocampus, forming olfactory afferent pathways to the hippocampus. The piriform cortex and cortical amygdaloid nuclei have rich connectivity with the amygdaloid nuclei, forming olfactory afferent pathways to the amygdala. The piriform cortex and other areas of the olfactory cortex also project to the lateral hypothalamus, forming the olfactory afferent pathways to the hypothalamus.

The olfactory tubercle is unique among areas of the olfactory cortex and thus appears to be functionally distinct from other areas of the olfactory cortex. Although it has a cortical organization, principal neurons in the olfactory tubercle are GABAergic medium spiny neurons (Millhouse and Heimer 1984). These medium spiny neurons do not send association fibers to other areas of the olfactory cortex but send inhibitory output to the neurons in the ventral pallidum. The ventral pallidum neurons are GABAergic neurons that send inhibitory outputs to neurons in the mediodorsal nucleus of the thalamus, dopaminergic neurons in the ventral tegmental area, and neurons in the lateral hypothalamus. Together with the accumbens, the olfactory tubercle forms the ventral striatum (Heimer 2003;

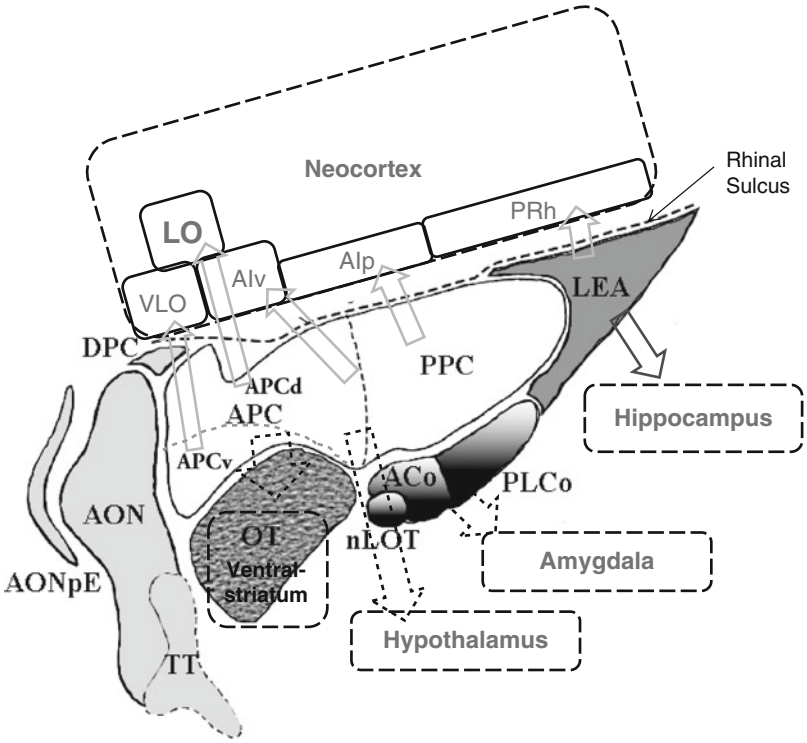

Fig. 1.8 Major olfactory afferent pathways from the olfactory cortex to the neocortex, hippocampus, amygdala, hypothalamus, and ventral striatum. Unrolled map of areas in the olfactory cortex is reconstructed based on Fig. 1.5. Olfactory peduncle areas include anterior olfactory nucleus (*AON*), anterior olfactory nucleus pars externa (*AONpE*), tenia tecta (*TT*), and dorsal peduncular cortex (*DPC*). The three subdivisions of the piriform cortex are the ventral subdivision of the anterior piriform cortex (*APCv*), the dorsal subdivision of APC (*APCd*), and the posterior piriform cortex (PPC). The olfactory tubercle (*OT*) is part of the ventral striatum. Cortical amygdaloid nuclei include the nucleus of the lateral olfactory tract (*nLOT*), the anterior cortical amygdaloid nucleus (*ACo*), and the posterolateral cortical amygdaloid nucleus (*PLCo*). Lateral entorhinal area (*LEA*) forms the pathway to the hippocampus. Each target area in the neocortex is surrounded by a *solid line*. *VLO* ventrolateral orbital cortex, *LO* lateral orbital cortex, *AIv* ventral agranular insular cortex, *AIp* posterior agranular insular cortex, *PRh* perirhinal cortex

Ikemoto 2003, 2007; Ikemoto et al. 2005; Switzer et al. 1982) and is thought to have a key role in the olfactory cortex–ventral striatum–ventral pallidum–thalamus–frontal cortex loop (see Chap. 8).

In addition to these major afferent pathways, a variety of associational and top-down axonal projections occur across different regions of the central olfactory system. The central olfactory system thus forms large-scale neuronal networks that connect local circuits in the olfactory bulb, olfactory cortex, orbitofrontal cortex, agranular insular cortex, thalamus, hypothalamus, amygdala, hippocampus, and ventral striatum. Olfactory researchers are now struggling to understand the

functional logic of the large-scale networks of the central olfactory system that enables human and animals to translate external odor information to appropriate behavioral outputs.

As described in the previous section, the information processing mode in the large-scale networks of the olfactory system depends heavily on the sniff cycle. Therefore, olfactory researchers are interested in the question of "when" in the sniff cycle the central olfactory system translates the external odor information to behavioral outputs. During the on-line inhalation phase of the sniff, what type of information processing occurs in the large-scale networks of the central olfactory system? During the inhalation phase, how and via which pathways is the odor information transferred in the large-scale networks? In parallel with the transition from inhalation phase to exhalation phase, the information processing mode and the direction of information streams appear to change. It is largely unknown, however, how the large-scale networks of the central olfactory system change the information processing mode at different phases of the sniff cycle. Future research will address these questions, which are particularly important in understanding the workings of the central olfactory system.

References

Amaral D, Lavenex P (2007) Hippocampal neuroanatomy. In: Andersen P, Morris R, Amaral D, Bliss T, O'Keefe J (eds) The hippocampus book. Oxford University Press, New York

Axel R (1995) The molecular logic of smell. Sci Am 273:154–159

Buck L, Axel R (1991) A novel multigene family may encode odorant receptors: a molecular basis for odor recognition. Cell 65:175–187

Buzsaki G (2006) Rhythms of the brain. Oxford University Press, New York

Doty RL (1986) Odor-guided behavior in mammals. Experientia (Basel) 42:257–271

Ekstand JJ, Domroese ME, Johnson DM, Feig SL, Knodel SM (2001) A new subdivision of anterior piriform cortex and associated deep nucleus with novel features of interest for olfaction and epilepsy. J Comp Neurol 434:289–307

Fukunaga I, Berning M, Kollo M, Schmaltz A, Schaefer AT (2012) Two distinct channels of olfactory bulb output. Neuron 75:320–329

Gautam SH, Verhagen JV (2012) Retronasal odor representations in the dorsal olfactory bulb of rats. J Neurosci 32:7949–7959

Haberly LB, Price JL (1977) The axonal projection patterns of the mitral and tufted cells of the olfactory bulb in the rat. Brain Res 129:152–157

Heimer L (2003) A new anatomical framework for neuropsychiatric disorders and drug abuse. Am J Psychiatry 160:1726–1739

Homma I, Masaoka Y (2008) Breathing rhythms and emotions. Exp Physiol 93:1011–1021

Igarashi KM, Ieki N, An M, Yamaguchi Y, Nagayama S et al (2012) Parallel mitral and tufted cell pathways route distinct odor information to different targets in the olfactory cortex. J Neurosci 32:7970–7985

Ikemoto S (2003) Involvement of the olfactory tubercle in cocaine reward: intracranial self-administration studies. J Neurosci 23:9305–9311

Ikemoto S (2007) Dopamine reward circuitry: two projection systems from the ventral midbrain to the nucleus accumbens-olfactory tubercle complex. Brain Res Rev 56:27–78

Ikemoto S, Qin M, Liu ZH (2005) The functional divide for primary reinforcement of D-amphetamine lies between the medial and lateral ventral striatum: is the division of the accumbens core, shell, and olfactory tubercle valid? J Neurosci 25:5061–5065
Illig KR (2005) Projections from orbitofrontal cortex to anterior piriform cortex in the rat suggest a role in olfactory information processing. J Comp Neurol 488:224–231
Kepecs A, Uchida N, Mainen ZF (2006) The sniff as a unit of olfactory processing. Chem Senses 31:167–179
Luskin MB, Price JL (1983) The topographic organization of associational fibers of the olfactory system in the rat, including centrifugal fibers to the olfactory bulb. J Comp Neurol 216:264–291
Mainland J, Sobel N (2006) The sniff is part of the olfactory percept. Chem Senses 31:181–196
Manabe H (2008) Behavioral state-dependent coordinated change in the respiration pattern and the signal processing mode in the olfactory cortex and hippocampus. University of Tokyo, Tokyo
Manabe H, Mori K (2013) Sniff rhythm-paced fast and slow gamma-oscillations in the olfactory bulb: relation to tufted and mitral cells and behavioral states. J Neurophysiol 110:1593–1599
Millhouse OE, Heimer L (1984) Cell configurations in the olfactory tubercle of the rat. J Comp Neurol 228:571–597
Mori K, Sakano H (2011) How is the olfactory map formed and interpreted in the mammalian brain? Annu Rev Neurosci 34:467–499
Mori K, Nagao H, Yoshihara Y (1999) The olfactory bulb: coding and processing of odor molecule information. Science 286:711–715
Mori K, Manabe H, Narikiyo K, Onisawa N (2013) Olfactory consciousness and gamma oscillation couplings across the olfactory bulb, olfactory cortex, and orbitofrontal cortex. Front Psychol 4:743
Murakami M, Kashiwadani H, Kirino Y, Mori K (2005) State-dependent sensory gating in olfactory cortex. Neuron 46:285–296
Nagao H, Yoshihara Y, Mitsui S, Fujisawa H, Mori K (2000) Two mirror-image sensory maps with domain organization in the mouse main olfactory bulb. Neuroreport 11:3023–3027
Neville KR, Haberly LB (2004) Olfactory cortex. In: Shepherd GM (ed) The synaptic organization of the brain. Oxford University Press, New York, pp 415–454
O'Keefe J (2007) Hippocampal neurophysiology in the behaving animal. In: Andersen P, Morris R, Amaral D, Bliss T, O'Keefe J (eds) The hippocampus book. Oxford University Press, New York, pp 475–548
Paxinos G, Franklin KBJ (2001) The mouse brain in stereotaxic coordinates. Academic, London
Price JL (1985) Beyond the primary olfactory cortex: olfactory-related areas in the neocortex, thalamus and hypothalamus. Chem Senses 10:239–258
Ray JP, Price JL (1992) The organization of the thalamocortical connections of the mediodorsal thalamic nucleus in the rat, related to the ventral forebrain-prefrontal cortex topography. J Comp Neurol 323:167–197
Shepherd GM, Chen WR, Greer CA (2004) Olfactory bulb. In: Shepherd GM (ed) The synaptic organization of the brain. Oxford University Press, New York, pp 165–216
Shipley MT, Ennis M (1996) Functional organization of olfactory system. J Neurobiol 30:123–176
Switzer RC 3rd, Hill J, Heimer L (1982) The globus pallidus and its rostroventral extension into the olfactory tubercle of the rat: a cyto- and chemoarchitectural study. Neuroscience 7:1891–1904
VanRullen R, Koch C (2003) Is perception discrete or continuous? Trends Cogn Sci 7:207–213
Wachowiak M (2011) All in a sniff: olfaction as a model for active sensing. Neuron 71:962–973
Welker WI (1964) Analysis of sniffing in the albino rat. Behavior 22:223–244
Wilson DA, Sullivan RM (1999) Respiratory airflow pattern at the rat's snout and an hypothesis regarding its role in olfaction. Physiol Behav 66:41–44
Wilson DA, Sullivan RM (2011) Cortical processing of odor objects. Neuron 72:506–519
Wyatt TD (2009) Fifty years of pheromones. Nature (Lond) 457:262–263
Yamaguchi M, Manabe H, Murata K, Mori K (2013) Reorganization of neuronal circuits of the central olfactory system during postprandial sleep. Front Neural Circuits 7:132

Chapter 2
Odor and Pheromone Molecules, Receptors, and Behavioral Responses

Kazushige Touhara

Abstract Knowledge about chemosensory signals, receptors, olfactory neural network, and behavioral outputs has grown rapidly. Thus, the molecular logic that mediates recognition and discrimination of chemosensory signals has been revealed. Here, I first summarize the current understanding of mammalian olfaction, from the odorant or pheromone, to the receptor, and finally to the behavioral output. I then discuss important questions to be solved in the future and give some insights. Specifically, how should we categorize volatile compounds that are received by olfactory systems in animals? What should be the next focus of research in the field of olfactory receptors? How can we connect a receptor response to a cognate, biologically meaningful odorant or pheromone with the respective behavioral or physiological output at the level of neural circuitry?

Keywords Chemosensory • Insect • Mouse • Odorant • Olfactory receptor • Pheromone

2.1 Introduction

For terrestrial animals, most odorants are small volatile organic compounds with molecular weights of less than 300. For fish, however, "odorants" are generally water soluble, not volatile. Moreover, a molecule that functions as an odorant for one species does not necessarily function as an odorant for other species. For example, although humans cannot smell CO_2, insects and mice can. Therefore, it

K. Touhara (✉)
Department of Applied Biological Chemistry, Graduate School of Agricultural and Life Sciences, The University of Tokyo, Tokyo 113-8657, Japan

JST ERATO Touhara Chemosensory Signal Project, Graduate School of Agricultural and Life Sciences, The University of Tokyo, Tokyo 113-8657, Japan
e-mail: ktouhara@mail.ecc.u-tokyo.ac.jp

K. Mori (ed.), *The Olfactory System: From Odor Molecules to Motivational Behaviors*,
DOI 10.1007/978-4-431-54376-3_2,

is not easy to define the word odorant; nevertheless, it is fair to say that odorants are small chemicals that are perceived by an animal's olfactory sensory system.

The estimated number of volatile organic compounds that function as odorants is thought to be 0.4–0.5 million, and the odor quality of each compound differs from that of every other compound. Among various volatile organic compounds, some molecules are biologically important for some species and function as information about food, predators, sex, and social or metabolic status of an individual. If compounds are utilized for communication within one species, they are usually defined as pheromones (Karlson and Luscher 1959). However, some such odorants may convey individuality and allow for one individual to be distinguished from other individuals; such intraspecies odorants could then be defined as signature odors, rather than pheromones (Wyatt 2010). Thus, volatiles can be categorized on the basis of biological role, meaning, or function.

The mechanisms underlying volatile sensing have been debated for a long time. After the discovery of the gene family comprising olfactory receptor (OR) genes (Buck and Axel 1991), the stereospecific receptor theory appeared to be proven. During the past decade or so, genome projects have generated an abundance of information about the OR multigene family in various species (Nei et al. 2008). Along with collection of the genomic information, many ORs have been deorphanized, and the combinatorial coding model has become a rule used to explain the sophisticated discriminatory power of the olfactory system (Touhara and Vosshall 2009). However, a repertoire of synthetic odorants has been used for most studies; therefore, the real in vivo role of each OR has not been assessed because information about the natural odorants detected by organisms via ORs in natural environments is generally lacking.

A signal from volatiles sensed by peripheral olfactory receptor neurons is sent to the olfactory bulb, the first neural center of the olfactory system, and eventually to higher brain areas (Mori and Sakano 2011). The network of neural projections to the glomeruli in the olfactory bulb is constructed so that the combinatorial receptor code for each odorant is sent without being mixed with any other code. The neuronal hardwiring of odorant coding that exists in the olfactory bulb does not seem to exist within the regions of the brain that are involved in olfaction and odor perception (Caron et al. 2013; Sosulski et al. 2011). Molecular biology and neuroscience techniques are being used to elucidate the neural networks and mechanisms for odorant discrimination by the mammalian brain, but examination of these complex phenomena has been very challenging. Furthermore, the mechanisms by which specific behaviors or neuroendocrine changes are induced by odorants or pheromones at the level of neural networks have not been fully elucidated.

Here, I first summarize the current understanding of mammalian olfaction from the odorant or pheromone, to the receptor, and finally to the behavioral output; I then focus on the three important questions I have just described and that are stated explicitly as follows. (1) How should we categorize volatile organic compounds that are received by olfactory systems in animals? (2) Having accumulated knowledge of receptor–ligand interactions, what should be the next focus of research in the field of olfactory receptors? (3) How can we connect, in terms of neural networks, a receptor response to a cognate, biologically meaningful odorant with the respective behavioral or physiological output?

2.2 Odor and Pheromone Molecules

2.2.1 General Odorants: From Food, Predator, or Nonrelevant Species

Among volatile odorants derived from various animals, insects, plants, and microorganisms in the external world, odorants emitted from nonrelevant species are neutral or do not possess any meaning for individuals of one or more species, and thus do not elicit any specific behavior. Some odorants, however, become important information for individuals of some species when they are emitted from relevant foods or predators, because each individual, regardless of species, has to find food and may have to avoid predators to survive. The odorants that are beneficial only to perceivers, those that perceive odorant-derived information, and not to the emitter are called kairomones. Conversely, odorants that are advantageous only to emitters, such as antifeedant volatiles from plants, are called allomones. Odorants that benefit both the perceiver and emitter are called synomones. Together, all three classes of odorants—kairomones, allomones, and synomones—are called allelochemicals (Wyatt 2003).

Allelochemicals tend to be highly volatile so that they are transmitted for a long distance (Fig. 2.1). In other words, individual animals can sense these volatile long-transmittable odorants as information about foods so that they can perceive food that is far away and follow the food signal from a long distance, or as information about predators so that they can take an action to escape while at a safe distance. In addition, the threshold concentration of these odorants for the receptors in perceivers is usually low, and such odorants tend to exhibit a relatively strong smell at low concentrations. So-called general odorants include neutral odorants from nonrelevant species and allelochemicals from relevant species.

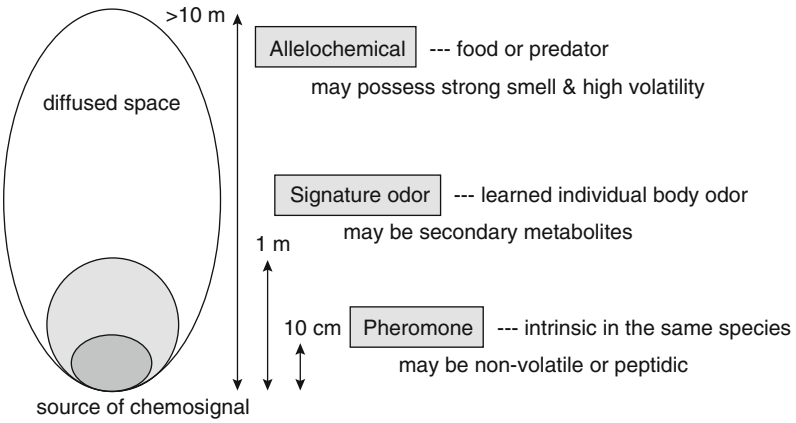

Fig. 2.1 Relationship between function and chemical property of chemosensory signals

2.2.2 Signature Odors: Recognition of Individuals Within the Species

Recognition of conspecifics is achieved by using various sensory modalities, such as vision and sound, which are physical information, and odorants and pheromones, which are chemical information. Among the modalities, olfaction is the most important tool for intraspecies communication for most animal species. Chemical compounds that provide within-species information can be divided into two categories: signature odors, which convey differences between individuals, and pheromones, which are crucial signals for survival and mating (Wyatt 2010). The main difference between signature odors and pheromones is that pheromones elicit intrinsic, within-sex or between-sex behavioral or endocrine changes; in contrast, signature odors are information about particular individuals and do not necessarily cause such changes, but signature odors do mediate how the perceiver feels or behave toward the emitter regardless of sex. For example, in humans, the preference observed in the T-shirt experiments is the result not of pheromones but of signature odors; in contrast, menstrual-cycle synchronization, also called the dormitory effect, is caused by pheromone(s), although the active compound(s) has (have) not been isolated. Behavioral responses to signature odors do not have to be common among all individuals within a species; these responses can differ case by case and from individual to individual.

Signature odors can provide information about siblings, parents, or friends. Moreover, signature odors are not usually conveyed by a single compound, but are the result of subtle differences in the compositions of body odors. Sources of body odor can include sweat, urine, saliva, and tears, which are all secreted compounds that can differ between individuals. The differences are thought to be generated from genetic variation such as major histocompatibility complex (MHC) molecules (Yamazaki et al. 1999). Additionally, signature odors can differ within a single individual depending on the individual's metabolic status. Odor composition may change when an individual is infected by a virus or contracts a disease (Shirasu and Touhara 2011). Signature odors are often less volatile than general odorants because the distance between conspecific individuals is often much shorter than that between heterospecific individuals (Fig. 2.1). The compounds that convey signature odors may be relatively heavy, such as secondary metabolites from fatty acid metabolism that are easily affected by health condition. Differences between signature odors are discriminated by approximately 1,000 ORs in the main olfactory system in a combinatorial fashion; in contrast, pheromones are perceived via selective receptor(s) and pinpoint recognition.

2.2.3 Pheromones: Innate Intraspecies Signals Necessary for Survival and Mating

The original definition of pheromone was an intraspecies signal that causes innate and specific behavioral or endocrine effects in other conspecific individuals

(Karlson and Luscher 1959). In some cases, such as the trail pheromone in ants, a pheromone elicits a specific behavior in all animals within the same species regardless of sex, but in most cases, pheromone signals convey sex-specific information. Sex pheromones are the most important for the species to leave offspring. Sex pheromones are usually species specific to ensure reproductive isolation. However, during the course of evolution, pheromones utilized in two completely different species may converge to become the same compound: for example, a current elephant pheromone is a current moth pheromone (Rasmussen and Schulte 1998). Additionally, a single compound can elicit sexual behaviors in multiple species, as is the case among even-toed ungulates such as sheep and goats. In both such cases, pheromones are not strictly species specific; therefore, the definition of pheromone has to be revised to include a much wider range of pheromone actions in animals. It is important to note that pheromone-elicited behaviors are intrinsic, not learned behaviors as are signature odor-elicited behaviors. Additionally, an odorant that functions as a pheromone for one species could function as a kairomone or even as a general odorant (that conveys only species-specific and not sex-specific information) for another species.

Chemical properties vary greatly among currently known pheromones. Pheromones are not necessarily volatile; for example, a pheromone can be a nonvolatile peptide or protein, so long as the compound is transmitted from one individual to another (Touhara and Vosshall 2009). In insects, sex pheromones are generally volatile and can attract an opposite-sex conspecific from a long distance. In contrast, in mammals, some sex pheromones are transmitted to an opposite-sexed conspecific via direct contact, and mammalian pheromones are sometimes peptide or proteins (Touhara 2008) (Fig. 2.1). Many mammalian species, excluding some primates, possess a second olfactory system called the vomeronasal system wherein many nonvolatile peptide pheromones are sensed (Touhara and Vosshall 2009). There are two major advantages of peptide pheromones: (1) they are encoded by the genome, and therefore stable throughout life; (2) they are not volatile, and therefore stay at the deposition site and are effective for a long period of time. Whether a pheromone used is volatile or nonvolatile depends on at least three things: (1) the environmental situation, (2) the distance the signal should be transferred, and (3) the length of time that the signal should persist.

2.3 Olfactory Receptors: Genes and Functions

2.3.1 Vertebrate Odorant Receptors

Titus Lucretius Carus, a Roman poet and philosopher, proposed that a variety of odors exist because each odorant possesses a unique structure (Lucretius 1995). In the mid-twentieth century, this concept was formally established as the stereospecific receptor theory (Amoore 1963), and it provided an explanation for

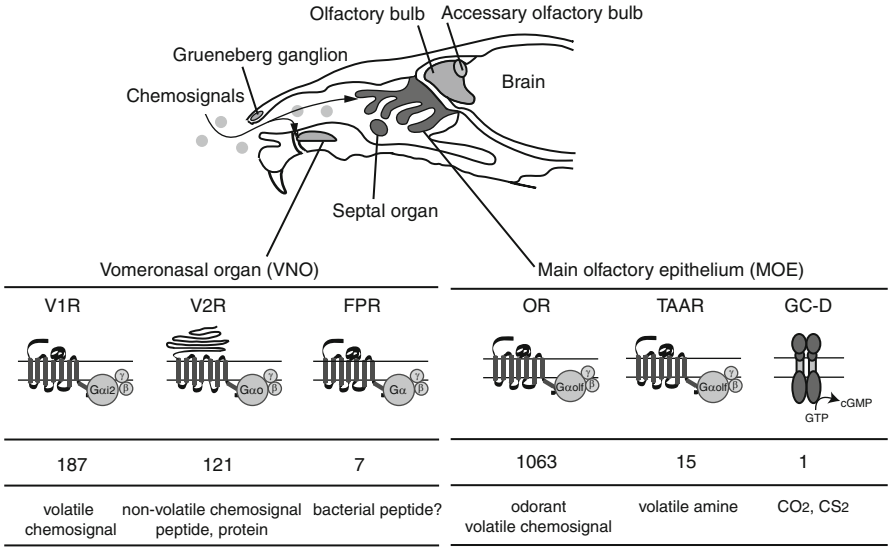

Fig. 2.2 Anatomical view of the olfactory systems and the numbers and ligands of chemosensory receptors in mice. *V1R* vomeronasal receptor type 1, *V2R* vomeronasal receptor type 2, *FPR* formyl peptide receptors, *OR* odorant receptors, *TAAR* trace amine-associated receptors, *GC-D* guanylate cyclase D

the molecular mechanisms underlying the remarkable discriminatory power of olfactory sensing systems. The receptor theory postulates that there are receptor sites for odorants and that odor perception occurs only when the structure of an odorant molecule and the binding site match. There were other theories, including vibrational theory, puncturing theory, radiational theory, and absorption theory. However, only the stereospecific receptor theory was consistently supported by empirical evidence and ultimately proven with the discovery of the OR family in 1991 (Buck and Axel 1991); this family comprises thousands of proteins each encoded by the respective gene and that recognizes a specific functional group, molecular size, length of odorant molecule, or some combination of these (Fig. 2.2).

The vertebrate OR family belongs to the G protein-coupled receptor (GPCR) superfamily, and most members possess a seven-transmembrane region and several amino acid sequence motifs (e.g., the DRY and/or NPXXY motifs that are common among GPCRs) (Touhara and Vosshall 2009). Recently solved three-dimensional (3D) structures of GPCRs indicate that the DRY motif present at the end of transmembrane region 3 (TM3) is involved in G-protein coupling (Rasmussen et al. 2011). Several amino acids in the intracellular loop and the C-terminal domain are involved in G-protein recognition (Kato et al. 2008). ORs appear to have a coupling selectivity for the G_s family, which includes $G\alpha_s$, and for $G\alpha_{olf}$ as well as $G\alpha_{15}$, which is a promiscuous G protein (Kato and Touhara 2009). The physiological endogenous G protein in olfactory sensory neurons is $G\alpha_{olf}$, which is involved in odor signal transduction, but $G\alpha_s$ or $G\alpha_{15}$ is used in heterologous expression experiments to monitor an increase in cAMP or calcium ion, respectively (Touhara 2007).

Highly effective assays of OR function that use heterologous cells such as HEK293 cells or *Xenopus* oocytes have been developed, revealing that individual ORs could recognize several structurally similar odorants and that each odorant could be recognized by a subset of ORs (Touhara 2007). Thus, the discrimination of a vast range of odorants is established by a combination of ORs that are activated by each odorant (Touhara and Vosshall 2009). The binding pocket was identified by mutation analyses and appears to reside within the transmembrane regions of TM3, TM6, and TM7 (Katada et al. 2005). Relatively weak hydrophobic interactions are thought to be the main forces driving odorant molecule recognition. Consistently, EC_{50} values for OR–odorant pairs are greater than those of other GPCR–ligand pairs; in olfactory sensory neuron and in heterologous cells, EC_{50} values among OR–odorant pairs range over two orders of magnitude, from 1 μM to several hundred micromoles (μM). This weak binding appears to help broaden the ligand spectrum of each OR and to ensure the role of the OR family in sensing a variety of odorants in the environment.

Even now, 15 years after the first success in functional characterization of an OR, only 10 % of ORs have been paired with a cognate odorant via heterologous cell assay by screening compounds that are commercially available or can be obtained from fragrance companies (Saito et al. 2009). In addition, approximately 90 % of all the olfactory sensory neurons tested in one study did not respond to any of 125 synthetic odorants used in the study, although these synthetic odorants represented a wide and diverse variety of structures (Nara et al. 2011). These findings indicate that most cognate ligands are absent from current odorant collections. Moreover, biologically relevant naturally occurring ligands for ORs are distinct from odorants in laboratory collections. Specifically, natural ligands are derived from foods, predators, competitors, urine, feces, secretions of conspecific or heterospecific individuals, or some combination of these sources. All natural ligands are secondary metabolites derived from the metabolism of fatty acids or of amino acids. Recently, Yoshikawa et al. developed a highly efficient OR assay with no background that can be used to purify natural ligands for ORs. For example, they used crude extracts, OR assay-guided fractionation, and chemical analysis to identify (*Z*)-5-tetradecen-1-ol, a putative fatty acid metabolite, as a natural ligand for Olfr288 in male urine that attracted females (Yoshikawa et al. 2013). In another study, they identified natural ligands for OR37 and showed that these were also fatty acid derivatives, specifically C14–C18 aldehydes (Bautze et al. 2012), although the functional proof in heterologous cells has not been provided. This assay and approach can be used to identify more naturally occurring ligand–OR pairs in the future.

Since the discovery of the first OR family in rats, genome projects have revealed that many animal taxa—from *Amphioxus*, a primitive chordate species, to humans—have OR proteins (Niimura 2009). Two major characteristics of the OR gene family are that (1) the family comprises hundreds to as many as a few thousand multigenes, and (2) a significant portion of these genes are pseudogenes (Nei et al. 2008). OR genes in each species appear to have a history of extensive duplication and pseudogenization that is unique to the respective species. The proportion of pseudogenization of the family argues about the molecular evolution

pressure by which sensory modalities are utilized to communicate in the life of each organism. We can also speculate that duplicated ORs probably play a crucial role for respective species in detecting important volatiles such as allelochemicals and pheromones, and that ORs that have been lost are not critical for persistence of the respective species within its current or recent environment. The molecular evolution of the OR family tells us much information about the history of development of the sensory systems in every animal species.

2.3.2 Vomeronasal Receptor

The vomeronasal organ (VNO) was discovered by a Danish surgeon, Ludwig Jacobson, in 1813; the VNO has a dead-ended elongated "c"-shaped lumen in a football-like capsule and is located under the nasal cavity. The VNO is considered a second olfactory system that detects various external substances from the external environment (Munger et al. 2009; Touhara and Vosshall 2009). Active pumping by a blood vessel that surrounds the vomeronasal cavity is required to take up compounds, and sniffing in rodents, or flehmen in cats or horses, is associated with VNO-mediated olfaction. The vomeronasal cavity is open to both the nasal and oral cavities; this anatomy indicates that there are two routes for chemical transport into the VNO. Surgical or genetic ablation of the VNO results in a loss of various social and sexual behaviors, suggesting that the VNO receives compounds utilized for chemical communication between individuals, including pheromones and allelochemicals (Dulac and Torello 2003).

Multiple types of GPCRs are expressed in the VNO (Touhara and Vosshall 2009) (Fig. 2.2). The vomeronasal receptor type 1 (V1R) subfamily belongs to the rhodopsin type class A GPCRs and consists of 170 members that are expressed together with $G\alpha_i$ in the apical layer of the vomeronasal epithelium in mice. The V2R subfamily comprises 128 members and is expressed with $G\alpha_o$ in the basal layer of the vomeronasal epithelium; this subfamily belongs to the class C GPCR family, which is characterized by a long N-terminal domain resembling that in the glutamate receptor. V1Rs recognize small volatile or nonvolatile organic compounds, whereas V2Rs appear to sense relatively large nonvolatile cues such as peptides and proteins (Touhara and Vosshall 2009). Formyl peptide receptors (FPRs) are another group of GPCRs that are expressed in the VNO; FPRs are thought to play a role in recognizing information of infected microorganisms or diseases (Liberles et al. 2009; Riviere et al. 2009). Each vomeronasal neuron expresses only 1 of 300 possible receptor types (VR or FPR) mutually exclusively, except V2R2, which is ubiquitously expressed in a fashion similar to that of neurons in the main olfactory system. The one neuron–one receptor rule is a molecular basis for a neural network to allow for signal transmission to the brain without mixing the information.

The VNO almost certainly has roles in sensing pheromones and allelochemicals, yet few ligand–receptor pairs have been identified. The most likely reason for the

delay in deorphanizing VRs is the difficulty in expressing VRs in heterologous cells (Dey and Matsunami 2011). However, the fact that each vomeronasal neuron expresses only one type of receptor allows us to identify a candidate receptor by double-labeling cells with a marker for neural activation and each VR gene. The mouse sex peptide pheromone ESP1 with its cognate receptor V2Rp5 was the first ligand–VR pair identified with this approach (Haga et al. 2010). The recognition was confirmed by transgenic introduction of a fluorescently tagged V2Rp5 into vomeronasal sensory neurons and subsequent functional characterization of exogenously expressed V2Rp5. More expanded characterization of the VR family in respect of chemical cues has been carried out by the same double-labeling approach (Isogai et al. 2011). This double-labeling approach has been used to characterize more VR family members that have a distinct function such as recognition of sex-specific cues, predator cues, and so on. In addition, MUP and MHC peptides were identified as cognate ligands of other VR2 proteins. Reportedly, MHC peptides may be recognized by V2r1b (Leinders-Zufall et al. 2009). The interaction mode between V2Rs and the cognate ligands resembles that of glutamate receptors and taste receptors, each of which possesses a binding site within the long extracellular N-terminal domain (Yoshinaga et al. 2013).

One family of V1R ligands constitutes sulfated steroids such as androgen, estrogen, pregnanolone, and glucocorticoid (Isogai et al. 2011). Some V1R neurons show high selectivity to only one type of sulfated steroid, whereas many other V1R neurons recognize several types of sulfated steroids, as was seen with ORs; these findings indicated that both broadly and narrowly tuned V1Rs exist in the repertoire (Meeks et al. 2010; Nodari et al. 2008). Among these, several steroid ligand–V1R pairs have so far been suggested (Isogai et al. 2011). V1Rs may function in sensing not only sex information but also signature odors that represent the metabolic status of an individual. The specificity and selectivity of V2Rs appear to be higher than those of V1Rs. The characterization of function and structure of VRs will reveal the purposes for which animals have developed the vomeronasal system and why higher primate species have lost the organ.

2.3.3 Other Receptor Families and Olfactory Subsystems in Vertebrates

Approximately 15 years after the discovery of the conventional OR family, trace amine-associated receptors (TAARs), a family of 7TM receptors that may function as amine compound receptors in the brain, were demonstrated to be expressed in a subset of olfactory sensory neurons in the olfactory epithelium (Liberles and Buck 2006) (Fig. 2.2). Mice, humans, and zebrafish have 15, 6, and 109 TAARs, respectively. TAARs are receptors tuned to odorants with amino groups such as phenylethylamine, methyl piperidine, thyramine, or triethyl amine (Ferrero et al. 2012; Zhang et al. 2013). Taken together these findings indicate that

TAARs make up a second class of the OR family. These ligands signal the presence of dead animals or predators. TAARs, similar to conventional ORs, are expressed in olfactory sensory neurons in a mutually exclusive manner.

In addition to the olfactory and vomeronasal epithelium, there are other tissues or organs in the nasal cavity that express chemosensory receptors, including ORs, VRs, FPRs, and TAARs (Munger et al. 2009) (Fig. 2.2). The septal organ is located in the anteroventral part of the olfactory epithelium and expresses some ORs. The function of the septal organ is not clear, but it can recognize a variety of odorant molecules. The Grueneberg ganglion (GG) is located at the entrance of the nose of mammals and is an olfactory subsystem that appears to express various chemosensory receptors, including OR, VR, and TAAR. The GG may be involved in detection of alarm pheromones (Brechbuhl et al. 2013) and cold temperatures (Schmid et al. 2010).

2.3.4 Ligand-Gated Chemosensory Channels in Insects

Although insect ORs appear to comprise 7-TM-domain proteins, they do not share amino acid sequence homology with GPCRs or with vertebrate ORs, indicating that insect ORs are not GPCRs (Touhara and Vosshall 2009). Interestingly, the topology of the TMs in insect ORs was found to be opposite to that of a typical GPCR; specifically, the C-terminus of an insect OR is outside the cell and the N-terminus is intracellular, suggesting that insect ORs are atypical 7-TM receptors (Benton et al. 2006). The first indication that the insect OR may be a channel came from the work on silkmoth pheromone receptors; specifically, the coexpression of an OR and a conserved olfactory receptor coreceptor (Orco) resulted in a robust cation channel activity that was distinct from any known channels present in *Xenopus* oocytes (Nakagawa et al. 2005). Electrophysiological and pharmacological studies using heterologous cells demonstrated that the insect ORs indeed formed heteromeric ligand-gated cation channels (Sato et al. 2008; Wicher et al. 2008) and that both subunits contribute to the formation of channel pore structure (Nakagawa et al. 2012). There are 60–400 kinds of ORs in each insect species, suggesting that the insect OR complex comprises the largest cation channel family. In addition to the OR family of ion channels, another family of channels, called ionotropic receptors (IRs), also contributes to the sensing of various odorant molecules (Rytz et al. 2013). IRs are similar to ionotropic glutamate receptors, possess a 3-TM structure, and form a heterocomplex as OR–Orco (Abuin et al. 2011).

Assays for insect ORs or IRs are usually carried out either in HEK293 cells or in *Xenopus laevis* oocytes (Touhara and Vosshall 2009). The heterocomplex permeates various cations; therefore, calcium imaging or electrophysiology can be applied to monitor the responses to cognate ligands. The odorant-binding site of the OR complex resides in the OR side and not in the Orco (Nichols and Luetje 2010). The activity of insect OR channels are regulated by various nonodorous chemicals such as DEET, VUAA1, and cyclic nucleotides (Ditzen et al. 2008;

Jones et al. 2011; Nakagawa and Touhara 2013). The regulation of activity by various chemicals at multiple binding sites in the complex is a unique strategy that has emerged in the insect olfactory system. The 3D structure of the complex will reveal how similar the receptors are to other channels and how distinct they are from vertebrate ORs.

We do not know the origin of the odorant receptor channels in insects at this moment, but it is fair to say that insects have adapted to use ligand-gated channels to sense chemical cues from the external environment for some purposes. Two possible reasons for this evolutionary trajectory can be proposed. First, the response speed of a ligand-gated channel is much faster than that of a G protein-coupled receptor. This difference in kinetics may ensure that insects can quickly judge the direction in which they should fly or move. Second, ligand-gated channels do not require an energy cost, whereas ATP is required from GPCR-mediated signaling cascades, which may be advantageous for the event that occurs in the small intracellular environment of insect antennae. Of course, there are some drawbacks. For example, a ligand-gated channel cannot amplify a signal as a GPCR can. Thus, much higher density of receptors in the membrane is required for channels to give signals equivalent to GPCRs. In any case, insects have, during the course of evolution, acquired an olfactory sensing mechanism that is distinct from that in vertebrate species.

2.4 Behavioral or Physiological Responses

2.4.1 Intrinsic or Learned Behavior/Releasing or Priming Effects

Chemical signals sensed via the olfactory system elicit various behaviors and endocrinological changes and cause animals to respond to and adapt to environmental changes. Behaviors can be divided into two categories: intrinsic behaviors that occur without consciousness versus learned behaviors that are acquired by experience or learning. A good example is the mammary pheromone in rabbits; the mammary pheromone, 2-methyl-but-2-enal, in milk induces the opening of a pup's mouth, thereby promoting nipple attachment and subsequent suckling behavior (Schaal et al. 2003). This behavior is intrinsic, and pups never open their mouth to other odorants. However, if a mixture that contains the pheromone and a certain other odorant is applied several times to a pup, the pup becomes responsive to the other odorant without the pheromone (Coureaud et al. 2006). This is a learned behavior, which is distinguishable from the intrinsic pheromonal behavior. In mice, it has been reported that initiation of suckling is dependent on maternal signature odors that are learned and recognized before the first suckling (Logan et al. 2012). Conceivably, the neural circuitries underlying intrinsic and learned behaviors are quite different.

Table 2.1 Examples of ligand–receptor pairs and the corresponding behaviors

Species	Ligand	Receptor	Behavior	References
Silkmoth	Bombykol	BmOr1	Male attraction	Nakagawa et al. (2005)
Silkworm	*cis*-Jasmone	BmOr56[a]	Attraction	Tanaka et al. (2009)
Fly	cVA	DmOr67d	Aggregation, aggression, courtship	Kurtovic et al. (2007), Datta et al. (2008)
		DmOr65a	Aggression, courtship	Liu et al. (2011), Ejima et al. (2007)
Fly	PA	IR84a	Courtship	Grosjean et al. (2011)
Fly	Acid	IR64a	Avoidance	Ai et al. (2010)
Fly	Geosmin	DmOr56a	Avoidance	Stensmyr et al. (2012)
Mouse	ESP1	V2Rp5	Female sexual receptive behavior	Haga et al. (2010)
Mouse	MTMT	MOR244-3[a]	Female attraction	Duan et al. (2012)
Mouse	Z5:14-OH	Olfr288[a]	Female attraction	Yoshikawa et al. (2013)
Mouse	Amine	TAAR5	Avoidance	Dewan et al. (2013)

cVA cis-vaccenyl acetate, *PA* phenyl acetaldehyde, *ESP1* exocrine gland-secreting peptide, *MTMT* methanethiomethanthiol

[a]Relationship between receptor and behavior has not been proved

Although an odorant or pheromone induces various obvious behaviors such as avoidance or sexual attraction, the effects are not obvious as a specific behavior in many cases in mammalian species. Even without an obvious output, some endocrinological changes occur in the brain or inside the body, and such changes affect reproductive function or alter endocrine status to prepare for some subsequent stimuli. An obvious behavior is called a releasing effect because the effect is released as a phenotype, whereas the physiological or endocrinological effect is called a priming effect because the animal becomes primed for a subsequent and appropriately timed output. A canonical example of a releasing effect is the sexual behavior of silkmoths. The female sex pheromone, bombykol, itself releases the full sexual attractive behavior of male silkmoths. A canonical example of a priming effect is puberty acceleration of female mice, which is induced by urine from male mice, which is a prepared status for mating (Colby and Vandenberg 1974). In humans, most intrinsic olfactory or pheromonal effects are considered priming effects.

2.4.2 From Receptor to Behavior

Recent progress in identification of the specific receptors for various chemosignals has made it possible to analyze the neural circuitry responsible for behavioral outputs (Table 2.1). For example, in insects, bombykol is recognized by the specific receptor, BmOR1, and the signal is sent to the macroglomerular complex, which in turn regulates sexual behavior (Sakurai et al. 2004). *cis*-Jasmone released from mulberry leaves attracts silkworms via BmOR56 (Tanaka et al. 2009). cVA is recognized by Or67d and Or65a in fruit flies, and the signals are sent to the specific

glomeruli through which the sexually dimorphic behaviors are induced (Datta et al. 2008; Ejima et al. 2007; Kurtovic et al. 2007; Liu et al. 2011). DmOr56a is involved in innate aversion to geosmin, a microbial odorant (Stensmyr et al. 2012). IR64a and IR84a regulate avoidance and courtship behaviors, respectively (Ai et al. 2010; Grosjean et al. 2011). The attractive behavior of flies to apple cider vinegar is regulated by the specific OR-glomerulus line (Semmelhack and Wang 2009). DmGr21a and Gr63a together are sufficient for olfactory CO_2 chemosensation in *Drosophila* (Jones et al. 2007). These pathways appear to be labeled, and thus, if the target OR is replaced with another OR, the fly shows the same behavior to the cognate ligand of the replaced OR.

In mammals, not many pheromone–receptor pairs have been revealed. Currently, the most clear-cut pair is ESP1–V2Rp5 (Haga et al. 2010). The ESP1 signal, which is sent to the accessory olfactory bulb via V2Rp5, is further sent to the amygdala and ventromedial hypothalamus areas. The pheromone effect of ESP1, as well as the neural responses in those brain regions, is completely gone in V2Rp5 knockout mice, suggesting that the ESP1 signal is mediated by a single specific vomeronasal receptor, V2Rp5. This narrowly tuned sensing mechanism differs from the combinatorial coding scheme for general odorants.

In addition to the vomeronasal system, various behaviors are elicited through the main olfactory system. For example, MTMT and Z5-14:OH, which are included in mature male urine, attract female mice, although Z5-14:OH requires other urinary compound(s) for the activity. One of the ORs for MTMT is MOR244-3 (Duan et al. 2012), and the one for Z5-14:OH is Olfr288 (Yoshikawa et al. 2013). There appear to be a few additional ORs for these compounds. Olfactory sensory neurons expressing all these ORs project their axons to the ventral region in the olfactory bulb. Although it is different from the vomeronasal system, the behavioral output may be mediated by a few OR signals that are received by a specific region in the olfactory bulb (Kobayakawa et al. 2007). Similarly, muscone, an odorant that is used widely in cosmetic industries because of its fascinating animalic scent, appeared to be recognized by one or few ORs that include MOR215-1 and via a restricted region in the olfactory bulb (Shirasu et al. 2014). This rather specific neural pathway for odor perception was confirmed by a recent study; specifically, the removal of a single TAAR gene results in a deficit in the aversion of mice to predator odors (Dewan et al. 2013). Thus, the main olfactory system possesses both redundant and nonredundant signal recognition abilities to survive in the environment.

2.5 Future Questions to Be Solved

2.5.1 Evolution of Chemosensory Signaling Molecules

Chemical signals in the environment are structurally diverse. Many are small volatile organic compounds, but nonvolatile compounds such as peptides or proteins are also signals. As I described earlier, it seems that the period or distance for which a

compound can be conveyed through the open air space is the determinant of whether that compound is used as a food or predator signal, as a signature signal within the same species, or as a mating partner signal. Of course, many chemicals are neutral for any given species. Any physiologically important signal can be supposed to be a neutral signal for the species in the beginning, but at some point, the species starts to use the chemical, which was originally neutral, as a physiological signal. When this scenario happens within a single species, the chemical often becomes a pheromone. Thus, any compound in the environment has the potential to be used as a chemosensory signal for some species in some context. The question is how does one compound among myriad potential odorants become useful as an important odorant signal for individuals in the species. The selection process is supposed to be affected by (1) the environment in which the animals live, (2) the methods they utilize to communicate with each other, and (3) the lifestyle the animals lead. But for this complex scenario to occur, the corresponding receptor and the neural circuitry after the receptor activation have to be ready to send the information to the brain and elicit appropriate behavioral or endocrine outputs. How chemosensory signals, their receptors, and the neural network are coevolved is the next big question to be solved.

2.5.2 Odorant Dynamics and Kinetics

The sensitivity of an odorant or pheromone receptor is at most up to the nM–μM range, which is much larger than the concentration range of hormone–receptor or antigen–antibody interactions. Then, how can we explain the fact that the perceptional threshold concentration of some odorants such as mercaptan or isovaleric acid is as low as a part per thousand (ppt) level? Odorant molecules have to enter into and go through the olfactory mucous layer to access the receptor sites on olfactory neural cilia. Some physical or chemical mechanisms must exist for absorbing and concentrating odorants from the nasal cavity into the mucus to establish concentrations high enough to activate ORs. A binding protein hypothesis (Ko et al. 2010) is hard to accept kinetically because odorant signaling is much faster than the time that takes to bind to the protein and to be released from it before an odorant reaches the receptor site. Moreover, metal such as copper enhances the sensitivity of receptors that sense sulfuryl compounds dramatically, although this does not apply to all ORs (Duan et al. 2012). Another question is where does an odorant in the mucus go after it finishes activating a receptor? There are many metabolic enzymes in the olfactory mucus that are secreted from nasal and Bowman's glands or supporting cells. It has been proposed that odorants are degraded and therefore removed by the mucosal enzymes (Thiebaud et al. 2013). However, some of the enzymatic reactions in the mucus appear to be fast and to occur before odorants reach the receptor site, resulting in affecting the perception (Nagashima and Touhara 2010). Thus, it remains to be shown (1) how exactly odorants travel from the air space into a receptor-binding site to achieve a concentration high enough to activate the receptor and (2) what is the fate of an odorant after the mission of activating an OR is completed in the mucous layer.

2.5.3 Physiological Odorant Receptor Function

Since the discovery of the OR family, the functional analysis of ORs has revealed the molecular logic for odorant recognition and discrimination. This logic resembles a combinatorial coding model in which each odorant is recognized by multiple ORs and each OR in turn recognizes a set of structurally similar odorants. ORs are defined as either a broadly tuned receptor or a narrowly tuned receptor depending on how broad or specific the ligand spectrum is. However, this categorization is sometimes biased in two aspects. One aspect is that the odorant repertoire, which is utilized for structure–activity relationship studies of ORs, is not broad enough in terms of structural diversity, and in addition, the repertoire includes many odorants that do not exist at an amount to be sensed by the olfactory system in nature. Another aspect is that natural odorants in the environment where each species lives are quite distinct from the odorant repertoire to be used for screening ligands for ORs in the laboratory. Even though some ORs apparently recognize a wide spectrum of odorants in laboratory experiments and could therefore be called broadly tuned receptors, only one naturally occurring ligand may exist for that OR and the structures of the natural ligand could be totally different from those of the synthetic ligands, and thus, the receptor should actually be categorized as a narrowly tuned receptor. Three examples of natural ligand–receptor pairs have been reported: Z5:14-OH-Olfr288 (Yoshikawa et al. 2013), MTMT-MOR244-3 (Duan et al. 2012), and OR37-C14–C18 aldehydes (Bautze et al. 2012). Olfr288 appears to recognize a broad range of lactone compounds and aliphatic alcohols in laboratory experiments but is actually narrowly tuned to Z5:14-OH in a natural environment. The most important task ahead in the field of OR function is the construction of a complete physiological matrix of ligand-by-OR pairs that are used as chemical communication between mice in nature. Such a matrix could reveal the function of each mouse OR in a physiological context.

2.5.4 Development of Sensory Circuitry to Behavior

Response specificity between species and sexual dimorphism of behavior between conspecifics are presumed to be determined by differences at the level of molecules, receptors, and neural circuitry. The most extreme case is found in the insect pheromone world. The composition of pheromone molecules is slightly different even between closely related species; the difference is discriminated by the receptors, and this discrimination establishes reproductive isolation. Sex pheromone receptors in moths usually exhibit sex-biased expression to ensure that the signal is received by the opposite sex. In mammals, regulation at the level of the receptor is not that strict, as there is no bias in expression of sex pheromone receptors. Rather, mammals establish sexual dimorphism in the brain that is constructed depending on sex hormones. How this specific neural circuitry is established is currently unknown. Furthermore, we do not know how many receptors are necessary to be activated to

elicit a certain behavior. In the case of pheromones, activation of one specific receptor is often enough to induce a behavior. However, predator signals often activate multiple receptors to elicit avoidance behavior, but we do not know whether activation of one among such a group of receptors is enough or whether the activation pattern is important. Recent evidence of a TAAR-mediated nonredundant signal supports the former hypothesis (Dewan et al. 2013). A future question to be solved is how the sensory circuitry from receptor to brain is constructed to respond to various external signals that are crucial for the survival of individuals.

2.6 Conclusions

In the past decade or so, the base of knowledge about chemosensory signals, receptors, olfactory neural network, and behavioral outputs has grown rapidly. The molecular logic that mediates recognition and discrimination of chemosensory signals has been revealed. Nevertheless, chemosensory signals are diverse and their functions differ between species; therefore, a comprehensive dogma of olfaction had not been adopted. Moreover, as is obvious with the molecular evolution of chemosensory receptor genes, the whole olfactory system is changing quickly and this change occurs at every level of olfaction: the signal, the receptor, and the neural circuitry. Therefore, olfactory systems develop and evolve to accomplish different purposes for different organisms that depend on where and how the respective organisms live. We humans use olfaction for more sophisticated purposes, such as appreciating deliciousness when eating and sniffing aromas to relax. Deciphering the molecular and neural mechanisms that determine how olfactory input affects emotion and desire will definitely help understand how we sense and respond to our external environments and how we are different from other animals. Each of these advances in understanding will be important for eventually solving myriad human social diseases and improving the quality of life.

Note Added in Proof The recently published book, Pheromone Signaling: Methods and Protocols (Springer, 2013), covers a wide spectrum of experimental approaches utilized in the area of pheromone research.

Acknowledgments This work was supported in part by grants from MEXT, JSPS, and the JST ERATO project in Japan. I thank current and past Touhara laboratory members for critical reading of the manuscript.

References

Abuin L, Bargeton B, Ulbrich MH, Isacoff EY, Kellenberger S, Benton R (2011) Functional architecture of olfactory ionotropic glutamate receptors. Neuron 69:44–60

Ai M, Min S, Grosjean Y, Leblanc C, Bell R, Benton R, Suh GS (2010) Acid sensing by the *Drosophila* olfactory system. Nature (Lond) 468:691–695

Amoore JE (1963) Stereochemical theory of olfaction. Nature (Lond) 198:271–272

Bautze V, Bar R, Fissler B, Trapp M, Schmidt D, Beifuss U, Bufe B, Zufall F, Breer H, Strotmann J (2012) Mammalian-specific OR37 receptors are differentially activated by distinct odorous fatty aldehydes. Chem Senses 37:479–493

Benton R, Sachse S, Michnick SW, Vosshall LB (2006) Atypical membrane topology and heteromeric function of *Drosophila* odorant receptors in vivo. PLoS Biol 4:e20

Brechbuhl J, Moine F, Klaey M, Nenniger-Tosato M, Hurni N, Sporkert F, Giroud C, Broillet MC (2013) Mouse alarm pheromone shares structural similarity with predator scents. Proc Natl Acad Sci USA 110:4762–4767

Buck L, Axel R (1991) A novel multigene family may encode odorant receptors: a molecular basis for odor recognition. Cell 65:175–187

Caron SJ, Ruta V, Abbott LF, Axel R (2013) Random convergence of olfactory inputs in the *Drosophila* mushroom body. Nature (Lond) 497:113–117

Colby DR, Vandenberg JG (1974) Regulatory effects of urinary pheromones on puberty in the mouse. Biol Reprod 11:268–279

Coureaud G, Moncomble AS, Montigny D, Dewas M, Perrier G, Schaal B (2006) A pheromone that rapidly promotes learning in the newborn. Curr Biol 16:1956–1961

Datta SR, Vasconcelos ML, Ruta V, Luo S, Wong A, Demir E, Flores J, Balonze K, Dickson BJ, Axel R (2008) The *Drosophila* pheromone cVA activates a sexually dimorphic neural circuit. Nature (Lond) 452:473–477

Dewan A, Pacifico R, Zhan R, Rinberg D, Bozza T (2013) Non-redundant coding of aversive odours in the main olfactory pathway. Nature (Lond) 497:486–489

Dey S, Matsunami H (2011) Calreticulin chaperones regulate functional expression of vomeronasal type 2 pheromone receptors. Proc Natl Acad Sci USA 108:16651–16656

Ditzen M, Pellegrino M, Vosshall LB (2008) Insect odorant receptors are molecular targets of the insect repellent DEET. Science 319:1838–1842

Duan X, Block E, Li Z, Connelly T, Zhang J, Huang Z, Su X, Pan Y, Wu L, Chi Q et al (2012) Crucial role of copper in detection of metal-coordinating odorants. Proc Natl Acad Sci USA 109:3492–3497

Dulac C, Torello AT (2003) Molecular detection of pheromone signals in mammals: from genes to behaviour. Nat Rev Neurosci 4:551–562

Ejima A, Smith BP, Lucas C, van der Goes van Naters W, Miller CJ, Carlson JR, Levine JD, Griffith LC (2007) Generalization of courtship learning in *Drosophila* is mediated by *cis*-vaccenyl acetate. Curr Biol 17:599–605

Ferrero DM, Wacker D, Roque MA, Baldwin MW, Stevens RC, Liberles SD (2012) Agonists for 13 trace amine-associated receptors provide insight into the molecular basis of odor selectivity. ACS Chem Biol 7:1184–1189

Grosjean Y, Rytz R, Farine JP, Abuin L, Cortot J, Jefferis GS, Benton R (2011) An olfactory receptor for food-derived odours promotes male courtship in *Drosophila*. Nature (Lond) 478:236–240

Haga S, Hattori T, Sato T, Sato K, Matsuda S, Kobayakawa R, Sakano H, Yoshihara Y, Kikusui T, Touhara K (2010) The male mouse pheromone ESP1 enhances female sexual receptive behaviour through a specific vomeronasal receptor. Nature (Lond) 466:118–122

Isogai Y, Si S, Pont-Lezica L, Tan T, Kapoor V, Murthy VN, Dulac C (2011) Molecular organization of vomeronasal chemoreception. Nature (Lond) 478:241–245

Jones WD, Cayirlioglu P, Kadow IG, Vosshall LB (2007) Two chemosensory receptors together mediate carbon dioxide detection in *Drosophila*. Nature (Lond) 445:86–90

Jones PL, Pask GM, Rinker DC, Zwiebel LJ (2011) Functional agonism of insect odorant receptor ion channels. Proc Natl Acad Sci USA 108:8821–8825

Karlson P, Luscher M (1959) Pheromones: a new term for a class of biologically active substances. Nature (Lond) 183:55–56

Katada S, Hirokawa T, Oka Y, Suwa M, Touhara K (2005) Structural basis for a broad but selective ligand spectrum of a mouse olfactory receptor: mapping the odorant-binding site. J Neurosci 25:1806–1815

Kato A, Touhara K (2009) Mammalian olfactory receptors: pharmacology, G protein coupling and desensitization. Cell Mol Life Sci 66:3743–3753

Kato A, Katada S, Touhara K (2008) Amino acids involved in conformational dynamics and G protein coupling of an odorant receptor: targeting gain-of-function mutation. J Neurochem 107:1261–1270

Ko HJ, Lee SH, Oh EH, Park TH (2010) Specificity of odorant-binding proteins: a factor influencing the sensitivity of olfactory receptor-based biosensors. Bioprocess Biosyst Eng 33:55–62

Kobayakawa K, Kobayakawa R, Matsumoto H, Oka Y, Imai T, Ikawa M, Okabe M, Ikeda T, Itohara S, Kikusui T et al (2007) Innate versus learned odour processing in the mouse olfactory bulb. Nature (Lond) 450:503–508

Kurtovic A, Widmer A, Dickson BJ (2007) A single class of olfactory neurons mediates behavioural responses to a *Drosophila* sex pheromone. Nature (Lond) 446:542–546

Leinders-Zufall T, Ishii T, Mombaerts P, Zufall F, Boehm T (2009) Structural requirements for the activation of vomeronasal sensory neurons by MHC peptides. Nat Neurosci 12:1551–1558

Liberles SD, Buck LB (2006) A second class of chemosensory receptors in the olfactory epithelium. Nature (Lond) 442:645–650

Liberles SD, Horowitz LF, Kuang D, Contos JJ, Wilson KL, Siltberg-Liberles J, Liberles DA, Buck LB (2009) Formyl peptide receptors are candidate chemosensory receptors in the vomeronasal organ. Proc Natl Acad Sci USA 106:9842–9847

Liu W, Liang X, Gong J, Yang Z, Zhang YH, Zhang JX, Rao Y (2011) Social regulation of aggression by pheromonal activation of Or65a olfactory neurons in *Drosophila*. Nat Neurosci 14:896–902

Logan DW, Brunet LJ, Webb WR, Cutforth T, Ngai J, Stowers L (2012) Learned recognition of maternal signature odors mediates the first suckling episode in mice. Curr Biol 22:1998–2007

Lucretius (1995) On the nature of things: De rerum natura. (Anthony M. Esolen, transl.) The Johns Hopkins University, Baltimore)

Meeks JP, Arnson HA, Holy TE (2010) Representation and transformation of sensory information in the mouse accessory olfactory system. Nat Neurosci 13:723–730

Mori K, Sakano H (2011) How is the olfactory map formed and interpreted in the mammalian brain? Annu Rev Neurosci 34:467–499

Munger SD, Leinders-Zufall T, Zufall F (2009) Subsystem organization of the mammalian sense of smell. Annu Rev Physiol 71:115–140

Nagashima A, Touhara K (2010) Enzymatic conversion of odorants in nasal mucus affects olfactory glomerular activation patterns and odor perception. J Neurosci 30:16391–16398

Nakagawa T, Touhara K (2013) Extracellular modulation of the silkmoth sex pheromone receptor activity by cyclic nucleotides. PLoS One 8:e63774

Nakagawa T, Sakurai T, Nishioka T, Touhara K (2005) Insect sex-pheromone signals mediated by specific combinations of olfactory receptors. Science 307:1638–1642

Nakagawa T, Pellegrino M, Sato K, Vosshall LB, Touhara K (2012) Amino acid residues contributing to function of the heteromeric insect olfactory receptor complex. PLoS One 7:e32372

Nara K, Saraiva LR, Ye X, Buck LB (2011) A large-scale analysis of odor coding in the olfactory epithelium. J Neurosci 31:9179–9191

Nei M, Niimura Y, Nozawa M (2008) The evolution of animal chemosensory receptor gene repertoires: roles of chance and necessity. Nat Rev Genet 9:951–963

Nichols AS, Luetje CW (2010) Transmembrane segment 3 of *Drosophila melanogaster* odorant receptor subunit 85b contributes to ligand–receptor interactions. J Biol Chem 285:11854–11862

Niimura Y (2009) On the origin and evolution of vertebrate olfactory receptor genes: comparative genome analysis among 23 chordate species. Genome Biol Evol 1:34–44

Nodari F, Hsu FF, Fu X, Holekamp TF, Kao LF, Turk J, Holy TE (2008) Sulfated steroids as natural ligands of mouse pheromone-sensing neurons. J Neurosci 28:6407–6418

Rasmussen LE, Schulte BA (1998) Chemical signals in the reproduction of Asian (*Elephas maximus*) and African (*Loxodonta africana*) elephants. Anim Reprod Sci 53:19–34

Rasmussen SG, DeVree BT, Zou Y, Kruse AC, Chung KY, Kobilka TS, Thian FS, Chae PS, Pardon E, Calinski D et al (2011) Crystal structure of the beta2 adrenergic receptor–Gs protein complex. Nature (Lond) 477:549–555

Riviere S, Challet L, Fluegge D, Spehr M, Rodriguez I (2009) Formyl peptide receptor-like proteins are a novel family of vomeronasal chemosensors. Nature (Lond) 459:574–577

Rytz R, Croset V, Benton R (2013) Ionotropic receptors (IRs): chemosensory ionotropic glutamate receptors in *Drosophila* and beyond. Insect Biochem Mol Biol 43:888–897

Saito H, Chi Q, Zhuang H, Matsunami H, Mainland JD (2009) Odor coding by a mammalian receptor repertoire. Sci Signal 2:ra9

Sakurai T, Nakagawa T, Mitsuno H, Mori H, Endo Y, Tanoue S, Yasukochi Y, Touhara K, Nishioka T (2004) Identification and functional characterization of a sex pheromone receptor in the silkmoth *Bombyx mori*. Proc Natl Acad Sci USA 101:16653–16658

Sato K, Pellegrino M, Nakagawa T, Vosshall LB, Touhara K (2008) Insect olfactory receptors are heteromeric ligand-gated ion channels. Nature (Lond) 452:1002–1006

Schaal B, Coureaud G, Langlois D, Ginies C, Semon E, Perrier G (2003) Chemical and behavioural characterization of the rabbit mammary pheromone. Nature (Lond) 424:68–72

Schmid A, Pyrski M, Biel M, Leinders-Zufall T, Zufall F (2010) Grueneberg ganglion neurons are finely tuned cold sensors. J Neurosci 30:7563–7568

Semmelhack JL, Wang JW (2009) Select *Drosophila* glomeruli mediate innate olfactory attraction and aversion. Nature (Lond) 459:218–223

Shirasu M, Touhara K (2011) The scent of disease: volatile organic compounds of the human body related to disease and disorder. J Biochem (Tokyo) 150:257–266

Shirasu M, Yoshikawa K, Takai Y, Nakashima A, Takeuchi H, Sakano H, Touhara K (2014) Olfactory receptor and neural pathway responsible for highly selective sensing of musk odors. Neuron 81:165–178

Sosulski DL, Bloom ML, Cutforth T, Axel R, Datta SR (2011) Distinct representations of olfactory information in different cortical centres. Nature (Lond) 472:213–216

Stensmyr MC, Dweck HK, Farhan A, Ibba I, Strutz A, Mukunda L, Linz J, Grabe V, Steck K, Lavista-Llanos S et al (2012) A conserved dedicated olfactory circuit for detecting harmful microbes in *Drosophila*. Cell 151:1345–1357

Tanaka K, Uda Y, Ono Y, Nakagawa T, Suwa M, Yamaoka R, Touhara K (2009) Highly selective tuning of a silkworm olfactory receptor to a key mulberry leaf volatile. Curr Biol 19:881–890

Thiebaud N, Veloso Da Silva S, Jakob I, Sicard G, Chevalier J, Menetrier F, Berdeaux O, Artur Y, Heydel JM, Le Bon AM (2013) Odorant metabolism catalyzed by olfactory mucosal enzymes influences peripheral olfactory responses in rats. PLoS One 8:e59547

Touhara K (2007) Deorphanizing vertebrate olfactory receptors: recent advances in odorant-response assays. Neurochem Int 51:132–139

Touhara K (2008) Sexual communication via peptide and protein pheromones. Curr Opin Pharmacol 8:759–764

Touhara K, Vosshall LB (2009) Sensing odorants and pheromones with chemosensory receptors. Annu Rev Physiol 71:307–332

Wicher D, Schafer R, Bauernfeind R, Stensmyr MC, Heller R, Heinemann SH, Hansson BS (2008) *Drosophila* odorant receptors are both ligand-gated and cyclic-nucleotide-activated cation channels. Nature (Lond) 452:1007–1011

Wyatt TD (2003) Pheromones and animal behavior: communication by smell and taste. Oxford University Press, Oxford

Wyatt TD (2010) Pheromones and signature mixtures: defining species-wide signals and variable cues for identity in both invertebrates and vertebrates. J Comp Physiol A Neuroethol Sens Neural Behav Physiol 196:685–700

Yamazaki K, Beauchamp GK, Singer A, Bard J, Boyse EA (1999) Odortypes: their origin and composition. Proc Natl Acad Sci USA 96:1522–1525

Yoshikawa K, Nakagawa H, Mori N, Watanabe H, Touhara K (2013) An unsaturated aliphatic alcohol as a natural ligand for a mouse odorant receptor. Nat Chem Biol 9:160–162

Yoshinaga S, Sato T, Hirakane M, Esaki K, Hamaguchi T, Haga-Yamanaka S, Tsunoda M, Kimoto H, Shimada I, Touhara K et al (2013) Structure of the mouse sex peptide pheromone ESP1 reveals a molecular basis for specific binding to the class-C G-protein-coupled vomeronasal receptor. J Biol Chem 288:16064–16072

Zhang J, Pacifico R, Cawley D, Feinstein P, Bozza T (2013) Ultrasensitive detection of amines by a trace amine-associated receptor. J Neurosci 33:3228–3239

Chapter 3
Olfactory Map Formation in the Mouse

Hitoshi Sakano

Abstract In the mouse olfactory system, each olfactory sensory neuron (OSN) expresses only one functional odorant receptor (OR) species. Furthermore, OSN axons bearing the same OR converge to a specific projection site in the olfactory bulb (OB), forming a glomerular structure. Based on these two basic principles, odor information detected in the olfactory epithelium is converted to a topographic map of activated glomeruli in the OB. During embryonic development, the olfactory map is formed by the combination of two genetically programmed processes. One is OR-dependent projection along the anterior-posterior axis, and the other is OR-independent projection along the dorsal-ventral axis. The map is further refined in an activity-dependent manner during the neonatal period. Here, we discuss a recent progress of neural map formation in the mouse olfactory system.

Keywords Axonal projection • Baseline activity • cAMP • Glomerular map • GPCR • Odorant receptors • Olfactory neurons

3.1 Introduction

In the mouse olfactory system, odorants are detected with approximately 1,000 different odorant receptor (OR) species expressed in the cilia of olfactory sensory neurons (OSNs) (Buck and Axel 1991). Each OSN in the olfactory epithelium (OE) expresses only one functional OR gene in a mutually exclusive and monoallelic manner (Serizawa et al. 2004). Furthermore, OSNs expressing the same OR

H. Sakano (✉)
Department of Brain Function, School of Medicine, University of Fukui, 23-3 Shimo-aizuki, Matsuoka, Fukui 910-1193, Japan

Department of Biophysics and Biochemistry, Graduate School of Science, University of Tokyo, 2-11-16 Yayoi, Bunkyo-ku, Tokyo 113-0032, Japan
e-mail: sakano@mail.ecc.u-tokyo.ac.jp

K. Mori (ed.), *The Olfactory System: From Odor Molecules to Motivational Behaviors*,
DOI 10.1007/978-4-431-54376-3_3,

species converge their axons to a specific location in the OB, forming a glomerular structure (Mombaerts et al. 1996) (Fig. 3.1a, b). Because a given OR responds to multiple odorants and a given odorant activates multiple OR species (Malnic et al. 1999), the odor information detected in the OE is topographically represented as the pattern of activated glomeruli in the OB (Mori and Sakano 2011) (Fig. 3.1c).

A remarkable feature of axonal projection in the mouse olfactory system is that ORs play an instructive role in projecting OSN axons to the OB. For dorsal-ventral (dorsoventral, D-V) projection, anatomical location of OSN cells within the OE regulates both OR gene choice and expression levels of axon guidance molecules, for example, Neuropilin-2 (Nrp2) and Semaphorin-3F (Sema3F), thus indirectly correlating the OR identity to the glomerular location along the D-V axis (Miyamichi et al. 2005; Takeuchi et al. 2010) (Fig. 3.2a, left). However, anterior-posterior (anteroposterior, A-P) projection is totally independent of the positional information of OSN cells, but instead dependent on the expressed OR species (Fig. 3.2a, right). We have previously reported that A-P targeting is regulated by OR-derived cAMP signals (Imai et al. 2006). In the OB, A-P projection molecules such as Neuropilin-1 (Nrp1) and Plexin-A1 (PlxnA1) are detected on axon termini of OSNs, forming a complementary gradient along the A-P axis (Imai and Sakano 2008).

OR-derived cAMP signals also regulate the expression of glomerular segregation molecules (e.g., Kirrel2 and Kirrel3) for map refinement through local sorting of OSN axons (Serizawa et al. 2006) (Fig. 3.2b). In contrast to A-P projection molecules, glomerular segregation molecules show mosaic distribution in the glomerular map. A naris occlusion experiment indicated that stimulus-driven neuronal activity contributes to the local sorting of OSN axons, but not to global targeting along the A-P axis (Nakashima et al. 2013).

How is it, then, that global A-P targeting and local sorting are differentially regulated by the expressed OR molecules? What are the sources of the cAMP signals, and how are the signals generated? Here, we discuss recent progress of neural map formation in the mouse olfactory system.

3.2 Axonal Projection Along the D-V Axis

For OSN projection along the D-V axis, there is a close correlation between the anatomical locations of OSNs in the OE and their axonal projection sites in the OB (Astic et al. 1987). The preservation of the spatial relationship of neuronal cell bodies and their projection sites is widely seen in other brain regions, including the visual system (McLaughlin and O'Leary 2005; Luo and Flanagan 2007; Petersen 2007). In the mouse olfactory system, two sets of repulsive signaling molecules, Nrp2/Sema3F and Robo2/Slit1, have been reported to participate in D-V projection (Walz et al. 2002; Cho et al. 2007; Cloutier et al. 2002) (Fig. 3.3, left). D-zone axons expressing a guidance receptor, Robo2, navigate to the D domain of the OB through the repulsive effects of the Slit ligands expressed in the V domain of the OB

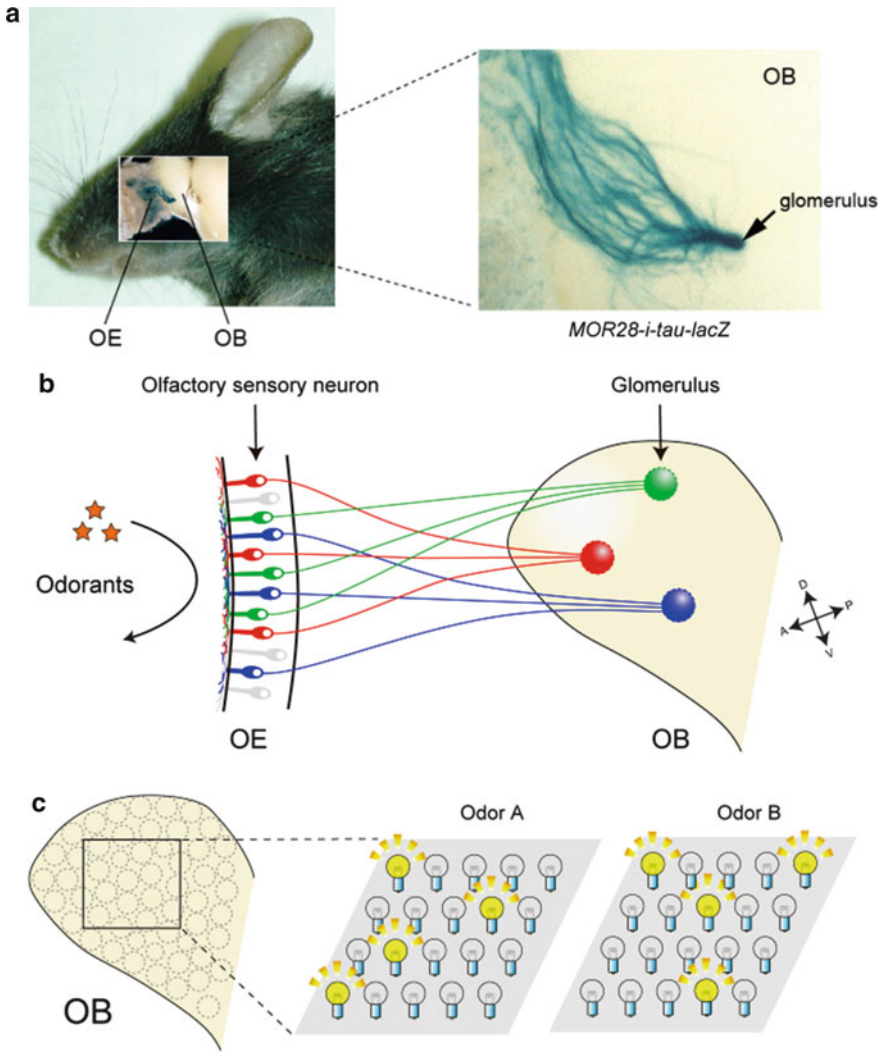

Fig. 3.1 The mouse olfactory system. (**a**) Projection and convergence of olfactory sensory neuron (OSN) axons. MOR28-expressing OSN axons are shown in *blue*, stained with X-gal in the transgenic mouse, MOR28-ires-tau-lacZ. OSNs expressing the *MOR28* transgene converge their axons to a specific glomerulus in the olfactory bulb (OB) (*arrow*). (**b**) In the olfactory epithelium (*OE*), each OSN expresses only one functional *OR* gene in a mono-allelic manner. Furthermore, OSN axons expressing the same OR species target to a specific site in the OB, forming a glomerular structure. (**c**) Odor signals received in the OE are converted to a topographic map of activated glomeruli in the OB. *OE* olfactory epithelium, *OB* olfactory bulb, *D* dorsal, *V* ventral, *A* anterior, *P* posterior

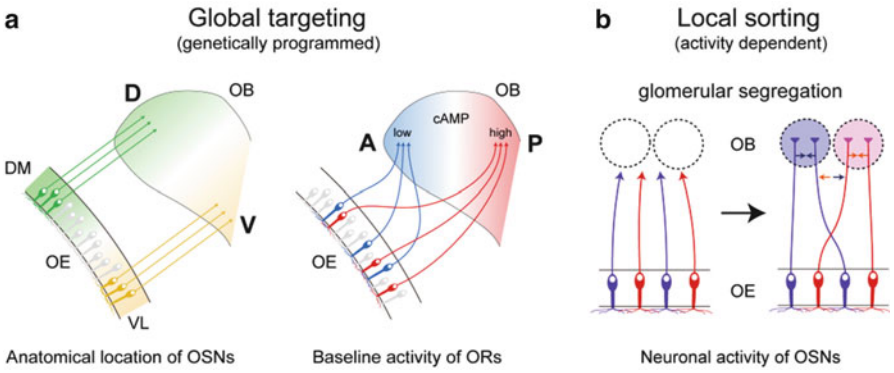

Fig. 3.2 Global targeting and local sorting of OSN axons. (**a**) OSN axons are guided to approximate destinations in the OB by a combination of D-V patterning and A-P patterning. D-V projection is regulated by the anatomical locations of OSNs within the OE. A-P projection is achieved through cAMP signals induced by OR baseline activities. These processes, forming a coarse map topography, are genetically programmed and are independent of neuronal activity. (**b**) During the neonatal period, the map is further refined in an activity-dependent manner. Glomerular segregation occurs via adhesive and repulsive interactions of neighboring axons. *DM* dorsomedial, *VL* ventrolateral, *D* dorsal, *V* ventral, *A* anterior, *P* posterior, *OE* olfactory epithelium, *OB* olfactory bulb

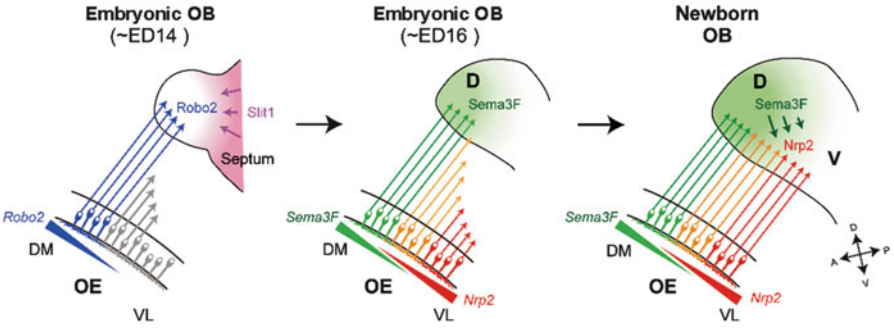

Fig. 3.3 OSN projection along the D-V axis. In the OE, D-zone OSNs mature first and extend their axons to the OB. These axons express Robo2 and project to the embryonic OB with the aid of repulsive interactions with Slit1 (*left*). Axonal extension of OSNs occurs sequentially along the DM-VL axis of the OE as the OB grows ventrally during embryonic development. In OSNs, an axon guidance receptor, Nrp2, and its repulsive ligand, Sema3F, are expressed in a complementary and graded manner. Sema3F is secreted in the anterodorsal region of the OB by early-arriving D-zone axons (*middle*). Sequential projection of OSN axons helps to establish the topographic order along the D-V axis. Sema3F secreted by the D-zone axons in the OB prevents the late-arriving $Nrp2^{+}$ axons from invading the dorsal region of the OB (*right*) (Takeuchi et al. 2010). *DM* dorsomedial, *VL* ventrolateral, *D* dorsal, *V* ventral, *A* anterior, *P* posterior, *ED* embryonic day

(Cho et al. 2007). These molecules are assumed to contribute to the separation of D and V domains (Takeuchi et al. 2010; Cho et al. 2007). Vertebrate OR genes are phylogenetically divided into two distinct classes: class I and class II. Class I ORs, known as fish-type receptors, are expressed exclusively in the D zone of the OE, and OSNs expressing them project their axons to the most anterodorsal area in the OB (Zhang et al. 2004; Tsuboi et al. 1999). In addition to the class I ORs, approximately 300 class II ORs are also expressed in the same D zone, but their corresponding glomeruli reside on the periphery of the class I area in the OB (Miyamichi et al. 2005). The remaining class II ORs are expressed in the V zone, and their glomeruli are found in the ventrolateral area in the OB. Thus, the glomerular map seems to be subdivided into three compartments along the D-V axis in the OB: a dorsal domain for class I ORs (D_I), a surrounding domain for class II ORs (D_{II} domain), and a ventral domain for class II ORs (V domain) (Kobayakawa et al. 2007; Bozza et al. 2009). More recently, D-zone OSNs expressing trace amine-associated receptors (TAARs) were found to form a group of glomeruli on the boundary of D_I and D_{II} domains in the OB (Pacifico et al. 2012).

In situ hybridization and a high-throughout microarray analysis demonstrated that most class I OR genes were D zone specific (Zhang et al. 2004; Tsuboi et al. 1999). Class I ORs originally identified in fish (Ngai et al. 1993) represent the ancient group in the OR repertoire. Class I ORs in fish bind nonvolatile odorants such as amino acids, whereas class II ORs are specialized to recognize airborne odorants. It is possible that the ancestral class I OR genes evolved independently of the class II OR genes, and that both the expression zone in the OE and the projection zone in the OB were conserved during evolution.

3.3 Projection of V-Zone Axons to the Ventral OB

Although OR genes expressed by OSNs that project to the D domain of the OB are distributed throughout the D zone (Tsuboi et al. 1999), V-zone-specific OR genes exhibit spatially limited expression in the OE. Each OR gene possesses its unique expression area, which is distributed in an overlapping and continuous manner along the dorsomedial–ventrolateral (DM-VL) axis of the OE. The relative order of OR expression areas is very well correlated with the order of corresponding glomeruli along the D-V axis in the OB (Miyamichi et al. 2005). How is this positional information of neurons translated to their target sites during olfactory map formation? Nrp2 is expressed on OSN axons in such a way to form a gradient in the OB along the D-V axis. Loss-of-function and gain-of-function experiments demonstrated that Nrp2 indeed regulates the axonal projection of OSNs along the D-V axis (Takeuchi et al. 2010). In the analogy of the visual system, the repulsive ligand, Sema3F, was initially expected to be produced by the cells in the target OB. Curiously, however, *Sema3F* transcripts were detected in the OE but not in the OB. Knockout (KO) mice in which Sema3F expression was specifically blocked in OSNs showed mistargeting of $Nrp2^+$ axons along the D-V axis (Takeuchi

et al. 2010). These findings indicate that, in the olfactory system, an axon guidance receptor, Nrp2, and its repulsive ligand, Sema3F, are both produced by OSNs and essential to the segregation of D-zone and V-zone axons.

Expression levels of D-V targeting molecules are closely correlated with the expressed OR species. However, the transcription of *Nrp2* and *Sema3F* is not downstream of OR signaling (Nakashima et al. 2013). It has been reported that OR gene choice is not purely stochastic along the DM-VL axis, but dependent upon anatomical location in the OE (Miyamichi et al. 2005). This idea was further supported by the experiment using transgenic mice in which the coding sequence of the *MOR28* gene is deleted and replaced by green fluorescent protein, GFP (Serizawa et al. 2003). In these mice, the choice of the secondary OR gene in GFP-positive OSNs was not random, and primarily limited to a group of OR genes whose expression areas and transcription levels of the Nrp2 are comparable to those of the coding-deleted OR gene. If D-V guidance molecules are not regulated by OR-derived signals, how are their expression levels determined and correlated with the expressed OR species? We speculate that both OR gene choice and Nrp2 expression levels are commonly regulated by positional information, and are likely determined by cell lineage resulting in the use of specific sets of transcription factors.

3.4 Sequential Projection of OSN Axons Along the D-V Axis

Complementary expression of Nrp2 and Sema3F genes in OSNs initially suggested that their repulsive interactions occur among OSN axons before they reach the target. This, however, is not the case because D-zone axons and V-zone axons are already segregated in separate axon bundles. This segregation in the trajectory of OSN axons was not noticeably affected by the OSN-specific Sema3F KO. Where and how, then, does Seama3F interact with $Nrp2^+$ OSN axons?

To study the developmental regulation of OSN projection, we analyzed the embryonic OE and OB for the expression of various axonal markers (Takeuchi et al. 2010). $Robo2^+$ D-zone OSNs were found to mature earlier than $Nrp2^+$ V-zone OSNs. Gap43 (a marker of growing axons) and olfactory marker protein (a marker of mature OSNs) first appear in the D-zone OSNs and demonstrate graded expression, DM-high and VL-low, in the embryonic OE. D-zone OSNs appear to mature earlier than V-zone OSNs. Axonal projection takes place in a sequential manner starting with the dorsal OB and expanding toward the ventral region (Takeuchi et al. 2010; Sullivan et al. 1995) (Fig. 3.3). These observations indicate an intriguing possibility that a repulsive ligand, Sema3F, secreted by early-arriving D-zone axons is deposited in the anterodorsal OB to serve as a guidance cue to repel late-arriving V-zone axons that express Nrp2 receptor (Takeuchi et al. 2010) (Fig. 3.3).

In addition, $Robo2^+$ D-zone axons are guided to the dorsal region of the OB by repulsive interactions with secreted ligands (Cho et al. 2007; Nguyen-Ba-Charvet

et al. 2008). One of the Robo2 ligands, Slit1, is detected in the septum and ventral OB during early developmental stages. In the KO for the Robo/Slit system, OSN axons mistarget to surrounding non-OB tissues (Nguyen-Ba-Charvet et al. 2008). Repulsive interactions between Robo2 and Slit1 appear to restrict the first wave of OSN projection to the anterodorsal OB (Fig. 3.3, left). During development, the glomerular map expands ventrally and the embryonic OB represents the prospective dorsal OB. Spatiotemporal regulation of axonal projection of OSNs aided by Robo2 and Slit1, and the graded expression of Nrp2 and Sema3F, contribute to establish the topographic order in the olfactory map along the D-V axis (Takeuchi et al. 2010).

3.5 Roles of Ensheathing Glial Cells in D-V Projection

As already described, two sets of axon guidance molecules, Nrp2/Sema3F and Robo2/Slit1, have important roles in D-V targeting of OSN axons. It has been shown that another set of repulsive-signaling molecules, Robo1 and Slits, are required for D-V targeting (Cho et al. 2007; Nguyen-Ba-Charvet et al. 2008). Interestingly, Robo1 is not produced by OSNs, but rather by olfactory ensheathing cells (OECs) (Nguyen-Ba-Charvet et al. 2008). Based on the results with mutant mice in which OSN projection is ablated, it was indicated that the OSN axons are associated with the Robo1$^+$ OECs. These observations suggest an intriguing possibility that the repulsive function of Robo1 is supplied to the dorsal OSN axons by associated OECs. It has been reported that glial cells have a number of supporting functions for neuronal cells and their axons, for example, supplying growth factors to neurons. However, it was not previously known that glial cells supply the repulsive function of axon guidance receptors to associated axons.

In the Robo1 KO, axon guidance/targeting is severely affected for D-zone OSNs, but not for V-zone OSNs (Nguyen-Ba-Charvet et al. 2008; Aoki et al. 2013); this probably occurs because Robo1$^+$ OECs are present in the lamia propria (LP) only when early-arriving D-zone axons go through the LP. Robo1$^+$ OECs are no longer found when late-arriving V-zone axons reach the LP (Aoki et al. 2013). Such temporal regulation of Robo1 expression may explain the differential effect of Robo1 KO on D- and V-zone OSN axons. What is the ligand for Robo1 and where is it expressed? It has been reported that Robo1 interacts with Slit1 in a repulsive manner in vitro (Nguyen-Ba-Charvet et al. 2008). We also found that Slit2 is expressed in the ventral region of the olfactory pit before ED11.5 (Aoki et al. 2013). At later stages on ED13.5 and 15.5, Slit1 is found in the septum and in the ventral region of the OB, respectively. We hypothesize that Slit2 in the ventral region of the olfactory pit and Slit1 in the septum are needed for the proper trajectory of dorsal OSN axons, and that Slit1 in the ventral OB plays a role in D-V targeting of OSN axons.

For D-V targeting, at least three sets of axon guidance receptors and ligands are involved. First, the repulsive function of Robo1 provided by associated glial cells is

essential to guide the dorsal OSN axons to the embryonic OB (Aoki et al. 2013). Next, Robo2 is needed to restrict the targeting of D-zone axons to the embryonic OB, and then, Nrp2 is required for establishing the topographic order along the D-V axis (Takeuchi et al. 2010).

3.6 OR-Instructed OSN Projection Along the A-P Axis

It is well established that each OSN expresses only one functional OR gene, regulated by a negative feedback mechanism (Serizawa et al. 2004). Furthermore, the olfactory map is composed of discrete glomeruli, each representing a single OR species (Mombaerts et al. 1996; Ressler et al. 1994; Vassar et al. 1994). The instructive role of the OR protein in OSN projection was demonstrated by the coding-swap and coding-deletion experiments of OR genes (Serizawa et al. 2003; Wang et al. 1998; Feinstein and Mombaerts 2004). Because OSNs expressing the same OR are scattered within the OE for A-P projection, topographic organization must occur during the process of axonal projection to the OB. In contrast to D-V projection, where relative positional information is preserved between the periphery and target, there is no such correlation for the projection along the A-P axis. Based on the observation that OR molecules are detected not only on cilia but also in axon termini of OSNs (Feinstein and Mombaerts 2004; Barnea et al. 2004; Strotmann et al. 2004), it was once thought that the OR protein itself may act as an axon guidance receptor detecting the target cues in the OB and also mediate homophilic interactions among "like" axons (Mombaerts 2006). Although these models were attractive, recent studies argue against them. Instead of directly acting as guidance receptors or axon-sorting molecules, ORs appear to regulate transcription levels of A-P targeting and glomerular segregation molecules by OR-derived cAMP signals (Imai et al. 2006). Supporting this idea, topographic map and glomerular formation in the OB are severely affected by the KO of adenylyl cyclase type III (ACIII) that is essential to cAMP production (Nakashima et al. 2013; Chesler et al. 2007; Col et al. 2007).

We found that axons expressing a mutant OR, I7 (RDY), that cannot activate G proteins, remained in the anterior region of the OB and failed to converge to a specific glomerulus (Imai et al. 2006). However, coexpression of a constitutively active G_s mutant restored axonal convergence and glomerular formation defects. Partial rescue was also observed with the constitutively active mutants of protein kinase, PKA, and a transcription factor, CREB. Thus, transcriptional regulation mediated by G_s and PKA is required for OSN projections. Furthermore, constitutively active G_s or dominant-negative PKA, when coexpressed with wild-type OR-I7, causes a posterior or anterior shift of I7 glomeruli, respectively (Imai et al. 2006). These findings suggest that the quantitative levels of OR-derived cAMP signals determine A-P positioning of glomeruli in the OB. OSNs producing high levels of cAMP project their axons to the posterior OB whereas those producing low levels target the anterior OB. When protein levels of Nrp1 were measured

in axon termini of OSNs within glomeruli, Nrp1 was found in an anterior-low/posterior-high gradient in the OB. Increases or decreases of Nrp1 expression in OSNs caused posterior or anterior glomerular shifts, respectively (Imai et al. 2009). Furthermore, the A-P topography of the glomerular map was perturbed in mice deficient for Nrp1 or Sema3A. These observations indicated that each OR species generates a unique level of cAMP signals that regulates expression of A-P targeting molecules, for example, Nrp1 and its repulsive ligand, Sema3A.

3.7 Pretarget Axon Sorting Within Bundles

How then do the guidance molecules regulate olfactory map formation? Interestingly, map order along the A-P axis emerges in axon bundles of OSNs, well before they reach the target. For neural map formation, Sperry (1963) proposed the "chemoaffinity model" in 1963, in which target cells present chemical cues to guide axons to their destination. Since then, it has been thought that the topography of the neural map is determined by interactions between guidance receptors expressed at axon termini and positional cues present on the target (Fig. 3.4, left). However, OSN axons projecting to distinct destinations are presorted in the axon bundle before arrival at the OB (Imai et al. 2009; Satoda et al. 1995).

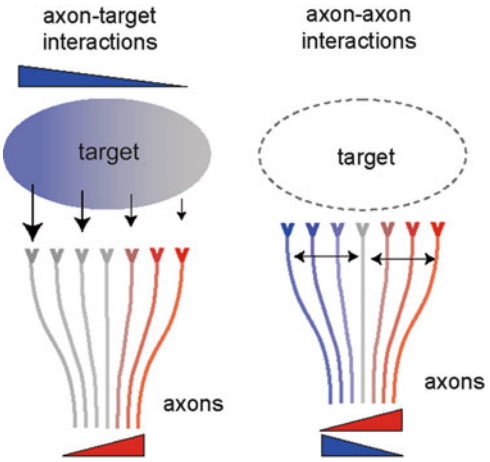

Fig. 3.4 Axon–target versus axon–axon interactions in neural map formation. Preservation of the relative spatial relationships of projecting axons between origin and target sites is a general feature of neural map formation. In the vertebrate visual system, graded expression of Eph receptors on retinal axons and their repulsive ligands, ephrins, from the superior colliculus regulates axonal projection of retinal ganglion cells (*left*). In the mouse olfactory system, topographic order emerges in axon bundles well before they reach the target, suggesting pretarget axon–axon interactions. An axon guidance receptor, Nrp1, and its repulsive ligand, Sema3A, are both expressed by OSNs in the OE in a complementary manner and mediate pretarget axon sorting within the bundles (*right*)

This observation suggests that pretarget mechanisms play important roles in the topographic map formation in the mouse olfactory system (Fig. 3.4). Indeed, A-P topography of OSN axons can be formed even in the *Gli3* mutant that completely lacks the OB (St John et al. 2003). We found that Nrp1 and Sema3A are both expressed in OSNs in a complementary manner. Within the axon bundles, Nrp1-low/Sema3A-high axons are sorted to the central compartment of the bundle, whereas Nrp1-high/Sema3A-low axons are confined to the outer-lateral compartment (Imai et al. 2009). OSN-specific KO of Nrp1 or Sema3A not only perturbed axon sorting within the bundle, but also caused an anterior shift of glomeruli in the OB (Imai et al. 2009). These results indicated that pretarget axon sorting within the bundle contributes to the establishment of topographic order along the A-P axis. Theoretically, however, axon–axon interactions alone cannot determine the axis of the map. Guidance cues on the target, as well as intermediary cues, may help orient the presorted axons to a correct orientation on the target.

3.8 Activity-Dependent Glomerular Segregation and Map Refinement

During embryonic development, a coarse map topography is established by a combination of D-V patterning and A-P patterning (Fig. 3.2a). However, neighboring glomerular structures are intermingled in the newborn animal, and discrete glomeruli emerge during the neonatal period. After OSN axons reach their approximate destinations in the OB, further refinement of the glomerular map needs to occur through fasciculation of axon termini in an activity-dependent manner (Serizawa et al. 2006) (Fig. 3.2b). To study how OR-specific axon sorting is controlled, we searched for a group of genes whose expression profiles correlate with the expressed OR species, and such genes were indeed identified (Fig. 3.5). The genes include those that code for homophilic adhesive molecules, such as Kirrel2 and Kirrel3 (Serizawa et al. 2006), which have an important role in the attraction of “like” axons. Repulsive signaling molecules, such as ephrinA and EphA receptors, are also expressed in a complementary and OR-specific manner in OSN axons. Therefore, interactions between two subsets of axons, one that is ephrinA-high/EphA-low and the other that is ephrinA-low/EphA-high, may be important for the segregation of “non-like” axons (Fig. 3.5). We assume that a specific set of adhesive and repulsive molecules, whose expression levels are determined by OR molecules, regulate the axonal fasciculation of OSNs for map refinement (Serizawa et al. 2006). It is not clear at this point how many sets of sorting molecules are involved in glomerular segregation. However, several sets of adhesion/repulsion molecules should be enough to segregate neighboring glomerular structures.

Differing from the global targeting of OSN axons during embryonic development, local sorting appears to occur in an activity-dependent manner in the neonatal animal. Blocking neuronal activity by the overexpression of an inward rectifying potassium channel, Kir2.1, severely affects glomerular segregation (Nakashima et al. 2013;

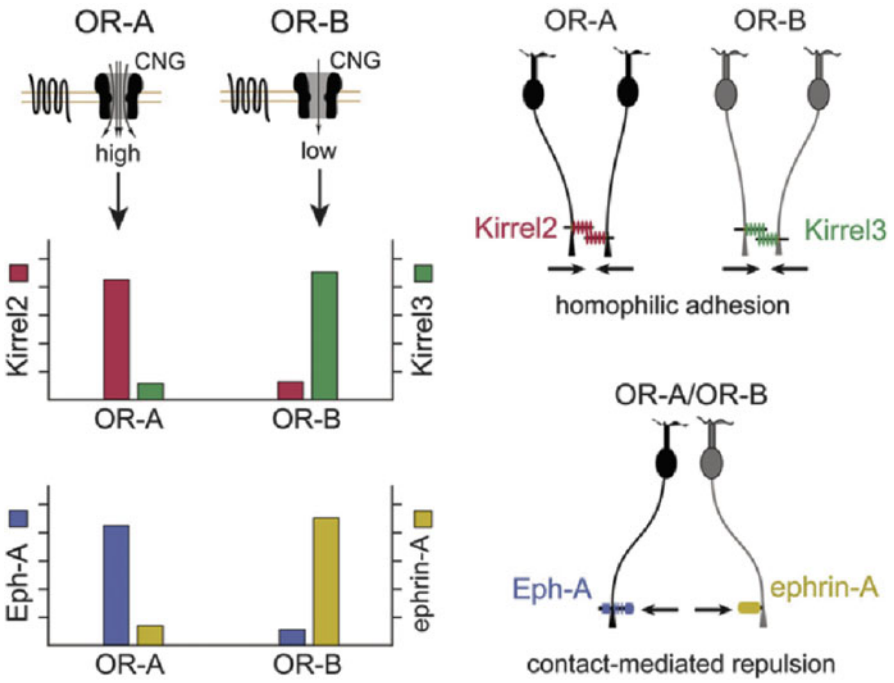

Fig. 3.5 Local sorting of OSN axons for glomerular segregation. OR-specific and activity-dependent expression of adhesion and repulsion molecules (*left*) (Serizawa et al. 2006). OSNs expressing activity-high OR-A would produce higher levels of Kirrel2 and EphA but lower levels of Kirrel3 and ephrin-A. In contrast, OSNs expressing activity-low OR-B would express higher levels of Kirrel3 and ephrin-A but lower levels of Kirrel2 and EphA. Schematic diagrams depict how Kirrel2, Kirrel3, EphA, and ephrin-A contribute to the OR-specific segregation of axon termini (*right*). OSNs expressing the same type of OR fasciculate their axons by homophilic adhesive interactions of Kirrel2 or Kirrel3. Axon termini of OSNs expressing different types of ORs are separated by the repulsive interaction between EphA and ephrin-A

Yu et al. 2004). Mice that are mosaic KO for CNGA2, a component of cyclic nucleotide-gated (CNG) channels, reveal segregation of CNGA2-positive and CNGA2-negative glomeruli for the same OR (Serizawa et al. 2006; Zheng et al. 2000). Interestingly, expression levels of glomerular segregation molecules were affected by unilateral naris occlusion. In the occluded naris, Kirrel2 expression was downregulated and Kirrel3 expression was upregulated, whereas expression of the A-P guidance receptors Nrp1 and PlxnA1 was not affected (Nakashima et al. 2013). These results indicate that stimulus-driven OR activity contributes to the local sorting of OSN axons but does not affect global targeting along the A-P axis.

We examined whether odorous stimuli can change the expression profile of glomerular segregation molecules (Nakashima et al. 2013). Transgenic mice in which the *MOR29B* gene is tagged with *IRES-gapEYFP* were housed in the presence of vanillin, a ligand for MOR29B. When the mice were exposed to vanillin, Kirrel2 expression was dramatically increased. Interestingly, however,

Nrp1 expression was not affected by vanillin exposure in the MOR29B-positive OSNs. These results indicate that the expression of glomerular segregation molecules is regulated by ligand-induced OR signals, whereas the expression of A-P-targeting molecules is likely to be driven by ligand-independent OR activity.

3.9 Agonist-Independent GPCR Activity That May Regulate A-P Targeting

As already described, OR-derived signals that regulate A-P targeting molecules are not affected by extrinsic stimuli or odor ligands. Furthermore, neuronal activity is not involved in the regulation. Then, what kind of OR activity could be responsible for A-P targeting, and how is it generated? We hypothesized that OR baseline activity may be regulating A-P targeting. G protein-coupled receptors (GPCRs), including ORs, are known to possess two different conformation states, active and inactive (Kobilka and Deupi 2007). Agonists stabilize the receptor in an active form, whereas inverse agonists lock it in an inactive form. In the absence of agonists and inverse agonists, GPCRs produce a baseline level of cAMP by spontaneously flipping between active and inactive conformations (Fig. 3.6a). For different OR species, variable but specific levels of baseline activities can be detected (Nakashima et al. 2013; Reisert 2010). This agonist-independent activity had long been considered to be noise created by GPCRs, and its functional role was not fully appreciated. Because naris occlusion did not affect the expression of A-P targeting molecules, we assumed that the ligand-independent OR activity may regulate A-P targeting of OSN axons. To examine this possibility, we attempted to generate the activity mutants of ORs. The initial experiment with ORs was not successful because of challenges of achieving adequate membrane expression in the heterologous system. In addition, the vast diversity of OR family proteins and the lack of three-dimensional (3D) structural information made prediction and screening of activity mutants difficult for OR molecules.

In contrast, β2-adrenergic receptor (β2-AR), a GPCR with the highest sequence homology to ORs, is much easier to express in transfected cells and shares many functional similarities with ORs. When expressed in OSNs with the OR gene promoter, β2-AR maintains the "one neuron–one receptor rule," couples with the α-subunit of G_s or G_{olf}, and substitutes ORs for receptor-instructed axonal projection (Feinstein et al. 2004). Furthermore, β2-AR has advantages of being well characterized for distinct receptor functions. Based on mutational studies, the key amino acid residues in the β2-AR that are required for G-protein coupling, ligand binding, and the generation of agonist-independent activity are well characterized (Ballesteros et al. 2001; O'Dowd et al. 1988; Savarese and Fraser 1992). Recently, the 3D structures of β2-AR in its active state and in a complex with a stimulatory G protein, G_s, have been determined (Rasmussen et al. 2011a, b). As a result of these favorable features, we selected β2-AR for the transgenic analysis of the agonist-independent GPCR activity in axonal projection of OSNs.

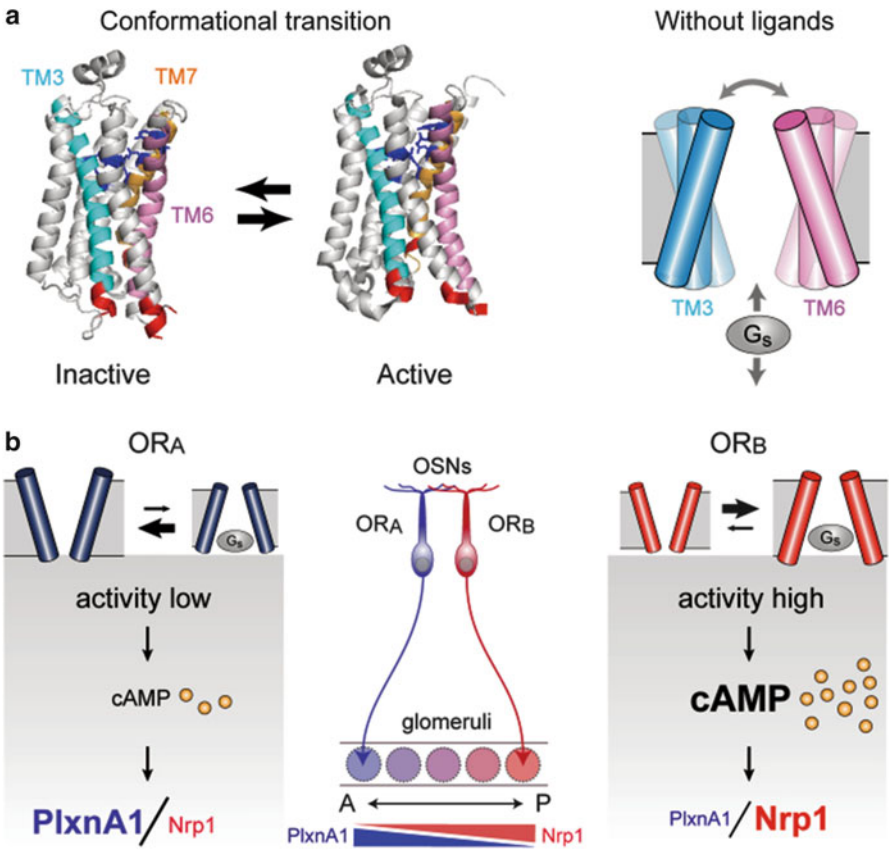

Fig. 3.6 Generation of baseline activity of GPCRs. (**a**) G protein-coupled receptors (GPCRs) possess two different conformations, active and inactive. Three-dimensional structures of β2-AR (*left*) are modified from Rasmussen et al. (2011a, b). In the absence of ligands, GPCRs spontaneously interchange between the active and inactive conformations, generating agonist-independent baseline activity (*right*). (**b**) Each OR possesses a unique level of baseline activity and generates a specific amount of cAMP using G_s, but not G_{olf}. The levels of cAMP signals are converted to transcription levels of A-P targeting molecules, e.g., Nrp1 and PlxnA1. Activity-high axons project to the posterior OB, whereas activity-low axons project to the anterior OB (Nakashima et al. 2013). *TM* transmembrane domain, *OR* odorant receptor

3.10 Transgenic Analysis of Baseline Activity Mutants

Among the β2-AR mutations analyzed, some affected both agonist-independent and agonist-dependent activities, whereas others affected only one of the two activities (Nakashima et al. 2013). We predict that mutations affecting G-protein activation would alter both agonist-dependent and -independent activities, whereas those altering ligand interactions would change agonist-dependent activity. Mutations that affect conformational transitions should alter the agonist-independent

receptor activity. For further transgenic studies, we selected three β2-AR mutants from the collection, which significantly altered agonist-independent receptor activity but not the agonist-dependent activity.

We generated transgenic mice expressing the mutant or wild-type (WT) β2-AR using an OR gene promoter (Nakashima et al. 2013); this was performed by replacing the *MOR23* coding sequence with that of *β2-AR* in the *MOR23* minigene cassette. The glomerular locations were studied for the WT and mutant β2-ARs tagged with different fluorescent markers. The activity-low β2-AR mutants generated glomeruli anterior to that of the WT. In contrast, the activity-high mutation caused a posterior shift of glomeruli. This finding showed a good correlation between the agonist-independent activities of β2-ARs and their corresponding glomerular locations in the OB along the A-P axis. We also examined the expression levels of A-P-targeting molecules in the β2-AR glomeruli (Nakashima et al. 2013). Nrp1 expression levels in β2-AR-expressing OSNs were increased by the activity-high mutation but lowered by the activity-low mutations (Fig. 3.6b). Expression levels of PlxnA1 were also affected by the activity mutation. However, the results were inverse compared with those of Nrp1 because Nrp1 expression is inversely regulated by cAMP signals. It is notable that expression levels of glomerular segregation molecules such as Kirrel2 and Kirrel3 were not affected at all by the baseline activity mutations, indicating that glomerular segregation molecules are regulated by distinct OR signals.

To examine whether the correlation between the agonist-independent activities and glomerular locations holds true for natural ORs, we performed the following experiments. We dissected the mouse OB into three sections: anterior, middle, and posterior. Thirty OR genes were cloned, transfected into HEK293 cells, and analyzed for their activities without ligands (Nakashima et al. 2013) by the luciferase reporter assay (Saito et al. 2009). ORs cloned from the anterior OB produced relatively lower levels of agonist-independent activities, whereas those from the posterior OB generated higher levels. Therefore, the agonist-independent OR activity appears to be the major determinant of expression levels of A-P targeting molecules. It should be noted that for natural ORs, the promoter activities, protein stabilities, and membrane transport could be additional factors affecting total cAMP signal levels.

3.11 Differential Usages of G_s and G_{olf} in OSNs

Our studies demonstrated that OR-instructed A-P targeting and glomerular segregation are differentially regulated by two distinct OR-derived cAMP signals. To address how these two types of regulation are separately controlled during development, we analyzed the onset of expression for various genes involved in axon guidance and signal transduction in OSNs (Nakashima et al. 2013). At ED13.5, hybridization signals were detected for A-P-targeting molecules (e.g., Nrp1), but not for glomerular segregation molecules (e.g., Kirrel2). Kirrel2 expression became prominent only at the late stage of embryonic development. We also analyzed the onset of G_s, G_{olf}, and

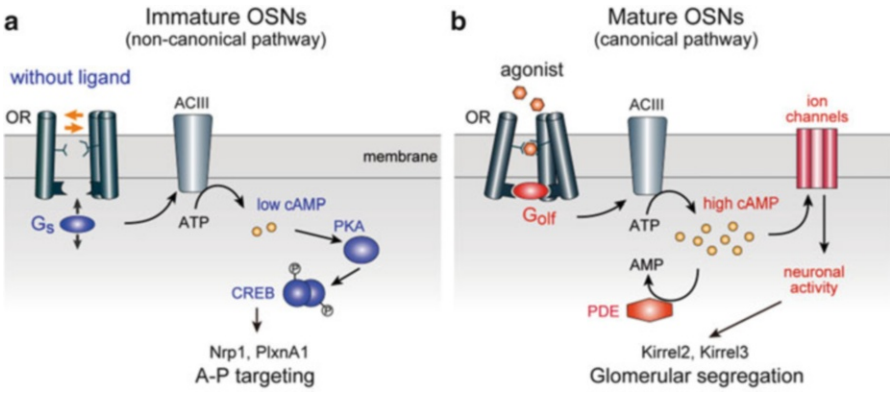

Fig. 3.7 Canonical and noncanonical signal transduction pathways in OSNs. (**a**) A-P targeting is regulated by agonist-independent OR activity using a noncanonical signaling pathway. In immature OSNs, each OR generates a unique level of cAMP by agonist-independent baseline activity via G_s and ACIII. The level of cAMP signals is converted to the transcription level of A-P targeting molecules, e.g., Nrp1 and PlxnA1, through the cAMP-activated PKA pathway, phosphorylating the transcription factor CREB. (**b**) Glomerular segregation is regulated by stimulus-driven neuronal activity using a canonical signal transduction pathway. In mature OSNs, different ORs generate different levels of neuronal activity using extrinsic stimuli, which ultimately determine the transcription levels of glomerular segregation molecules, e.g., Kirrel2 and Kirrel3. *OR* odorant receptor, *AC* adenylyl cyclase, *PKA* protein kinase A, *CREB* cAMP responsive element-binding protein, *PDE* phosphodiesterase

other signal transduction molecules. Hybridization signals were detected for G_s at ED13.5. In contrast, G_{olf} is expressed at ED17.5, but not at ED13.5, indicating that G_{olf} is not required for the expression of A-P-targeting molecules.

G_s and G_{olf} are structurally similar, sharing 88 % amino acid identity, and both mediate OR signals and activate ACIII in OSNs. However, their functional differences in the cellular context were not fully recognized. What could be the reason that G_s and G_{olf} are differentially expressed in OSNs during development? We examined the biochemical properties of G_s and G_{olf} in mediating OR signals. We generated G_s and G_{olf} fusion proteins for different ORs, whose agonists have been established. Both agonist-independent and agonist-dependent cAMP signals were measured in vitro by the dual luciferase assay using β2-AR as a control. We detected much higher agonist-independent cAMP signals with G_s than with G_{olf}, whereas ligand response properties were similar between G_s and G_{olf} (Nakashima et al. 2013). We concluded that G_s mediates agonist-independent activity more efficiently than G_{olf}. This notion was further confirmed by the loss-of-function experiments using KO mice of G_s and G_{olf}. It was found that expression of A-P targeting molecules was affected by the G_s conditional KO in OSNs, whereas the glomerular segregation molecules were unaffected. In contrast, G_{olf} KO affected glomerular segregation but not A-P targeting. Taken together, our results demonstrated that G_s plays a major role in regulating A-P targeting in immature OSNs, followed by the role of G_{olf} for glomerular segregation in mature OSNs (Fig. 3.7).

3.12 Functional Modules in the Olfactory Map

The mammalian main olfactory system mediates various responses, including aversive behaviors to spoiled foods and fear responses to predator odors. Because a particular odorant interacts with many different odorant receptor species, multiple sets of glomeruli are activated in both D and V domains of the OB. However, little is known about how the topographic information in the OB is transmitted to and interpreted in the brain to elicit various behaviors. To address these questions, mutant mice were generated in which the OSNs in a specific area of the OE are ablated with diphtheria toxin. Using the D-zone-specific OMACS promoter (Oka et al. 2003), a ΔD mutant was made, in which the D_I and D_{II} domains of the OB were devoid of glomerular structures (Kobayakawa et al. 2007). The ΔD mice lacked innate responses to aversive odorants and predator smell, even though they were capable of detecting them and could be conditioned for aversion or fear using the remaining glomeruli in the V domain. Our unpublished observations indicate that the D domain contains multiple subdomains for various innate responses, including male–male aggression and female nursing behaviors. We also generated and analyzed the ΔII mutant using the class II OR promoter, in which glomeruli were absent in the D_{II} and V domains of the OB (Kobayakawa et al. 2007). Interestingly, the ΔII mutant demonstrated avoidance behaviors toward aversive odorants; for example, 2MB acid and iso-amyl amine both activate D_I and V domain glomeruli, but not D_{II} glomeruli. Interestingly, however, the ΔII mice failed to demonstrate innate fear responses to the smell of predators, such as fox smell, tri-methyl-thyazoline (TMT). The D_I domain appears to contain glomeruli for aversive responses to spoiled food smell and irritating odorants, whereas the D_{II} domain mediates fear responses to predators (Kobayakawa et al. 2007). It was once thought that both D and V domain glomeruli contribute equally to the processing of odor information in the glomerular map. However, the mouse main olfactory system seems to be composed of at least three functional modalities: D_I, D_{II}, and V. D_I and D_{II} are for innate odor responses with hard-wired circuits and V is for learned responses based on memory (Fig. 3.8). As seen in the immune system, the mammalian olfactory system appears to have maintained innate responses in parallel with acquired/adaptive responses during evolution.

3.13 Conclusions

The olfactory map is formed by the combination of OR-dependent (A-P targeting) and OR-independent (D-V targeting) processes (Fig. 3.2a). These processes are genetically programmed and are independent from neuronal activity. The map is further refined in an activity-dependent manner during the neonatal period (Fig. 3.2b). Our recent studies revealed that A-P targeting and glomerular segregation molecules are separately regulated by distinct signals of ORs, even though both

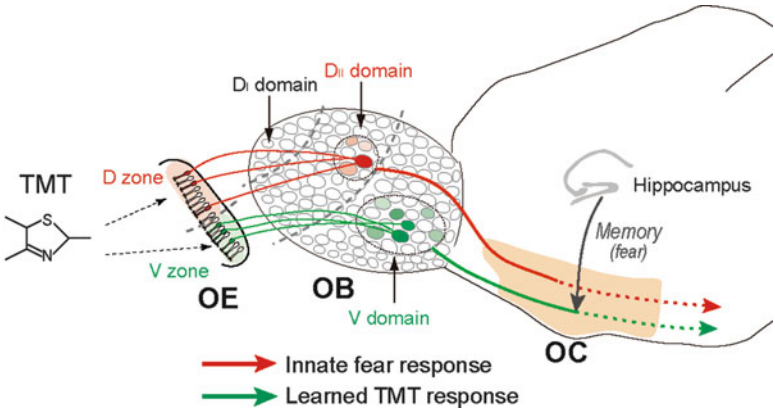

Fig. 3.8 Two independent neural pathways in the mouse olfactory system. A predator odorant, tri-methyl-thiazoline (TMT), is detected by two sets of glomeruli, one in the D_{II} domain and the other in the V domain of the OB (Kobayakawa et al. 2007). TMT activates two different neuronal pathways: one for the innate fear response (*red*) and the other for the learned fear response based on memory (*green*). *OB* olfactory bulb, *OE* olfactory epithelium, *OC* olfactory cortex

are using OR-derived cAMP as a second messenger (Nakashima et al. 2013). Glomerular segregation is regulated by stimulus-driven neuronal activity using the canonical signal transduction pathway, whereas A-P targeting is regulated by agonist-independent baseline activity of ORs using the noncanonical pathway (Fig. 3.7). How these two types of signals are separately transduced can be explained by the following. One mechanism would be temporal insulation. Different OR signals are processed for cAMP production at different stages of olfactory development. Our studies indicated that cAMP signals for A-P projection and glomerular segregation are separately processed with distinct signal transduction molecules at immature and mature stages, respectively. Differences between the two types of regulation may also be the result of the subcellular localization of ORs, namely, cilia in mature OSNs compared to axon termini in immature OSNs.

Although spatial and temporal insulation of two distinct OR signals may be important for differential regulation, the difference in the source of cAMP signals appears to be the major basis for the difference in the distribution of A-P targeting (graded) and glomerular segregation (mosaic) molecules in the glomerular map. Our study demonstrated that the equilibrium of conformational transition of GPCRs without ligands determines the steady-state levels of cAMP in immature OSNs, which ultimately determine the expression levels of A-P-targeting molecules (Fig. 3.6). In contrast, expression of glomerular segregation molecules is regulated by the stimulus-driven neuronal activity in mature OSNs. Amounts of stimuli appear to be the major determinant of the expression levels of glomerular segregation molecules (Fig. 3.5). Thus, OR-specific rate-limiting factors of cAMP production differ between the agonist-independent and -dependent processes.

Until recently, GPCR studies had been focused on their ligand-dependent functions. As the baseline activity had long been considered to be noise created by GPCRs, its biological role was not fully appreciated. However, recent studies of 3D structures of β2-AR (Rasmussen et al. 2011a, b) have revealed the inner workings of various GPCRs: the extracellular cavity determines ligand specificity and firing rates, whereas the intracellular cavity determines the G-protein selectivity and levels of baseline activities. The olfactory system makes use of extensive functionality of the largest family of GPCRs: G_s utilizes intracellular diversity of ORs for axonal wiring specificity during development, whereas G_{olf} utilizes extracellular diversity to detect various environmental stimuli after birth and also to regulate olfactory map refinement (Fig. 3.7).

After 23 years since the discovery of the OR gene (Buck and Axel 1991), it is now clear what defines the identity of OSNs in OR-instructed axonal projection. Our studies have revealed that the equilibrium of conformational transitions set by each OR is what determines the transcription levels of A-P targeting molecules in OSNs (Nakashima et al. 2013).

Acknowledgments This work was supported by the CREST Program of the Japan Science and Technology Agency and a Specially Promoted Research Grant from the Ministry of Education, Culture, Sports, Science and Technology of Japan.

References

Aoki M, Takeuchi H, Nakashima A, Nishizumi H, Sakano H (2013) Possible roles of robo1$^+$ ensheathing cells in guiding dorsal-zone olfactory sensory neurons in mouse. Dev Neurobiol 73:828–840

Astic L, Saucier D, Holley A (1987) Topographical relationships between olfactory receptor cells and glomerular foci in the rat olfactory bulb. Brain Res 424:144–152

Ballesteros JA, Jensen AD, Liapakis G, Rasmussen SG, Shi L, Gether U, Javitch JA (2001) Activation of the β2-adrenergic receptor involves disruption of an ionic lock between the cytoplasmic ends of transmembrane segments 3 and 6. J Biol Chem 276:29171–29177

Barnea G, O'Donnell S, Mancia F, Sun X, Nemes A, Mendelsohn M, Axel R (2004) Odorant receptors on axon termini in the brain. Science 304:1468

Bozza T, Vassalli A, Fuss S, Zhang JJ, Weiland B, Pacifico R, Feinstein P, Mombaerts P (2009) Mapping of class I and class II odorant receptors to glomerular domains by two distinct types of olfactory sensory neurons in the mouse. Neuron 61:220–233

Buck L, Axel R (1991) A novel multigene family may encode odorant receptors: a molecular basis for odor recognition. Cell 65:175–187

Chesler AT, Zou DJ, Le Pichon CE, Peterlin ZA, Matthews GA, Pei X, Miller MC, Firestein S (2007) A G protein/cAMP signal cascade is required for axonal convergence into olfactory glomeruli. Proc Natl Acad Sci USA 104:1039–1044

Cho JH, Lepine M, Andrews W, Parnavelas J, Cloutier JF (2007) Requirement for Slit-1 and Robo-2 in zonal segregation of olfactory sensory neuron axons in the main olfactory bulb. J Neurosci 27:9094–9104

Cloutier JF, Giger RJ, Koentges G, Dulac C, Kolodkin AL, Ginty DD (2002) Neuropilin-2 mediates axonal fasciculation, zonal segregation, but not axonal convergence, of primary accessory olfactory neurons. Neuron 33:877–892

Col JA, Matsuo T, Storm DR, Rodriguez I (2007) Adenylyl cyclase-dependent axonal targeting in the olfactory system. Development (Camb) 134:2481–2489

Feinstein P, Mombaerts P (2004) A contextual model for axonal sorting into glomeruli in the mouse olfactory system. Cell 117:817–831

Feinstein P, Bozza T, Rodriguez I, Vassalli A, Mombaerts P (2004) Axon guidance of mouse olfactory sensory neurons by odorant receptors and the β2 adrenergic receptor. Cell 117:833–846

Imai T, Sakano H (2008) Odorant receptor-mediated signaling in the mouse. Curr Opin Neurobiol 18:251–260

Imai T, Suzuki M, Sakano H (2006) Odorant receptor-derived cAMP signals direct axonal targeting. Science 314:657–661

Imai T, Yamazaki T, Kobayakawa R, Kobayakawa K, Abe T, Suzuki M, Sakano H (2009) Pre-target axon sorting establishes the neural map topography. Science 325:585–590

Kobayakawa K, Kobayakawa R, Matsumoto H, Oka Y, Imai T, Ikawa M, Okabe M, Ikeda T, Itohara S, Kikusui T, Mori K, Sakano H (2007) Innate versus learned odour processing in the mouse olfactory bulb. Nature (Lond) 450:503–508

Kobilka BK, Deupi X (2007) Conformational complexity of G-protein coupled receptors. Trends Pharmacol Sci 28:397–406

Luo L, Flanagan JG (2007) Development of continuous and discrete neural maps. Neuron 56:284–300

Malnic B, Hirono J, Sato T, Buck LB (1999) Combinatorial receptor codes for odors. Cell 96:713–723

McLaughlin T, O'Leary DD (2005) Molecular gradients and development of retinotopic maps. Annu Rev Neurosci 28:327–355

Miyamichi K, Serizawa S, Kimura HM, Sakano H (2005) Continuous and overlapping expression domains of odorant receptor genes in the olfactory epithelium determine the dorsal/ventral positioning of glomeruli in the olfactory bulb. J Neurosci 25:3586–3592

Mombaerts P (2006) Axonal wiring in the mouse olfactory system. Annu Rev Cell Dev Biol 22:713–737

Mombaerts P, Wang F, Dulac C, Chao SK, Nemes A, Mendelsohn M, Edmondson J, Axel R (1996) Visualizing an olfactory sensory map. Cell 87:675–686

Mori K, Sakano H (2011) How is the olfactory map formed and interpreted in the mammalian brain? Annu Rev Neurosci 34:467–499

Nakashima A, Takeuchi H, Imai T, Saito H, Kiyonari H, Abe T, Chen M, Weinstein LS, Yu CR, Storm DR, Nishizumi H, Sakano H (2013) Agonist-independent GPCR activity regulates axon targeting of olfactory sensory neurons. Cell 154:1314–1325

Ngai J, Dowling MM, Buck LB, Axwl R, Chess A (1993) The family of genes encoding odorant receptors in the channel catfish. Cell 72:657–666

Nguyen-Ba-Charvet KT, Di Meglio T, Fouquet C, Chedotal A (2008) Robos and slits control the pathfinding and targeting of mouse olfactory sensory axons. J Neurosci 28:4244–4249

O'Dowd BF, Hnatowich M, Regan JW, Leader WM, Caron MG, Lefkowitz RJ (1988) Site-directed mutagenesis of the cytoplasmic domains of the human β2-adrenergic receptor. Localization of regions involved in G protein-receptor coupling. J Biol Chem 263:15985–15992

Oka Y, Kobayakawa K, Nishizumi H, Miyamichi K, Hirose S, Tsuboi A, Sakano H (2003) O-MACS, a novel member of the medium-chain acyl-CoA synthetase family, specifically expressed in the olfactory epithelium in a zone-specific manner. Eur J Biochem 270:1995–2004

Pacifico R, Dewan A, Cawley D, Guo C, Bozza T (2012) An olfactory subsystem that mediates high-sensitivity detection of volatile amines. Cell Rep 2:76–88

Petersen CC (2007) The functional organization of the barrel cortex. Neuron 56:339–355

Rasmussen SG, Choi HJ, Fung JJ, Pardon E, Casarosa P, Chae PS, Devree BT, Rosenbaum DM, Thian FS, Kobilka TS, Schnapp A, Konetzki I, Sunahara RK, Gellman SH, Pautsch A, Steyaert J, Weis WI, Kobilka BK (2011a) Structure of a nanobody-stabilized active state of the β(2) adrenoceptor. Nature (Lond) 469:175–180

Rasmussen SG, DeVree BT, Zou Y, Kruse AC, Chung KY, Kobilka TS, Thian FS, Chae PS, Pardon E, Calinski D, Mathiesen JM, Shah ST, Lyons JA, Caffrey M, Gellman SH, Steyaert J, Skiniotis G, Weis WI, Sunahara RK, Kobilka BK (2011b) Crystal structure of the β2 adrenergic receptor-Gs protein complex. Nature (Lond) 477:549–555

Reisert J (2010) Origin of basal activity in mammalian olfactory receptor neurons. J Gen Physiol 136:529–540

Ressler KJ, Sullivan SL, Buck LB (1994) Information coding in the olfactory system: evidence for a stereotyped and highly organized epitope map in the olfactory bulb. Cell 79:1245–1255

Saito H, Chi Q, Zhuang H, Matsunami H, Mainland JD (2009) Odor coding by a mammalian receptor repertoire. Sci Signal 2:ra9

Satoda M, Takagi S, Ohta K, Hirata T, Fujisawa H (1995) Differential expression of two cell surface proteins, neuropilin and plexin, in *Xenopus* olfactory axon subclasses. J Neurosci 15:942–955

Savarese TM, Fraser CM (1992) In vitro mutagenesis and the search for structure–function relationships among G protein-coupled receptors. Biochem J 283:1–19

Serizawa S, Miyamichi K, Nakatani H, Suzuki M, Saito M, Yoshihara Y, Sakano H (2003) Negative feedback regulation ensures the one receptor-one olfactory neuron rule in mouse. Science 302:2088–2094

Serizawa S, Miyamichi K, Sakano H (2004) One neuron–one receptor rule in the mouse olfactory system. Trends Genet 20:648–653

Serizawa S, Miyamichi K, Takeuchi H, Yamagishi Y, Suzuki M, Sakano H (2006) A neuronal identity code for the odorant receptor-specific and activity-dependent axon sorting. Cell 127:1057–1069

Sperry RW (1963) Chemoaffinity in the orderly growth of nerve fiber patterns and connection. Proc Natl Acad Sci USA 50:703–710

St. John JA, Clarris HJ, McKeown S, Royal S, Key B (2003) Sorting and convergence of primary olfactory axons are independent of the olfactory bulb. J Comp Neurol 464:131–140

Strotmann J, Levai O, Fleischer J, Schwarzenbacher K, Breer H (2004) Olfactory receptor proteins in axonal processes of chemosensory neurons. J Neurosci 24:7754–7761

Sullivan SL, Bohm S, Ressier KJ, Horowitz LF, Buck LB (1995) Target-independent pattern specification in the olfactory epithelium. Neuron 15:779–789

Takeuchi H, Inokuchi K, Aoki M, Suto F, Tsuboi A, Matsuda I, Suzuki M, Aiba A, Serizawa S, Yoshihara Y, Fujisawa H, Sakano H (2010) Sequential arrival and graded secretion of Sema3F by olfactory neuron axons specify map topography at the bulb. Cell 141:1056–1067

Tsuboi A, Yoshihara S, Yamazaki N, Kasai H, Asai-Tsuboi H, Komatsu M, Serizawa S, Ishii T, Matsuda Y, Nagawa F, Sakano H (1999) Olfactory neurons expressing closely linked and homologous odorant receptor genes tend to project their axons to neighboring glomeruli on the olfactory bulb. J Neurosci 19:8409–8418

Vassar R, Chao SK, Sitcheran R, Nunez JM, Vosshall LB, Axel R (1994) Topographic organization of sensory projections to the olfactory bulb. Cell 79:981–991

Walz A, Rodriguez I, Mombaerts P (2002) Aberrant sensory innervation of the olfactory bulb in neuropilin-2 mutant mice. J Neurosci 22:4025–4035

Wang F, Nemes A, Mendelsohn M, Axel R (1998) Odorant receptors govern the formation of a precise topographic map. Cell 93:47–60

Yu CR, Power J, Barnea G, O'Donnell S, Brown HE, Osborne J, Axel R, Gogos JA (2004) Spontaneous neural activity is required for the establishment and maintenance of the olfactory sensory map. Neuron 42:553–566

Zhang X, Rogers M, Tian H, Zhang X, Zou DJ, Liu J, Ma M, Shepherd GM, Firestein SJ (2004) High-throughput microarray detection of olfactory receptor gene expression in the mouse. Proc Natl Acad Sci USA 101:14168–14173

Zheng C, Feinstein P, Bozza T, Rodriguez I, Mombaerts P (2000) Peripheral olfactory projections are differentially affected in mice deficient in a cyclic nucleotide-gated channel subunit. Neuron 26:81–91

Chapter 4
Odor Maps in the Olfactory Bulb

Kensaku Mori

Abstract The olfactory bulb is the first relay station of the central olfactory system in the mammalian brain and contains a few thousand glomeruli on its surface. Individual glomeruli represent a single type of odorant receptor, and the glomerular sheet of the olfactory bulb forms odorant receptor maps. This chapter summarizes the spatial organization of the odorant receptor-representing glomerular maps of the rodent olfactory bulb, focusing on (1) the domain organization of each glomerular map, (2) "intrabulbar projections" of tufted cell axons that precisely and topographically connect the lateral and medial maps, (3) molecular feature clusters of glomeruli in the olfactory bulb, and (4) functional compartmentalization of the glomerular maps.

Keywords Clusters • Domains • Glomeruli • Intrabulbar projections • Odor map • Odorant receptor • Olfactory bulb • Two mirror-symmetrical glomerular maps

4.1 Glomerular Modules

As shown in Chap. 3, axons of olfactory sensory neurons (OSNs) expressing a given odorant receptor (OR) converge to a fixed projection site, forming a glomerulus in each of two olfactory maps in the olfactory bulb (Imai and Sakano 2007; Mombaerts 2006; Mori and Sakano 2011). Thus, an individual glomerulus in the olfactory bulb represents a single OR species. Within each glomerulus, OSN axons form excitatory synapses on the terminal tufts of primary dendrites of projection neurons, the tufted cells and mitral cells (Mori 1987; Shepherd et al. 2004). Because each tufted or mitral cell projects a single primary dendrite to a single glomerulus, an individual glomerulus together with its associated tufted and mitral cells form a

K. Mori (✉)
Department of Physiology, Graduate School of Medicine, The University of Tokyo, Bunkyo-ku, Tokyo 118-0033, Japan
e-mail: moriken@m.u-tokyo.ac.jp

K. Mori (ed.), *The Olfactory System: From Odor Molecules to Motivational Behaviors*,
DOI 10.1007/978-4-431-54376-3_4,

single structural and functional module (glomerular module or glomerular unit) (see Fig. 7.1 in Chap. 7). In the mouse, each olfactory bulb contains approximately 1,800 OR-representing glomerular modules that are arranged at stereotypical positions and thus form glomerular maps (Mori and Sakano 2011; Mori et al. 2006). In this sense, the olfactory bulb resembles primary sensory areas of the neocortex in which functional columns are spatially arranged in a modality-specific manner and form sensory maps.

4.2 Each Olfactory Bulb Has Two Mirror-Symmetrical Glomerular Maps That Are Connected Precisely with Tufted Cell Axon Collaterals

In the mouse olfactory bulb, an individual OR is typically represented by a stereotypic pair of glomeruli located at two different sites, one at the rostrodorsolateral half and the other at the caudoventromedial half of the olfactory bulb (Mombaerts et al. 1996; Ressler et al. 1994; Vassar et al. 1994). Because of the dual representation, each olfactory bulb has two mirror-symmetrical glomerular maps: a lateral map and a medial map (Figs. 4.1b, 4.2) (Nagao et al. 2000). The lateral map receives olfactory axon inputs from OSNs distributed in the rostrodorsolateral part of the ipsilateral olfactory epithelium, whereas the medial map receives olfactory axon inputs from those in the caudoventromedial part of the olfactory epithelium (Astic and Saucier 1986; Saucier and Astic 1986; Schoenfeld et al. 1994).

Each functional pair of glomerular modules is precisely and reciprocally linked via the axon collaterals of tufted cells (external, middle, and internal tufted cells), which are called intrabulbar projections (Fig. 4.3) (Belluscio et al. 2002; Cummings and Belluscio 2010; Igarashi et al. 2012; Liu and Shipley 1994; Lodovichi et al. 2003; Schoenfeld et al. 1985; Zhou and Belluscio 2008). For example, tufted cells associated with a given glomerular module (glomerulus A or B in Fig. 4.3) in the lateral map extend axon collaterals through the internal plexiform layer (IPL) to the dendrites of granule cells located beneath the isofunctional glomerular module (glomerulus A′ or B′ in Fig. 4.3) in the medial map. It can be speculated that these granule cells are tufted cell-targeting granule cells that form dendrodendritic reciprocal synaptic connections with tufted cell dendrites (Fig. 4.3, see also Chap. 7). Because sister tufted cells belonging to a particular glomerulus and tufted cell-targeting granule cells form local tufted cell circuits (see Chap. 7), tufted cell circuits in the glomerular module A or B may interact preferentially with tufted cell circuits of the isofunctional glomerular modules A′ or B′, respectively, via the precise "intrabulbar projections." In striking contrast, intrabulbar axon collaterals of mitral cells do not participate in the precise "intrabulbar projections."

The "intrabulbar projections" of tufted cell axon collaterals are thought to coordinate responses of two mirror-symmetrical glomerular maps, but detailed functional roles of the precise reciprocal connections are not well understood

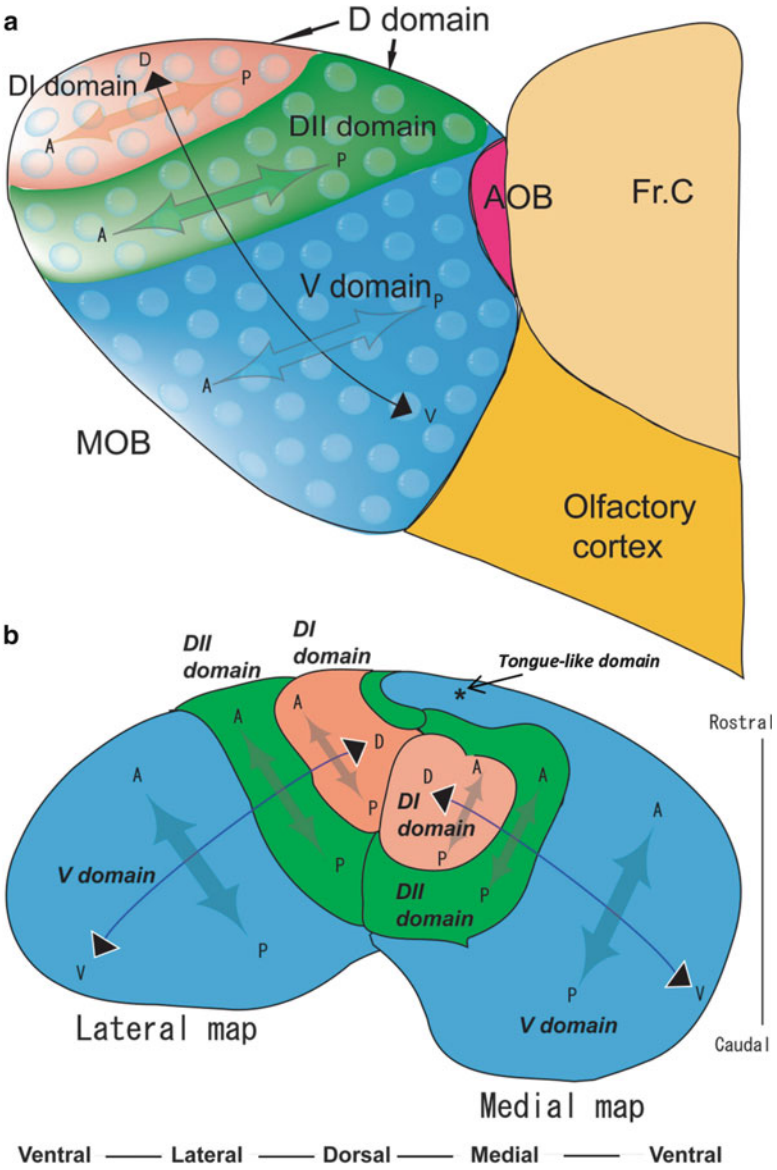

Fig. 4.1 Glomerular map of the olfactory bulb. (**a**) *Lateral view* of the domain organization of glomeruli in the lateral map of the rodent main olfactory bulb (*MOB*). *Double-headed colored arrows* indicate the anterior-posterior (anteroposterior, A-P) axis of each domain; *black arrows* indicate the dorsal-ventral (dorsoventral, D-V) axis of the lateral map. *AOB* accessory olfactory bulb, *DI* class I part of the dorsal (D) domain, *DII* class II part of the D domain, *Fr.C* frontal cortex. (**b**) A dorsal centered view of an unrolled flattened map of glomerular layer of the MOB. *Double-headed gray arrows* indicate the A-P axis of each domain of the lateral and medial maps; *black arrows* indicate the D-V axis of the lateral and medial maps. In mice, an individual OR is typically represented by a pair of glomeruli: one in the lateral map and the other in the medial map. However, for a small subset of ORs, each OR is represented only by a single glomerulus. Some of these glomeruli are located in the *tongue-like domain* (*asterisk*). (Modified from Mori and Sakano 2011)

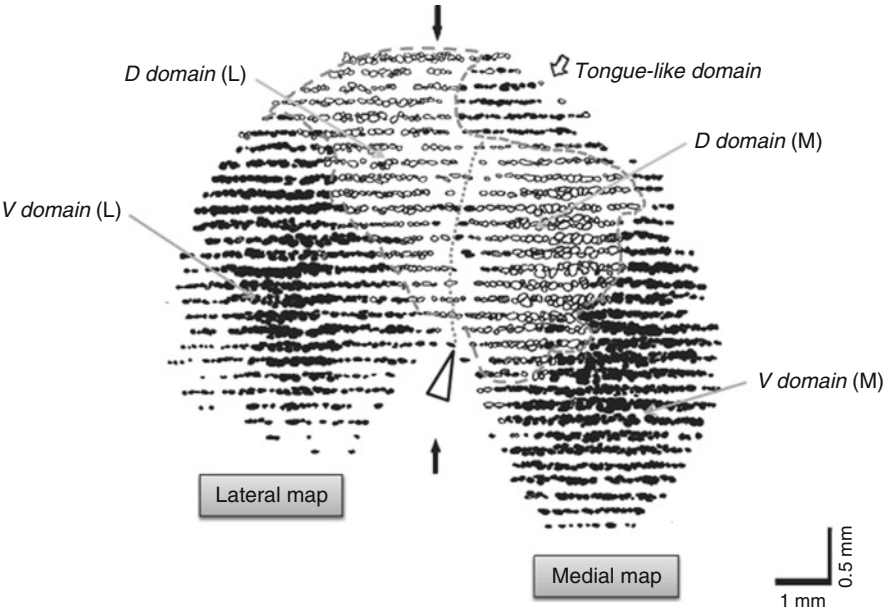

Fig. 4.2 Unrolled flattened maps of glomeruli showing OCAM-positive domain (V-domain) and OCAM-negative domain (D-domain) in the mouse olfactory bulb. The flattened glomerular layers with OCAM-positive glomeruli (*filled spots*) and OCAM-negative glomeruli (*open spots*) were aligned from rostral to caudal using the dorsal edge (*filled arrows*) of the frontal sections of the olfactory bulb. A *dotted line* with an *open triangle* indicates a possible dorsal boundary between the lateral (*L*) and medial (*M*) maps. *Open arrow* indicates the tongue-like domain. Unit length along the rostrocaudal axis is twice that of the circumferential to better illustrate the organization of glomeruli in the unrolled map. (Modified with permission from Nagao et al. 2000)

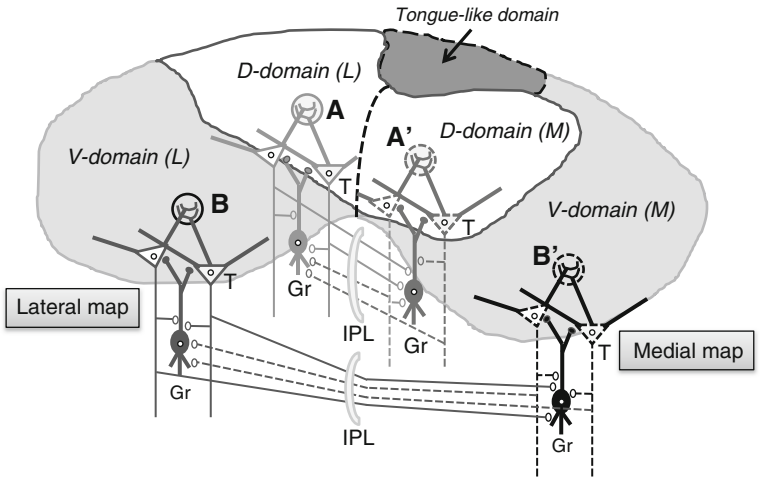

Fig. 4.3 Intrabulbar projections of tufted cell axon collaterals. Tufted cells associated with a given glomerular module (glomerulus *A* or *B*) in the lateral map extend axon collaterals through the internal plexiform layer (*IPL*) to the dendrites of granule cells (*Gr*) located beneath the isofunctional glomerular module (glomerulus A' or B') in the medial map. The intrabulbar projection of tufted cell axon collaterals reciprocally connects isofunctional glomerular modules in the lateral and medial maps. Axons of tufted cells whose somata are in the lateral map are shown by *solid lines*; those in the medial map are illustrated by *dashed lines*

(Cummings and Belluscio 2008). Because tufted cell circuits in each glomerular module are thought to be responsible for the generation of sniff rhythm-paced early-onset fast gamma oscillations (see Chap. 7), one possible functional role of the "intrabulbar projections" is the coordination of fast gamma oscillations between isofunctional glomerular modules. It has been shown that the precise intrabulbar projections of tufted cell axon collaterals are achieved during postnatal development and undergo olfactory activity-dependent refinement during both development and adulthood (Cummings and Belluscio 2010; Marks et al. 2006). Olfactory deprivation by naris closure disrupts the intrabulbar projection, and reopening of the naris recovers the precise intrabulbar projection. These results suggest that the intrabulbar projections of tufted cells maintain a continuous level of activity-dependent plasticity throughout life.

In addition to the intrabulbar projections, each tufted cell projects axons to focal targets in the pars externa of the anterior olfactory nucleus (AONpE) (Igarashi et al. 2012; Schoenfeld and Macrides 1984). The axonal projection of tufted cells to the AONpE is organized in a topographic fashion such that the dorsoventral axis of the glomerular map in the olfactory bulb is conserved precisely in the dorsoventral axis of the axonal targets in the AONpE (Schoenfeld and Macrides 1984; Yan et al. 2008). As is described in Chap. 7, each tufted cell also projects axons to focal targets in the pars principalis of the anterior olfactory nucleus, the rostroventral part of the anterior piriform cortex, and the rostrolateral part of the olfactory tubercle. Each tufted cell may send specific OR information to focal targets both in the olfactory bulb and in the olfactory peduncle areas of the olfactory cortex.

4.3 Domain Organization of Glomerular Map

Based on the OR species (Zhang and Firestein 2002), glomeruli are grouped into specific compartments, such as domains at stereotypical positions in the olfactory bulb. Figure 4.1a shows the domain arrangement in the lateral view of the olfactory bulb. Glomeruli in the main olfactory bulb are grouped into two domains, dorsal and ventral, arranged in parallel with the anteroposterior axis of the olfactory bulb. Glomeruli in the dorsal domain (D domain) receive olfactory axon inputs from OSNs in the dorsal zone of the olfactory epithelium. Therefore, D-domain glomeruli represent dorsal-zone ORs. Glomeruli in the ventral domain (V domain) receive olfactory axon inputs from OSNs that are distributed in the ventral zone of the olfactory epithelium (Yoshihara et al. 1997). Glomeruli in the V domain therefore represent ventral-zone ORs. Olfactory axons that project to the V domain express olfactory cell adhesion molecule (OCAM), whereas those that project to the D domain lack OCAM expression (Fig. 4.2). Over the course of embryonic development, the D-domain glomeruli are formed first in the olfactory bulb, and the glomerular map expands ventrally (Takeuchi et al. 2010).

As shown in Fig. 4.1, the D-domain glomeruli are further grouped into two domains, DI and DII, according to the expressed OR species (Bozza et al. 2009; Kobayakawa et al. 2007; Tsuboi et al. 2006). The DI domain occupies the

rostrodorsal part of the D domain and the DII domain surrounds the DI domain (Fig. 4.1b). Glomeruli in the DI domain represent class I (fish-type) ORs, whereas DII glomeruli represent class II (terrestrial-type) ORs. OSNs expressing class I ORs and those expressing class II ORs are intermingled in the dorsal zone of the olfactory epithelium. However, the two subsets of OSNs project their axons to separate dorsal domains in the olfactory bulb.

Trace amine-associated receptors (TAARs) are a small family of evolutionally conserved ORs (Liberles and Buck 2006). A majority of olfactory TAARs are represented by a cluster of glomeruli located in the caudal part of the D domain near the boundary between DI and DII domains (Pacifico et al. 2012). The cluster of TAARs-representing glomeruli is referred as the DIII domain.

As described earlier, each of the lateral and medial maps is divided into DI, DII, and V domains arranged in parallel to the anteroposterior axis. A comparison between the lateral and medial maps using the unrolled flattened maps indicates that each map has its own anteroposterior–dorsoventral axis coordinates, although the two maps are arranged in roughly a mirror-symmetrical manner (Fig. 4.1b).

A majority of ORs are represented by a pair of glomeruli in the mouse olfactory bulb. However, a small subset ORs is represented only by a single glomerulus. The rostromedioventral domain (so-called tongue-like domain shown in Figs. 4.1b, 4.2, and 4.3) of the glomerular map is unique in that it contains glomeruli representing the single glomerulus ORs. For example, OSNs expressing a given member of OR37 family genes converge axons only to a single glomerulus, and glomeruli for the different OR37 subtypes are grouped together in the rostromedioventral domain (Bader et al. 2012). Interestingly, mitral/tufted cells associated with the OR37 glomeruli show a unique pattern of axonal projection. They project axons directly to the medial amygdala, paraventricular nucleus, and supraoptic nucleus of the hypothalamus (Bader et al. 2012).

4.4 Molecular Feature Clusters of Glomeruli

Glomeruli in the olfactory bulb can also be grouped into subsets by the odorant selectivity, or molecular receptive range (MRR) property, of individual glomeruli. Mapping the odor-induced glomerular activity and the MRR properties of glomeruli demonstrated that (1) individual glomeruli typically respond to a range of odorants that share a specific combination of molecular features, and that (2) each glomerulus appears to be unique in its MRR property (Kikuta et al. 2013; Mori et al. 2006). In addition, glomeruli with similar MRR properties tend to gather and form molecular feature clusters at stereotypical positions in the glomerular map (Johnson and Leon 2007; Johnson et al. 2009; Matsumoto et al. 2010; Mori et al. 2006; Takahashi et al. 2004).

Figure 4.4a shows molecular feature clusters of glomeruli superimposed on the domain organization at the dorsal surface of mouse olfactory bulb (Matsumoto et al. 2010). Fatty acids, aliphatic aldehydes, and amines have distinct unpleasant

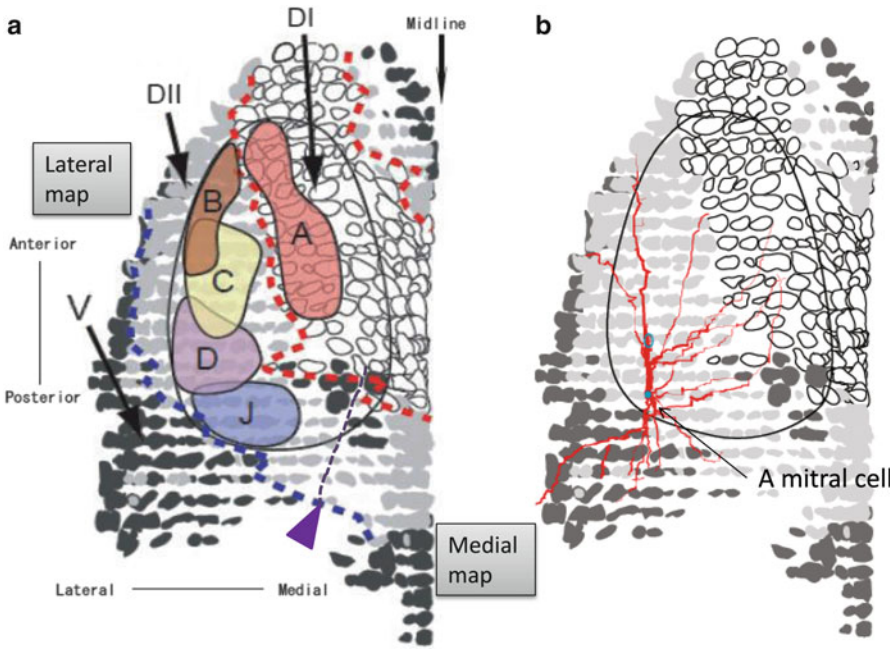

Fig. 4.4 Reconstructed glomerular map of the dorsal part of the mouse olfactory bulb. (**a**) Molecular feature clusters *A*–*J* are superimposed on the domain organization of the standard glomerular map. The *large black contour line* indicates the optically imaged region for determining the molecular feature clusters. *DI* DI domain (glomeruli shown by *open spots*), *DII* DII domain (glomeruli shown by *light gray spots*), *V* V-domain (glomeruli shown by *dark gray spots*). The boundaries between the DI and DII domains and between the DII and V domains are indicated by *red* and *blue dotted lines*. A *purple broken line* with *purple triangle* indicates a possible boundary between the lateral and medial maps. (**b**) Reconstructed dendritic tree of a single mitral cell (shown by *red*) whose soma is located in the DII domain is superimposed on the standard glomerular map to estimate the spatial distribution of the lateral dendrites of a single mitral cell in reference to the domain organization of glomerular maps. The standard map and the mitral cell were obtained from different mice. (Modified with permission from Matsumoto et al. 2010)

odors that characterize spoiled foods. Glomeruli in cluster A respond to fatty acid and aliphatic aldehyde odorants. The cluster A glomeruli also respond to alkyl amine odorants that contain an amino group ($-NH_3$) and are located in the lateral part of the DI domain adjacent to the DII domain.

A small cluster of glomeruli located caudomedially to the cluster A respond to amine odorants including trimethylamine but not to fatty acids (this cluster is not shown in Fig. 4.4a; cf. posteromedial amine-selective cluster in Takahashi et al. 2004). The amine-selective cluster of glomeruli appears to correspond to the TAARs-representing cluster of glomeruli (in DIII domain) (Pacifico et al. 2012).

Cluster B, which responds to aliphatic alcohol odorants and a wide range of aliphatic ketone odorants, is located in the anterior part of the DII domain. It should be noted that the aliphatic alcohols and ketones do not activate cluster A glomeruli.

Glomeruli in cluster C, which respond to phenol odorants (e.g., cresol and ethyl phenol) and phenylethyl odorants (e.g., guaiacol and creosole) are located in the DII domain just posterior to cluster B.

Cluster D glomeruli are activated by aliphatic and aromatic ketone odorants and are located posterior to cluster C. Cluster J glomeruli that respond to thiazole and thiazoline odorants (including the fox odor tri-methyl-thyazoline) are located in the caudal part of the DII domain in the lateral map. Thus, clusters B, C, D, and J are invariably arranged from the anterior to the posterior region in the DII domain. Molecular feature clusters are also found in the V domain of the olfactory bulb (Igarashi and Mori 2005). The spatial arrangement of the molecular feature clusters A–D and J appears to be conserved between rats and mice (Matsumoto et al. 2010).

In human sensory psychophysical studies, a variety of correlations have been reported between the molecular features of odorants and their perceived "odor quality" (Amoore et al. 1964; Beets 1970; Moncrieff 1967; Mori et al. 2006; Rossiter 1996). Although the molecular structure–odor relationships are complex and cannot be explained in simple terms, it can be speculated that the molecular feature clusters of glomeruli might be part of the neural representation of basic odor quality. In addition, the molecular feature maps provide a basis for understanding how the olfactory cortex read the odor maps in the olfactory bulb.

4.5 Functional Compartmentalization in the Olfactory Map

Odors emitted by predators signify danger and induce fear responses such as freezing in rodents (Dielenberg and McGregor 2001; Hebb et al. 2002, 2004). Trimethyl thiazoline (TMT) is a fox odor known to induce a freezing response in mice and rats. TMT activates glomeruli in cluster J of the DII domain and many glomeruli in the V domain. Ablation of glomeruli in the D domain including the DII domain abolishes the TMT-induced fear response in mice (Kobayakawa et al. 2007), suggesting that TMT-responsive glomeruli in the DII domain are responsible for the TMT-induced fear responses.

Spoiled foods produce amines and fatty acids, and these odors induce innate aversive responses in rats and mice (Dielenberg and McGregor 2001) and activate multiple glomeruli in various areas of the olfactory bulb. However, only cluster A glomeruli in the DI domain are responsible for fatty acid-induced aversive responses (Kobayakawa et al. 2007).

These results raise the possibility of functional compartmentalization of the glomerular map of the olfactory bulb: TMT-responsive glomeruli and other predator odor-responsive glomeruli in the DII domain might be specialized for inducing fear responses to the predator odors, and fatty acid and amine-responsive glomeruli in the DI domain might be specialized for inducing aversive responses to spoiled foods.

A single glomerular module consists of a glomerulus together with sister tufted cells and mitral cells. Each granule cell also might mainly associate with a single glomerular module (Willhite et al. 2006). Mitral and tufted cells belonging to a particular glomerular module extend lateral dendrites in the external plexiform layer and thus can interact with mitral and tufted cells belonging to other glomerular modules via dendrodendritic reciprocal synaptic connections with granule cell inhibitory interneuron (Migliore et al. 2010) (see Chap. 7). To estimate the extent of dendritic projection of a single mitral cell in reference to the glomerular maps, we superimposed the dendritic tree of a mitral cell (whose soma was located in the DII domain) on a standard glomerular map of the dorsal surface of the mouse main olfactory bulb (Fig. 4.4b). It can be seen that a single mitral cell extends a lateral dendrite widely covering not only wide areas of the DII domain but also DI and V domains. Thus, a number of glomerular modules can interact globally across wide areas of the olfactory bulb via the long lateral dendrites of mitral cells.

In contrast, external tufted cells and middle tufted cells extend shorter lateral dendrites, suggesting that interactions among glomerular modules via these tufted cell dendrites are more spatially restricted. Therefore, tufted cells and mitral cells appear to read the glomerular OR maps in a different manner, as is discussed in more detail in Chap. 7.

References

Amoore JE, Johnston JW Jr, Rubin M (1964) The sterochemical theory of odor. Sci Am 210:42–49

Astic L, Saucier D (1986) Anatomical mapping of the neuroepithelial projection to the olfactory bulb in the rat. Brain Res Bull 16:445–454

Bader A, Klein B, Breer H, Strotmann J (2012) Connectivity from OR37 expressing olfactory sensory neurons to distinct cell types in the hypothalamus. Front Neural Circuits 6:84

Beets MG (1970) The molecular parameters of olfactory response. Pharmacol Rev 22:1–34

Belluscio L, Lodovichi C, Feinstein P, Mombaerts P, Katz LC (2002) Odorant receptors instruct functional circuitry in the mouse olfactory bulb. Nature (Lond) 419:296–300

Bozza T, Vassalli A, Fuss S, Zhang J, Weiland B et al (2009) Mapping of class I and class II odorant receptors to glomerular domains by two distinct types of olfactory sensory neurons in the mouse. Neuron 61:220–233

Cummings DM, Belluscio L (2008) Charting plasticity in the regenerating maps of the mammalian olfactory bulb. Neuroscientist 14:251–263

Cummings DM, Belluscio L (2010) Continuous neural plasticity in the olfactory intrabulbar circuitry. J Neurosci 30:9172–9180

Dielenberg RA, McGregor IS (2001) Defensive behavior in rats towards predatory odors: a review. Neurosci Biobehav Rev 25:597–609

Hebb AL, Zacharko RM, Dominguez H, Trudel F, Laforest S, Drolet G (2002) Odor-induced variation in anxiety-like behavior in mice is associated with discrete and differential effects on mesocorticolimbic cholecystokinin mRNA expression. Neuropsychopharmacology 27:744–755

Hebb AL, Zacharko RM, Gauthier M, Trudel F, Laforest S, Drolet G (2004) Brief exposure to predator odor and resultant anxiety enhances mesocorticolimbic activity and enkephalin expression in CD-1 mice. Eur J Neurosci 20:2415–2429

Igarashi K, Mori K (2005) Spatial representation of hydrocarbon odorants in the ventrolateral zones of the rat olfactory bulb. J Neurophysiol 93:1007–1019

Igarashi KM, Ieki N, An M, Yamaguchi Y, Nagayama S et al (2012) Parallel mitral and tufted cell pathways route distinct odor information to different targets in the olfactory cortex. J Neurosci 32:7970–7985
Imai T, Sakano H (2007) Roles of odorant receptors in projecting axons in the mouse olfactory system. Curr Opin Neurobiol 17:507–515
Johnson B, Leon M (2007) Chemotopic odorant coding in a mammalian olfactory system. J Comp Neurol 503:1–34
Johnson B, Xu Z, Ali S, Leon M (2009) Spatial representations of odorants in olfactory bulbs of rats and mice: similarities and differences in chemotopic organization. J Comp Neurol 514:658–673
Kikuta S, Fletcher ML, Homma R, Yamasoba T, Nagayama S (2013) Odorant response properties of individual neurons in an olfactory glomerular module. Neuron 77:1122–1135
Kobayakawa K, Kobayakawa R, Matsumoto H, Oka Y, Imai T et al (2007) Innate versus learned odour processing in the mouse olfactory bulb. Nature (Lond) 450:503–508
Liberles SD, Buck LB (2006) A second class of chemosensory receptors in the olfactory epithelium. Nature (Lond) 442:645–650
Liu WL, Shipley MT (1994) Intrabulbar associational system in the rat olfactory bulb comprises cholecystokinin-containing tufted cells that synapse onto the dendrites of GABAergic granule cells. J Comp Neurol 346:541–558
Lodovichi C, Belluscio L, Katz LC (2003) Functional topography of connections linking mirror-symmetric maps in the mouse olfactory bulb. Neuron 38:265–276
Marks CA, Cheng K, Cummings DM, Belluscio L (2006) Activity-dependent plasticity in the olfactory intrabulbar map. J Neurosci 26:11257–11266
Matsumoto H, Kobayakawa K, Kobayakawa R, Tashiro T, Mori K, Sakano H (2010) Spatial arrangement of glomerular molecular-feature clusters in the odorant-receptor class domains of the mouse olfactory bulb. J Neurophysiol 103:3490–3500
Migliore M, Hines ML, McTavish TS, Shepherd GM (2010) Functional roles of distributed synaptic clusters in the mitral-granule cell network of the olfactory bulb. Front Integr Neurosci 4:122
Mombaerts P (2006) Axonal wiring in the mouse olfactory system. Annu Rev Cell Dev Biol 22:713–737
Mombaerts P, Wang F, Dulac C, Chao SK, Nemes A et al (1996) Visualizing an olfactory sensory map. Cell 87:675–686
Moncrieff RW (1967) The chemical senses. Leonard Hill, London
Mori K (1987) Membrane and synaptic properties of identified neurons in the olfactory bulb. Prog Neurobiol 29:275–320
Mori K, Sakano H (2011) How is the olfactory map formed and interpreted in the mammalian brain? Annu Rev Neurosci 34:467–499
Mori K, Takahashi Y, Igarashi K, Yamaguchi M (2006) Maps of odorant molecular features in the mammalian olfactory bulb. Physiol Rev 86:409–433
Nagao H, Yoshihara Y, Mitsui S, Fujisawa H, Mori K (2000) Two mirror-image sensory maps with domain organization in the mouse main olfactory bulb. Neuroreport 11:3023–3027
Pacifico R, Dewan A, Cawley D, Guo C, Bozza T (2012) An olfactory subsystem that mediates high-sensitivity detection of volatile amines. Cell Rep 2:76–88
Ressler KJ, Sullivan SL, Buck LB (1994) Information coding in the olfactory system: evidence for a stereotyped and highly organized epitope map in the olfactory bulb. Cell 79:1245–1255
Rossiter KJ (1996) Structure–odor relationships. Chem Rev 96:3201–3240
Saucier D, Astic L (1986) Analysis of the topographical organization of olfactory epithelium projections in the rat. Brain Res Bull 16:455–462
Schoenfeld TA, Macrides F (1984) Topographic organization of connections between the main olfactory bulb and pars externa of the anterior olfactory nucleus in the hamster. J Comp Neurol 227:121–135
Schoenfeld TA, Marchand JE, Macrides F (1985) Topographic organization of tufted cell axonal projections in the hamster main olfactory bulb: an intrabulbar associational system. J Comp Neurol 235:503–518

Schoenfeld TA, Clancy AN, Forbes WB, Macrides F (1994) The spatial organization of the peripheral olfactory system of the hamster. Part I: receptor neuron projections to the main olfactory bulb. Brain Res Bull 34:183–210

Shepherd G, Chen WR, Greer CA (eds) (2004) Olfactory bulb. Oxford University Press, New York, pp 165–216

Takahashi Y, Kurosaki M, Hirono S, Mori K (2004) Topographic representation of odorant molecular features in the rat olfactory bulb. J Neurophysiol 92:2413–2427

Takeuchi H, Inokuchi K, Aoki M, Suto F, Tsuboi A et al (2010) Sequential arrival and graded secretion of Sema3F by olfactory neuron axons specify map topography at the bulb. Cell 141:1056–1067

Tsuboi A, Miyazaki T, Imai T, Sakano H (2006) Olfactory sensory neurons expressing class I odorant receptors converge their axons on an antero-dorsal domain of the olfactory bulb in the mouse. Eur J Neurosci 23:1436–1444

Vassar R, Chao SK, Sitcheran R, Nunez JM, Vosshall LB, Axel R (1994) Topographic organization of sensory projections to the olfactory bulb. Cell 79:981–991

Willhite DC, Nguyen KT, Masurkar AV, Greer CA, Shepherd GM, Chen WR (2006) Viral tracing identifies distributed columnar organization in the olfactory bulb. Proc Natl Acad Sci USA 103:12592–12597

Yan Z, Tan J, Qin C, Lu Y, Ding C, Luo M (2008) Precise circuitry links bilaterally symmetric olfactory maps. Neuron 58:613–624

Yoshihara Y, Kawasaki M, Tamada A, Fujita H, Hayashi H et al (1997) OCAM: A new member of the neural cell adhesion molecule family related to zone-to-zone projection of olfactory and vomeronasal axons. J Neurosci 17:5830–5842

Zhang X, Firestein S (2002) The olfactory receptor gene superfamily of the mouse. Nat Neurosci 5:124–133

Zhou Z, Belluscio L (2008) Intrabulbar projecting external tufted cells mediate a timing-based mechanism that dynamically gates olfactory bulb output. J Neurosci 28:9920–9928

Chapter 5
Zebrafish Olfactory System

Yoshihiro Yoshihara

Abstract Similar to other animal species, fishes efficiently use the sense of smell for locating food, detecting danger, communicating social information, and memorizing beneficial and detrimental conditions. This review summarizes recent advances in our knowledge of the olfactory system in the zebrafish (*Danio rerio*), which has become one of the most useful and important model organisms in neurobiology. Olfactory receptors belonging to the OR, V1R, V2R, and TAAR families are differentially expressed in three types of the olfactory sensory neurons (ciliated, microvillus, and crypt) in the olfactory epithelium. In the olfactory bulb, nine glomerular clusters are clearly delineated by anatomical features and molecular markers, serving as functional units important for odor information categorization, coding, and processing. Individual output neurons of the olfactory bulb project axons to a combination of four major target regions in the forebrain: the posterior zone of dorsal telencephalon, the ventral nucleus of ventral telencephalon, the posterior tuberculum, and the right habenula. Distinct modes of odor information decoding are employed by the individual olfactory centers: either nonselective or biased as well as either diffuse or convergent, which contribute to eliciting different physiological and behavioral responses. By taking advantage of its small brain, transparency of larvae, and amenability to various genetic and imaging techniques, zebrafish will pave the way toward understanding the functional organization of the olfactory system as a whole.

Keywords Alarm pheromone • Foraging behavior • Glomerular clusters • Higher olfactory centers • Odor map • Olfactory conditioning • Olfactory imprinting • Sex pheromone • Zebrafish

Y. Yoshihara (✉)
RIKEN Brain Science Institute, 2-1 Hirosawa, Wako, Saitama 351-0198, Japan
e-mail: yoshihara@brain.riken.jp

K. Mori (ed.), *The Olfactory System: From Odor Molecules to Motivational Behaviors*,
DOI 10.1007/978-4-431-54376-3_5,

5.1 Introduction

Many chemical cues pervade the aquatic environment of fish, activate the olfactory system, and elicit various physiological and behavioral responses. Fish can detect a huge variety of odorants that are emitted from objects and dissolved in the water, such as amino acids, nucleotides, bile acids, amines, steroids, and prostaglandins. The fish olfactory system is highly elaborated to receive and discriminate these odorant molecules, to transmit their signals to the brain, and to evoke fundamental behaviors important for survival of individuals and preservation of species, including food finding, predator avoidance, social communication, mate choice, and spawning migration (Sorensen and Caprio 1998; Zielinski and Hara 2007; Yoshihara 2009).

Zebrafish, a freshwater small teleost fish commonly available in pet shops, offers numerous advantages over other vertebrates for biological studies. Zebrafish are easy to grow and produce large clutches of eggs (100–200 per mating) through external fertilization (Westerfield 1995). The embryos develop quickly, hatching as early as 3 days post fertilization (dpf), and start to swim at 5 dpf. The zebrafish embryos are optically transparent throughout early developmental stages, enabling us to observe organogenesis and morphogenesis in vivo. In particular, transgenic expression of green fluorescent protein (GFP) and its derivatives in selected cell types greatly facilitates the live imaging of dynamic developmental events such as cell division, cell migration, and neural circuit formation. Furthermore, it has recently become possible to image functional neural activities in living transgenic embryos in which genetically engineered, highly sensitive Ca^{2+} indicators are expressed (Ahrens et al. 2013; Muto et al. 2013).

Another major advantage of using the zebrafish is its amenability of various genetic engineering techniques in both forward and reverse directions, including mutagenesis, transgenesis, gene knockdown, and gene knockout. Most recently, in particular, the whole genome sequence of zebrafish has been reported (Howe et al. 2013), and disruptive mutations in more than 38 % of all known protein-coding regions were identified (Kettleborough et al. 2013). These mutant fish will become available to the scientific community, which undoubtedly accelerate the zebrafish research in all fields of biology. In addition to these basic techniques, more advanced genetic methods have been developed in the zebrafish, such as the Tol2 transposon-mediated gene trap approach combined with the Gal4/UAS system (Asakawa et al. 2008: Koide et al. 2009), retrovirus-mediated large-scale enhancer trap screening (Ellingsen et al. 2005), Cre/loxP- and/or Gal4/UAS-mediated single-cell mosaic labeling analysis (Sato et al. 2007a; Miyasaka et al. 2009; Miyasaka et al. 2014), and TALEN- or CRISPR/Cas-mediated genome editing (Bedell et al. 2012; Hwang et al. 2013; Zu et al. 2013). Thus, the zebrafish is one of the most useful vertebrate species with which we can perform both forward and reverse genetic analyses, similar to *Drosophila melanogaster* and *Caenorhabditis elegans*.

This review highlights recent progress in our knowledge on the zebrafish olfactory system with special emphasis on neuroanatomical and functional correlates.

5.2 Olfactory Sensory Neurons

In many mammals, two functionally distinct classes of chemicals (odorants and pheromones) are detected by different types of sensory neurons located in two anatomically segregated olfactory organs in the nose: the olfactory epithelium (OE) and the vomeronasal organ (Buck 2000; Mombaerts 2004). Volatile odorants are received by a huge repertoire of odorant receptors (ORs: ~1,200 genes in mice) expressed by ciliated olfactory sensory neurons (OSNs) in the OE, and the information is transferred to the main olfactory bulb (OB). On the other hand, pheromones are mostly received by two families of vomeronasal receptors, V1Rs and V2Rs (each ~150 genes in mice), expressed by microvillus sensory neurons in the vomeronasal organ, which project axons to the accessory OB. In addition, recent studies have identified trace amine-associated receptors (TAARs) as the fourth family of olfactory receptors that are expressed by ciliated OSNs and take charge of specific pheromone or kairomone signaling (Liberles and Buck 2006; Ferrero et al. 2011; Li et al. 2013; Dewan et al. 2013).

In contrast, the anatomical organization of the olfactory system in fish species is different from that of mammals. Teleost fishes including zebrafish possess only a single type of olfactory organ called the olfactory rosette that contains three morphologically distinct types of OSNs: ciliated, microvillus, and crypt OSNs (Fig. 5.1) (Hansen and Zeiske 1998; Hansen et al. 2003, 2004). All these OSN types innervate the same OB via a tightly fasciculated bundle of olfactory nerves. Two major types of OSNs are the ciliated and microvillus neurons that differ from one another with respect to morphology and their relative positions in the OE. The ciliated OSNs are situated in the deep layer of the OE, project a long dendrite, and extend several long cilia into the lumen of the nasal cavity. The microvillus OSNs are located in the superficial layer, project a shorter dendrite, and emanate tens of short microvilli. The third OSN type is crypt cells, which account for only a small population in the OE, are located in the most superficial part of the OE, and have unique ovoid cell bodies bearing microvilli as well as submerged short cilia.

5.3 Olfactory Receptors

The ciliated, microvillus, and crypt OSNs display distinct profiles of functional molecular expression (Yoshihara 2009). The most noteworthy and functionally important is the expression of different families of olfactory receptors. The zebrafish genome harbors ~140 OR-type, 6 V1R-type, ~50 V2R-type, and ~100 TAAR-type olfactory receptor genes (Alioto and Ngai 2005, 2006; Hashiguchi and Nishida 2006, 2007; Ngai and Alioto 2007; Saraiva and Korsching 2007). The expression of OR-type olfactory receptors is observed in ciliated OSNs in teleost fishes, whereas V2R-type olfactory receptors are found in the microvillus OSNs (Cao et al. 1998; Speca et al. 1999; Hansen et al. 2004; Sato et al. 2005). It has been

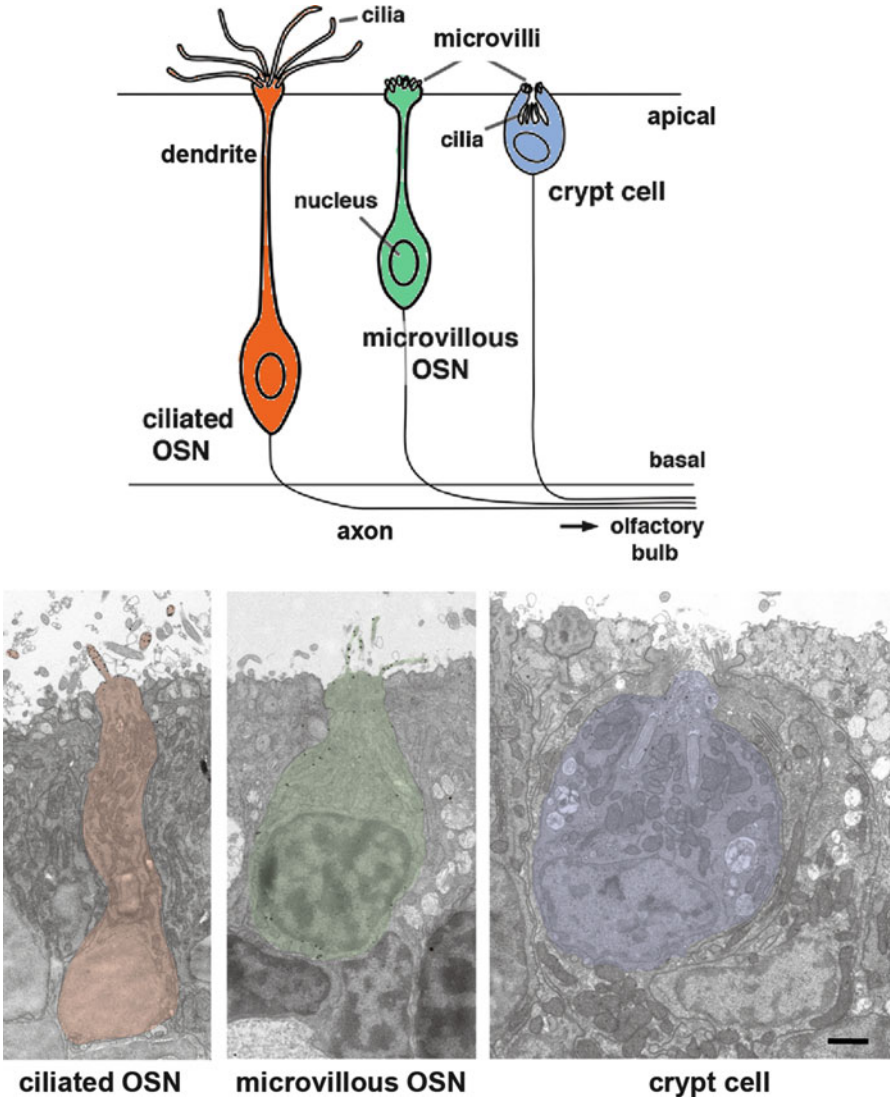

Fig. 5.1 Three types of olfactory sensory neurons (*OSN*s) in zebrafish. The *upper drawing* depicts morphological features of ciliated (*orange*), microvillus (*green*), and crypt (*blue*) OSNs. *Lower panels* show representative electron microscopic images of three OSNs. (Courtesy of Drs. Takumi Akagi and Tsutomu Hashikawa, RIKEN Brain Science Institute)

reported that mammalian ORs detect hydrophobic, volatile molecules, and V2Rs recognize hydrophilic, highly water-soluble compounds (Mombaerts 2004). Therefore, it is likely that the ciliated and microvillus OSNs in fish also take charge of detecting chemical compounds with different physical properties (e.g., hydrophobic bile acids vs. hydrophilic amino acids) through the two distinct families of olfactory

receptors (ORs andV2Rs). Several lines of evidence support this notion, based on molecular biological, electrophysiological, and activity-dependent labeling experiments (Michel and Derbidge 1997; Speca et al. 1999; Michel 1999; Lipschitz and Michel 2002; Nikonov and Caprio 2007). In contrast, V1R-type olfactory receptors are expressed in either the crypt cells or a small subset of the microvillus OSNs (unpublished observations). Intriguingly, the crypt cells express only one of the six V1R-type olfactory receptors, V1R4 (Oka et al. 2012).

The gene repertoires of OR-, V1R-, and V2R-type olfactory receptors in zebrafish are significantly smaller than those in mouse by an order of magnitude (Shi and Zhang 2009). In contrast, the zebrafish genome is equipped with as many as ~100 genes for TAAR-type olfactory receptors that far exceed TAAR genes in any other organisms examined (e.g., 6 in human, 17 in rat, 16 in mouse, 13 in Fugu fish) (Gloriam et al. 2005; Korsching 2009; Shi and Zhang 2009). Such a huge diversity of TAAR genes in the zebrafish suggests the possibility that this fish species can detect and discriminate various amine compounds. Although it remains unknown what physiological and behavioral responses are induced by amines in the environmental water, it is likely that these amines play some important roles as odorants, pheromones, or kairomones in the zebrafish.

In mouse, each OSN expresses only one type of OR gene of a repertoire of ~1,200 genes equipped in the genome (Chess et al. 1994; Serizawa et al. 2003; Mori and Sakano 2011). This "one neuron–one receptor" rule enables individual OSNs to respond to a range of odorants that bind to the expressed ORs. In other words, OSNs expressing a given OR are tuned to a particular molecular receptive range. Is the one neuron–one receptor rule applicable also to the zebrafish olfactory system? Individual OR-type olfactory receptor genes are expressed in a small population of OSNs, ranging from 0.5 % to 2 % (Barth et al. 1996). Double-fluorescence in situ hybridization experiments revealed that most combinations of two OR-type receptor probes label nonoverlapping populations of OSNs (Barth et al. 1997; Sato et al. 2007b). These results support the notion that the zebrafish OSNs fundamentally obey the one neuron–one receptor rule. However, two exceptional cases have been reported for particular olfactory receptors, in which "one neuron–multiple receptors" is true. One is the case for a subpopulation of ciliated OSNs expressing the OR103 family members: OR103-1-positive OSNs simultaneously express OR103-2 and/or OR103-5 (Sato et al. 2007b). Coexpression of multiple chemosensory receptors has been shown in several populations of OSNs in *C. elegans* and *Drosophila* (Troemel et al. 1995; Goldman et al. 2005). For example, a single AWC neuron in *C. elegans* expresses multiple olfactory receptors, responds to various odorants without discrimination, and mediates attractive behavior to all these odorants (Bargmann et al. 1993; Troemel et al. 1995). By analogy, it is likely that zebrafish do not need to discriminate a range of odorants received by the individual OR103 subfamily members. These OSNs expressing multiple OR103 members thus may integrate odor information at the most peripheral level, leading to particular behavioral or endocrine responses. The other case is a broad expression of a V2R-type receptor, OlfCc1 (VR5.3; V2rl1), in almost all microvillus OSNs (Sato et al. 2005). This situation is reminiscent of *Drosophila* Orco (Or83b) and mouse V2R2 olfactory receptors (Larsson et al. 2004; Martini

et al. 2001). *Drosophila* Orco is broadly expressed in almost all OSNs together with a selectively expressed OR and plays a general role as a hetero-dimerization partner for the selected regular OR to constitute a cation channel (Sato et al. 2008; Wicher et al. 2008). In conclusion, both "one neuron–one receptor" and "one neuron–multiple receptor" cases are observed in zebrafish, probably depending on the divergence of relevant functions in distinct types of OSNs.

5.4 Glomeruli

Glomeruli are spherical neuropils deployed on the surface of the OB where odor information is transmitted across a synapse from OSNs to the second-order neurons in the OB. Orderly arranged glomerular architecture is observed in fishes, similar to mammals and insects. There are about 140 glomeruli in zebrafish, among which 27 glomeruli are clearly identifiable whereas others are ambiguous, tiny, or sometimes fused (Baier and Korsching 1994; Braubach et al. 2012). Although the boundaries of individual glomeruli in zebrafish are, in most cases, not so clear as those in mice and *Drosophila*, a unique feature of glomerular organization is observed in the zebrafish: the presence of easily discernible glomerular clusters (Fig. 5.2). Based on their spatial locations, shapes, and molecular markers, nine glomerular clusters can be delineated and designated as dorsal glomerular cluster (dG), dorso-lateral (dlG), lateral (lG), medio-anterior (maG), medio-posterior (mpG), medio-dorsal (mdG), ventro-anterior (vaG), ventro-medial (vmG), and ventro-posterior (vpG) (Braubach et al. 2012). Individual glomerular clusters display characteristic molecular receptive ranges and play crucial roles as functional units for coding of structurally and functionally different odor categories (see following).

A recent study revealed that the zebrafish OB glomeruli can be classified into two distinct groups with respect to developmental process, anatomical size, and structural/functional stability: early-generated, highly stereotypic, large, stable glomeruli versus later-developing, smaller, plastic glomeruli (Braubach et al. 2013). The maturation of small glomeruli is heavily dependent on olfactory experience, and they are variable across individuals, whereas large and identifiable glomeruli grow steadily irrespective of sensory inputs. Thus, the two types of glomeruli form at different times and display distinct maturation mechanisms in either sensory input-dependent or input-independent manners, probably reflecting their involvement in different types of olfactory outputs: experience-dependent plastic responses versus hard-wired innate responses.

5.5 Olfactory Axon Projection

A number of neuroanatomical tracing studies were conducted for analysis of neural circuitry in the fish olfactory system (Morita and Finger 1998; Hamdani et al. 2001; Hamdani and Doving 2002, 2006; Hansen et al. 2003). For example, a lipophilic

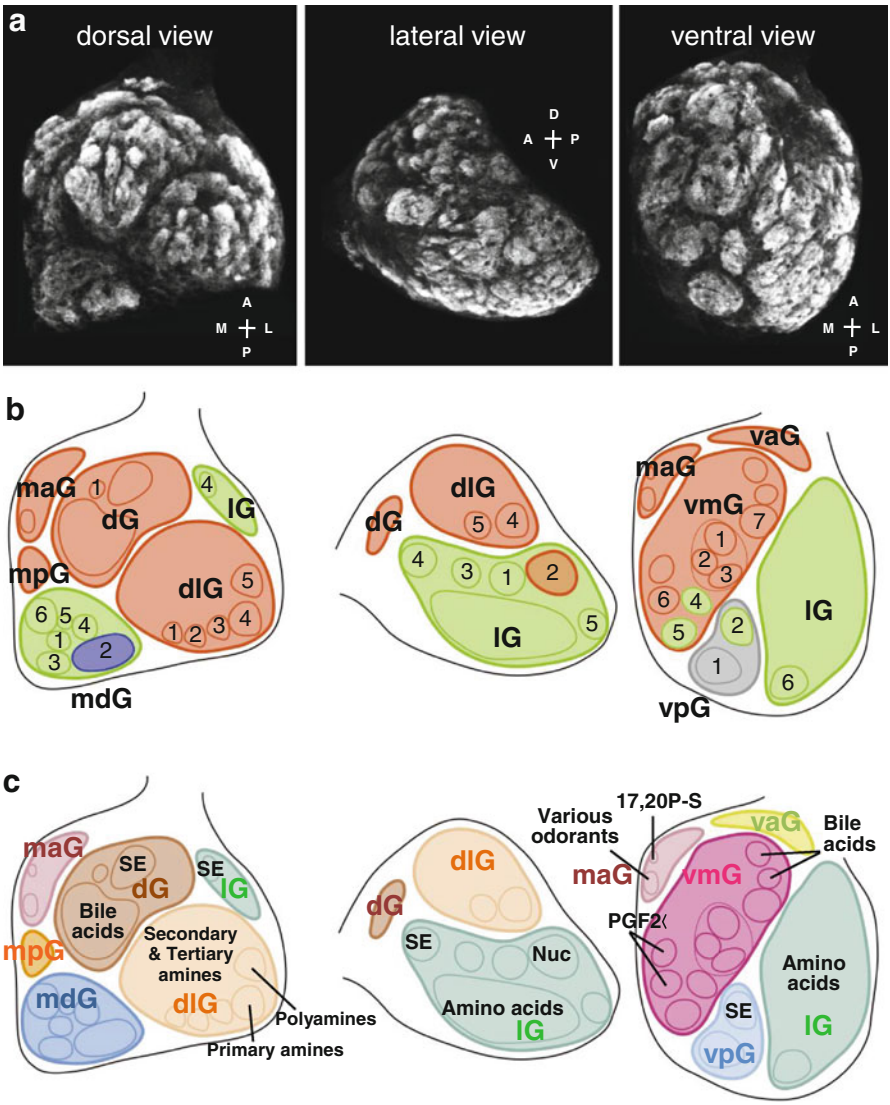

Fig. 5.2 Glomerular clusters and odor map in the zebrafish olfactory bulb (*OB*). (**a**) Whole-mount OB immunostained with anti-SV2 antibody, viewed from dorsal, lateral, and ventral sides. (**b**) Eight glomerular clusters and 29 identifiable glomeruli. (**c**) Odor map. *Nuc* nucleotides, *SE* skin extract, *dG* dorsal glomerular, *dlG* dorso-lateral, *lG* lateral, *maG* medio-anterior, *mpG* medio-posterior, *mdG* medio-dorsal, *vaG* ventro-anterior, *vmG* ventro-medial, *vpG* ventro-posterior

fluorescent tracer, DiI, was injected into a small area of the OB, taken up by olfactory axon terminals in glomeruli, and retrogradely transported to the OE. Subsequently, the types of DiI-labeled OSNs were determined on the basis of cellular morphology and location in the OE. Their results implied a tendency of

axonal segregation from the distinct types of OSNs to different regions of the OB. However, it was impossible with such a conventional tracing method to elucidate detailed patterns of axon projection from the distinct types of OSNs to individual glomeruli.

The introduction of genetic technology such as transgenesis and gene trap approaches opened a new avenue in the zebrafish olfactory research and unambiguously solved the issue on axonal wiring from the OE to the OB (Miyasaka et al. 2005, 2007; Sato et al. 2005, 2007b; Koide et al. 2009). The two major types of OSNs, ciliated and microvillus OSNs, can be differentially labeled with spectrally distinct fluorescent proteins (e.g., RFP and Venus) under the control of zebrafish OMP and TRPC2 gene promoters, respectively (Sato et al. 2005). In these double transgenic zebrafish (OMP-RFP; TRPC2-Venus), fluorescence images of whole-mount OB clearly show that the ciliated OSNs project axons mostly to the dorsal and medial regions of the OB, whereas the microvillus OSNs project axons to the lateral region. A careful histological analysis of OB sections indicates that the two distinct types of OSNs innervate different glomeruli in a mutually exclusive manner. Importantly, there is no double-positive glomerulus that receives convergent inputs from both types of OSNs. Together with immunohistochemical results with several marker antibodies (Braubach et al. 2012) and transgene expression patterns in specific subsets of OSNs in several gene trap lines (Koide et al. 2009), the primary olfactory projection in the zebrafish is summarized in Fig. 5.2b. According to the nomenclature of identifiable glomeruli and glomerular clusters in the zebrafish OB by Braubach et al. (2012), the ciliated OSNs project their axons to the maG, vaG, dG, and dlG clusters, mpG glomerulus, lG2 glomerulus, and most of vmG glomeruli, whereas the microvillus OSNs innervate all glomeruli in the lG cluster except for lG2, one of the two vpG glomeruli, and several mdG glomeruli. The third minor type of OSNs, crypt cells, send axons to at least one particular glomerulus mdG2, as demonstrated by the immunohistochemical staining of the OB with antibody against crypt cell-specific S100 calcium-binding protein (Germana et al. 2004, 2007; Oka et al. 2012; Braubach et al. 2012). These segregated neural pathways are important prerequisites for representation of distinct olfactory information on the OB as an "odor map" (see following).

5.6 Odor Map

The odor map is a central representation of chemical structural features in odorants that are systematically arranged on a two-dimensional glomerular sheet of the first relay station along the olfactory neural circuitry (Mori et al. 1999; Mori and Sakano 2011). In other words, each glomerulus represents a single olfactory receptor and is tuned to specific molecular features of odorants that can activate the receptor. The concept of the odor map was first described in the rabbit OB by electrophysiological single-unit recording of spike discharges from mitral and tufted cells to odor stimuli (Mori et al. 1992) and subsequently confirmed in various mammalian and

insect species upon the emergence and refinement of neural activity imaging techniques (Rubin and Katz 1999; Uchida et al. 2000; Wang et al. 2003; Mori et al. 2006; Vosshall and Stocker 2007; Mori and Sakano 2011).

A series of pioneering studies measuring glomerular activities with conventional voltage-sensitive dyes or Ca^{2+} indicators demonstrated the existence of an odor map also in the zebrafish OB (Friedrich and Korsching 1997, 1998; Fuss and Korsching 2001). Thereafter, genetically engineered Ca^{2+} probes (e.g., Inverse Pericam; GCaMP) were introduced to analyze the developmental and functional aspects of the zebrafish OB odor map in a more detailed and comprehensive manner (Li et al. 2005; unpublished observation). Furthermore, an immunohistochemical analysis using anti-phosphorylated Erk (MAP kinase) antibody has recently turned out to be a convenient and powerful tool to visualize glomerular activation upon odorant stimulation (unpublished observation). These findings revealed that various kinds of water-soluble compounds are represented on the surface of the OB in a highly systematic fashion and that the glomerular clusters play important roles as functional units for coding of different categories of odorants (Fig. 5.2c). For example, the dG cluster responds predominantly to bile acids, whereas the dlG cluster is exclusively devoted to amines (see following). Although the majority of glomeruli display specific activation to particular odorants, there is one glomerulus in the maG cluster that responds to various different odorants without selectivity. This glomerulus might function as a "generalist" to elicit olfactory alertness, responding to the presence of any odor stimuli (unpublished observation).

5.6.1 *Amino Acids*

Amino acids strongly attract fishes as food-derived odorants (Steele et al. 1990, 1991; Koide et al. 2009). Zebrafish are capable of discriminating between different amino acids (Miklavc and Valentincic 2012). Amino acids are detected mostly by microvillus OSNs through binding to V2R-type olfactory receptors (Speca et al. 1999; Hansen et al. 2003; Luu et al. 2004) and activate multiple glomeruli in the lG cluster (Friedrich and Korsching 1997, 1998; Fuss and Korsching 2001). Structural features of side chains in individual amino acids (e.g., long or short; hydrophilic or hydrophobic; acidic, neutral, or basic) are represented as a combinatorial code in spatially confined glomerular groups in the lateral cluster.

5.6.2 *Bile Acids*

Bile acids are biliary steroids synthesized in the liver, stored in the gallbladder, secreted into the intestine, and reabsorbed by the enterohepatic system. Interestingly, various fishes produce species-specific bile acid derivatives, such as cyprinol sulfate in carp (*Cyprinus carpio*), petromyzonol sulfate in sea lamprey

(*Petromyzon marinus*), and myxinol disulfate in hagfish (*Mixni*) (Hagey et al. 2010), suggesting their potential roles in olfactory-mediated social interaction. In the sea lamprey, for example, specific bile acids are released into the environment to act as sex and migratory pheromones, respectively (Li et al. 2002; Sorensen et al. 2005). In zebrafish, taurocholic acid activates a population of OSNs (Michel and Lubomudrov 1995) and induces a significant attractive response (Koide et al. 2009). Bile acids activate ciliated OSNs possibly via the OR-type olfactory receptors -G_{olf}- cyclic AMP signaling cascade (Hansen et al. 2003; unpublished observation). In the zebrafish OB, various bile acids elicit strong responses in the dG cluster and the anterior part of the vmG cluster (Friedrich and Korsching 1998; unpublished observation). The activity patterns induced by different bile acids show a similar but not identical distribution, indicating that distinct molecular features in bile acids are represented in the dG and vmG clusters in a combinatorial manner.

5.6.3 Amines

Although the physiological functions as odorants are enigmatic, amines should be definitely important olfactory stimuli to zebrafish from the following three reasons. First, the zebrafish genome is equipped with the largest number of amine receptors, TAARs, in all animal species examined (Gloriam et al. 2005; Korsching 2009; Shi and Zhang 2009). Second, several amine compounds induce strong electro-olfactogram responses in the zebrafish OE (Michel et al. 2003). Third, the dlG cluster in the OB is almost completely devoted to amine responses (unpublished observation). The dlG is composed of several tens of small glomeruli, among which five glomeruli (dlG1-5) are identifiable based on their unique position, morphology, and molecular expression (Braubach et al. 2012). Distinct glomeruli in the dlG tend to be activated by structurally different categories of amines: dlG4 by primary amines, dlG5 by polyamines, and many glomeruli in the anterior part of dlG by secondary and tertiary amines. Thus, there is a clear topographic map for structural features of amines in the dlG.

5.6.4 Nucleotides

Nucleotides such as ATP, IMP, and ITP induce excitatory responses in fish OE and bulbar neurons (Kang and Caprio 1995; Nikonov and Caprio 2001), possibly acting as feeding cues together with amino acids (Carr 1988). An immunohistochemical analysis with anti-phospho-Erk antibody revealed that nucleotides activate a small population of OSNs bearing a short dendrite and locating in the apical portion of OE (unpublished observation). However, these OSNs are positive for OMP promoter-driven RFP, but negative for TRPC2 promoter-driven GFP (Sato et al. 2005). Thus, nucleotides appear to activate a peculiar subset of ciliated OSNs whose morphology is similar to that of microvillus OSNs. Because the amine moiety is

contained in structure of purines and pyrimidines, it is likely that nucleotides are detected by ciliated OSNs expressing TAARs. In the OB, nucleotides activate a specific single glomerulus lG2 belonging to the lG cluster (Koide et al., in preparation). Although all other glomeruli in the lG cluster are innervated by microvillus OSNs, only the lG2 is innervated by G_{olf}-positive ciliated OSNs (Braubach et al. 2012). However, it remains largely unknown what physiological or behavioral responses are induced by nucleotides as olfactory stimulants in zebrafish.

5.6.5 Sex Pheromones

Two classes of sex pheromones, primers and releasers, acting on different steps of reproductive responses have been identified in various teleost fishes: steroid derivatives and prostaglandins, respectively (see following for details). In zebrafish OB, two sex pheromones evoke neural responses in only one or two glomeruli (Friedrich and Korsching 1998; Koide et al., in preparation). A primer pheromone, 17α,20β-dihydroxy-4-pregnen-3-one-20-sulfate (17,20P-S), activates a single or few glomeruli in the maG cluster, whereas a releaser pheromone, prostaglandin F2α (PGF2α), activates two glomeruli in the vmG cluster.

5.6.6 Skin Extract

In various fish species, putative alarm pheromones released from the injured skin of conspecifics induce robust aversive responses of other nearby fish (see following). Although two candidate molecules were reported as alarm pheromones in zebrafish (Pfeiffer et al. 1985; Mathuru et al. 2012), their validity still remains controversial. When the conspecific skin extract, a mixture of various compounds including a putative alarm pheromone, is applied to the OE, three glomerular foci are specifically activated in the OB: the anterior part of the dG cluster, the most anterior glomerulus (lG4) in the lG cluster, and one glomerulus (vpG2) in the vpG cluster (unpublished observation). At present, however, it remains unknown which glomerulus (or glomerular combination) is responsible for mediating the aversive responses to the alarm pheromone.

In addition to the aforementioned spatial representation of odorant structural features on the OB, several electrophysiological and activity imaging studies proposed the temporal coding of odor quality and intensity and the odor information processing by neuronal populations in the fish OB (Kang and Caprio 1995; Friedrich and Laurent 2001; Friedrich et al. 2004; Niessing and Friedrich 2010; Wiechert et al. 2010). For details, see reviews by Laberge and Hara (2001), Friedrich (2006), and Friedrich et al. (2009).

5.7 Higher Olfactory Centers

Odorant and pheromone information represented on the glomerular map of the OB is next transferred via the second-order projection neurons, mitral cells, to several distinct regions in the forebrain. In these higher olfactory centers, the information is decoded and processed in different manners to perceive, discriminate, and memorize odorants, to change hormonal secretion and reproductive activity, and to elicit various olfactory behaviors such as attraction to foods, escape from predators, social communication with company, and spawning migration to home rivers. Compared with a wealth of knowledge on functional correlates in the OE and OB, little has been elucidated on the molecular, cellular, and circuit mechanisms underlying odor coding and processing in higher olfactory centers in fish (Nikonov et al. 2005). However, physiological and anatomical studies have begun to shed light on basic principles of odor information representation and computation in the secondary olfactory circuitry of zebrafish (Yaksi et al. 2009; Miyasaka et al. 2009; Blumhagen et al. 2011). In particular, the most recent study combining a genetic single-neuron labeling method with the image registration system has uncovered a nearly comprehensive axon projection map from the OB to higher bran centers in zebrafish larvae (Miyasaka et al. 2014).

The OB output neurons project axons to the four major target regions in the forebrain: the posterior zone of dorsal telencephalon (Dp), the ventral nucleus of ventral telencephalon (Vv), the posterior tuberculum (PT), and the right habenula (rHb) (Fig. 5.3). In addition, approximately one-third of OB output neurons send axonal branches back into the OB ipsilaterally, contralaterally, or both. The higher olfactory centers receive odor information from OB glomeruli (and glomerular clusters) in a highly specific manner, either nonselective or biased as well as either diffuse or convergent, which is important for eliciting different olfactory outputs.

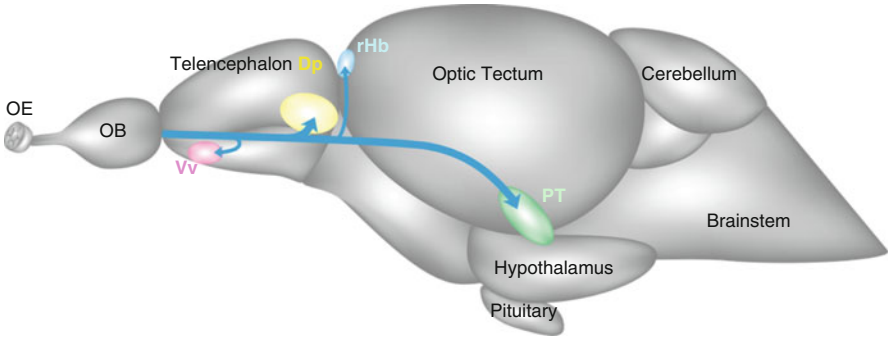

Fig. 5.3 Secondary olfactory pathway from the *OB* to higher brain centers. The four major targets of OB output neurons are highlighted: Dp (*yellow*), Vv (*pink*), rHb (*light blue*), and PT (*green*)

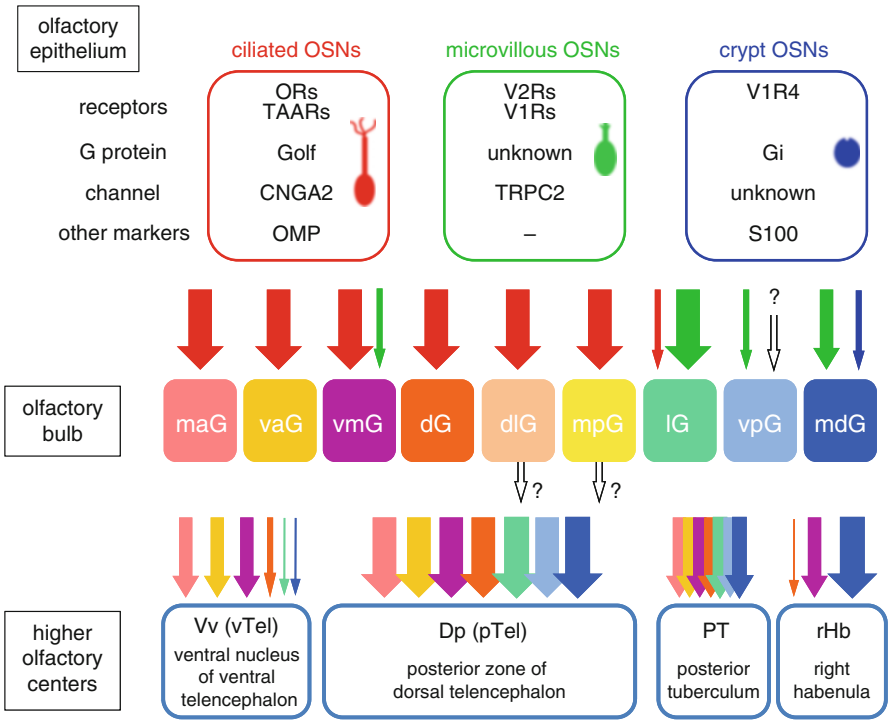

Fig. 5.4 Odor information flows from the olfactory epithelium (*OE*) to the OB and further to higher olfactory centers. Three types of OSNs express distinct receptors and other functional molecules and project axons to different sets of glomerular clusters. The odor information received by distinct glomerular clusters in the OB is next transferred to the four brain regions in higher olfactory centers, where different modes of odor information decoding are performed: either nonselective or biased and either sparse or convergent

5.7.1 Posterior Zone of the Dorsal Telencephalon (Dp)

The Dp, a pallial structure located in the dorsoposterior telencephalon, constitutes the largest part of the secondary olfactory centers in zebrafish. Genetic single-neuron visualization revealed that all the labeled OB output neurons project axons to the Dp with extensive overlap. Within the Dp, the large core region samples intermingled inputs from all the glomerular clusters (Fig. 5.4), thus transforming topographic information in the OB to broad and sparse representations (Miyasaka et al. 2014). An optical imaging study showed that individual Dp neurons extract information about discrete combinations of odorant molecular features from ensembles of glomeruli to establish representations of higher-order olfactory objects (Yaksi et al. 2009). These anatomical and functional features of the central Dp indicate that it may correspond to the piriform cortex in mammals (Ghosh et al. 2011; Miyamichi et al. 2011; Sosulski et al. 2011; Igarashi et al. 2012) and the mushroom body in *Drosophila* (Jefferis et al. 2007; Lin et al. 2007;

Caron et al. 2013), where information from the OB and the antennal lobe is computed for odor discrimination and olfactory memory. In contrast, the marginal portion of Dp is divided into several subregions that receive biased inputs from particular glomerular clusters. Thus, these Dp subregions could specifically respond to distinct categories of odorants (Miyasaka et al. 2014). This notion is supported by the fact that the anterior and posterior parts of Dp show biased responses to bile acids and amino acids, respectively (Yaksi et al. 2009).

5.7.2 Ventral Nucleus of the Ventral Telencephalon (Vv)

Another telencephalic target of OB output neurons is the Vv, a subpallial region in the ventro-anterior telencephalon. Although the Vv is thought to be equivalent to the septum and striatum in mammals, based on the expression patterns of molecular markers (Ganz et al. 2012; Wullimann and Mueller 2004), it remains largely unknown what brain functions the Vv neurons exert in fish. In contrast to the Dp, which is innervated by all the OB output neurons, the Vv receives massive inputs from particular glomerular clusters: maG, vaG, vmG, and dG (Fig. 5.4) (Miyasaka et al. 2014). These four glomerular clusters are innervated by ciliated OSNs expressing OR-type olfactory receptors that detect socially relevant odor cues such as bile acids and prostaglandins. Because the Vv neurons are reciprocally connected with the preoptic and hypothalamic areas (Rink and Wullimann 2004), the Vv might have some role in transformation of the odor and pheromone information into various social behaviors and endocrine responses.

5.7.3 Posterior Tuberculum (PT)

In addition to the two major telencephalic targets, the OB output neurons directly send axons to two diencephalic regions in zebrafish. One is the posterior tuberculum (PT), a hypothalamus-related region containing groups of dopaminergic neurons (Schweitzer et al. 2012). One or two axon branches of OB output neurons emanate from the posterior telencephalon, extend a long distance through the medial forebrain bundle, and finally reach the PT (Miyasaka et al. 2014). These axons appear to make close contacts with the dopaminergic neurons in the PT. The PT receives convergent inputs from all the glomerular clusters (Fig. 5.4), suggesting a wide range of responsiveness of PT neurons to various odor stimuli. In the sea lamprey, a group of dopaminergic neurons in the PT mediates olfactory-locomotor transformation by relaying the odor information from the OB to the reticulospinal neurons via the mesencephalic locomotor region (Ren et al. 2009; Derjean et al. 2010). Therefore, it is likely that the OB–PT pathway drives the descending neural circuitry for locomotion also in zebrafish, irrespective of odor classes and output

responses, either attraction or aversion. A small population of dopaminergic neurons in the zebrafish PT sends ascending projection to the ventral telencephalon (Tay et al. 2011), which is reminiscent of dopaminergic neurons in the ventral tegmental area and the substantia nigra in mammals. Thus, the OB–PT pathway might be also involved in controlling brain functions such as motivation, reward, and emotions.

5.7.4 Right Habenula (rHb)

The habenula is an epithalamic structure conserved among all vertebrate species. In mammals, the habenula relays information from the forebrain to the midbrain nuclei such as the interpeduncular nucleus, the raphe nuclei, the substantia nigra, and the ventral tegmental area to regulate the activities of serotonergic and dopaminergic systems. The mammalian habenula is subdivided into medial and lateral nuclei, which correspond to the dorsal and ventral habenula in zebrafish, respectively (Amo et al. 2010). The dorsal habenula in zebrafish exhibits prominent left–right asymmetry in terms of the developmental timing, molecular expression, and size ratio of medial and lateral subnuclei (Bianco and Wilson 2009; Okamoto et al. 2012). The medial and lateral subnuclei of the dorsal habenula innervate the ventral and dorsal parts of the interpeduncular nucleus, respectively (Aizawa et al. 2005). Two prominent features are observed in the neural connection from the OB to the habenula. First, the habenula receives strongly biased olfactory inputs predominantly from two glomerular clusters, mdG and vmG (Fig. 5.4) (Miyasaka et al. 2014). Therefore, it is likely that the OB–habenula pathway may constitute part of a hard-wired circuit conveying particular odor information to evoke stereotyped responses such as innate olfactory behavior. Second, the OB output neurons project axons only to the right habenula (rHb) but not to the left habenula, displaying clear left–right asymmetry of neural circuitry (Miyasaka et al. 2009). Within the rHb, axon termination is specifically observed in the medial subnucleus, suggesting that the odor information conveyed to the rHb is next transferred to the ventral part of the interpeduncular nucleus. Two recent studies reported that the habenula plays a crucial role in controlling fear responses in zebrafish (Agetsuma et al. 2010; Lee et al. 2010), although the involvement of olfactory inputs has not yet been investigated.

5.8 Olfactory Behaviors in Zebrafish

Finding foods, escaping from danger, and mating with a partner are the most basic behaviors commonly observed in various animal species. Odorants and pheromones in the aquatic environment activate olfactory receptors and neural circuits, mediating these innate behaviors also in zebrafish. In addition, zebrafish can be utilized

for analyses of odor-associated short-term memory (olfactory conditioning), as well as extremely long-lasting memory (olfactory imprinting) reminiscent of salmon homing behavior.

5.8.1 Foraging Behavior

Attraction toward food sources is one of the fundamental behaviors needed for animals to survive. Amino acids contained in the diet are indispensable for fishes not only as nutrients but also as odorants. Zebrafish exhibit robust appetitive behavior to amino acids including attraction and increased turning, recognizing them as potential feeding cues (Steele et al. 1990, 1991: Braubach et al. 2009). When a hungry zebrafish is placed into a tank of water with amino acids pumped into one corner, the fish tend to spend more time near the amino acids (Fig. 5.5c). The primary olfactory circuitry mediating this attractive behavior was elucidated by a combination of genetic, anatomical, and behavioral approaches (Koide et al. 2009). First, three gene trap and transgenic zebrafish lines were established in which the Gal4 transactivator is expressed in three distinct populations of OSNs innervating different glomerular clusters (Fig. 5.5a,b). Next, synaptic transmission from each population of OSNs to the OB neurons was selectively blocked by Gal4/UAS-mediated expression of tetanus neurotoxin that specifically cleaves VAMP2 (synaptobrevin), a synaptic vesicle protein required for exocytosis (Fig. 5.5d). The attractive response of zebrafish to amino acids was completely abolished only when the synaptic transmission to the lG cluster was silenced. These results clearly demonstrate the functional significance of the OSNs innervating the lG in the amino acid-mediated feeding behavior in zebrafish. However, it remains totally unknown how the amino acid information in the lG is read and transformed by neurons in higher olfactory centers to elicit the attractive response.

5.8.2 Alarm Response

In 1938, the Austrian ethologist Karl von Frisch discovered the existence of an alarm substance, the so-called Schreckstoff (German for “scary stuff”), in minnows (von Frisch 1938). When a minnow in a shoal was accidentally injured, von Frisch noticed that the other fish in the same tank displayed conspicuously frightened reactions: darting and freezing. Subsequent experiments demonstrated that putative alarm substances are contained in specialized cells (alarm substance cells or club cells) in the fish skin, released into water upon injury, and activate specific olfactory neural circuitry in its shoaling company to notify the presence of danger (Lebedeva et al. 1975; Pfeiffer 1977; Kasumyan and Lebedeva 1975). The Schreckstoff-induced alarm response is observed in the superorder Ostariophysi that includes approximately two-third of freshwater fish species including zebrafish.

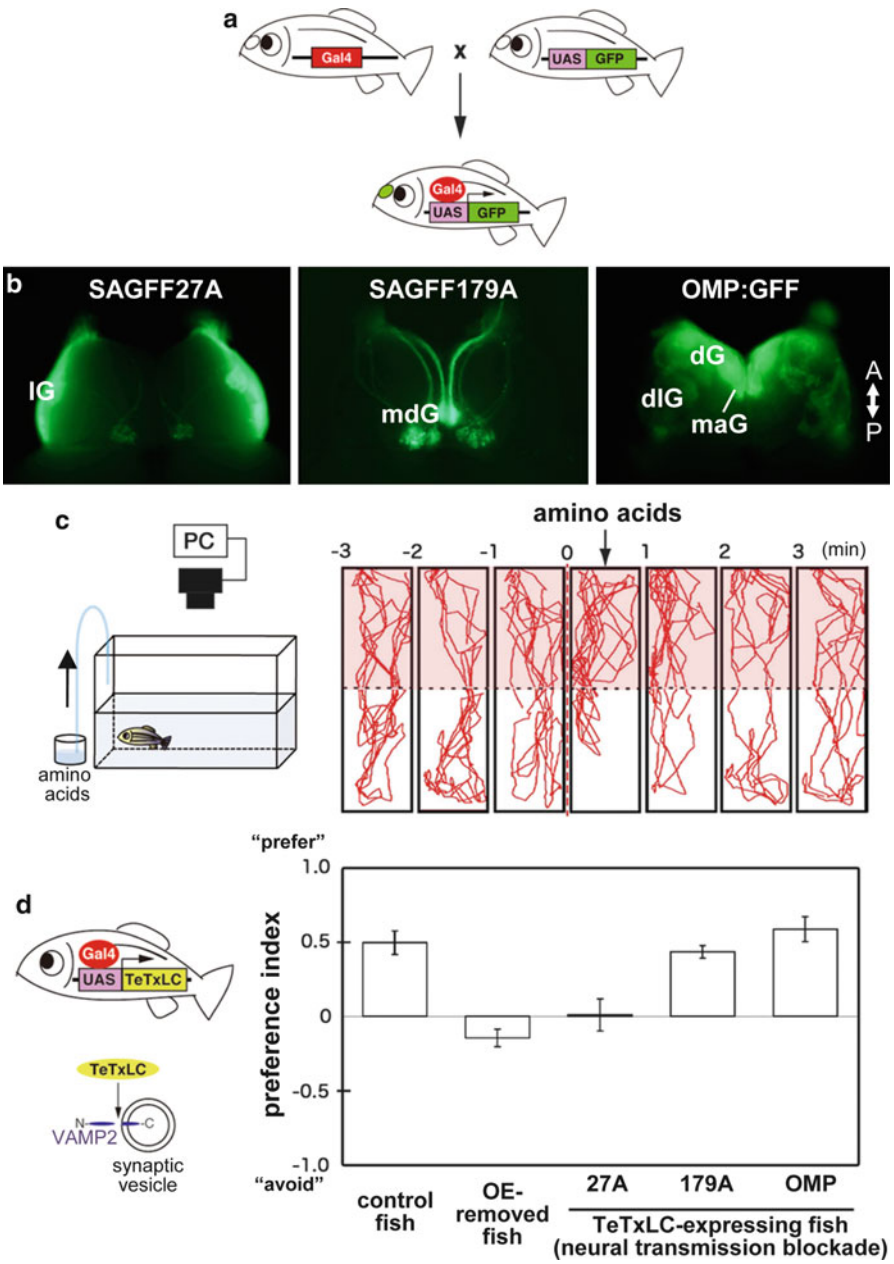

Fig. 5.5 Genetic dissection of olfactory neural circuitry mediating attraction to amino acids. (**a**) A principle of Gal4/UAS system in zebrafish. (**b**) GFP fluorescence in whole-mount OBs from three transgenic lines expressing Gal4 and GFP in different populations of OSNs. Axon innervations of differential glomerular clusters are observed among the three transgenic lines. (**c**) *Left*: A behavioral assay setup. *Right*: Representative swimming paths of zebrafish on amino acid application. Results are presented for every 1 min before and after the application of amino acid mixture. (**d**) Synaptic transmission blockade by forced expression of tetanus neurotoxin (TeTxLC). *Left*: TeTxLC-mediated blockade of synaptic transmission by specific cleavage of VAMP2 in synaptic vesicles. *Right*: The attractive responses to amino acids for individual genotypes are represented by the preference index (*Y*-axis). The OE-removed fish and the SAGFF27A; UAS: TeTxLC double-transgenic fish show no preference, demonstrating the importance of the lateral glomerular cluster in the attraction to amino acids. (Modified from Koide et al. 2009)

Upon application of a conspecific skin extract, most zebrafish display a robust, biphasic response in the bottom of a tank: burst swimming followed by freezing (Speedie and Gerlai 2008). Although two structurally unrelated molecules were reported as candidates of fish alarm substances, hypoxanthine-3*N*-oxide (Pfeiffer et al. 1985) and chondroitin sulfate (Mathuru et al. 2012), the real identity of Schreckstoff is still a mystery. As already mentioned, our calcium imaging and anti-phospho-Erk immunohistochemical experiments have identified three glomerular foci in the zebrafish OB that are strongly activated by the skin extract (unpublished observation). It is conceivable that plural components in the skin extract activating different glomeruli may coordinately evoke the alarm response through some coincidence-detection mechanism in higher olfactory centers.

5.8.3 Reproductive Behavior

Two types of sex pheromones, steroids and prostaglandins, that have been identified in female goldfish are secreted at different steps of the estrus cycle and sequentially act on male fish for successful reproduction (Sorensen et al. 1998; Sorensen and Caprio 1998). Two steroid derivatives, 17α,20β-dihydroxy-4-pregnen-3-one (17,20P) and its sulfated form (17,20P-S), are secreted from female goldfish at a preovulatory stage and act on males as primer pheromones that change the male endocrine-gonadal responses (Stacey et al. 1989). 17,20P and 17,20P-S evoke a rapid increase in luteinizing hormone release from the pituitary, leading to spermatogenesis in several hours (DeFraipont and Sorensen 1993). In zebrafish, only 17,20P-S appears an active pheromone that is sensed by a small subset of ciliated OSNs and activates a single or few glomeruli in the maG cluster (Friedrich and Korsching 1998; unpublished observation). During ovulation in zebrafish as well as goldfish, prostaglandin F2α (PGF2α) and its metabolite 15-keto-PGF2α are synthesized and secreted in female urine, acting on male fish as releaser pheromones (Sorensen et al. 1988). The male sexual behavior upon stimulation with these releaser pheromones includes increased swimming activity, attraction to females, nudging (abdomen touch), and quivering. PGF2α and 15-keto-PGF2α activate a selective olfactory pathway involving two glomeruli in the vmG cluster in zebrafish (Friedrich and Korsching 1998; unpublished observation). Future studies are awaited for the identification of pheromonal receptors for 17,20P-S and PGF2α, and the dissection of higher-order neural circuitry mediating endocrine and behavioral responses evoked by these sex pheromones.

5.8.4 Olfactory Conditioning

Similar to other animal species, fish can be conditioned to associate odors with either aversive or attractive stimuli. The aversive conditioning experiments include electrical shock to catfish (Little 1977), lithium chloride injection to goldfish

(Manteifel and Karelina 1996), and conspecific skin extract (Schreckstoff) exposure to zebrafish (Suboski et al. 1990), all of which were associated with particular odorants. In contrast, fish also can associate odorants with positive reinforcement stimuli such as food rewards (Herbert and Atema 1977; Valentincic et al. 2000; Braubach et al. 2009; Miklavc and Valentincic 2012). Thus, zebrafish can learn and memorize odor-associated behavioral tasks reliably in standard conditioning paradigms. Hence, it is now possible to analyze these learning behaviors with a combination of genetic, optical imaging, electrophysiological, and neuroanatomical methods for elucidation of neural circuit mechanisms underlying olfactory memory and behavioral plasticity.

5.8.5 Olfactory Imprinting

One of the most widely known olfactory imprinting behaviors is homing of salmon to their mother-rivers. Juvenile salmon imprint on the odors of their natal stream, then migrate to sea, and grow up to be adults. After several years in the sea, the adult salmon return to their home river for reproduction by navigating through the environment using various sensory cues including the odors of their natal stream (Scholz et al. 1976; Dittman and Quinn 1996; Yamamoto et al. 2010). Although zebrafish do not display homing behavior in nature, Harden et al. (2006) reported that zebrafish in laboratories can form and retain olfactory memories experienced in juveniles, similar to those observed in salmons. Zebrafish were exposed to an artificial odorant, phenylethyl alcohol (PEA), for the first 3 weeks post fertilization, then raised in ordinary water up to adult stage, and subjected to a preference test in a Y-maze. As a result, the PEA-exposed zebrafish showed significant preference to this odorant whereas the control fish did not. Thus, zebrafish clearly remember the odor to which they were exposed as juveniles, rendering this fish species as an attractive model organism for studying olfactory imprinting or long-lasting olfactory memory.

5.9 Conclusions and Perspectives

These two decades since the discovery of odorant receptor genes by Buck and Axel (1991) have witnessed great advances in our understanding of the functional architecture of the primary olfactory system. Multigene families encoding odorant and pheromone receptors were identified in various animal species (see Chap. 2 by Touhara). The axon guidance mechanism for establishing neural connectivity patterns from the OE to the OB was clarified (see Chap. 3 by Sakano). The concept of the "odor map" was established as the internal representation of odorant molecular features in the OB, demonstrating the importance of glomerular modules as functional units for odor coding and processing (see Chap. 4 by Mori). Therefore, it

is high time for us to contemplate, hypothesize, and investigate the functional architecture of the secondary and tertiary olfactory circuitry from the OB to the cortex and beyond, linking odor inputs to various higher-order brain functions such as perception, emotion, memory, decision making, and consciousness. In our efforts toward understanding the olfactory system as a whole, the zebrafish will undoubtedly become an ideal model vertebrate in the next decade, with its tiny but well-organized brain, sophisticated olfactory circuits, and robust olfactory behaviors, as well as amenability of various state-of-the-art genetic techniques.

Acknowledgments The author thanks Nobuhiko Miyasaka, Tetsuya Koide, Noriko Wakisaka, Miwa Masuda, and Yoichi Yabuki for help in preparation of the figures and critical reading of the manuscript, and Takumi Akagi and Tsutomu Hashikawa in the Support Unit for Animal Resources Development, RIKEN BSI Research Resources Center for help in electron microscopy. This work was supported in part by a Grant-in-Aid for Scientific Research (B) and a Grant-in-Aid for Scientific Research on Innovative Areas (Systems Molecular Ethology) from the Ministry of Education, Culture, Sports, Science, and Technology of Japan, and a Grant from the Human Frontier Science Program (HFSP).

References

Agetsuma M, Aizawa H, Aoki T, Nakayama R, Takahoko M, Goto M, Sassa T, Amo R, Shiraki T, Kawakami K, Hosoya T, Higashijima S, Okamoto H (2010) The habenula is crucial for experience-dependent modification of fear responses in zebrafish. Nat Neurosci 13:1354–1356

Ahrens MB, Orger MB, Robson DN, Li JM, Keller PJ (2013) Whole-brain functional imaging at cellular resolution using light-sheet microscopy. Nat Methods 10:413–420

Aizawa H, Bianco IH, Hamaoka T, Miyashita T, Uemura O, Concha ML, Russell C, Wilson SW, Okamoto H (2005) Laterotopic representation of left-right information onto the dorso-ventral axis of a zebrafish midbrain target nucleus. Curr Biol 15:238–243

Alioto TS, Ngai J (2005) The odorant receptor repertoire of teleost fish. BMC Genomics 6:173. doi:10.1186/1471-2164-6-173

Alioto TS, Ngai J (2006) The repertoire of olfactory C family G protein-coupled receptors in zebrafish: candidate chemosensory receptors for amino acids. BMC Genomics 7:309. doi:10.1186/1471-2164-7-309

Amo R, Aizawa H, Takahoko M, Kobayashi M, Takahashi R, Aoki T, Okamoto H (2010) Identification of the zebrafish ventral habenula as a homolog of the mammalian lateral habenula. J Neurosci 30:1566–1574

Asakawa K, Suster ML, Mizusawa K, Nagayoshi S, Kotani T, Urasaki A, Kishimoto Y, Hibi M, Kawakami K (2008) Genetic dissection of neural circuits by Tol2 transposon-mediated Gal4 gene and enhancer trapping in zebrafish. Proc Natl Acad Sci USA 105:1255–1260

Baier H, Korsching S (1994) Olfactory glomeruli in the zebrafish form an invariant pattern and are identifiable across animals. J Neurosci 14:219–230

Bargmann CI, Hartwieg E, Horvitz HR (1993) Odorant-selective genes and neurons mediate olfaction in *C. elegans*. Cell 74:515–527

Barth AL, Nicholas JJ, Ngai J (1996) Asynchronous onset of odorant receptor expression in the developing zebrafish olfactory system. Neuron 16:23–34

Barth AL, Dugas JC, Ngai J (1997) Noncoordinate expression of odorant receptor genes tightly linked in the zebrafish genome. Neuron 19:359–369

Bedell VM, Wang W, Campbell JM, Poshusta TL, Starker CG, Krug RG 2nd, Tan W, Penheiter SG, Ma AC, Leung AY, Fahrenkrug SC, Carlson DF, Voytas DF, Clark KJ, Essner JJ, Ekker

SC (2012) In vivo genome editing using a high-efficiency TALEN system. Nature (Lond) 491:114–118
Bianco IH, Wilson SW (2009) The habenular nuclei: a conserved asymmetric relay station in the vertebrate brain. Philos Trans R Soc Lond B Biol Sci 364:1005–1020
Blumhagen F, Zhu P, Shum J, Scharer YP, Yaksi E, Deisseroth K, Friedrich RW (2011) Neuronal filtering of multiplexed odour representations. Nature (Lond) 479:493–498
Braubach OR, Wood HD, Gadbois S, Fine A, Croll RP (2009) Olfactory conditioning in the zebrafish (*Danio rerio*). Behav Brain Res 198:190–198
Braubach OR, Fine A, Croll RP (2012) Distribution and functional organization of glomeruli in the olfactory bulbs of zebrafish (*Danio rerio*). J Comp Neurol 520:2317–2339
Braubach OR, Miyasaka N, Koide T, Yoshihara Y, Croll RP, Fine A (2013) Experience-dependent versus experience-independent postembryonic development of distinct groups of zebrafish olfactory glomeruli. J Neurosci 33:6905–6916
Buck LB (2000) The molecular architecture of odor and pheromone sensing in mammals. Cell 100:611–618
Buck L, Axel R (1991) A novel multigene family may encode odorant receptors: a molecular basis for odor recognition. Cell 65:175–187
Cao Y, Oh BC, Stryer L (1998) Cloning and localization of two multigene receptor families in goldfish olfactory epithelium. Proc Natl Acad Sci USA 95:11987–11992
Caron SJ, Ruta V, Abbott LF, Axel R (2013) Random convergence of olfactory inputs in the *Drosophila* mushroom body. Nature (Lond) 497:113–117
Carr WES (1988) The molecular nature of chemical stimuli in the aquatic environment. In: Atema J, Fay RR, Popper AN, Tavolga WN (eds) Sensory biology of aquatic animals. Springer, New York, pp 3–27
Chess A, Simon I, Cedar H, Axel R (1994) Allelic inactivation regulates olfactory receptor gene expression. Cell 78:823–834
DeFraipont M, Sorensen PW (1993) Exposure to the pheromone 17α,20β-dihydroxy-4-pregnen-3-one enhances behavioral spawning success, sperm production, and sperm motility of male goldfish. Anim Behav 46:245–256
Derjean D, Moussaddy A, Atallah E, St.-Pierre M, Auclair F, Chang S, Ren X, Zielinski B, Dubac R (2010) A novel neural substrate for the transformation of olfactory inputs into motor output. PLoS Biol 8:e1000567
Dewan A, Pacifico R, Zhan R, Rinberg D, Bozza T (2013) Non-redundant coding of aversive odours in the main olfactory pathway. Nature (Lond) 497:486–489
Dittman A, Quinn T (1996) Homing in Pacific salmon: mechanisms and ecological basis. J Exp Biol 199:83–91
Ellingsen S, Laplante MA, Konig M, Kikuta H, Furmanek T, Hoivik EA, Becker TS (2005) Large-scale enhancer detection in the zebrafish genome. Development (Camb) 132:3799–3811
Ferrero DM, Lemon JK, Fluegge D, Pashkovski SL, Korzan WJ, Datta SR, Spehr M, Fendt M, Liberles SD (2011) Detection and avoidance of a carnivore odor by prey. Proc Natl Acad Sci USA 108:11235–11240
Friedrich RW (2006) Mechanisms of odor discrimination: neurophysiological and behavioral approaches. Trends Neurosci 29:40–47
Friedrich RW, Korsching SI (1997) Combinatorial and chemotopic odorant coding in the zebrafish olfactory bulb visualized by optical imaging. Neuron 18:737–752
Friedrich RW, Korsching SI (1998) Chemotopic, combinatorial, and noncombinatorial odorant representations in the olfactory bulb revealed using a voltage-sensitive axon tracer. J Neurosci 18:9977–9988
Friedrich RW, Laurent G (2001) Dynamic optimization of odor representations by slow temporal patterning of mitral cell activity. Science 291:889–894
Friedrich RW, Habermann CJ, Laurent G (2004) Multiplexing using synchrony in the zebrafish olfactory bulb. Nat Neurosci 7:862–871
Friedrich RW, Yaksi E, Judkewitz B, Wiechert MT (2009) Processing of odor representations by neuronal circuits in the olfactory bulb. Ann N Y Acad Sci 1170:293–297

Fuss SH, Korsching SI (2001) Odorant feature detection: activity mapping of structure response relationships in the zebrafish olfactory bulb. J Neurosci 21:8396–8407
Ganz J, Kaslin J, Freudenreich D, Machate A, Geffarth M, Brand M (2012) Subdivisions of the adult zebrafish subpallium by molecular marker analysis. J Comp Neurol 520:633–655
Germana A, Montalbano G, Laura R, Ciriaco E, dell Calle ME, Vega JA (2004) S100 protein-like immunoreactivity in the crypt olfactory neurons of the adult zebrafish. Neurosci Lett 371:196–198
Germana A, Paruta S, Germana GP, Ochoa-Erena FJ, Montalbano G, Cobo J, Vega JA (2007) Differential distribution of S100 protetin and calretinin in mechanosensory and chemosensory cells of adult zebrafish (*Danio rerio*). Brain Res 1162:48–55
Ghosh S, Larson SD, Hefzi H, Marnoy Z, Cutforth T, Dokka K, Baldwin KK (2011) Sensory maps in the olfactory cortex defined by long-range viral tracing of single neurons. Nature (Lond) 472:217–220
Gloriam DEI, Bjarnadottir TK, Yan YL, Postlethwait JH, Schioth HB, Fredriksson R (2005) The repertoire of trace amine G-protein-coupled receptors: large expansion in zebrafish. Mol Phylogenet Evol 35:470–482
Goldman AL, Van der Goes van Naters W, Lessing D, Warr CG, Carlson JR (2005) Coexpression of two functional odor receptors in one neuron. Neuron 45:661–666
Hagey LR, Moller PR, Hofmann AF, Krasowski MD (2010) Diversity of bile salts and amphibians: evolution of a complex biochemical pathway. Physiol Biochem Zool 83:308–321
Hamdani EH, Doving KB (2002) The alarm reaction in crucian carp is mediated by olfactory neurons with long dendrites. Chem Senses 27:395–398
Hamdani EH, Doving KB (2006) Specific projection of the sensory crypt cells in the olfactory system in crucian carp, *Carassius carassius*. Chem Senses 31:63–67
Hamdani EH, Alexander G, Doving KB (2001) Projection of sensory neurons with microvilli to the lateral olfactory tract indicates their participation in feeding behaviour in crucian carp. Chem Senses 26:1139–1144
Hansen A, Zeiske E (1998) The peripheral olfactory organ of the zebrafish, *Danio rerio*: an ultrastructural study. Chem Senses 23:39–48
Hansen A, Rolen SH, Anderson K, Morita Y, Caprio J, Finger TE (2003) Correlation between olfactory receptor cell type and function in the channel catfish. J Neurosci 23:347–359
Hansen A, Anderson KT, Finger TE (2004) Differential distribution of olfactory receptor neurons in goldfish: structural and molecular correlates. J Comp Neurol 477:347–359
Harden MV, Newton LA, Lloyd RC, Whitlock KE (2006) Olfactory imprinting is correlated with changes in gene expression in the olfactory epithelia of the zebrafish. J Neurobiol 66:1452–1466
Hashiguchi Y, Nishida M (2006) Evolution and origin of vomeronasal-type odorant receptor gene repertoire in fishes. BMC Evol Biol 6:76
Hashiguchi Y, Nishida M (2007) Evolution of trace amine-associated receptor (TAAR) gene family in vertebrates: lineage-specific expansions and degradations of a second class of vertebrate chemosensory receptors expressed in the olfactory epithelium. Mol Biol Evol 24:2099–2107
Herbert P, Atema J (1977) Olfactory discrimination of male and female conspecifics in bullhead catfish, *Ictalurus nebulosus*. Biol Bull 153:429–430
Howe K, Clark MD et al (2013) The zebrafish reference genome sequence and its relationship to the human genome. Nature (Lond) 496:498–503
Hwang WY, Fu Y, Reyon D, Maeder ML, Tsai SQ, Sander JD, Peterson RT, Yeh JR, Joung JK (2013) Efficient genome editing in zebrafish using a CRISPR-Cas system. Nat Biotechnol 31:227–229
Igarashi KM, Ieki N, An M, Yamaguchi Y, Nagayama S, Kobayakawa K, Kobayakawa R, Tanifuji M, Sakano H, Chen WR, Mori K (2012) Parallel mitral and tufted cell pathways route distinct odor information to different targets in the olfactory cortex. J Neurosci 32:7970–7985

Jefferis GS, Potter CJ, Chan AM, Marin EC, Rohlfing T, Maurer CR Jr, Luo L (2007) Comprehensive maps of *Drosophila* higher olfactory centers: spatially segregated fruit and pheromone representation. Cell 128:1187–1203

Kang J, Caprio J (1995) Electrophysiological response of single olfactory bulb neurons to amino acids in the channel catfish, *Ictalurus punctatus*. J Neurophysiol 74:1421–1434

Kasumyan AO, Lebedeva NY (1975) New data on the nature of the alarm pheromone in cyprinids. J Ichthyol 19:109–114

Kettleborough RN, Busch-Nentwich EM, Harvey SA, Dooley CM, de Bruijn E, van Eeden F, Sealy I, White RJ, Herd C, Nijman IJ, Fenyes F, Mehroke S, Scahill C, Gibbons R, Wali N, Carruthers S, Hall A, Yen J, Cuppen E, Stemple DL (2013) A systematic genome-wide analysis of zebrafish protein-coding gene function. Nature (Lond) 496:494–497

Koide T, Miyasaka N, Morimoto K, Asakawa K, Urasaki A, Kawakami K, Yoshihara Y (2009) Olfactory neural circuitry for attraction to amino acids revealed by transposon-mediated gene trap approach in zebrafish. Proc Natl Acad Sci USA 106:9884–9889

Korsching S (2009) The molecular evolution of teleost olfactory receptor gene families. Results Probl Cell Differ 47:37–55

Laberge F, Hara TJ (2001) Neurobiology of fish olfaction: a review. Brain Res Rev 36:41–59

Larsson MC, Domingos AI, Jones WD, Chiappe E, Amrein H, Vosshall LB (2004) *Or83b* encodes a broadly expressed odorant receptor essential for *Drosophila* olfaction. Neuron 43:703–714

Lebedeva NY, Malyukina GA, Kasumyan AO (1975) The natural repellent in the skin of cyprinids. J Ichthyol 15:472–480

Lee A, Mathuru AS, Teh C, Kibat C, Korzh V, Penney TB, Jesuthasan S (2010) The habenula prevents helpless behavior in larval zebrafish. Curr Biol 20:2211–2216

Li W, Scott AP, Siefkes MJ, Yan H, Liu Q, Yun SS, Gage DA (2002) Bile acid secreted by male sea lamprey that acts as a sex pheromone. Science 296:138–141

Li J, Mack JA, Souren M, Yaksi E, Higashijima S, Mione M, Fetcho JR, Friedrich RW (2005) Early development of functional spatial maps in the zebrafish olfactory bulb. J Neurosci 25:5784–5795

Li Q, Korzan WJ, Ferrero DM, Chang RB, Roy DS, Buchi M, Lemon JK, Kaur AW, Stowers L, Fendt M, Liberles SD (2013) Synchronous evolution of an odor biosynthesis pathway and behavioral response. Curr Biol 23:11–20

Liberles SD, Buck LB (2006) A second class of chemosensory receptors in the olfactory epithelium. Nature (Lond) 442:645–650

Lin HH, Lai JS, Chin AL, Chen YC, Chiang AS (2007) A map of olfactory representation in the *Drosophila* mushroom body. Cell 128:1205–1217

Lipschitz DL, Michel WC (2002) Amino acid odorants stimulate microvillar sensory neurons. Chem Senses 27:277–286

Little EE (1977) Conditioned cardiac response to the olfactory stimuli of amino acids in the channel catfish, *Ictalurus punctatus*. Physiol Behav 27:691–697

Luu P, Acher F, Bertrand HO, Fan J, Ngai J (2004) Molecular determinants of ligand selectivity in a vertebrate odorant receptor. J Neurosci 24:10128–10137

Manteifel YB, Karelina MA (1996) Conditioned food aversion in the goldfish, *Carassius auratus*. Comp Biochem Phys A 115:31–35

Martini S, Silvotti L, Shirazi A, Ryba NJP, Tirindelli R (2001) Co-expression of putative pheromone receptors in the sensory neurons of the vomeronasal organ. J Neurosci 21:843–848

Mathuru AS, Kibat C, Cheong WF, Shui G, Wenk MR, Friedrich RW, Jesuthasan S (2012) Chondroitin fragments are odorants that trigger fear behavior in fish. Curr Biol 22:538–544

Michel WC (1999) Cyclic nucleotide-gated channel activation is not required for activity-dependent labeling of zebrafish olfactory receptor neurons by amino acids. Biol Signals Recept 8:338–347

Michel WC, Derbidge DS (1997) Evidence of distinct amino acid and bile salt receptors in the olfactory system of the zebrafish, *Danio rerio*. Brain Res 764:179–187

Michel WC, Lubomudrov LM (1995) Specificity and sensitivity of the olfactory organ of the zebrafish, *Danio rerio*. J Comp Physiol A 177:191–199

Michel WC, Sanderson MJ, Olson JK, Lipschitz DL (2003) Evidence of a novel transduction pathway mediating detection of polyamines by the zebrafish olfactory system. J Exp Biol 206:1697–1706

Miklavc P, Valentincic T (2012) Chemotopy of amino acids on the olfactory bulb predicts olfactory discrimination capabilities of zebrafish *Danio rerio*. Chem Senses 37:65–75

Miyamichi K, Amat F, Moussavi F, Wang C, Wickersham I, Wall NR, Taniguchi H, Tasic B, Huang ZJ, He Z, Callaway EM, Horowitz MA, Luo L (2011) Cortical representations of olfactory input by trans-synaptic tracing. Nature (Lond) 472:191–196

Miyasaka N, Sato Y, Yeo SY, Hutson LD, Chien CB, Okamoto H, Yoshihara Y (2005) Robo2 is required for establishment of a precise glomerular map in the zebrafish olfactory system. Development (Camb) 132:1283–1293

Miyasaka N, Knaut H, Yoshihara Y (2007) Cxcl12/Cxcr4 chemokine signaling is required for placode assembly and sensory axon pathfinding in the zebrafish olfactory system. Development (Camb) 134:2459–2468

Miyasaka N, Morimoto K, Tsubokawa T, Higashijima S, Okamoto H, Yoshihara Y (2009) From the olfactory bulb to higher brain centers: genetic visualization of secondary olfactory pathways in zebrafish. J Neurosci 29:4756–4767

Miyasaka N, Arganda-Carreras I, Wakisaka N, Masuda M, Seung HS, Yoshihar Y (2014) Olfactory projectomes in the zebrafish forebrain revealed by genetic single-neuron labeling. Nat Commun 5:3639. doi: 10.1038/ncomms4639

Mombaerts P (2004) Genes and ligands for odorant, vomeronasal and taste receptors. Nat Rev Neurosci 5:263–278

Mori K, Sakano H (2011) How is the olfactory map formed and interpreted in the mammalian brain? Annu Rev Neurosci 34:467–499

Mori K, Mataga N, Imamura K (1992) Differential specificities of single mitral cells in rabbit olfactory bulb for a homologous series of fatty acid odor molecules. J Neurophysiol 67:786–789

Mori K, Nagao H, Yoshihara Y (1999) The olfactory bulb: coding and processing of odor molecule information. Science 286:711–715

Mori K, Takahashi YK, Igarashi KM, Yamaguchi M (2006) Maps of odorant molecular features in the mammalian olfactory bulb. Physiol Rev 86:409–433

Morita Y, Finger TE (1998) Differential projections of ciliated and microvillous olfactory receptor cells in the catfish, *Ictalurus punctatus*. J Comp Neurol 398:539–550

Muto A, Ohkura M, Abe G, Nakai J, Kawakami K (2013) Real-time visualization of neuronal activity during perception. Curr Biol 23:307–311

Ngai J, Alioto TS (2007) Genomics of odor receptors in zebrafish. In: Firestein S, Beauchamp GK (eds) The senses: a comprehensive reference, vol 4, Olfaction and taste. Academic Press, Oxford/San Diego, pp 553–560

Niessing J, Friedrich RW (2010) Olfactory pattern classification by discrete neuronal network states. Nature (Lond) 465:47–52

Nikonov AA, Caprio J (2001) Electrophysiological evidence for a chemotopy of biological relevant odors in the olfactory bulb of the channel catfish. J Neurophysiol 86:1869–1876

Nikonov AA, Caprio J (2007) Highly specific olfactory receptor neurons for types of amino acids in the channel catfish. J Neurophysiol 98:1909–1918

Nikonov AA, Finger TE, Caprio J (2005) Beyond the olfactory bulb: an odotopic map in the forebrain. Proc Natl Acad Sci USA 102:18688–18693

Oka Y, Saraiva LR, Korsching SI (2012) Crypt neurons express a single V1R-related ora gene. Chem Senses 37:219–227

Okamoto H, Agetsuma M, Aizawa H (2012) Genetic dissection of the zebrafish habenula, a possible switching board for selection of behavioral strategy to cope with fear and anxiety. Dev Neurobiol 72:386–394

Pfeiffer W (1977) The distribution of fright reaction and alarm substance cells in fishes. Copeia 4:653–665

Pfeiffer W, Riegelbauer G, Meier G, Sheibler B (1985) Effect of hypoxanthine-3(N)-oxide and hypoxanthine-1(N)-oxide on central nervous excitation of the black tetra *Gymnocorymbus*

ternetzi (Characidae, Ostariophysi, Pisces) indicated by dorsal light response. J Chem Ecol 11:507–523

Ren X, Chang S, Laframboise A, Green W, Dubac R, Zielinski B (2009) Projections from the accessory olfactory organ into the medial region of the olfactory bulb in the sea lamprey (*Petromyzon marinus*): a novel vertebrate sensory structure? J Comp Neurol 516:105–116

Rink E, Wullimann MF (2004) Connections of the ventral telencephalon (subpallium) in the zebrafish (*Danio rerio*). Brain Res 1011:206–220

Rubin BD, Katz LC (1999) Optical imaging of odorant representations in the mammalian olfactory bulb. Neuron 23:499–511

Saraiva LR, Korsching SI (2007) A novel olfactory receptor gene family in teleost fish. Genome Res 17:1448–1457

Sato Y, Miyasaka N, Yoshihara Y (2005) Mutually exclusive glomerular innervation by two distinct types of olfactory sensory neurons revealed in transgenic zebrafish. J Neurosci 25:4889–4897

Sato T, Hamaoka T, Aizawa H, Hosoya T, Okamoto H (2007a) Genetic single-cell mosaic analysis implicates ephrinB2 reverse signaling in projections from the posterior tectum to the hindbrain in zebrafish. J Neurosci 27:5271–5279

Sato Y, Miyasaka N, Yoshihara Y (2007b) Hierarchical regulation of odorant receptor gene choice and subsequent axonal projection of olfactory sensory neurons in zebrafish. J Neurosci 27:1606–1615

Sato K, Pellegrino M, Nakagawa T, Nakagawa T, Vosshall LB, Touhara K (2008) Insect olfactory receptors are heteromeric ligand-gated ion channels. Nature (Lond) 452:1002–1006

Scholz AT, Horrall RM, Cooper JC, Hasler AD (1976) Imprinting to chemical cues: the basis for home stream selection in salmon. Science 192:1247–1249

Schweitzer J, Lohr H, Filippi A, Driever W (2012) Dopaminergic and noradrenergic circuit development in zebrafish. Dev Neurobiol 72:256–268

Serizawa S, Miyamichi K, Nakatani H, Suzuki M, Saito M, Yoshihara Y, Sakano H (2003) Negative feedback regulation ensures the one receptor-one olfactory neuron rule in mouse. Science 302:2088–2094

Shi P, Zhang J (2009) Extraordinary diversity of chemosensory receptor gene repertoires among vertebrates. Results Probl Cell Differ 47:1–23

Sorensen PW, Caprio J (1998) Chemoreception. In: Evans DH (ed) The physiology of fishes, 2nd edn. CRC Press, Boca Raton, pp 375–405

Sorensen PW, Hara TJ, Stacey NE, Goetz FW (1988) F prostaglandins function as potent olfactory stimulants comprising the post-ovulatory sex pheromone in the goldfish. Biol Reprod 39:1039–1050

Sorensen PW, Christensen TA, Stacey NE (1998) Discrimination of pheromonal cues in fish: emerging parallels with insects. Curr Opin Neurobiol 8:458–467

Sorensen PW, Fine JM, Dvornikovs V, Jeffrey CS, Shao F, Wang J, Vrieze LA, Anderson KR, Hoye TR (2005) Mixture of new sulfated steroids functions as a migratory pheromone in the sea lamprey. Nat Chem Biol 1:324–328

Sosulski DL, Bloom ML, Cutforth T, Axel R, Datta SR (2011) Distinct representations of olfactory information in different cortical centres. Nature (Lond) 472:213–216

Speca DJ, Lin DM, Sorensen PW, Isacoff EY, Ngai J, Dittman AH (1999) Functional identification of a goldfish odorant receptor. Neuron 23:497–498

Speedie N, Gerlai R (2008) Alarm substance induced behavioral responses in zebrafish (*Danio rerio*). Behav Brain Res 188:168–177

Stacey NE, Sorensen PW, Van der Kraak GJ, Dulka JG (1989) Direct evidence that 17α,-20β-dihydroxy-4-pregnen-3-one functions as a goldfish primer pheromone: preovulatory release is closely associated with male endocrine system. Gen Comp Endocrinol 75:62–70

Steele CW, Owens DW, Scarfe AD (1990) Attraction of zebrafish *Brachydanio rerio* to alanine and its suppression by copper. J Fish Biol 36:341–352

Steele CW, Scarfe AD, Owens DW (1991) Effects of group size on the responsiveness of zebrafish *Brachydanio rerio* to alanine, a chemical attractant. J Fish Biol 38:553–564

Suboski MD, Bain S, Carty AE, McQuoid LM, Seelen MI, Seifert M (1990) Alarm reaction in acquisition and social transmission of simulated-predator recognition by zebra danio fish (*Brachydanio rerio*). J Comp Psychol 104:101–112

Tay TL, Ronneberger O, Ryu S, Nitschke R, Driever W (2011) Comprehensive catecholaminergic projectome analysis reveals single-neuron integration of zebrafish ascending and descending dopaminergic systems. Nat Commun 2:171

Troemel ER, Chou JH, Dwyer ND, Colbert HA, Bargmann CI (1995) Divergent seven transmembrane receptors are candidate chemosensory receptors in *C. elegans*. Cell 83:207–218

Uchida N, Takahashi YK, Tanifuji M, Mori K (2000) Odor maps in the mammalian olfactory bulb: domain organization and odorant structural features. Nat Neurosci 3:1035–1043

Valentincic T, Metelko J, Ota D, Pirc V, Blejec A (2000) Olfactory discrimination of amino acids in brown bulhead catfish. Chem Senses 25:21–29

von Frisch K (1938) Zur psychologie des Fische-Schwarmes. Naturwissenschaften 26:601–606

Vosshall LB, Stocker RF (2007) Molecular architecture of smell and taste in *Drosophila*. Annu Rev Neurosci 30:505–533

Wang JW, Wong AM, Flores J, Vosshall LB, Axel R (2003) Two-photon calcium imaging reveals an odor-evoked map of activity in the fly brain. Cell 112:271–282

Westerfield M (1995) The zebrafish book, 3rd edn. University of Oregon Press, Eugene

Wicher D, Schafer R, Bauernfeind R, Stensmyr MC, Heller R, Heinemann SH, Hansson BS (2008) Drosophila odorant receptors are both ligand-gated and cyclic-nucleotide-activated cation channels. Nature (Lond) 452:1007–1011

Wiechert MT, Judkewitz B, Riecke H, Friedrich RW (2010) Mechanisms of pattern decorrelation by recurrent neuronal circuits. Nat Neurosci 13:1003–1010

Wullimann MF, Mueller T (2004) Teleostean and mammalian forebrains contrasted: evidence from genes to behavior. J Comp Neurol 475:143–162

Yaksi E, von Saint Paul F, Niessing J, Bundschuh ST, Friedrich RW (2009) Transformation of odor representations in target areas of the olfactory bulb. Nat Neurosci 12:474–482

Yamamoto Y, Hino H, Ueda H (2010) Olfactory imprinting of amino acids in lacustrine sockeye salmon. PLoS One 5:e8633

Yoshihara Y (2009) Molecular genetic dissection of the zebrafish olfactory system. Results Probl Cell Differ 47:97–120

Zielinski BS, Hara TJ (2007) Olfaction. In: Hara T, Zielinski B (eds) Fish physiology, vol 25, Sensory systems neuroscience. Academic Press, San Diego/London, pp 1–43

Zu Y, Tong X, Wang Z, Liu D, Pan R, Li Z, Hu Y, Luo Z, Huang P, Wu Q, Zhu Z, Zhang B, Lin S (2013) TALEN-mediated precise genome modification by homologous recombination in zebrafish. Nat Methods 10:329–331

Chapter 6
Interneurons in the Olfactory Bulb: Roles in the Plasticity of Olfactory Information Processing

Masahiro Yamaguchi

Abstract Odor information is substantially modulated in the first relay of the central nervous system, the olfactory bulb (OB). This chapter focuses on how the large number of local inhibitory interneurons in the OB contribute to the structural and functional plasticity of the OB neuronal circuits, and odor information processing within them. The major OB interneurons, granule cells (GCs) and periglomerular cells (PGCs), form the characteristic synaptic structures, called dendrodendritic reciprocal synapses with excitatory projection neurons, the mitral and tufted cells. Dendrodendritic synaptic inhibition of OB interneurons induces feedback inhibition, lateral inhibition, and synchronization to mitral/tufted cells. Dendrodendritic synaptic inhibition is regulated by various signals, including olfactory sensory inputs, top-down inputs from the olfactory cortex (OC), and neuromodulatory signals. Outputs from mitral/tufted cells are in turn substantially influenced by these signals via the plasticity of dendrodendritic inhibition of OB interneurons. A second intriguing property of OB interneurons is that they are continually generated throughout life, conferring high plasticity on the OB neuronal circuits. The life-and-death decision of adult-born GCs is regulated by sensory experience and the behavioral state of the animal, indicating that the fate decision of new OB interneurons is also under the control of multiple signals. Further, behavioral analysis of mice with suppression of adult neurogenesis revealed abnormalities in many kinds of odor-guided behaviors. These observations collectively indicate that the structural and functional plasticity of OB interneurons plays crucial roles in odor information processing, and that this plasticity contributes to the expression of proper olfactory behaviors.

M. Yamaguchi (✉)
Department of Physiology, Graduate School of Medicine, The University of Tokyo, 7-3-1 Hongo, Bunkyo-ku, Tokyo 113-0033, Japan

Japan Science and Technology Agency, CREST, Tokyo, Japan
e-mail: yamaguti@m.u-tokyo.ac.jp

K. Mori (ed.), *The Olfactory System: From Odor Molecules to Motivational Behaviors*,
DOI 10.1007/978-4-431-54376-3_6, © Springer Japan 2014

Keywords Adult neurogenesis • Behavioral state • Cell elimination • Dendrodendritic synapse • Interneuron • Neuromodulatory input • Sensory input • Slow-wave sleep • Top-down input

6.1 Introduction

The olfactory bulb (OB) is the first relay of odor information processing in the central nervous system. In rodents, the OB is located at the rostral end of the brain, where it forms part of the telencephalon. It receives sensory input from the olfactory sensory neurons (OSNs) in the olfactory epithelium and sends the information to the olfactory cortex (OC). Dendrites of excitatory projection neurons in the OB, the mitral cells and tufted cells, form synapses with OSN axons to receive odor inputs, and their axons form synapses with dendrites of pyramidal cells in the OC to send the odor information to higher cortical regions.

Odor information processing in the OB has been an attractive target of analysis. One reason for this is the rather simple structure of OB neuronal circuits: different types of neurons and their synaptic connections are well organized in a laminated fashion, which is advantageous in both the structural and functional analysis of the neuronal circuits. A second reason is that analysis is facilitated by the identification of odorant receptors and axonal convergence of OSNs on topographically fixed glomeruli.

A remarkable feature of OB neuronal circuits is that local inhibitory interneurons outnumber excitatory projection neurons. In contrast to most brain regions, where a smaller number of local interneurons regulate the activity of a larger number of projection neurons, the OB has a larger number of local interneurons participating in the regulation of mitral/tufted cells. This fact indicates that odor information received from the OSNs is substantially modulated in the OB neuronal circuits by local interneurons before it is transferred to the OC.

This chapter focuses on OB interneurons, with particular regard to the contribution of these interneurons to the structural and functional plasticity of OB neuronal circuits. The structural organization and activity of OB interneurons are plastically regulated by a variety of signal systems. These signal systems in turn plastically modulate the outputs from mitral and tufted cells. The first topic in this chapter is how OB interneurons regulate the activity of mitral and tufted cells via the characteristic synaptic structure, dendrodendritic reciprocal synapses. Dendrodendritic synaptic inhibition is regulated by various signals, including olfactory sensory input, top-down inputs from the OC, and neuromodulatory signals.

The next topic of this chapter describes the adult neurogenesis of OB interneurons. OB interneurons are generated throughout life, a characteristic that provides highly plastic features to the OB neuronal circuits. Utilization of adult-born OB interneurons is regulated by olfactory sensory inputs and also by the behavioral state of the animal. OB interneurons undergo extensive turnover and are considered to contribute to the maintenance and plastic reorganization of OB neuronal circuits.

The contribution of adult-born OB interneurons to olfactory behaviors is also discussed.

Through a comprehensive discussion of these topics, this chapter states that odor information is substantially modulated as early as in the first relay, the OB, and that OB neuronal circuits work in concert with other cortical and subcortical brain regions. OB interneurons play central roles in the plastic odor information processing in the OB neuronal circuits.

6.2 Structure and Function of Interneurons in the OB

6.2.1 Local Interneurons in the OB Form Dendrodendritic Reciprocal Synapses with Projection Neurons

In most brain regions, a smaller number of local inhibitory neurons regulates the activity of a larger number of excitatory projection neurons. In the OB, in contrast, this relationship is reversed: local inhibitory neurons far outnumber excitatory projection neurons, mitral and tufted cells, by about two orders of magnitude (Kaplan et al. 1985; Parrish-Aungst et al. 2007). OB local interneurons consist of the two most abundant populations, granule cells (GCs) and periglomerular cells (PGCs) (Mori 1987; Shepherd et al. 2004). The number of GCs is one order larger than that of PGCs. The somata of GCs are densely packed in the granule cell layer (GCL) whereas those of PGCs are aligned around glomeruli in the glomerular layer (GL) (Fig. 6.1).

The characteristic synaptic structure in the OB is the dendrodendritic reciprocal synapse, between interneurons and projection neurons. In contrast to ordinary synapses between axons and dendrites, dendrites of OB interneurons make synapses with dendrites of mitral/tufted cells. The dendrodendritic synapse is reciprocal. In the case of GCs, the dendrodendritic synapse consists of a mitral/tufted-to-granule glutamatergic excitatory synapse and a granule-to-mitral/tufted GABAergic inhibitory synapse (Fig. 6.2). Historically, pioneering work by neuroanatomists Camillo Golgi and Santiago Ramón y Cajal suggested that GCs in the OB lack axons (Golgi 1875; Cajal 1890). Because of this peculiar morphology, the functions of GCs, including whether they are actually neurons, long remained obscure, although Cajal and his student T. Blanes raised the possibility that GC dendrites may emit signals similar to axons (Blanes 1897). Many decades later, advances in electrophysiological recordings and computational modeling of neuronal circuits led to the suggestion that GCs were the major source of inhibitory synaptic input to mitral/tufted cells, and the existence of dendrodendritic reciprocal synapses was proposed (Shepherd 1963; Rall et al. 1966). In fact, this unique synaptic structure was identified by electron microscopic analysis (Hirata 1964; Andres 1965; Price and Powell 1970a, b). Eventually, the concept of dendrodendritic reciprocal synapses was established both in structure and in function (Rall and Shepherd 1968; for review, Shepherd et al. 2007).

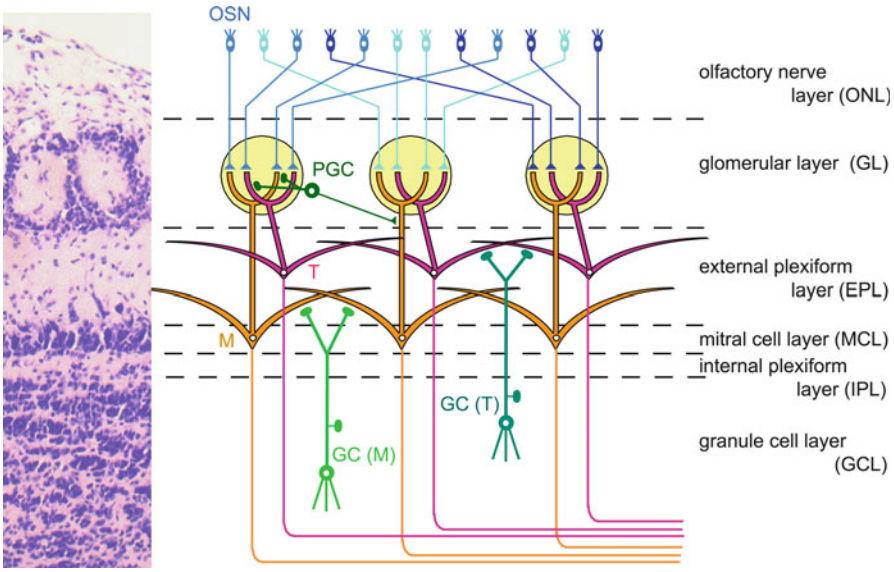

Fig. 6.1 Neuronal circuits of the olfactory bulb (OB). Layer structure of the OB. A Nissl-stained coronal section is shown on the *left*. Names of individual layers and their abbreviations are shown on the *right*. Axons of olfactory sensory neurons (*OSN*s) in the olfactory epithelium expressing the same type of odorant receptors (*light blue*, *blue*, *dark blue*) converge onto the same glomeruli (*yellow circles*). Mitral cells (*M*) and tufted cells (*T*) extend primary dendrites to a single glomerulus. Lateral dendrites of mitral cells distribute in the deep sublamina of the *EPL*; those of tufted cells distribute in the superficial sublamina of the EPL. A mitral cell-targeting granule cell (GC) (GC (M)) forms dendrodendritic synaptic contacts with mitral cell lateral dendrites. A tufted cell-targeting GC (GC (T)) forms dendrodendritic synaptic contacts with tufted cell lateral dendrites. A periglomerular cell (PGC) makes dendrodendritic synaptic contacts with mitral/tufted cells in a single glomerulus

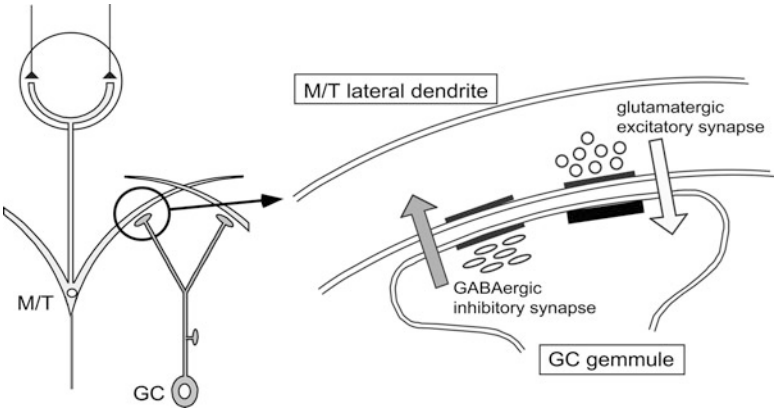

Fig. 6.2 Dendrodendritic reciprocal synapses between OB interneurons and mitral/tufted cells. A schema of a dendrodendritic reciprocal synapse between the lateral dendrite of a mitral/tufted cell (M/T) and the gemmule of a GC apical dendrite. A mitral/tufted-to-granule glutamatergic excitatory synapse and a granule-to-mitral/tufted GABAergic inhibitory synapse are arranged side by side in the contact site. Synaptic densities and synaptic vesicles are illustrated

GCs are GABAergic local inhibitory interneurons that lack axons. They extend apical dendrites into the external plexiform layer (EPL) and basal dendrites within the GCL (Fig. 6.1). Apical dendrites of GCs form dendrodendritic reciprocal synapses with lateral dendrites of mitral/tufted cells in the EPL. A given GC makes such dendrodendritic reciprocal synapses with mitral/tufted cells belonging to the same glomerular unit, namely, those extending primary dendrites to the same glomerulus, and with mitral/tufted cells belonging to different glomerular units, namely, those extending primary dendrites to different glomeruli. Accordingly, GCs modulate the activity of mitral/tufted cells within and across glomerular units.

The second major type of interneuron, PGCs, typically extend dendrites into a single glomerulus (Fig. 6.1). Within the glomerulus, PGC dendrites receive excitatory inputs from the OSNs via axodendritic synapses and from mitral or tufted cell primary dendrites via dendrodendritic synapses. A PGC sends inhibitory output via dendrodendritic synapses to mitral/tufted cell primary dendrites and thereby modulates the activity of mitral/tufted cells in a given glomerular unit (Shepherd et al. 2004). PGCs also have axons that innervate mitral/tufted cells of different glomerular units and thereby modulate the activity of mitral/tufted cells across glomerular units. The OB also contains another type of inhibitory neuron called short axon cells, whose function has attracted recent interest but remains largely unknown (Schneider and Macrides 1978; Eyre et al. 2008; Boyd et al. 2012).

Although the dendrodendritic synapses are the sole route of output from GCs, the synapses are not the only route of excitatory inputs to GCs. GCs also receive glutamatergic synaptic input from pyramidal cells in the olfactory cortex (OC) via axodendritic synapses in the GCL (Fig. 6.3). Pyramidal cells in the OC project axon collaterals massively back to the OB. The top-down centrifugal axons distribute mostly to the GCL of the OB and terminate on inhibitory interneurons such as GCs and short axon cells (Luskin and Price 1983; Boyd et al. 2012; Markopoulos et al. 2012). Thus, GCs are excited both by olfactory sensory inputs transmitted from mitral/tufted cells via the dendrodendritic synapses and by the activities of the OC pyramidal cells via the top-down axodendritic synapses. PGCs are also considered to receive top-down inputs from the OC, albeit it to a lesser degree than that to GCs.

6.2.2 Physiological Properties of OB Interneurons and Their Role in the Modulation of Mitral and Tufted Cell Activity

Dendritic spines of GCs that form reciprocal synapses in the EPL are larger in size than ordinary spines and are specifically called gemmules. At the site of contact of a mitral/tufted cell lateral dendrite and a GC gemmule, a mitral/tufted-to-granule excitatory synapse and a granule-to-mitral/tufted inhibitory synapse are positioned side by side in close proximity. This structure efficiently generates feedback inhibition on the lateral dendrite of the mitral/tufted cell (Fig. 6.4, left).

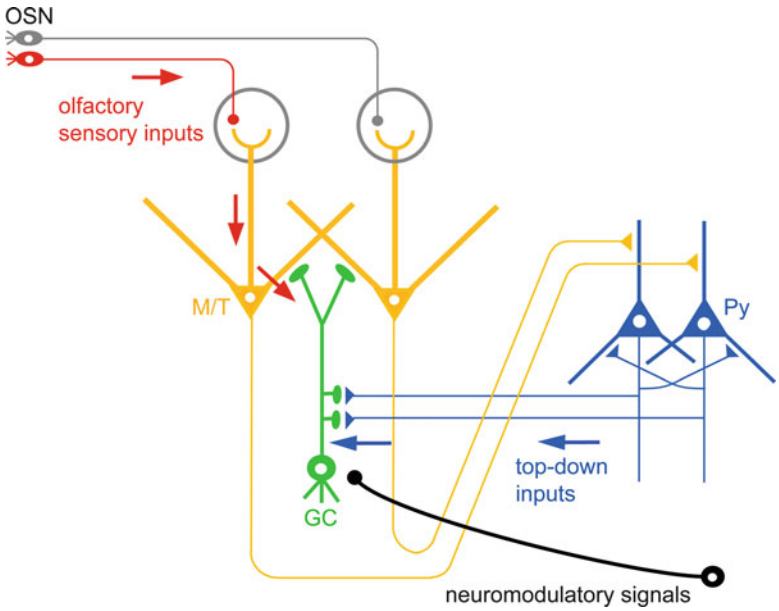

Fig. 6.3 Signals to OB interneurons. GCs receive excitatory synaptic inputs from mitral/tufted cells (M/T) via dendrodendritic synapses. These inputs represent olfactory sensory inputs (*red arrows*). GCs also receive top-down excitatory synaptic inputs from pyramidal cells (Py) in the OC via axodendritic synapses (*blue arrows*). These inputs represent the firing activity of OC pyramidal cells. GCs receive neuromodulatory signals (*black*) including noradrenergic, cholinergic, and serotonergic inputs

This feedback inhibition can occur at local sites at dendrites without the firing activity of GCs (Jahr and Nicoll 1982; Schoppa et al. 1998; Isaacson and Strowbridge 1998). The activation of a mitral/tufted-to-granule excitatory synapse induces an increase in calcium in the GC gemmule, which then activates GABA release at the granule-to-mitral/tufted inhibitory synapse from the GC gemmule to the mitral/tufted cell lateral dendrite. Calcium influx in the GC gemmule through NMDAR crucially promotes GABA release (Schoppa et al. 1998; Isaacson and Strowbridge 1998; Chen et al. 2000; Halabisky et al. 2000).

Lateral dendrites of individual mitral or tufted cells extend as long as 1–1.5 mm, which covers almost half of the circumference of the OB (Mori et al. 1983; Orona et al. 1984). Because an action potential in a given mitral/tufted cell can propagate throughout the length of the lateral dendrites (Xiong and Chen 2002; Debarbieux et al. 2003), the firing activity of a mitral/tufted cell activates many dendrodendritic reciprocal synapses formed with many GCs along the lateral dendrites, by which individual dendrodendritic reciprocal synapses provide feedback inhibition to the mitral/tufted cell dendrites. One proposed role of this feedback inhibition is regulation of the spiking rate and timing of mitral/tufted cells. Pharmacological blockade of GABAergic inputs increases the firing rate of mitral/tufted cells during odor stimulation and also perturbs the prompt cessation of their firing at the end of odor stimulation (Margrie et al. 2001).

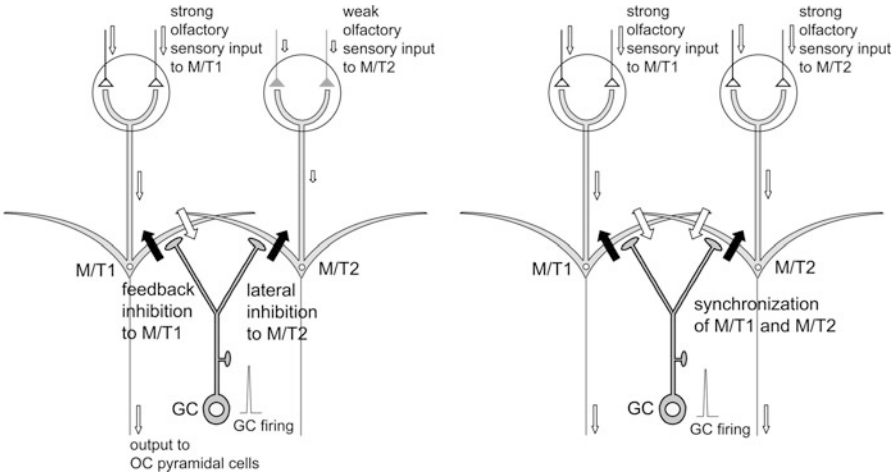

Fig. 6.4 Modulation of mitral/tufted cell activity by dendrodendritic synaptic inhibition from OB interneurons. *Left*: A mitral/tufted cell (M/T1) receives strong olfactory sensory input and another mitral/tufted cell (M/T2) receives weak olfactory sensory input. A GC forms dendrodendritic reciprocal synapses with these mitral/tufted cells and fires action potentials in response to the strong excitatory synaptic input via the dendrodendritic synapse with M/T1 (*thick white arrow*). The GC sends inhibition to M/T1 (feedback inhibition; *thick black arrow*). The GC sends inhibition also to M/T2 (lateral inhibition; *thick black arrow*), as a result of the propagation of action potentials to the dendrodendritic synapse with M/T2. This lateral inhibition suppresses the output from M/T2, which receives weak olfactory sensory input, and enhances the output contrast between M/T1 and M/T2. *Right*: Both mitral/tufted cells (M/T1 and M/T2) receive strong olfactory sensory input. A GC forming dendrodendritic reciprocal synapses with these mitral/tufted cells fires action potentials in response to the strong excitatory synaptic input via the dendrodendritic synapse with M/T1 and M/T2. Because of the propagation of action potentials to the entire dendritic tree of the GC, the GC sends simultaneous inhibition to M/T1 and M/T2 via the dendrodendritic synapses. The temporally coordinated inhibition of M/T1 and M/T2 leads to the synchronized firing of M/T1 and M/T2

In addition to feedback inhibition, the dendrodendritic synapses also coordinate the activity of individual populations of mitral/tufted cells, based on the connectivity provided by the formation of dendrodendritic synapses from a given GC with many mitral/tufted cells. One mode of this coordination is called lateral inhibition (Fig. 6.4). Strong excitatory inputs from a subset of mitral/tufted cells induce spiking activities in GCs. The spiking activity propagates in the entire dendritic tree of the GCs, which then activates many dendrodendritic synapses on the GC dendrites (Chen et al. 2000; Egger et al. 2003). The granule-to-mitral/tufted synaptic inhibition is targeted not only to mitral/tufted cells involved in the GC excitation (feedback inhibition), but also to mitral/tufted cells that do not contribute to the GC excitation (lateral inhibition). The lateral inhibition suppresses weakly activated or nonactivated mitral/tufted cells and contributes to the contrast enhancement of mitral/tufted cell activity (Yokoi et al. 1995), and is thereby considered to potentiate odor discrimination ability in mice (Abraham et al. 2010).

Activation of dendrodendritic synaptic inhibition by GC firing requires voltage-gated calcium channels (Halabisky et al. 2000; Chen et al. 2000), which is in striking contrast to the dispensability of these channels in the feedback activation of dendrodendritic synaptic inhibition (Schoppa et al. 1998; Isaacson and Strowbridge 1998; Chen et al. 2000; Halabisky et al. 2000). This observation suggests that feedback inhibition and lateral inhibition are differentially regulated and differentially contribute to odor information processing. Subthreshold activity of GC dendrites can also spread in entire dendritic trees without firing activity, in which the spread is dependent on low-threshold, voltage-gated calcium channels (Egger et al. 2005). Lateral inhibition without GC firing is also considered to play a role in odor information processing.

Another mode of coordination by dendrodendritic synapses is the synchronization of mitral/tufted cells (Fig. 6.4). In local field potential (LFP) recording, the OB shows oscillatory activity at high frequency (gamma range, 30–80 Hz) which is enhanced by odor stimulation (Adrian 1950; Rall and Shepherd 1968). Single-unit recordings of mitral/tufted cells showed that their firing activity is phase locked to the oscillatory LFP, and that the synchronous firing of different mitral/tufted cell firing becomes evident during odor stimulation (Kashiwadani et al. 1999). Pharmacological blockade of synaptic inhibition in the MCL and EPL significantly diminishes this gamma oscillation (Lagier et al. 2004). Further, patch clamp recordings from mitral cell pairs showed that their synchronous firing is dependent on synaptic inhibition from GCs, which occurs synchronously in different mitral cells (Schoppa 2006). It is likely that synchronous recovery of mitral/tufted cells from dendrodendritic synaptic inhibition-mediated hyperpolarization triggers synchronized firing of mitral/tufted cells (Schoppa 2006). Although the function of this synchronized firing of mitral/tufted cells is not yet known, it is assumed that it effectively activates pyramidal cells in the OC that receive converged projection from many mitral/tufted cells (Mori et al. 1999). Oscillatory strength in the OB correlates with the efficacy of olfactory learning (Martin et al. 2006; Beshel et al. 2007).

In contrast to GCs, a given PGC typically forms dendrodendritic synapses with primary dendrites of mitral/tufted cells in a single glomerulus. PGC dendrites also form synapses on the axon terminals of OSNs that mediate retrograde inhibition to OSNs (Murphy et al. 2005). PGCs are therefore considered to primarily regulate odor-induced activities in particular glomeruli. In summary, OB interneurons modulate the activity of mitral/tufted cells by inducing feedback inhibition, lateral inhibition, and synchronization through dendrodendritic synaptic inhibition. Thus, odor information received from OSNs is substantially modulated by OB local interneurons before it is transferred to OC pyramidal cells.

6.2.3 Mechanisms of the Control of OB Interneuron Activity

Because dendrodendritic synapses are the sole outputs of GCs, the contribution of GCs to odor information processing is ultimately attributable to their dendrodendritic

synaptic inhibition of mitral/tufted cells. The activation of dendrodendritic synaptic output of GCs is regulated by a variety of signals. As discussed, one notable signal is glutamatergic input from mitral/tufted cells via dendrodendritic synapses in the EPL. This input reflects odor information from the external world, which is received by OSNs and transferred to GCs via mitral/tufted cells.

Another crucial signal is the glutamatergic top-down input from OC pyramidal cells to GC dendrites in the GCL (Fig. 6.3). Although GC dendrites in the GCL also receive axon collaterals of mitral/tufted cells, anatomical and functional studies indicate that top-down inputs from the OC are much more massive than these mitral/tufted cell collaterals (de Olmos et al. 1978; Haberly and Price 1978; Balu et al. 2007). Top-down inputs to GCs in the GCL release NMDAR at dendrodendritic synapses in the EPL from the magnesium blockade and facilitate the dendrodendritic synaptic inhibition of mitral cells, thereby providing a "gating" signal for the dendrodendritic inhibition (Halabisky and Strowbridge 2003). In addition, theta-burst stimulation of GC synapses in the GCL induces long-term potentiation of the dendrodendritic synaptic inhibition of mitral/tufted cells in the EPL (Gao and Strowbridge 2009). Recent in vivo studies have shown that optogenetic stimulation of OC pyramidal cells suppresses spontaneous and/or odor-induced firing activity of mitral cells (Boyd et al. 2012; Markopoulos et al. 2012). This effect is most likely mediated by the enhanced dendrodendritic synaptic inhibition of GCs that receive substantial top-down inputs from OC pyramidal cells. These results indicate that dendrodendritic synaptic inhibition in the OB is under the control of OC pyramidal cell activity.

In addition to the top-down glutamatergic synaptic inputs, the OB is targeted by subcortical neuromodulatory systems that include cholinergic input from the horizontal limb of the diagonal band of Broca, noradrenergic input from the locus ceruleus, and serotonergic input from the raphe nuclei (Fig. 6.3) (Shipley and Ennis 1996). Most of the neuromodulatory fibers to the OB terminate on local interneurons and directly regulate their activity (Shipley and Ennis 1996; Shepherd et al. 2004). Cholinergic fibers innervate all layers of the OB, from the GCL to the GL (Kasa et al. 1995). Effects of acetylcholine vary among different cell types expressing different types of receptors (Le Jeune et al. 1995). Acetylcholine increases the excitability of PGCs and mitral cells via nicotinic receptors (Castillo et al. 1999). In contrast, the effect of acetylcholine on GCs is mainly mediated via muscarinic receptors. Although its effect on GC excitability is controversial (Castillo et al. 1999; Pressler et al. 2007), muscarinic receptor activation partially suppresses the dendrodendritic inhibition from GCs to mitral cells in vivo (Tsuno et al. 2008). Given that cholinergic input is potentiated during waking periods (Brown et al. 2012), the cholinergic modulation of dendrodendritic synapses likely optimizes odor information processing during waking olfactory behavior. Partial suppression of dendrodendritic inhibition might facilitate the propagation of action potentials in lateral dendrites of mitral/tufted cells (Xiong and Chen 2002), and may allow an appropriate number of mitral/tufted cells to synchronize for proper odor information processing. Although the exact mechanisms are not known, the blockade of cholinergic signals in the OB perturbs olfactory learning and memory (Ravel et al. 1994; Devore et al. 2012).

Noradrenergic fibers from the locus ceruleus are distributed predominantly in the GCL (McLean et al. 1989), and GCs express several subtypes of adrenergic receptors (McCune et al. 1993; Nai et al. 2009). The influence of noradrenergic signals in dendrodendritic inhibition has been closely discussed with regard to the accessory OB of pregnant rodents. Female mice form olfactory recognition memory to male mouse pheromones at mating, and noradrenergic input to the accessory OB is crucial to this memory formation. The memory trace for this is considered to be deposited as a plastic change in dendrodendritic reciprocal synapses in the accessory OB (Kaba and Nakanishi 1995). Based on the observation that noradrenalin reduces dendrodendritic synaptic inhibition via α_2-receptors (Trombley and Shepherd 1992), a hypothesis was proposed that the mating-induced increase in noradrenalin transiently reduces granule-to-mitral dendrodendritic synaptic inhibition and that the resultant disinhibition of mitral-to-granule synaptic excitation leads to the long-term potentiation of granule-to-mitral dendrodendritic synaptic inhibition (Kaba and Nakanishi 1995). On the other hand, another study of the accessory OB showed that noradrenalin potentiates dendrodendritic synaptic inhibition via α1 receptors (Araneda and Firestein 2006). Although the results of these studies are contradictory, the effect of noradrenalin in the main OB was found to be concentration dependent: low doses of noradrenalin reduced dendrodendritic synaptic inhibition via α_2-receptors whereas intermediate doses increased this inhibition via α_1-receptors (Nai et al. 2009). The actual neuronal mechanisms of noradrenergic function awaits further study, but the importance of noradrenergic signals in olfactory behaviors has been widely documented. For example, activation of noradrenergic signals in the OB lowers the threshold for odor detection and discrimination (Escanilla et al. 2010), and blockade of signals in the OB perturbs olfactory learning (Sullivan et al. 1989; Veyrac et al. 2009).

Serotonergic fibers from the raphe nuclei predominantly innervate superficial layers of the OB, including GL (McLean and Shipley 1987). Serotonergic signals activate PGCs via serotonin 2C receptors, and the increased GABA release attenuates glutamate release from the OSNs (Petzold et al. 2009). Thus, serotonergic signals regulate odor inputs at a very early stage of information processing.

Taken together, these results indicate that the activity of OB interneurons and their dendrodendritic synaptic inhibition of mitral/tufted cells are regulated not only by odor inputs from the external world but also by the activity of the higher cortical region, the OC, and subcortical neuromodulatory centers. Indeed, the firing activity of mitral/tufted cells to odors is substantially modulated in a context- and behavioral state-dependent manner (Pager 1983; Kay and Laurent 1999; Doucette and Restrepo 2008; Doucette et al. 2011). Calcium imaging of the OB in vivo also showed that mitral/tufted cell activity is plastically modulated by odor experience (Kato et al. 2012). A large part of the plastic properties of mitral/tufted cell activity is considered to result from plasticity in the dendrodendritic synaptic inhibition of OB interneurons.

6.2.4 Subtypes of OB Interneurons

Although I have referred to GCs and PGCs as the two major populations of OB interneurons, they are in fact a heterogeneous population consisting of various subtypes. Knowledge of individual interneuron subtypes is important to understanding the function of OB neuronal circuits. Because the functions of individual subtypes are now little understood, the difference in OB interneuron subtypes in molecular expression and morphology is described here as a basis for the future understanding of their cooperative activity in odor information processing.

PGCs are subdivided into three nonoverlapping populations based on molecular expression, namely, the tyrosine hydroxylase (TH)-expressing, calretinin-expressing, and carbindin-expressing subtypes (Kosaka et al. 1995; Parrish-Aungst et al. 2007). A subset of TH-positive PGCs is thought to receive direct input from OSNs and send feed-forward inhibition to mitral/tufted cells via the dendrodendritic synapses, whereas carbindin-expressing PGCs are thought to not receive direct input from OSNs but rather to send dendrodendritic feedback inhibition to mitral/tufted cells in response to mitral/tufted-to-periglomerular excitatory inputs (Toida et al. 1998, 2000; Shao et al. 2009).

A small subset of GCs expresses calretinin, and their somata distribute to the MCL and the superficial sublamina of the GCL (Parrish-Aungst et al. 2007). A different subset of GCs express 5T4, a cell adhesion molecule with leucine-rich repeats in the extracellular domain, and their somata distribute mostly to the MCL (Imamura et al. 2006). Some GCs in the deep sublamina of the GCL express a calmodulin-binding protein neurogranin (Gribaudo et al. 2009). In contrast to PGCs, however, a majority of GCs do not express known protein markers for interneuron subtypes. Their molecular heterogeneity is therefore less understood.

The dendritic morphology of GCs differentiates GC subtypes in relationship to their connectivity to mitral/tufted cells. A subset of GCs ramifies apical dendrites preferentially in the deep sublamina of the EPL. They are presumed to form dendrodendritic synapses with mitral cells, whose lateral dendrites extend into the deep EPL (mitral cell-targeting GCs) (Fig. 6.1) (Mori 1987). Another GC subset ramifies apical dendrites preferentially in the superficial sublamina of the EPL. They are presumed to form dendrodendritic synapses with tufted cells, whose lateral dendrites extend into the superficial EPL (tufted cell-targeting GCs). 5T4-expressing GCs are considered to be a small subpopulation of tufted cell-targeting GCs (Imamura et al. 2006). The OB also contains a GC subtype whose apical dendrites do not extend into the EPL but form reciprocal synapses specifically with the somata of mitral cells (perisomatic-targeting GCs), although perisomatic-targeting synapses are also made by typical GCs that form dendrodendritic synapses in the EPL (Naritsuka et al. 2009). Somata of the mitral cell-targeting GCs tend to distribute to the deep sublamina of the GCL; those of the tufted cell-targeting GCs to the MCL and superficial sublamina of the GCL; and those of perisomatic-targeting GCs to the middle sublamina of the GCL (Mori 1987; Naritsuka et al. 2009).

It has been suggested that mitral cells and tufted cells constitute parallel pathways that handle different submodalities of odor information (Nagayama et al. 2004; Igarashi et al. 2012). It is possible that yet-unknown functional differences between mitral cell-targeting GCs and tufted cell-targeting GCs contribute to the different firing properties of mitral and tufted cells. In addition, subcellular targeting of interneurons is a crucial clue to the understanding of their function. In the hippocampus and neocortex, perisomatic-targeting interneurons play central roles in the synchronized firing of pyramidal cells (Sohal et al. 2009). In the OB, PGCs are targeted to the primary dendrites of mitral/tufted cells whereas GCs are targeted to the lateral dendrites and perisoma of mitral/tufted cells. Dendrodendritic synaptic inhibition of GCs to the proximal portion of mitral cell lateral dendrites inhibits the propagation of action potentials to the distal portion of the lateral dendrites (Xiong and Chen 2002), which presumably restricts the mitral/tufted cell population participating in lateral inhibition and synchronization. A closer understanding of the differential subcellular targeting of interneuron subtypes would reveal their differential roles in feedback inhibition, lateral inhibition, and synchronization of mitral/tufted cells.

6.3 Adult Neurogenesis of OB Interneurons

6.3.1 Adult OB Neurogenesis Provides Remarkable Plasticity in the OB Neuronal Circuit

The plasticity of OB neuronal circuits is further potentiated by an intriguing property of OB interneurons. Although the production of new neurons occurs only during the embryonic and neonatal periods in most brain regions, interneurons in the OB are continually generated even in adulthood (Lledo et al. 2006). In the olfactory system, OSNs in the olfactory epithelium turn over throughout life, with loss of old and incorporation of new cells. In spite of this turnover, the axonal targeting of OSNs expressing a given type of olfactory receptor to topographically fixed glomeruli is maintained (Gogos et al. 2000). OSNs are continually exposed to noxious stimuli from the external environment, such as viral infection and chemicals, and the continual generation of OSNs is thus considered to aid the maintenance of neuronal circuits despite the frequent loss of damaged OSNs. OB interneurons also turn over throughout life. In contrast to OSNs, however, turnover of OB interneurons provides a rich opportunity for extensive remodeling of the neuronal connectivity of OB neuronal circuits, which is likely not achievable by preexisting interneurons alone. As is explained in the following sections, the fact that utilization of new OB interneurons is plastically regulated by olfactory sensory experience and the behavioral state of the animal supports the notion that OB interneuron turnover contributes to the plasticity of neuronal circuits.

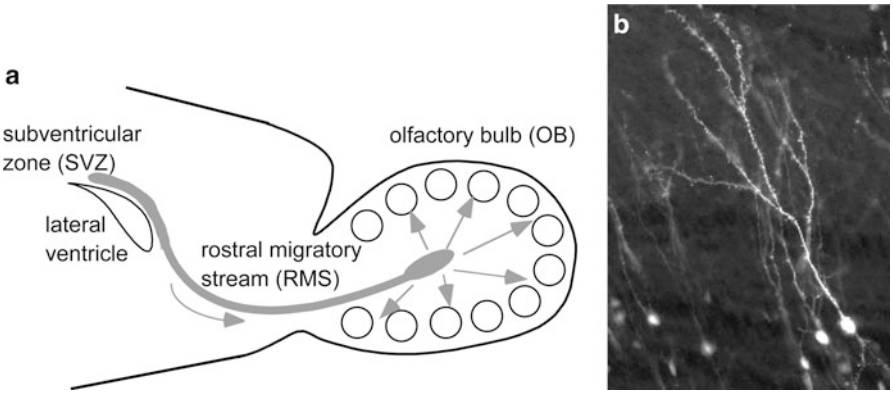

Fig. 6.5 Adult neurogenesis in the OB. **(a)** Neuronal precursors are generated in the subventricular zone (*SVZ*) around the lateral ventricle and migrate to the OB via a specific route called the rostral migratory stream (*RMS*). (**b**) Adult-born GCs are visualized by retrovirus-mediated green fluorescent protein (GFP) expression. GFP-expressing retrovirus was injected in the SVZ and the OB was analyzed 28 days after the injection

6.3.2 Generation and Synaptic Integration of Adult-Born OB Interneurons

Precursors of OB interneurons are produced in the subventricular zone (SVZ) of the lateral ventricle (Fig. 6.5). Embryonic precursors of interneurons in the ganglionic eminence and neocortex migrate to and settle down in the SVZ and continue to generate OB interneurons throughout life (Young et al. 2007). The newly generated neuronal precursors in the SVZ migrate along a specific route called the rostral migratory stream (RMS) to the OB, where they differentiate into GCs and PGCs (Fig. 6.5). Interneuron precursors in the SVZ are heterogeneous and differentiate into distinct subtypes of OB interneurons depending on their position in the SVZ (Merkle et al. 2007). Although generation of GCs and PGCs peaks during the late embryonic and early neonatal periods, it continues substantially in adulthood. The number of adult-born OB interneurons is indeed large: in rodents, at least several tens of thousands of neurons enter the OB each day (Alvarez-Buylla et al. 2001; Winner et al. 2002; Lledo et al. 2006), corresponding to roughly 1 % of the total number of OB interneurons.

Similar to embryonic and neonatal-born GCs, adult-born GCs receive glutamatergic synaptic contact from the same two major sources, mitral or tufted cells via dendrodendritic synapses in the EPL and pyramidal cells in the OC via axodendritic synapses in the GCL. Synaptic incorporation of adult-born GCs occurs roughly within 1 month after their generation (Petreanu and Alvarez-Buylla 2002; Carleton et al. 2003; Whitman and Greer 2007; Kelsch et al. 2008, 2010; Katagiri et al. 2011): axodendritic synaptic contacts from OC pyramidal cells occurs earlier, at

around day 14, synaptic contacts from mitral/tufted cell dendrites become apparent later, at around day 21, and all synaptic structures become indistinguishable from those of preexisting mature GCs by day 28.

6.3.3 *Selection of New GCs for Incorporation and Elimination*

Not all new interneurons in the OB are stably incorporated into the neuronal circuit. Under normal conditions only half of new GCs succeed in living longer than 1 month after generation: the other half are eliminated by apoptosis (Petreanu and Alvarez-Buylla 2002; Winner et al. 2002; Yamaguchi and Mori 2005). Although such a large loss of neurons seems to be a wasteful process, initial excess neurogenesis and subsequent elimination commonly occur in both embryonic and adult neurogenesis. Neuronal selection during embryonic development is crucial to refining the neuronal circuitry for proper information processing (Buss et al. 2006), and this seems to similarly apply to neuronal selection in adult neurogenesis. When apoptotic elimination of adult-born OB interneurons is suppressed by a caspase inhibitor, odor discrimination ability is disturbed (Mouret et al. 2009), possibly because inappropriately incorporated adult-born interneurons disturb proper information processing.

The life and death of new OB interneurons are not predetermined. The fate decision of new OB interneurons is regulated by the olfactory sensory experience and the behavioral state of the animal. Revealing the regulatory mechanisms of the life-and-death decision of new OB interneurons is important to understanding how adult-born OB interneurons contribute to the plasticity of olfactory information processing.

6.3.4 *Sensory Experience-Dependent Life-and-Death Decision of New GCs*

The life and death of adult-born GCs depends on olfactory sensory experience. An increased survival rate of adult-born GCs was observed in mice that were repeatedly exposed to novel odors (odor-enriched environment) (Rochefort et al. 2002). Conversely, the survival rate of adult-born GCs was decreased in anosmic mice lacking a cyclic nucleotide-gated channel in OSNs (Petreanu and Alvarez-Buylla 2002) and in the ipsilateral OB of mice with unilateral sensory input deprivation (Corotto et al. 1994; Saghatelyan et al. 2005; Yamaguchi and Mori 2005; Mandairon et al. 2006). Olfactory sensory deprivation by nostril occlusion remarkably increases the apoptosis of new GCs, which can be detected immunohistochemically by the activation of caspase-3 (Fig. 6.6a,b) (Yamaguchi and Mori 2005).

In general, sensory experience-dependent plastic change in the central nervous system is subject to the influence of time windows. For example, deprivation of visual input from one eye shifts the response property of binocular zone neurons in the visual cortex preferentially toward the nondeprived eye input (Hensch 2005). This ocular dominance plasticity occurs during a specific period after birth, called the critical period. Whether there is a critical period for adult-born GCs when their life and death is strongly influenced by olfactory sensory experience was examined. Newly generated GCs in adult mice were labeled by intraperitoneal BrdU injection, and the mice were then deprived of olfactory sensory input by nostril occlusion at various time periods after labeling. The results showed that sensory deprivation during days 14–28 after GC generation greatly reduced the survival of GCs, whereas deprivation before or after this period had no significant effect (Fig. 6.6c) (Yamaguchi and Mori 2005). Consistent with this, most apoptotic GCs were aged 14–28 days. These observations indicate that the sensory experience-dependent life-and-death decision of new GCs occurs during a critical time window at days 14–28 after their generation.

This time window corresponds to the period when adult-born GCs make extensive synaptic contacts with preexisting neurons (Petreanu and Alvarez-Buylla 2002; Carleton et al. 2003; Whitman and Greer 2007; Kelsch et al. 2008, 2010; Katagiri et al. 2011), suggesting that synaptic input plays a crucial role in the selection of adult-born GCs. Morphological examination of adult-born GCs in anosmic mice showed that young GCs destined for later elimination had already developed many synaptic structures in the EPL (Petreanu and Alvarez-Buylla 2002). Thus, it appears that the life-and-death decision of new GCs is conducted after they form synaptic contacts with preexisting neurons (Fig. 6.6d). The usability of individual new GCs may be determined with respect to their interaction with preexisting neurons in the neuronal circuit.

6.3.5 Behavioral State-Dependent Life-and-Death Decision of New GCs

Olfactory sensory experience is tightly linked to behavioral outputs of animals, such as food searching/eating, mating with partners, and escaping from predators, all of which are critical to the maintenance of life (Doty 1986). Because many odor-guided behaviors have to be newly acquired or updated to cope with a changing odor world, it is likely that neuronal circuits in the central olfactory system, including the OB, are reorganized on a daily basis during the odor experience and the acquisition/improvement of odor-guided behaviors. Thus, the life-and-death decision of new GCs may occur in association with olfaction-related behaviors, which consist of a sequence of different behavioral states. A remarkable alteration in behavioral state is the wake–rest/sleep cycle: after extensive waking olfactory behaviors, animals then take a rest or sleep. In the hippocampus and neocortex,

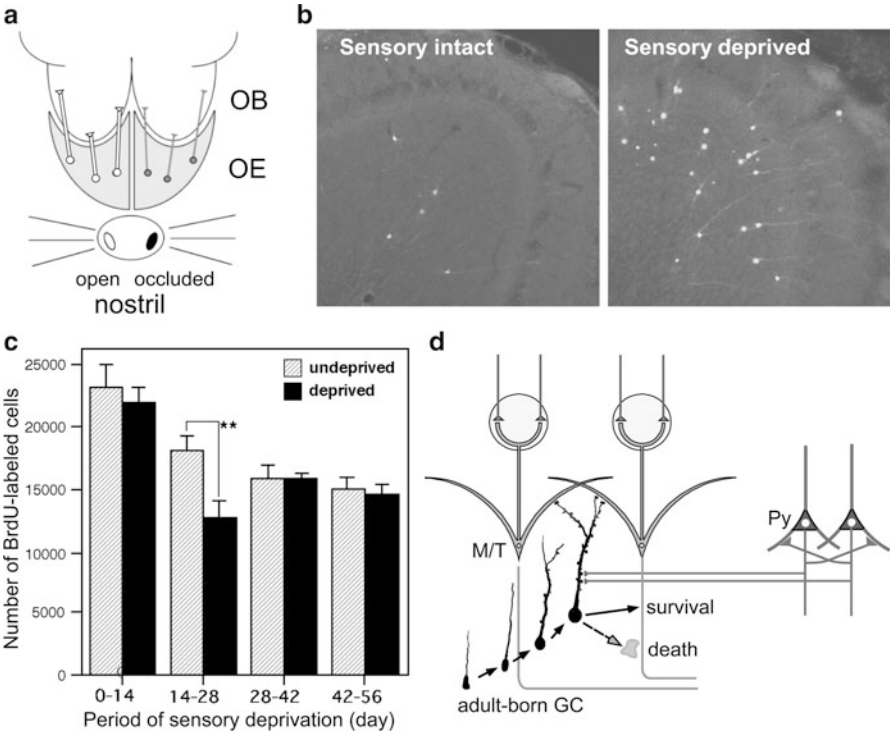

Fig. 6.6 Sensory experience-dependent life-and-death decision of adult-born GCs. (**a**) Deprivation of olfactory sensory input by single-nostril occlusion. Olfactory sensory input is conducted from the open nostril (*left*) to the same side of the olfactory epithelium (OE) and OB but is not conducted to the occluded side (*right*). (**b**) Caspase-3-activated apoptotic GCs in the OB (*white spots*). Compared to the sensory input-intact OB, a large number of apoptotic GCs is seen in the sensory-deprived OB. (**c**) Effect of sensory deprivation for 14 days at various periods after BrdU labeling on the survival of BrdU-labeled new GCs. Sensory deprivation during day 14–28 decreased survival; deprivation before or after this period showed no significant effect on survival. (**d**) A schema of the life-and-death decision of adult-born GCs. The sensory experience-dependent life-and-death decision of adult-born GCs is considered to occur during or after they form synaptic contacts with preexisting mitral/tufted cells (*M/T*) and pyramidal cells in the OC (*Py*). (Modified from Yamaguchi and Mori 2005)

reorganization of the neural circuits that accompanies the consolidation of spatial memory is considered to occur during the rest/sleep period that follows the spatial learning (Buzsaki 1989; Diekelmann and Born 2010).

On the supposition that the life-and-death decision of new GCs may occur during the time course of olfactory sensory experience and rest/sleep, we examined the fate decision of new GCs during feeding behavior, a typical olfactory behavior that is often followed by rest/sleep. Given that under ad libitum feeding conditions mice show sporadic and fragmented eating behavior, which is not suitable for efficient analysis, feeding behavior was controlled using a restricted feeding paradigm.

Food pellets were made available only during a fixed 4-h time window (11:00–15:00) each day (Fig. 6.7a). After habituation to this schedule, all mice showed extensive eating behavior during the first hour of food availability (11:00–12:00), and then showed grooming, resting, and sleeping, which are typical postprandial (after-meal) behaviors, during the subsequent hour (12:00–13:00). In the first 1 h of the eating period, no increase in apoptotic GCs was observed (Fig. 6.7b). Interestingly, however, apoptotic GCs increased approximately twofold during the next 1 h of postprandial behaviors. Perturbation of these postprandial behaviors remarkably suppressed this increase in GC apoptotic elimination, suggesting that they are important to it (Fig. 6.7b). Most of the apoptotic GCs were newly generated GCs aged 14–28 days.

Sleep is the most characteristic behavior during the postprandial period. Among various stages of sleep (light sleep, slow-wave sleep, and REM sleep), slow-wave sleep plays an important role in promoting GC elimination. The length of the slow-wave sleep roughly correlated with the number of apoptotic GCs. With regard to REM sleep, in contrast, this was rarely observed during this period; and when it did occur, its length showed no significant correlation with the magnitude of GC apoptosis. Interestingly, the length of slow-wave sleep during the period was only 10–30 min in total, indicating that short time periods of slow-wave sleep in the range of a "nap" can nevertheless strongly promote GC elimination. It should be emphasized that, although food-restricted mice sleep without preceding feeding, GC apoptosis did not increase during sleep periods outside the feeding time. The increased GC apoptosis is therefore not dependent on sleep alone, but on the combination of feeding and subsequent sleep episodes.

6.3.6 Integration of Sensory Experience and Behavioral States in the Life–and-Death Decision of New GCs: Two-Stage Model for Sensory Experience-Dependent GC Selection

The extent of apoptotic GC elimination during the postprandial period is regulated by olfactory sensory input. In mice that received unilateral sensory deprivation by chronic occlusion of one nostril and were then subjected to restricted feeding, the number of apoptotic GCs increased dramatically in the sensory-deprived OB during the postprandial period (Fig. 6.7c). Intriguingly, the number of apoptotic GCs at any period outside the feeding time did not differ from that in the OB without sensory deprivation, in spite of the fact that sensory deprivation was continuously maintained by chronic occlusion of the nostril. Thus, in food-restricted mice, the sensory experience-dependent life-and-death decision of new GCs occurred specifically during the postprandial period, indicating that this process is tightly linked to behavioral states with the sequence of olfactory sensory experience during feeding followed by sleep.

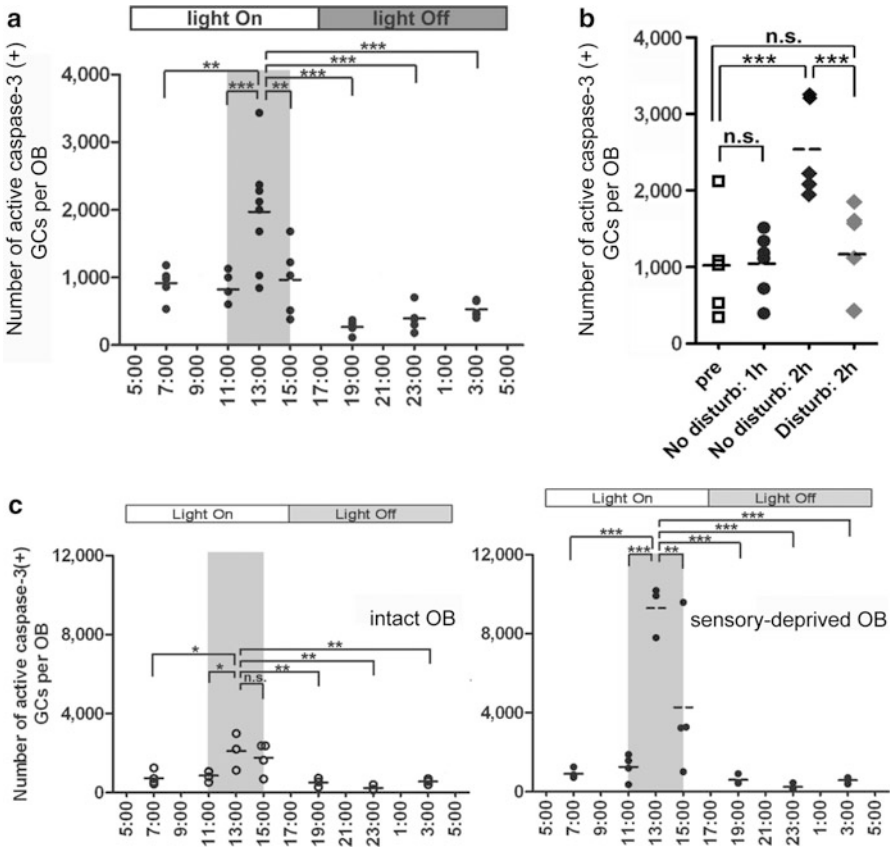

Fig. 6.7 Behavioral state-dependent life-and-death decision of adult-born GCs. (**a**) Apoptotic GCs increase during the feeding and postprandial periods. Mice were under restricted feeding in which food is supplied for only 4 h (11:00–15:00; *gray bar*) per day. On day 10 of restricted feeding, mice were analyzed at various circadian time points for caspase-3-activated apoptotic GCs in the OB. (**b**) Postprandial behaviors including sleep are crucial to the increase in GC elimination. After food delivery, mice were allowed to behave freely (*filled black dots*) for 1 or 2 h and then analyzed for caspase-3-activated apoptotic GCs. At 1 h after food presentation (No disturb: 1 h), the number of apoptotic GCs was not increased compared to that just before food delivery (pre). In contrast, at 2 h after food presentation (No disturb: 2 h), the apoptotic GC number was considerably increased. When postprandial behaviors, including rest, grooming, and sleep, were disturbed during the postprandial period (between 1 and 2 h after food delivery) (Disturb: 2 h), the apoptotic GC number was significantly suppressed. (**c**) In food-restricted mice, olfactory sensory input was deprived unilaterally by chronic occlusion of one nostril. The number of caspase-3-activated apoptotic GCs was examined at various circadian time points in the sensory input-intact (*left*) and sensory input-deprived (*right*) OB. The number of apoptotic GCs increased dramatically in the sensory-deprived OB during the postprandial period (13:00) compared to the sensory input-intact OB. In contrast, the apoptotic GC number just before the feeding time (11:00) and at any time period outside the feeding time were comparable between sensory-deprived and sensory input-intact OB. In **a**–**c**, each *dot* represents the number of caspase-3-activated GCs in one animal (average of *left* and *right* OBs for **a** and **b**; either side of OB for **c**). *Bars* represent the average. $*p < 0.05$; $**p < 0.01$; $***p < 0.001$; *n.s.* not significant; one-way ANOVA with post hoc Bonferroni test. (Modified from Yokoyama et al. 2011) with permission

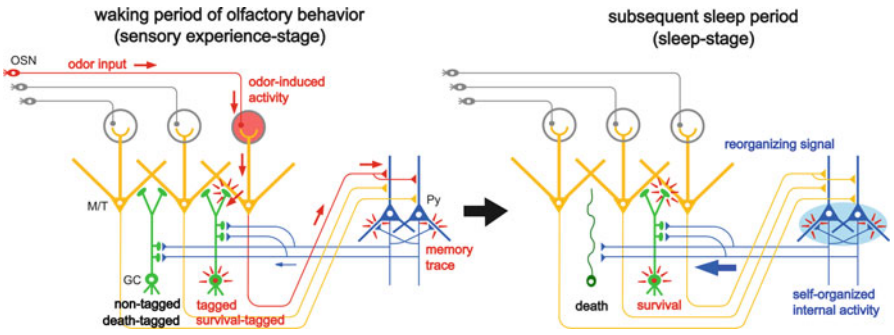

Fig. 6.8 Two-stage model for the sensory experience- and behavioral state-dependent life-and-death decision of adult-born GCs. Adult-born GCs (*green*) make dendrodendritic reciprocal synapses with mitral/tufted cells (*yellow*, M/T) and receive top-down synaptic contacts from pyramidal cells in the OC (*blue*, Py). *Left*: During the waking period of olfactory behavior (sensory experience stage), local sensory input from the OSNs (*red arrows*) activates a subset of mitral/tufted cells. Activated mitral/tufted cells activate a subset of adult-born GCs. The activated GCs might deposit "sensory experience-dependent tags" in the dendrodendritic reciprocal synapses or the cells themselves (*red marks*). Other adult-born GCs lacking activation by sensory experience are left "non-tagged" or "death-tagged." Activated mitral/tufted cells further activate pyramidal cells in the OC. The memory trace of the odor experience is deposited in the association fiber synapses among pyramidal cells in the OC (*red marks*). *Right*: During the subsequent sleep period (sleep-stage), association fiber synapses among pyramidal cells in the OC are reactivated and induce synchronized firing of the pyramidal cells. This self-organized internal activity of OC pyramidal cells (*blue oval*) is transferred to the adult-born GCs as synchronized top-down synaptic inputs (*thick blue arrow*). The synchronized top-down synaptic inputs may contribute to the putative "reorganizing signal" that promotes GC elimination during the postbehavioral sleep period. Adult-born GCs that are tagged by sensory experience during the preceding waking period survive; adult-born GCs that are not tagged (or death-tagged) are eliminated by the "reorganizing signal"

These observations led us to propose a "two-stage model" for the sensory experience-dependent selection of new GCs, in which the two stages represent olfactory sensory experience during food search and eating (sensory experience stage) followed by postprandial sleep (sleep stage) (Fig. 6.8) (Yokoyama et al. 2011; Yamaguchi et al. 2013). During the waking period, when mice show food-searching and eating behaviors, a subset of newly generated adult-born GCs receives olfactory sensory inputs from mitral/tufted cells via dendrodendritic synapses in the EPL, while the remaining subset does not (Fig. 6.8). We assume that new GCs that are activated by these olfactory sensory inputs receive a kind of synaptic tagging that works as a substrate for subsequent plastic change (Frey and Morris 1997; Redondo and Morris 2011). These GCs may be "tagged" in the dendrodendritic synapses or the cells themselves, whereas other GCs that are not activated by olfactory sensory input remain "non-tagged." Alternatively, activated new GCs might receive a "survival tag" while nonactivated new GCs receive a "death tag." Top-down axodendritic synapses from the OC pyramidal cells to new GCs might also be candidates for tagging, although whether and how a subset of

new GCs receives olfactory sensory experience-dependent top-down inputs remains unknown at present.

Importantly, although differential tagging of new GCs might occur during feeding behavior, the life-and-death decision of GCs is not made during feeding. During the subsequent postprandial period, the cell selection process is triggered and the increased GC apoptosis occurs. We hypothesized that some sort of "reorganizing signal" enters the OB during the postprandial period, typically during the postprandial slow-wave sleep period, and promotes GC selection according to the presence or absence or type of tag that the GCs received during the preceding waking period (Fig. 6.8). Adult-born GCs "tagged" or "survival-tagged" by sensory experience might be selected to survive by this "reorganizing signal" whereas other "non-tagged" or "death-tagged" adult-born GCs might be eliminated by it. The fate of individual adult-born GCs might be determined by the interplay between tagging that reflect the olfactory sensory experience during the waking period and the reorganizing signal that enters the OB during the subsequent sleep period.

This idea of a two-stage model of GC elimination is analogous to the two-stage model of memory formation and consolidation in the hippocampus. This model states that experience-dependent input induces memory trace formation during awake learning and that replay of the experience occurs for the reorganization and consolidation of neuronal circuits during subsequent sleep or rest (Buzsaki 1989; Diekelmann and Born 2010). Enhanced GC elimination during the postprandial period also resembles homeostatic synaptic downscaling during sleep (Tononi and Cirelli 2006; Vyazovskiy et al. 2008). It has been shown in the rodent neocortex and hippocampus that behavioral state modulates synaptic strength, with a net increase during waking and a reduction during sleep. Because a large number of adult-born GCs are recruited in the OB every day, elimination of adult-born GCs is necessary to maintaining the overall number of GCs in the entire OB within an appropriate range. This kind of downscaling may increase the ratio of useful versus useless GCs and thereby improve the signal-to-noise ratio for olfactory information processing, as has been proposed for the role of synaptic downscaling (Tononi and Cirelli 2006), and may make room for a successive cohort of new GCs to be integrated in preparation for the next round of new olfactory experience.

6.3.7 Possible Neuronal Mechanisms Underlying Sensory Experience- and Behavioral State-Dependent GC Selection

What are the neuronal mechanisms for the hypothetical reorganizing signal during postbehavioral sleep? One possibility is that the signal is contributed to by glutamatergic top-down inputs from the OC. Manabe et al. recorded single unit activities in the anterior piriform cortex (APC) in freely behaving rats and showed that numerous APC neurons fire synchronously during the slow-wave sleep state

(Manabe et al. 2011). LFP recordings further showed that the deep layer of the APC generates repetitive sharp negative potentials during the slow-wave sleep state that resemble hippocampal sharp waves in both shape and duration. These "olfactory cortex sharp waves" (OC-SPWs) in the APC are associated with synchronized spike discharges of APC neurons. Importantly, simultaneous recording of LFP in the APC and GCL of the OB revealed that sharp wave-like potentials in the OB occurred in close temporal proximity to OC-SPWs, indicating that the repetitive synchronous discharge activity of APC neurons during the slow-wave sleep state is transferred to the OB GCL as the synchronized top-down synaptic inputs. Given that the synchronized top-down inputs occur repeatedly during slow-wave sleep but not during waking or REM sleep (Manabe et al. 2011), these inputs are a plausible candidate for the slow-wave sleep state-specific reorganizing signal. The synchronous discharge of APC neurons during the slow-wave sleep is a self-organized internal activity, and might be a replay of the memory trace of odor experience formed during the waking period, which is deposited in the association fibers of the APC neurons (Fig. 6.8) (for details please refer to Manabe et al. 2011 and Yamaguchi et al. 2013). Further examination will clarify the causal relationship between top-down inputs and GC elimination.

GC elimination is promoted during postprandial sleep but not during sleep without preceding eating in food-restricted mice. However, OC-SPW-associated synchronized top-down inputs to GCs always occur during slow-wave sleep regardless of the presence or absence of preceding eating (Manabe et al. 2011; our unpublished observation). Synchronized top-down inputs from the OC alone may thus not be sufficient to trigger GC elimination. Deposition of putative tag signals during preceding waking may be prerequisite, and the life-and-death decision of new GCs might be determined after collation of the top-down reorganization signal with the putative deposited tag signals. Further, other behavioral state-dependent signals might also be involved. Neuromodulatory signals are activated during attentive behaviors and decline during slow-wave sleep (Brown et al. 2012). Noradrenergic input to the OB is potentiated in many olfactory behaviors (Brennan et al. 1990; Wellman 2000). Enhanced neuromodulatory signals during waking olfactory behavior might potentiate subsequent GC elimination during slow-wave sleep. The effects of noradrenergic or cholinergic signals on the survival of new GCs have been well documented (Cooper-Kuhn et al. 2004; Kaneko et al. 2006; Veyrac et al. 2009; Moreno et al. 2012).

The behavioral state-dependent life-and-death decision of adult-born GCs indicates that the fate of adult-born GCs is determined by the integration of various behavioral state-dependent signals. It is worth noting that the candidate signals, namely olfactory sensory inputs, top-down inputs from the OC, and neuromodulatory signals, overlap with those signals that regulate the activity of OB interneurons and their dendrodendritic synaptic inhibition. This observation implies that the function of OB interneurons and the life-and-death decision of adult-born OB interneurons are regulated by shared neuronal mechanisms, both of which would help the animal behave properly in response to ever-changing odor circumstances by utilizing the highly plastic properties of OB interneurons.

6.4 Coordination of Preexisting Interneurons and Newly Generated Interneurons in the OB

6.4.1 Relationship Between Preexisting and Newly Generated Interneurons for Constitution of the OB Neuronal Circuit

A large number of OB interneurons are continually generated in the adult. In rodents, roughly 1% of total OB interneurons are generated each day (Alvarez-Buylla et al. 2001; Winner et al. 2002; Lledo et al. 2006). Although the number declines with age, neurogenesis continues even in 2-year-old mice (Enwere et al. 2004). One question is to what extent do adult-born interneurons contribute to the overall constitution of the OB neuronal circuits in the adult. Although traditional techniques of BrdU- or retrovirus-mediated labeling of new neurons identify only a small fraction of adult-born neurons, recent advances in molecular and developmental biology have enabled the labeling of a much larger proportion and provided an estimation of the quantitative contribution of adult-born interneurons. A number of studies have used a tamoxifen-mediated Cre recombination system to permanently label adult-born OB interneurons by marker protein expression (Lagace et al. 2007; Ninkovic et al. 2007; Imayoshi et al. 2008). The proportion of labeled cells among total OB interneurons differed among studies, but all showed that the labeled cells gradually accumulate and increase in number for at least several months after the initiation of cell labeling. In one study, labeled adult-born GCs accounted for nearly 20 % of the total number of GCs, a proportion that remained stable between 4 and 9 months (Ninkovic et al. 2007). In another study, the proportion of labeled adult-born GCs continued to increase up to age 12 months to 60–70 % of GCs (Imayoshi et al. 2008). The former observation suggests the possibility that adult-born GCs may constitute a specific cohort of cells that are repeatedly replaced by much younger adult-born GCs, and the latter observation suggests that adult-born GCs may continue to accumulate and finally account for the majority of all GCs in the adult OB. Although the actual proportion of adult-born GCs awaits further confirmation, the two modes of contribution of adult-born GCs, repeated replacement and continual addition, are not mutually exclusive but rather may work together to differing extents under different conditions to maintain and modulate the OB neuronal circuits.

Besides the continual accumulation of adult-born GCs, preexisting old GCs are gradually lost from the neuronal circuits during adulthood. BrdU-labeled neonatal-born GCs decrease in number with age, by nearly half at 6 months old (Imayoshi et al. 2008). In the case of PGCs, an in vivo time-lapse imaging study showed the disappearance of old PGCs and appearance of new PGCs in the same observation field, with a turnover rate of approximately 3 % per month

(Mizrahi et al. 2006). These observations indicate that OB interneurons are turning over, with the elimination of old cells and incorporation of new ones. What then is the relationship between old and new interneurons in their turnover? Interestingly, genetic ablation of adult-born GCs did not influence the rate of neonate-born GC loss, suggesting that old GCs are lost irrespective of the supply of new neurons (Imayoshi et al. 2008). This observation in turn suggests that continuous neurogenesis is required to compensate for the loss of old interneurons. Consistent with this, enhanced elimination of preexisting GCs in a local area of the OB by local injection of immunotoxin facilitates the incorporation of newly generated GCs in the local OB area (Fig. 6.9a) (Murata et al. 2011). This observation further supports the idea that the elimination of old GCs and incorporation of new GCs are coordinated, such that new GCs compensate for the loss of old GCs and contribute to the maintenance of the GC population in local neuronal circuits of the OB. In addition to the plastic modulation of OB neuronal circuits, adult-born interneurons play fundamental roles in the maintenance of OB neuronal circuits.

6.4.2 Generation of Different Subtypes at Different Ages and Subtype-Specific Replacement of OB Interneurons

OB neuronal circuits contain various subtypes of interneurons. Recent studies have revealed that the turnover of OB interneurons is conducted in a subtype-specific manner (Fig. 6.9b). In the experiment of immunotoxin-mediated GC ablation, a subset of preexisting GCs that expresses metabotropic glutamate receptor type II (mGluR2) was specifically ablated (Murata et al. 2011). Following this subtype-specific ablation, incorporation of new GCs was preferentially promoted for the mGluR2-expressing subtype over the mGluR2-negative subtype. Similarly, laser ablation of TH-expressing PGCs was compensated by the integration of new TH-expressing PGCs in the same periglomerular positions where preexisting TH-expressing PGCs were present before ablation (Sawada et al. 2011). The constitution of OB neuronal circuits thus appears to be further maintained by subtype-specific compensatory mechanisms even under extensive turnover (Fig. 6.9c).

Although I have so far explained the role of subtype-specific turnover of OB interneurons in the compensation and maintenance of OB neuronal circuits, neurogenesis at different ages generates overlapping but different populations of interneuron subtypes. The calbindin-expressing PGC subtype is predominantly generated during the embryonic and neonatal period, whereas adult-born PGCs are mostly of the TH- or calretinin-expressing subtype (De Marchis et al. 2007; Ninkovic et al. 2007; Batista-Brito et al. 2008). Calretinin-expressing GCs are predominantly generated after birth, while 5T4-expressing GCs are generated throughout the embryonic and postnatal periods (Batista-Brito et al. 2008). Genetic

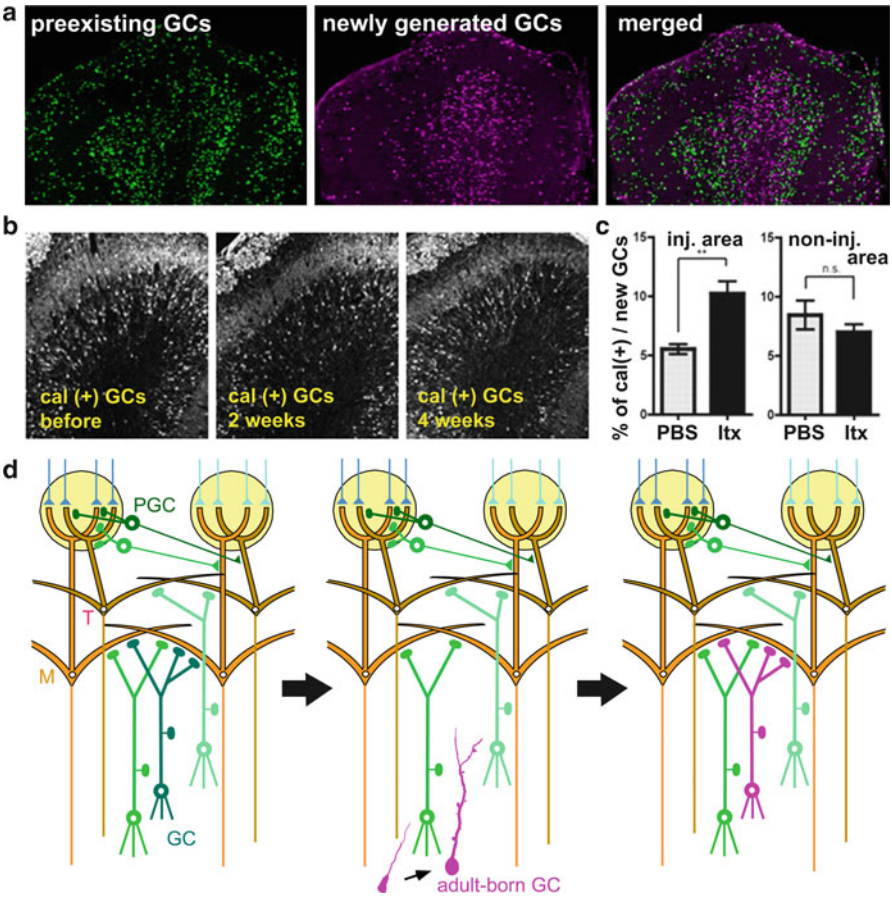

Fig. 6.9 Turnover of preexisting old GCs and newly generated GCs. (**a**) Newly generated GCs compensate for the loss of preexisting GCs. Preexisting old GCs were ablated in the local area of the OB by the local injection of immunotoxin. At 2 weeks after immunotoxin injection, preexisting GCs (*left panel*, *green*; labeled by BrdU analogue CldU) decreased in the local area. In the same local area, newly generated adult-born GCs (*middle panel*, *magenta*; labeled by another BrdU analogue, IdU) increased. *Right panel:* Merged view. (**b**) Ablation and recovery of a GC subtype. Calretinin-expressing GCs (*white*) are a subpopulation of mGluR2-expressing GCs. At 2 weeks after immunotoxin injection, calretinin-expressing GCs decreased from mGluR2-expressing GC-specific ablation (*middle panel*). At 4 weeks, calretinin-expressing GCs showed recovery in density in the ablated area (*right panel*). (**c**) In the immunotoxin (Itx)-injected area, incorporation of calretinin-expressing new GCs increased (*left panel*). This effect was not seen in the noninjected area of the same OB (*right panel*). (**d**) Conceptual schema of subtype-specific turnover of GCs and maintenance of OB neuronal circuits. Following the loss of a specific subtype of GC in an OB neuronal circuit (*middle panel*, loss of a GC with *dark green*), an adult-born GC (*magenta*) compensates for the lost subtype of GC (*right panel*, a GC with *magenta*). This subtype-specific turnover maintains the constitution of OB neuronal circuits during the continual loss and incorporation of GCs. *M* mitral cell, *T* tufted cell. (Modified from Murata et al. 2011)

analysis and transplantation studies of stem cells revealed that the generation of different interneuron subtypes originates from the heterogeneity of stem cells, rather than the putative subtype-specific instruction cues in the OB environment (Merkle et al. 2007; Young et al. 2007).

These observations raise the interesting possibility that the subtype constitution of OB neuronal circuits may gradually change with age, and that neurogenesis at different ages may contribute to odor information processing differently. BrdU labeling of new neurons showed that neonate-born GCs tend to locate in the superficial portion of the GCL while adult-born GCs locate in the deep portion (Lemasson et al. 2005; Imayoshi et al. 2008). Neonate-born GCs tend to extend dendrites into the superficial sublamina of the EPL, whereas adult-born GCs do so into the deep sublamina of the EPL (Kelsch et al. 2007). Given the distribution of mitral cell lateral dendrites in the deep EPL sublamina (Mori 1987), adult-born GCs may make dendrodendritic synaptic contacts preferentially with mitral cells and contribute to the odor information processing conveyed through mitral cell pathways.

Further analysis of the turnover of interneuron subtypes during odor-guided learning and memory formation would give clues to understanding the functional roles of individual interneuron subtypes and their turnover. Different interneuron subtypes respond differently to olfactory sensory experience. Olfactory sensory deprivation remarkably reduces the survival of TH-expressing PGCs compared to calbindin- or calretinin-expressing PGCs (Bastien-Dionne et al. 2010; Sawada et al. 2011). Olfactory sensory deprivation preferentially reduces the survival of newly generated GCs in the deep sublamina of the GCL (Mandairon et al. 2006). Proper control of interneuron subtype turnover may be important both for the maintenance and plastic modulation of OB neuronal circuits.

6.5 Contribution of OB New Neurons in Olfactory Behaviors

6.5.1 Methods for Addressing the Role of Adult Olfactory Neurogenesis

A central question for adult neurogenesis is how it contributes to brain functions. Recent studies in rodents are revealing the roles of olfactory neurogenesis in olfactory behaviors, although contradictory observations have occasionally appeared. The purpose of this section is to provide an overview of how adult neurogenesis has been experimentally addressed and what kinds of functional alteration have been observed in adult neurogenesis-modified animals. For details, please refer also to recent reviews (Lazarini and Lledo 2011; Breton-Provencher and Saghatelyan 2012; Kageyama et al. 2012).

Most studies are based on the loss-of-function approach, whereby olfactory behaviors are addressed in mice with suppressed adult olfactory neurogenesis. Four major techniques to suppress olfactory neurogenesis have been reported to date: antimitotic drug injection, γ-ray irradiation, genetic cell ablation, and utilization of gene-mutant mice. Each method has advantages and disadvantages. Injection of the antimitotic drug Ara-C into the lateral ventricle (LV)/SVZ effectively ablates proliferating cells in the SVZ and reduces the supply of new neurons to the OB. Continual application of Ara-C continues to suppress neurogenesis and drug removal restores it (Enwere et al. 2004). Ara-C application can therefore address the effect of both loss and recovery of olfactory neurogenesis. A major caveat is that application of the drug affects not only olfactory neurogenesis but also hippocampal neurogenesis (Breton-Provencher et al. 2009; Sultan et al. 2010). Some olfactory learning is known to depend on the hippocampus (Sauvage et al. 2008). On the other hand, γ-ray irradiation in restricted brain areas, including the SVZ, enables specific suppression of olfactory neurogenesis by sparing hippocampal neurogenesis. However, both Ara-C treatment and irradiation may have confounding effects on preexisting neuronal circuits, such as direct neuronal toxicity, or indirect effects through the induction of inflammation.

The genetic method utilizing drug-induced Cre recombinase activation provides a sophisticated way of suppressing adult neurogenesis. For example, induced expression of cytotoxic genes by tamoxifen-mediated activation of CreER recombinase causes cell death in adult-born neurons at desired time points (Imayoshi et al. 2008). The efficacy and specificity of this ablation system are crucially dependent on the availability of tissue- or cell type-specific promoters for expressing exogenous genes. Gene mutant mice showing impairment in olfactory neurogenesis offer a variety of materials to address the role of adult neurogenesis as well as the function of the genes of interest. Possible drawbacks of mutant mice are abnormalities other than olfactory neurogenesis and the recruitment of compensatory mechanisms for the gene mutation from developmental stages.

Many kinds of olfactory behaviors have been examined in these neurogenesis-suppressed mice, including spontaneous approaching behaviors to odors, acquisition of associative olfactory memory, retention of olfactory memory, and odor-guided social and reproductive behaviors. These behaviors differ greatly in motivation, difficulty of tasks, and expected outcomes of the behavioral responses. Although contradictory observations are often seen, the overall tendency of behaviors in olfactory neurogenesis-suppressed mice seems to be that spontaneous odor behaviors are somewhat spared, acquisition and retention of associative olfactory memory are somehow impaired, and social and reproductive olfactory behaviors are remarkably impaired. These effects are explained in the next section.

6.5.2 *Possible Roles of Adult Neurogenesis in Olfactory Behaviors*

When mice are repeatedly exposed to a given odor without any reward or avoidance cues, the exploratory time devoted to the odor gradually diminishes (habituation). If a different odor is applied after habituation to the first odor, however, the exploratory time increases (dishabituation). This habituation–dishabituation paradigm is frequently used to address a mice's ability in odor discrimination and the odor-detection threshold. In olfactory neurogenesis-suppressed mice, these functions do not appear to differ from those in intact mice (Imayoshi et al. 2008; Lazarini et al. 2009, but see Breton-Provencher et al. 2009). In contrast, when short-term olfactory memory is assessed by this habituation–dishabituation paradigm, apparent impairment is observed. When the same odor was presented twice at varying time intervals, intact mice showed reduced sniffing to the second presentation even after an interval of 120 min. However, mice injected with Ara-C in the LV did not show reduced sniffing to the second presentation as early as after 30 min, indicating that the Ara-C-injected mice did not retain memory of the odor for longer than 30 min (Breton-Provencher et al. 2009). A different odor presentation paradigm showed that repeated exposure to two different odors improves the ability to discriminate the odors, which is referred to as perceptual olfactory learning (Moreno et al. 2009, 2012). Perceptual olfactory learning is impaired in Ara-C-injected mice (Moreno et al. 2012). These observations indicate that olfactory neurogenesis contributes to olfactory learning even when odors are experienced without any association with reinforcing (attractive or aversive) cues.

In typical experiments of olfactory learning, animals learn to associate odor cues with specific reinforcing outcomes. When one odor is associated with a sugar/water reward while another odor is left unrewarded, mice become selectively attracted to the rewarded odor. In SVZ-irradiated mice and Ara-C-injected mice, this odor–reward associative learning was accomplished normally, but long-term retention of the memory over days was impaired (Lazarini et al. 2009; Sultan et al. 2010). In contrast, odor–sugar reward associative learning was maintained for more than a week in Ara-C-injected mice (Breton-Provencher et al. 2009) and over several months in mice with cell ablation using tamoxifen-dependent Cre-mediated cell toxicity (Imayoshi et al. 2008).

The reason for this discrepancy is not known but it might be attributable to the difference in the task paradigm (Lazarini and Lledo 2011; Mandairon et al. 2011; Breton-Provencher and Saghatelyan 2012). The studies showing impaired long-term memory utilized operant conditioning tasks, in which mice need to learn novel procedures to retrieve a reward, such as poking the nose into odor/water ports or searching in holes made on a platform. On the other hand, the studies showing no impairment used nonoperant (Pavlovian) conditioning tasks, in which mice can retrieve a reward without acquiring a novel procedure, just by digging into their bedding where the cued odor is present. Such differences in learning paradigm may recruit different brain regions to different extents and alter the dependency on OB

neurogenesis. Consistent with this notion, the survival of new GCs is substantially potentiated by performing operant tasks compared to nonoperant tasks (Mandairon et al. 2011).

The association of odor cues with noxious stimuli is also affected in neurogenesis-suppressed mice. When an odor was associated with electrical foot shock delivery, mice developed freezing behavior to the odor. In SVZ-irradiated mice, the freezing behavior occurred to the cued odor but the time duration was shorter than in intact mice. In contrast, the irradiated mice showed normal freezing behavior when an auditory cue was used for the association with foot shock (Valley et al. 2009). In mice with genetic and inducible ablation of adult-born neurons, freezing response to TMT, a predator's odor, was compromised when TMT was force associated with a sugar reward (Sakamoto et al. 2011).

Olfaction mediates a variety of social and reproductive behaviors, and the suppression of olfactory neurogenesis substantially affects these behaviors. Proliferation of progenitors in the SVZ of female mice is enhanced during pregnancy and after partition, which is mediated by the increased secretion of prolactin (Shingo et al. 2003). This prolactin-mediated enhanced neurogenesis is essential for the proper pup-fostering behavior of mothers (Larsen and Grattan 2010), for female mice to show preference to dominant males over subordinate males (Mak et al. 2007), and for male mice to recognize their own offspring (Mak and Weiss 2010). Irradiation of the SVZ in females impaired their recognition of male odors (Feierstein et al. 2010). Genetic and inducible ablation of adult-born neurons induces impairment in male-to-male aggressive behavior, male-to-female mating behavior, and the pup-fostering behavior of mothers (Sakamoto et al. 2011).

In addition to these loss-of-function studies, a recent optogenetic study used a gain-of-function approach. Photoactivation of new OB interneurons during odor discrimination learning facilitated the learning process, in which mice that received photoactivation accomplished the learning with a smaller number of trials (Alonso et al. 2012). Notably, this learning facilitation was evident when mice discriminated very similar odors but not when they discriminated dissimilar odors.

Overall, these studies indicate that adult neurogenesis in the OB contributes to various olfactory behaviors to varying extents. A possible interpretation for the seemingly variable contribution to different olfactory tasks is that adult neurogenesis may be much more involved in "difficult" tasks compared to "easy" tasks. The degree of difficulty in the olfactory tasks may relate to whether the tasks are operant or nonoperant, whether they require the discrimination of very similar odors or dissimilar odors, and whether they require the identification and discrimination of animals of the same species or different species, as well as nonliving odorous objects. Each of the former of these paired cases may represent a more difficult situation for the performance of proper olfactory behaviors. Difficult tasks may require much higher attention and motivation and additional learning/memory processes that must recruit many brain regions and signal systems. The function of adult-born OB interneurons may be fully potentiated by, and required for, situations in which many brain regions and signal systems are required to work in concert.

6.5.3 *Physiological Studies Addressing the Role of Adult Neurogenesis*

In contrast to the many behavioral studies, physiological analyses in adult neurogenesis-suppressed mice are limited and controversial. Patch clamp recordings of mitral cells in the OB slice of Ara-C-injected mice showed a reduced frequency of spontaneous inhibitory postsynaptic potentials, lesser strength of dendrodendritic inhibition, and decreased synchronized activity (Breton-Provencher et al. 2009). However, in vivo recordings under anesthesia in SVZ-irradiated mice showed no alteration in dendrodendritic synaptic inhibition following antidromic stimulation of mitral/tufted cells or in the odor-induced oscillatory LFP in the OB (Valley et al. 2009). Optogenetic activation of new OB interneurons showed that activation reduces spontaneous firing activity of mitral cells in vitro and also in vivo in head-restrained awake mice (Alonso et al. 2012). Interestingly, enhanced firing of mitral cells in response to odor stimuli was suppressed by optogenetic activation of new OB neurons to different extents, with weakly activated mitral cells showing much greater suppression than strongly activated mitral cells, thereby enhancing the contrast of odor responses among mitral cells (Alonso et al. 2012). The combination of behavioral analysis with electrophysiological and imaging analysis would facilitate understanding of how odor information processing by adult-born OB interneurons contributes to the expression of proper olfactory behaviors. Simultaneous analysis of wide brain regions might also be important, given the possible contribution of many brain regions and signal systems to OB interneuron-mediated odor information processing.

6.6 Conclusion

In the OB, odor information is substantially modulated by a large number of local interneurons. GCs and PGCs induce feedback inhibition, lateral inhibition, and synchronization to mitral/tufted cells via dendrodendritic synapses and regulate the firing activity of mitral/tufted cells. Notably, the dendrodendritic synaptic inhibition of mitral/tufted cells is plastically regulated not only by the odor inputs from the external world but also by the activity of the OC and subcortical neuromodulatory centers. In addition, continual generation of OB interneurons during adulthood potentiates the plasticity of OB neuronal circuits. The life-and-death decision of new GCs is dependent on the behavioral state of the animal, namely, the sequence of feeding behavior during waking and subsequent slow-wave sleep, suggesting that utilization of new OB interneurons is also regulated by the behavioral state-dependent activities of higher brain regions. The OB interneurons therefore establish neuronal circuits in which integration of multiple signals from many brain regions leads to the plastic modulation of mitral/tufted cell

activities. The importance of this OB interneuron-mediated information processing is supported by the behavioral analysis of adult neurogenesis-suppressed mice. These mice show impaired behaviors, particularly in difficult olfactory tasks, which likely require much higher attention and motivation and additional learning/memory processes and thereby recruit many brain regions and signal systems. Given that OB interneurons consist of various subtypes, revealing the subtype-specific functions and turnover would give further clues to understanding the adaptive roles of OB interneurons in the acquisition and updating of proper odor-guided behaviors in the ever-changing odor circumstances.

Acknowledgments This work was supported by a Grant-in-Aid for Scientific Research from JSPS, and a Grant-in-Aid for Scientific Research on Innovative Areas from MEXT.

References

Abraham NM, Egger V, Shimshek DR et al (2010) Synaptic inhibition in the olfactory bulb accelerates odor discrimination in mice. Neuron 65:399–411

Adrian ED (1950) The electrical activity of the mammalian olfactory bulb. Electroencephalogr Clin Neurophysiol 2:377–388

Alonso M, Lepousez G, Sebastien W et al (2012) Activation of adult-born neurons facilitates learning and memory. Nat Neurosci 15:897–904

Alvarez-Buylla A, Garcia-Verdugo J, Tramontin AD (2001) A unified hypothesis on the lineage of neuronal stem cells. Nat Rev Neurosci 2:287–293

Andres KH (1965) Der feinbau des bulbus olfactorius der ratte unter beonderer beruksachtigung der synaptischen verbandungen. Z Zellforsch Mikrosk Anat 65:530–561

Araneda RC, Firestein S (2006) Adrenergic enhancement of inhibitory transmission in the accessory olfactory bulb. J Neurosci 26:3292–3298

Balu R, Pressler RT, Strowbridge BW (2007) Multiple modes of synaptic excitation of olfactory bulb granule cells. J Neurosci 27:5621–5632

Bastien-Dionne PO, David LS, Parent A et al (2010) Role of sensory activity on chemospecific populations of interneurons in the adult olfactory bulb. J Comp Neurol 518:1847–1861

Batista-Brito R, Close J, Machold R et al (2008) The distinct temporal origins of olfactory bulb interneuron subtypes. J Neurosci 28:3966–3975

Beshel J, Kopell N, Kay LM (2007) Olfactory bulb gamma oscillations are enhanced with task demands. J Neurosci 27:8358–8365

Blanes T (1897) Sobre algunos puntos dudosos de la estructura del bulbo olfatorio (On some doubtful points concerning the structure of the olfactory bulb). Rev Trim Micrograf 3:99–127

Boyd AM, Sturgill JF, Poo C et al (2012) Cortical feedback control of olfactory bulb circuits. Neuron 76:1161–1174

Brennan P, Kaba H, Keverne EB (1990) Olfactory recognition: a simple memory system. Science 250:1223–1226

Breton-Provencher V, Saghatelyan A (2012) Newborn neurons in the adult olfactory bulb: unique properties for specific odor behavior. Behav Brain Res 227:480–489

Breton-Provencher V, Lemasson M, Peralta MR 3rd et al (2009) Interneurons produced in adulthood are required for the normal functioning of the olfactory bulb network and for the execution of selected olfactory behaviors. J Neurosci 29:15245–15257

Brown RE, Basheer R, McKenna JT et al (2012) Control of sleep and wakefulness. Physiol Rev 92:1087–1187

Buss RR, Sun W, Oppenheim RW (2006) Adaptive roles of programmed cell death during nervous system development. Annu Rev Neurosci 29:1–35

Buzsaki G (1989) Two-stage model of memory trace formation: a role for "noisy" brain states. Neuroscience 31:551–570

Cajal SR (1890–1891) Origen y terminación de las fibras nerviosas olfatorias (Origin and termination of the olfactory nerve fibers). Gaceta Sanitaria de Barcelona 3:133–139; 174–181; 206–212

Carleton A, Petreanu LT, Lansford R et al (2003) Becoming a new neuron in the adult olfactory bulb. Nat Neurosci 6:507–518

Castillo PE, Carleton A, Vincent JD et al (1999) Multiple and opposing roles of cholinergic transmission in the main olfactory bulb. J Neurosci 19:9180–9191

Chen WR, Xiong W, Shepherd GM (2000) Analysis of relations between NMDA receptors and GABA release at olfactory bulb reciprocal synapses. Neuron 25:625–633

Cooper-Kuhn CM, Winkler J, Kuhn HG (2004) Decreased neurogenesis after cholinergic forebrain lesion in the adult rat. J Neurosci Res 77:155–165

Corotto F, Henegar J, Maruniak J (1994) Odor deprivation leads to reduced neurogenesis and reduced neuronal survival in the olfactory bulb of the adult mouse. Neuroscience 61:739–744

De Marchis S, Bovetti S, Carletti B et al (2007) Generation of distinct types of periglomerular olfactory bulb interneurons during development and in adult mice: implication for intrinsic properties of the subventricular zone progenitor population. J Neurosci 27:657–664

de Olmos J, Hardy H, Heimer L (1978) The afferent connections of the main and the accessory olfactory bulb formations in the rat: an experimental HRP-study. J Comp Neurol 181:213–244

Debarbieux F, Audinat E, Charpak S (2003) Action potential propagation in dendrites of rat mitral cells in vivo. J Neurosci 23:5553–5560

Devore S, Manella LC, Linster C (2012) Blocking muscarinic receptors in the olfactory bulb impairs performance on an olfactory short-term memory task. Front Behav Neurosci 6:59

Diekelmann S, Born J (2010) The memory function of sleep. Nat Rev Neurosci 11:114–126

Doty RL (1986) Odor-guided behavior in mammals. Experientia (Basel) 42:257–271

Doucette W, Restrepo D (2008) Profound context-dependent plasticity of mitral cell responses in olfactory bulb. PLoS Biol 6:e258

Doucette W, Gire DH, Whitesell J et al (2011) Associative cortex features in the first olfactory brain relay station. Neuron 69:1176–1187

Egger V, Svoboda K, Mainen ZF (2003) Mechanisms of lateral inhibition in the olfactory bulb: efficiency and modulation of spike-evoked calcium influx into granule cells. J Neurosci 23:7551–7558

Egger V, Svoboda K, Mainen ZF (2005) Dendrodendritic synaptic signals in olfactory bulb granule cells: local spine boost and global low-threshold spike. J Neurosci 25:3521–3530

Enwere E, Shingo T, Gregg C et al (2004) Aging results in reduced epidermal growth factor receptor signaling, diminished olfactory neurogenesis, and deficits in fine olfactory discrimination. J Neurosci 24:8354–8365

Escanilla O, Arrellanos A, Karnow A et al (2010) Noradrenergic modulation of behavioral odor detection and discrimination thresholds in the olfactory bulb. Eur J Neurosci 32:458–468

Eyre MD, Antal M, Nusser Z (2008) Distinct deep short-axon cell subtypes of the main olfactory bulb provide novel intrabulbar and extrabulbar GABAergic connections. J Neurosci 28:8217–8229

Feierstein CE, Lazarini F, Wagner S et al (2010) Disruption of adult neurogenesis in the olfactory bulb affects social interaction but not maternal behavior. Front Behav Neurosci 4:176

Frey U, Morris RGM (1997) Synaptic tagging and long-term potentiation. Nature (Lond) 385:533–536

Gao Y, Strowbridge W (2009) Long-term plasticity of excitatory inputs to granule cells in the rat olfactory bulb. Nat Neurosci 12:731–733

Gogos JA, Osborne J, Nemes A et al (2000) Genetic ablation and restoration of the olfactory topographic map. Cell 103:609–620

Golgi C (1875) Sulla fina struttura dei bulbi olfactorii (On the fine structure of the olfactory bulb). Riv Sper Freniatr Med Leg 1:405–425
Gribaudo S, Bovetti S, Garzotto D et al (2009) Expression and localization of the calmodulin-binding protein neurogranin in the adult mouse olfactory bulb. J Comp Neurol 517:683–694
Haberly LB, Price JL (1978) Association and commissural fiber systems of the olfactory cortex of the rat. J Comp Neurol 178:711–740
Halabisky B, Strowbridge BW (2003) Gamma-frequency excitatory input to granule cells facilitates dendrodendritic inhibition in the rat olfactory bulb. J Neurophysiol 90:644–654
Halabisky B, Friedman D, Radojicic M et al (2000) Calcium influx through NMDA receptors directly evokes GABA release in olfactory bulb granule cells. J Neurosci 20:5124–5134
Hensch TK (2005) Critical period plasticity in local cortical circuits. Nat Rev Neurosci 6:877–888
Hirata Y (1964) Some observations on the fine structure of the synapses in the olfactory bulb of the mouse, with particular references to the atypical synaptic configurations. Arch Histol Jpn 24:293–302
Igarashi KM, Ieki N, An M et al (2012) Parallel mitral and tufted cell pathways route distinct odor information to different targets in the olfactory cortex. J Neurosci 32:7970–7985
Imamura F, Nagao H, Naritsuka H et al (2006) A leucine-rich repeat membrane protein, 5T4, is expressed by a subtype of granule cells with dendritic arbors in specific strata of the mouse olfactory bulb. J Comp Neurol 495:754–768
Imayoshi I, Sakamoto M, Ohtsuka T et al (2008) Roles of continuous neurogenesis in the structural and functional integrity of the adult forebrain. Nat Neurosci 11:1153–1161
Isaacson JS, Strowbridge BW (1998) Olfactory reciprocal synapses: dendritic signaling in the CNS. Neuron 20:749–761
Jahr CE, Nicoll RA (1982) An intracellular analysis of dendrodendritic inhibition in the turtle in vitro olfactory bulb. J Physiol 326:213–234
Kaba H, Nakanishi S (1995) Synaptic mechanisms of olfactory recognition memory. Rev Neurosci 6:125–141
Kageyama R, Imayoshi I, Sakamoto M (2012) The role of neurogenesis in olfaction-dependent behaviors. Behav Brain Res 227:459–463
Kaneko N, Okano H, Sawamoto K (2006) Role of cholinergic system in regulating survival of newborn neurons in the adult mouse dentate gyrus and olfactory bulb. Genes Cells 11:1145–1159
Kaplan MS, McNelly NA, Hinds JW (1985) Population dynamics of adult-formed granule neurons of the rat olfactory bulb. J Comp Neurol 239:117–125
Kasa P, Hlavati I, Dobo E et al (1995) Synaptic and non-synaptic cholinergic innervation of the various types of neurons in the main olfactory bulb of adult rat: immunocytochemistry of choline acetyltransferase. Neuroscience 67:667–677
Kashiwadani H, Sasaki YF, Uchida N et al (1999) Synchronized oscillatory discharges of mitral/tufted cells with different molecular receptive ranges in the rabbit olfactory bulb. J Neurophysiol 82:1786–1792
Katagiri H, Pallotto M, Nissant A et al (2011) Dynamic development of the first synapse impinging on adult-born neurons in the olfactory bulb circuit. Neural Syst Circuits 1:6
Kato HK, Chu MW, Isaacson JS et al (2012) Dynamic sensory representations in the olfactory bulb: modulation by wakefulness and experience. Neuron 76:962–975
Kay LM, Laurent G (1999) Odor- and context-dependent modulation of mitral cell activity in behaving rats. Nat Neurosci 2:1003–1009
Kelsch W, Mosley CP, Lin CW et al (2007) Distinct mammalian precursors are committed to generate neurons with defined dendritic projection patterns. PLoS Biol 5:2501–2512
Kelsch W, Lin CW, Lois C (2008) Sequential development of synapses in dendritic domains during adult neurogenesis. Proc Natl Acad Sci USA 105:16803–16808
Kelsch W, Sim S, Lois C (2010) Watching synaptogenesis in the adult brain. Annu Rev Neurosci 33:131–149

Kosaka K, Aika Y, Toida K et al (1995) Chemically defined neuron groups and their subpopulations in the glomerular layer of the rat main olfactory bulb. Neurosci Res 23:73–88

Lagace DC, Whitman MC, Nooman MA et al (2007) Dynamic contribution of nestin-expressing stem cells to adult neurogenesis. J Neurosci 27:12623–12629

Lagier S, Carleton A, Lledo PM (2004) Interplay between local GABAergic interneurons and relay neurons generates gamma oscillations in the rat olfactory bulb. J Neurosci 24:4382–4392

Larsen CM, Grattan DR (2010) Prolactin-induced mitogenesis in the subventricular zone of the maternal brain during early pregnancy is essential for normal postpartum behavioral responses in the mother. Endocrinology 151:3805–3814

Lazarini F, Lledo PM (2011) Is adult neurogenesis essential for olfaction? Trends Neurosci 34:20–30

Lazarini F, Mouthon MA, Gheusi G et al (2009) Cellular and behavioral effects of cranial irradiation of the subventricular zone in adult mice. PLoS One 4:e7017

Le Jeune H, Aubert I, Jourdan F et al (1995) Comparative laminar distribution of various autoradiographic cholinergic markers in adult rat main olfactory bulb. J Chem Neuroanat 9:99–112

Lemasson M, Saghatelyan A, Olivo-Marin JC et al (2005) Neonatal and adult neurogenesis provide two distinct populations of newborn neurons to the mouse olfactory bulb. J Neurosci 25:6816–6825

Lledo PM, Alonso M, Grubb MS (2006) Adult neurogenesis and functional plasticity in neuronal circuits. Nat Rev Neurosci 7:179–193

Luskin MB, Price J (1983) The topographic organization of associational fibers of the olfactory system in the rat, including centrifugal fibers to the olfactory bulb. J Comp Neurol 216:264–291

Mak GK, Weiss S (2010) Paternal recognition of adult offspring mediated by newly generated CNS neurons. Nat Neurosci 13:753–758

Mak GK, Enwere EK, Gregg C et al (2007) Male pheromone-stimulated neurogenesis in the adult female brain: possible role in mating behavior. Nat Neurosci 10:1003–1011

Manabe H, Kusumoto-Yoshida I, Ota M et al (2011) Olfactory cortex generates synchronized top-down inputs to the olfactory bulb during slow-wave sleep. J Neurosci 31:8123–8133

Mandairon N, Sacquet J, Jourdan F et al (2006) Long-term fate and distribution of newborn cells in the adult mouse olfactory bulb: influences of olfactory deprivation. Neuroscience 141:443–451

Mandairon N, Sultan S, Nouvian M et al (2011) Involvement of newborn neurons in olfactory associative learning? The operant or non-operant component of the task makes all the difference. J Neurosci 31:12455–12460

Margrie TW, Sakmann B, Urban NN (2001) Action potential propagation in mitral cell lateral dendrites is decremental and controls recurrent and lateral inhibition in the mammalian olfactory bulb. Proc Natl Acad Sci USA 98:319–324

Markopoulos F, Rokni D, Gire DH et al (2012) Functional properties of cortical feedback projections to the olfactory bulb. Neuron 76:1175–1188

Martin C, Gervais R, Messaoudi B et al (2006) Learning-induced oscillatory activities correlated to odour recognition: a network activity. Eur J Neurosci 23:1801–1810

McCune SK, Voigt MM, Hill JM (1993) Expression of multiple alpha adrenergic receptor subtype messenger RNAs in the adult rat brain. Neuroscience 57:143–151

McLean JH, Shipley MT (1987) Serotonergic afferents to the rat olfactory bulb: I. Origins and laminar specificity of serotonergic inputs in the adult rat. J Neurosci 7:3016–3028

McLean JH, Shipley MT, Nickell WT et al (1989) Chemoanatomical organization of the noradrenergic input from locus coeruleus to the olfactory bulb of the adult rat. J Comp Neurol 285:39–349

Merkle FT, Mirzadeh Z, Avarez-Buylla A (2007) Mosaic organization of neural stem cells in the adult brain. Science 317:381–384

Mizrahi A, Lu J, Irving R et al (2006) In vivo imaging of juxtaglomerular neuron turnover in the mouse olfactory bulb. Proc Natl Acad Sci USA 103:1912–1917

Moreno MM, Linster C, Escanilla O et al (2009) Olfactory perceptual learning requires adult neurogenesis. Proc Natl Acad Sci USA 106:17980–17985
Moreno MM, Bath K, Kuczewski N et al (2012) Action of the noradrenergic system on adult-born cells is required for olfactory learning in mice. J Neurosci 32:3748–3758
Mori K (1987) Membrane and synaptic properties of identified neurons in the olfactory bulb. Prog Neurobiol 29:275–320
Mori K, Kishi K, Ojima H (1983) Distribution of dendrites of mitral, displaced mitral, tufted, and granule cells in the rabbit olfactory bulb. J Comp Neurol 219:339–355
Mori K, Nagao H, Yoshihara Y (1999) The olfactory bulb: coding and processing of odor molecule information. Science 286:711–715
Mouret A, Lepousez G, Gras J et al (2009) Turnover of newborn olfactory bulb neurons optimizes olfaction. J Neurosci 29:12302–12314
Murata K, Imai M, Nakanishi S et al (2011) Compensation of depleted neuronal subsets by new neurons in a local area of the adult olfactory bulb. J Neurosci 31:10540–10557
Murphy GJ, Darcy DP, Isaacson JS (2005) Intraglomerular inhibition: signaling mechanisms of an olfactory microcircuit. Nat Neurosci 8:354–364
Nagayama S, Takahashi YK, Yoshihara Y et al (2004) Mitral and tufted cells differ in the decoding manner of odor maps in the rat olfactory bulb. J Neurophysiol 91:2532–2540
Nai Q, Dong HW, Hayar A et al (2009) Noradrenergic regulation of GABAergic inhibition of main olfactory bulb mitral cells varies as a function of concentration and receptor subtype. J Neurophysiol 101:2472–2484
Naritsuka H, Sakai K, Hashikawa T et al (2009) Perisomatic-targeting granule cells in the mouse olfactory bulb. J Comp Neurol 515:409–426
Ninkovic J, Mori T, Gotz M (2007) Distinct modes of neuron addition in adult mouse neurogenesis. J Neurosci 27:10906–10911
Orona E, Rainer EC, Scott JW (1984) Dendritic and axonal organization of mitral and tufted cells in the rat olfactory bulb. J Comp Neurol 226:346–356
Pager J (1983) Unit responses changing with behavioral outcome in the olfactory bulb of unrestrained rats. Brain Res 289:87–98
Parrish-Aungst S, Shipley MT, Erdelyi F et al (2007) Quantitative analysis of neuronal diversity in the mouse olfactory bulb. J Comp Neurol 501:825–836
Petreanu L, Alvarez-Buylla A (2002) Maturation and death of adult-born olfactory bulb granule neurons: role of olfaction. J Neurosci 22:6106–6113
Petzold GC, Hagiwara A, Murthy VN (2009) Serotonergic modulation of odor input to the mammalian olfactory bulb. Nat Neurosci 12:784–791
Pressler RT, Inoue T, Strowbridge BW (2007) Muscarinic receptor activation modulates granule cell excitability and potentiates inhibition onto mitral cells in the rat olfactory bulb. J Neurosci 27:10969–10981
Price JL, Powell TP (1970a) The morphology of the granule cells of the olfactory bulb. J Cell Sci 7:91–123
Price JL, Powell TP (1970b) The synaptology of the granule cells of the olfactory bulb. J Cell Sci 7:125–155
Rall W, Shepherd GM (1968) Theoretical reconstruction of field potentials and dendrodendritic synaptic interactions in olfactory bulb. J Neurophysiol 31:884–915
Rall W, Shepherd GM, Reese TS et al (1966) Dendrodendritic synaptic pathway for inhibition in the olfactory bulb. Exp Neurol 14:44–56
Ravel N, Elaagouby A, Gervais R (1994) Scopolamine injection into the olfactory bulb impairs short-term olfactory memory in rats. Behav Neurosci 108:317–324
Redondo RL, Morris RG (2011) Making memories last: the synaptic tagging and capture hypothesis. Nat Rev Neurosci 12:17–30
Rochefort C, Gheusi G, Vincent J et al (2002) Enriched odor exposure increases the number of newborn neurons in the adult olfactory bulb and improves odor memory. J Neurosci 22:2679–2689

Saghatelyan A, Roux P, Migliore M et al (2005) Activity-dependent adjustments of the inhibitory network in the olfactory bulb following early postnatal deprivation. Neuron 46:103–116
Sakamoto M, Imayoshi I, Ohtsuka T et al (2011) Continuous neurogenesis in the adult forebrain is required for innate olfactory responses. Proc Natl Acad Sci USA 108:8479–8484
Sauvage MM, Fortin NJ, Owens CB et al (2008) Recognition memory: opposite effects of hippocampal damage on recollection and familiarity. Nat Neurosci 11:16–18
Sawada M, Kaneko N, Inada H et al (2011) Sensory input regulates spatial and subtype-specific patterns of neuronal turnover in the adult olfactory bulb. J Neurosci 31:11587–11596
Schneider SP, Macrides F (1978) Laminar distributions of interneurons in the main olfactory bulb of the adult hamster. Brain Res Bull 3:73–82
Schoppa NE (2006) Synchronization of olfactory bulb mitral cells by precisely timed inhibitory inputs. Neuron 49:271–283
Schoppa NE, Kinzie JM, Sahara Y et al (1998) Dendrodendritic inhibition in the olfactory bulb is driven by NMDA receptors. J Neurosci 18:6790–6802
Shao Z, Puche AC, Kiyokage E et al (2009) Two GABAergic intraglomerular circuits differentially regulate tonic and phasic presynaptic inhibition of olfactory nerve terminals. J Neurophysiol 101:1988–2001
Shepherd GM (1963) Neuronal systems controlling mitral cell excitability. J Physiol 168:101–117
Shepherd GM, Chen W, Greer C (2004) Olfactory bulb. In: Shepherd G (ed) The synaptic organization of the brain, 5th edn. Oxford University Press, New York, pp 165–216
Shepherd GM, Chen WR, Willhite D et al (2007) The olfactory granule cell: from classical enigma to central role in olfactory processing. Brain Res Rev 55:373–382
Shingo T, Gregg C, Enwere E et al (2003) Pregnancy-stimulated neurogenesis in the adult female forebrain mediated by prolactin. Science 299:117–120
Shipley MT, Ennis M (1996) Functional organization of olfactory system. J Neurobiol 30:123–176
Sohal VS, Zhang F, Yizhar O et al (2009) Parvalbumin neurons and gamma rhythms enhance cortical circuit performance. Nature (Lond) 459:698–702
Sullivan RM, Wilson DA, Leon M (1989) Norepinephrine and learning-induced plasticity in infant rat olfactory system. J Neurosci 9:3998–4006
Sultan S, Mandairon N, Kermen F et al (2010) Learning-dependent neurogenesis in the olfactory bulb determines long-term olfactory memory. FASEB J 24:2355–2363
Toida K, Kosaka K, Heizmann CW et al (1998) Chemically defined neuron groups and their subpopulations in the glomerular layer of the rat main olfactory bulb: III. Structural features of calbindin D28K-immunoreactive neurons. J Comp Neurol 392:179–198
Toida K, Kosaka K, Aika Y et al (2000) Chemically defined neuron groups and their subpopulations in the glomerular layer of the rat main olfactory bulb. IV. Intraglomerular synapses of tyrosine hydroxylase-immunoreactive neurons. Neuroscience 101:11–17
Tononi G, Cirelli C (2006) Sleep function and synaptic homeostasis. Sleep Med Rev 10:49–62
Trombley PQ, Shepherd GM (1992) Noradrenergic inhibition of synaptic transmission between mitral and granule cells in mammalian olfactory bulb cultures. J Neurosci 12:3985–3991
Tsuno Y, Kashiwadani H, Mori K (2008) Behavioral state regulation of dendrodendritic synaptic inhibition in the olfactory bulb. J Neurosci 28:9227–9238
Valley MT, Mullen TR, Schultz LC et al (2009) Ablation of mouse adult neurogenesis alters olfactory bulb structure and olfactory fear conditioning. Front Neurosci 3:51
Veyrac A, Sacquet J, Nguyen V et al (2009) Novelty determines the effects of olfactory enrichment on memory and neurogenesis through noradrenergic mechanisms. Neuropsychopharmacology 34:786–795
Vyazovskiy VV, Cirelli C, Pfister-Genskow M et al (2008) Molecular and electrophysiological evidence for net synaptic potentiation in wake and depression in sleep. Nat Neurosci 11:200–208
Wellman PJ (2000) Norepinephrine and the control of food intake. Nutrition 16:837–842

Whitman MC, Greer CA (2007) Synaptic integration of adult-generated olfactory bulb granule cells: basal axodendritic centrifugal input precedes apical dendrodendritic local circuits. J Neurosci 27:9951–9961

Winner B, Cooper-Kuhn CM, Aigner R et al (2002) Long-term survival and cell death of newly generated neurons in the adult rat olfactory bulb. Eur J Neurosci 16:1681–1689

Xiong W, Chen WR (2002) Dynamic gating of spike propagation in the mitral cell lateral dendrites. Neuron 34:115–126

Yamaguchi M, Mori K (2005) Critical period for sensory experience-dependent survival of newly generated granule cells in the adult mouse olfactory bulb. Proc Natl Acad Sci USA 102:9697–9702

Yamaguchi M, Manabe H, Murata K et al (2013) Reorganization of neuronal circuits of the central olfactory system during postprandial sleep. Front Neural Circuits 7:132

Yokoi M, Mori K, Nakanishi S (1995) Refinement of odor molecule tuning by dendrodendritic synaptic inhibition in the olfactory bulb. Proc Natl Acad Sci USA 92:3371–3375

Yokoyama TK, Mochimaru D, Murata K et al (2011) Elimination of adult-born neurons in the olfactory bulb is promoted during the postprandial period. Neuron 71:883–897

Young KM, Fogarty M, Kessaris N et al (2007) Subventricular zone stem cells are heterogeneous with respect to their embryonic origins and neurogenic fates in the adult olfactory bulb. J Neurosci 27:8286–8296

Chapter 7
Parallel Tufted Cell and Mitral Cell Pathways from the Olfactory Bulb to the Olfactory Cortex

Shin Nagayama, Kei M. Igarashi, Hiroyuki Manabe, and Kensaku Mori

Abstract In the mammalian olfactory system, sniff-induced odor signals are conveyed from the olfactory bulb to the olfactory cortex by two types of projection neurons, tufted cells and mitral cells. This chapter summarizes recent advances in knowledge of the structural and functional differences between tufted cell and mitral cell circuits. Tufted cells and mitral cells show distinct patterns of lateral dendrite projection and make dendrodendritic reciprocal synaptic connections with different subtypes of granule cell inhibitory interneurons. Tufted cells and mitral cells thus form distinct local circuits within the olfactory bulb: small-scale tufted cell dendrodendritic circuits and larger-scale mitral cell dendrodendritic circuits. In addition, tufted cells and mitral cells differ dramatically in their axonal projection to the olfactory cortex. Individual tufted cells project axons to focal targets in the olfactory peduncle areas, whereas individual mitral cells send axons in a dispersed way to nearly all areas of the olfactory cortex, including nearly all parts of the piriform cortex. Furthermore, tufted cells and mitral cells differ strikingly in how they respond to odor inhalation. Compared with mitral cells, tufted cells show earlier-onset, higher-frequency spike discharges. Tufted cells are activated at a much lower odor concentration threshold than activating mitral cells. During an inhalation–exhalation sniff cycle, tufted cell circuits generate early-onset fast

S. Nagayama
Department of Neurobiology and Anatomy, The University of Texas Medical School at Houston, Houston, TX, USA
e-mail: shin.nagayama@uth.tmc.edu

K.M. Igarashi
Kavli Institute for Systems Neuroscience and Centre for Neural Computation, Norwegian University of Science and Technology, Trondheim, Norway
e-mail: kei.igarashi@ntnu.no

H. Manabe • K. Mori (✉)
Department of Physiology, Graduate School of Medicine, The University of Tokyo, Bunkyo-ku, Tokyo 118-0033, Japan
e-mail: hmanabe@m.u-tokyo.ac.jp; moriken@m.u-tokyo.ac.jp

K. Mori (ed.), *The Olfactory System: From Odor Molecules to Motivational Behaviors*, DOI 10.1007/978-4-431-54376-3_7, © Springer Japan 2014

gamma oscillation while mitral cell circuits give rise to later-onset slow gamma oscillation. From these structural and functional differences, we hypothesize that the two types of projection neurons play distinct roles in sending sniff-induced odor signals to the olfactory cortex. Specifically, tufted cells provide specificity-projecting circuits that send specific odor information to focal targets in the olfactory peduncle areas with early-onset fast gamma synchronization. In contrast, mitral cells give rise to dispersed-projection feed-forward "binding" circuits that transmit the response synchronization timing via their later-onset slow gamma synchronization to pyramidal cells distributed across all parts of the piriform cortex.

Keywords Dispersed-projection feed-forward "binding" circuits • Early-onset responses • Fast and slow gamma synchronizations • Glomerular module • Later-onset responses • Odor inhalation • Sniff cycle • Specificity-projecting circuits • Tufted and mitral cells

7.1 Introduction

As noted by pioneering neuro-anatomists such as Cajal (1955) and Golgi (1875), the most characteristic structure within the olfactory bulb is its numerous large round neuropils, called olfactory glomeruli (Fig. 7.1). Individual glomeruli receive converging axonal inputs from several thousands of olfactory sensory neurons that express an identical type of odorant receptor ("glomerular convergence rule"). Because of this remarkable convergence of olfactory sensory neuron axons (olfactory axons), individual glomeruli represent a single type of odorant receptor ("one receptor–one glomerulus rule") and can function as a detector of odorant molecular features.

Within each glomerulus, olfactory axons form excitatory synaptic connections on primary dendrites of tufted cells and mitral cells (Fig. 7.1). Because each tufted cell or mitral cell projects a primary dendrite to a single glomerulus, an individual glomerulus and its associated tufted and mitral cells form a structural and functional module (glomerular module or glomerular unit), which represents a single type of odorant receptor. The stereotyped spatial arrangement of numerous glomerular modules in the olfactory bulb seems to be equivalent to the spatial organization of functional columns in the sensory and motor areas of the neocortex. In this sense, the structural and functional organization of the olfactory bulb is similar to that of the neocortex.

As shown in Chap. 4, the spatial arrangement of approximately 1,000 glomerular modules in the rostrodorsolateral or caudoventromedial half of the mouse main olfactory bulb forms a sensory map (odorant receptor map) that represents ~1,000 types of odorant receptors and thus functions as ~1,000 different "molecular feature detectors." Each olfactory bulb has two such maps arranged in mirror image fashion (Mori et al. 1999; Mori and Sakano 2011; Nagao et al. 2000).

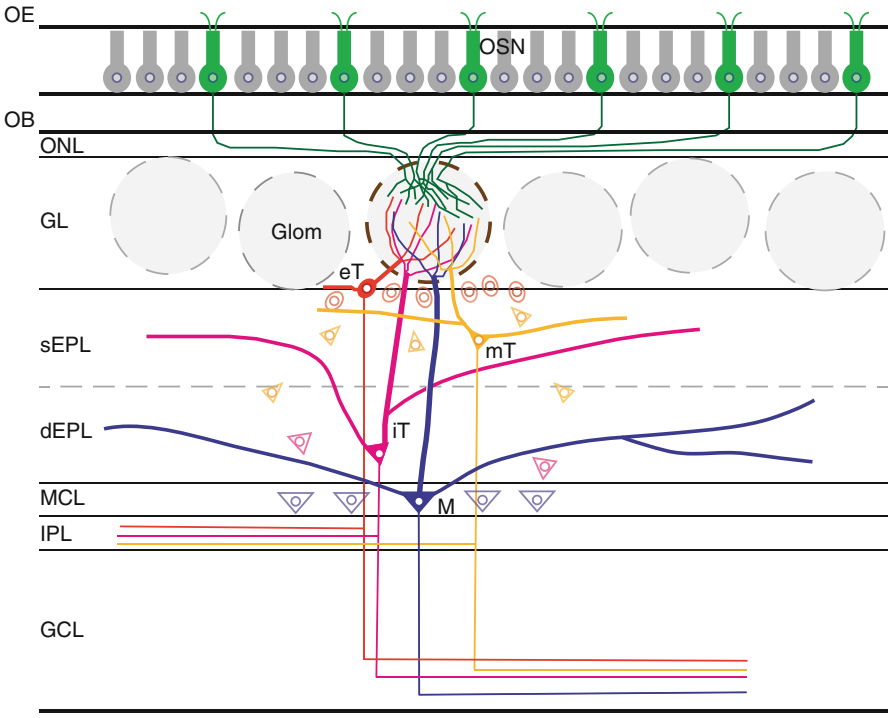

Fig. 7.1 Laminar structure of olfactory bulb circuit. Olfactory sensory neurons (*OSN*) in the olfactory epithelium (*OE*) send axons to the olfactory bulb (*OB*) and form synapses to dendrites of principal cells in structures called glomeruli (*glom*). The principal cells include mitral (*M*) cells and tufted cells, which are further divided into external tufted (*eT*) cells, middle tufted (*mT*) cells, and internal tufted (*iT*) cells. In the order from eT, mT, to iT cells, they have gradually larger cell bodies, and the cell bodies reside in gradually deeper part of the external plexiform layer (*EPL*). Mitral cells have a relatively large cell body in the mitral cell layer (*MCL*). Tufted cells extend relatively short secondary dendrites to the superficial half of the EPL (*sEPL*), whereas mitral cells extend long secondary dendrites in the deeper half of the external plexiform layer (*dEPL*). *ONL* olfactory nerve layer, *GL* glomerular layer, *IPL* internal plexiform layer, *GCL* granule cell layer

An apple emits dozens of different odorants. Each odorant activates a specific combination of odorant receptors. Thus, the apple activates a larger combination of glomerular modules. To perceive the odor of an apple, the central olfactory system needs to determine which combination of glomerular modules is activated by the inhaled odor. How does the ensemble of activated glomerular modules (molecular feature detectors) come to be associated to form an integrated perceptual olfactory image of an apple? The olfactory cortex is thought to play a major role in integrating the responses across different glomerular modules, as is described in Chap. 8. However, before rushing to explore the largely unknown field of the olfactory cortex, we first examine the question of how the signals of numerous glomerular modules are transmitted from the olfactory bulb to the olfactory cortex.

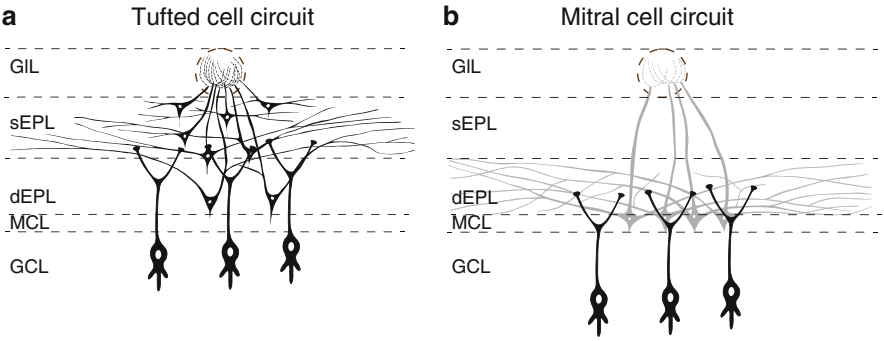

Fig. 7.2 Dissociation of tufted cell circuit and mitral cell circuit. (**a**) Tufted cells form dendrodendritic reciprocal synapses preferentially with the superficial granule cells, which have cell bodies in the superficial part of the granule cell layer and branch dendrites within the superficial EPL. (**b**) In contrast, mitral cells form synapses preferentially with the deep granule cells, which have cell bodies in the deep part of the granule cell layer and branch dendrites within the deep EPL

Odor signals received by glomerular modules are further processed by two distinct local circuits in the olfactory bulb: tufted cell circuits and mitral cell circuits (Fig. 7.2). The processed odor signals are then transmitted to the olfactory cortex via two parallel pathways: axons of tufted cells (tufted cell pathway) and axons of mitral cells (mitral cell pathway). It might be asked why the transmission of odor information from the olfactory bulb to the olfactory cortex requires two parallel pathways, and what functional role each pathway plays in odor information processing in the olfactory cortex. After reviewing the emerging view of the structural organization and functional properties of the two parallel pathways, we propose a model in which tufted cell and mitral cell pathways convey distinct signals to the olfactory cortex at different time windows of the inhalation–exhalation sniff cycle.

7.2 Structural Characteristics of Tufted Cells and Mitral Cells in the Mammalian Olfactory Bulb

The olfactory bulb has a cortical structure with a well-defined laminar organization (Fig. 7.1). Odor information is conveyed by olfactory axons that pass through the olfactory nerve layer and converge onto each glomerulus in the glomerular layer. Within the glomerulus, the odor signals are transferred to the terminal tuft of primary dendrites of tufted and mitral cells. Individual mitral cells have large cell bodies in the thin mitral cell layer. They extend remarkably long secondary (lateral) dendrites in the deep half of the external plexiform layer (EPL). Although morphological variations of mitral cells have been reported (Kikuta et al. 2013; Orona et al. 1984), many studies have considered them a single neuron type. Tufted cells show medium to small cell bodies distributed in the EPL and periglomerular region.

They have relatively shorter secondary dendrites in the superficial half of the EPL. Tufted cells are further classified into three subtypes. External tufted cells (eT in Fig. 7.1) have relatively small cell bodies in the periglomerular region and at the border between the glomerular layer and EPL. Middle tufted cells (mT) are medium-sized neurons whose somata are distributed in the superficial two-thirds of the EPL. Cell bodies of internal tufted cells (iT) are scattered sparsely in the deeper one-third of the EPL. Internal tufted cells are similar to mitral cells in size and morphology and are often called displaced mitral cells.

Tufted and mitral cells also differ in their development. Mitral cells are born in an earlier embryonic stage (E10–13d) than tufted cells (E13–17d) (Hinds 1968; Imamura and Greer 2013). The ascending axons of earlier-born mitral cells tend to pass through the deeper part of lateral olfactory tract (LOT), whereas axons of later-born cells pass through the superficial part (Inaki et al. 2004). Thus, tufted cell axons and mitral cell axons are segregated within the LOT. In addition, tufted cell axons are thinner than mitral cell axons in the LOT (Price and Sprich 1975). The difference in axon diameter is associated with the difference in spike conduction velocity in the LOT.

Tufted and mitral cells receive dual inhibitory interneuron controls, by GABAergic periglomerular cells in the glomerular layer and GABAergic granule cells in the granule cell layer. Interestingly, granule cells whose cell bodies are in the superficial part of the granule cell layer (superficial granule cells) tend to branch dendrites within the superficial EPL, whereas granule cells with their cell body in the deep part of the granule cell layer (deep granule cells) tend to branch dendrites within the deep EPL (Fig. 7.2) (Mori et al. 1983). Because tufted cells project secondary dendrites to the superficial EPL, tufted cells may form dendrodendritic reciprocal synapses preferentially with the superficial granule cells. The subtype of granule cells that have their dendrites in the superficial EPL is thus called tufted cell-targeting granule cells (Fig. 7.3). In contrast, mitral cells send long lateral dendrites to the deep EPL and thus preferentially form dendrodendritic reciprocal synapses with deep granule cells. These granule cells with dendrodendritic connections with mitral cells are called mitral cell-targeting granule cells (Fig. 7.2b).

As shown in Fig. 7.3, dozens of sister tufted cells and sister mitral cells project primary dendrites to a single glomerulus (Kikuta et al. 2013). Glomeruli in the rabbit olfactory bulb have a large diameter (160–210 μm) (Allison and Warwick 1949). Allison and Warwick counted the total number of glomeruli, tufted cells, and mitral cells in the rabbit main olfactory bulb, and estimated that a single glomerulus receives primary dendrites from an average of 68 sister tufted cells and 24 sister mitral cells (Allison and Warwick 1949). However, Royet reestimated these numbers and reported that each glomerular module is formed of an average of 10 sister mitral cells in rabbits (Royet et al. 1998). In mice, individual glomeruli are relatively small (50–120 μm) (Royet et al. 1988) and expect to receive about 20 sister mitral cells (Royet et al. 1998). From our data (Kikuta et al. 2013), we roughly estimate that a single glomerular module receives primary dendrites from about 20 sister mitral cells and 50 sister tufted cells.

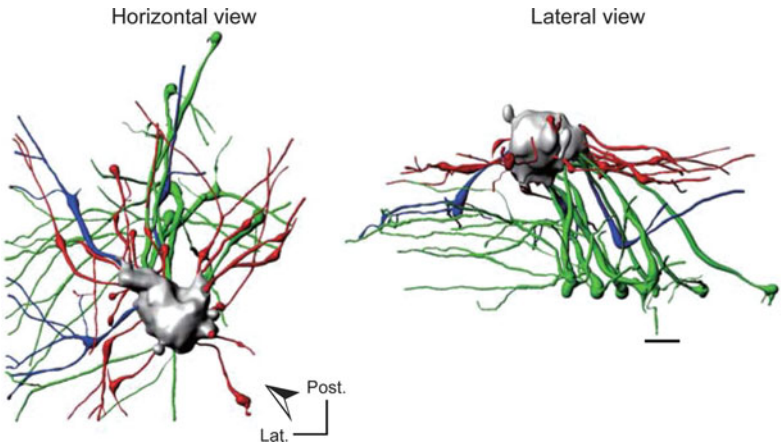

Fig. 7.3 Three-dimensional (3D) reconstruction of glomerular module. *Left* and *right images* show horizontal and lateral views of the single glomerular module, respectively. Sister cells associated with the glomerulus were labeled by single glomerulus dye injection and imaged by in vivo two-photon microscopy. *Arrowhead* in the horizontal view indicates the view angle for lateral view. *Gray* glomerulus, *red* juxtaglomerular cells (including periglomerular and external tufted cells), *blue* middle tufted cells, *green* mitral cells, *Post*. posterior, *Lat*. lateral. *Bar* 50 μm. (Reproduced, with permission, from Kikuta et al. 2013)

7.3 Tufted Cells and Mitral Cells Differ in Their Response to Odor Inhalation

Olfaction is mediated discretely by respiration (sniff) cycles, with each cycle composed of an inhalation phase followed by an exhalation phase (see Chap. 1). So, any study of the signal timing of neurons in the olfactory system should consider monitoring the sniff cycles of the test animals. One convenient method is to place a thermocouple in the nasal cavity and measure the temperature change that accompanies each sniff cycle: inhalation of external cool air causes cooling of the nasal cavity whereas exhalation of warm lung air causes warming. Simultaneous recording of the spike activities of tufted or mitral cells in response to odor inhalation will show that these are typically phase locked with the sniff cycle.

Recent studies show that tufted cells and mitral cells differ in their response to odor inhalation (Fukunaga et al. 2012; Igarashi et al. 2012; Nagayama et al. 2004; Phillips et al. 2012). For example, the odor concentration threshold for inducing spike responses in tufted cells is much lower than that for activating mitral cells. Tufted cells respond to odors at low concentration, whereas mitral cells respond only to those at high concentration. When the concentration of a stimulus odor is gradually increased, only the tufted cells respond when the concentration is low, whereas both types respond at the higher concentration.

The two cell types also differ in the firing frequencies of their odor responses. Tufted cells show high-frequency burst discharges, whereas mitral cells respond with lower-frequency burst discharges (Fig. 7.4).

A particularly noteworthy difference between tufted and mitral cells is their signal timing in reference to the inhalation–exhalation sniff cycle. The two types show spike responses at different phases of the sniff cycle (Fig. 7.4) (Fukunaga et al. 2012; Igarashi et al. 2012). In both freely behaving and anesthetized animals, tufted cells start to respond earlier than mitral cells. Tufted cells respond with early-onset high-frequency burst discharges, which start at the middle of the inhalation phase. In contrast, mitral cells respond with later-onset lower-frequency burst discharges that start at the transition phase from inhalation to exhalation.

Regarding the time window of signaling during the sniff cycle, external tufted cells and a subset of middle tufted cells show early-onset spike discharges that start at the rising phase of inhalation and continue up to the early or middle part of exhalation, suggesting that the spike output of these tufted cells strongly reflects the input from olfactory sensory neurons. In contrast, the signal timing of many mitral cells does not appear to reflect the direct input of olfactory sensory neurons. In addition to responses during the inhalation–exhalation transition phase, which might reflect direct inputs, many mitral cells also show spike discharges much later during the long exhalation phase, when the olfactory bulb is isolated from the external odor world (Fukunaga et al. 2012; Igarashi et al. 2012). In other words, many mitral cells show burst discharges during the off-line phase (see Chap. 1). Furthermore, some mitral cells show prolonged spike discharges even after the cessation of odor stimulation, suggesting that these responses are not directly driven by olfactory sensory neurons but may represent odor afterimages (Matsumoto et al. 2009; Patterson et al. 2013).

7.4 Neuronal Circuit Mechanisms for the Inhalation-Induced Early-Onset Responses of Tufted Cells and Later-Onset Responses of Mitral Cells

What mechanisms underlie the early-onset activity of tufted cells and later-onset activity of mitral cells? Recent studies using patch-clamp recordings from these cells showed that a single electrical stimulation of the olfactory axons induces two types of excitatory inputs, early-onset direct short-latency excitatory synaptic inputs and later-onset indirect slow depolarizing inputs (De Saint Jan et al. 2009; Gire and Schoppa 2009; Hayar et al. 2004; Najac et al. 2011). Recordings from external tufted cells show that olfactory axon stimulation induces strong short-latency excitatory synaptic responses, mediated by direct excitatory synaptic input from olfactory axon terminals (De Saint Jan et al. 2009). By contrast, mitral cells respond to a single electrical stimulation of olfactory axons with a small short-latency depolarization followed by a larger and long-lasting depolarization.

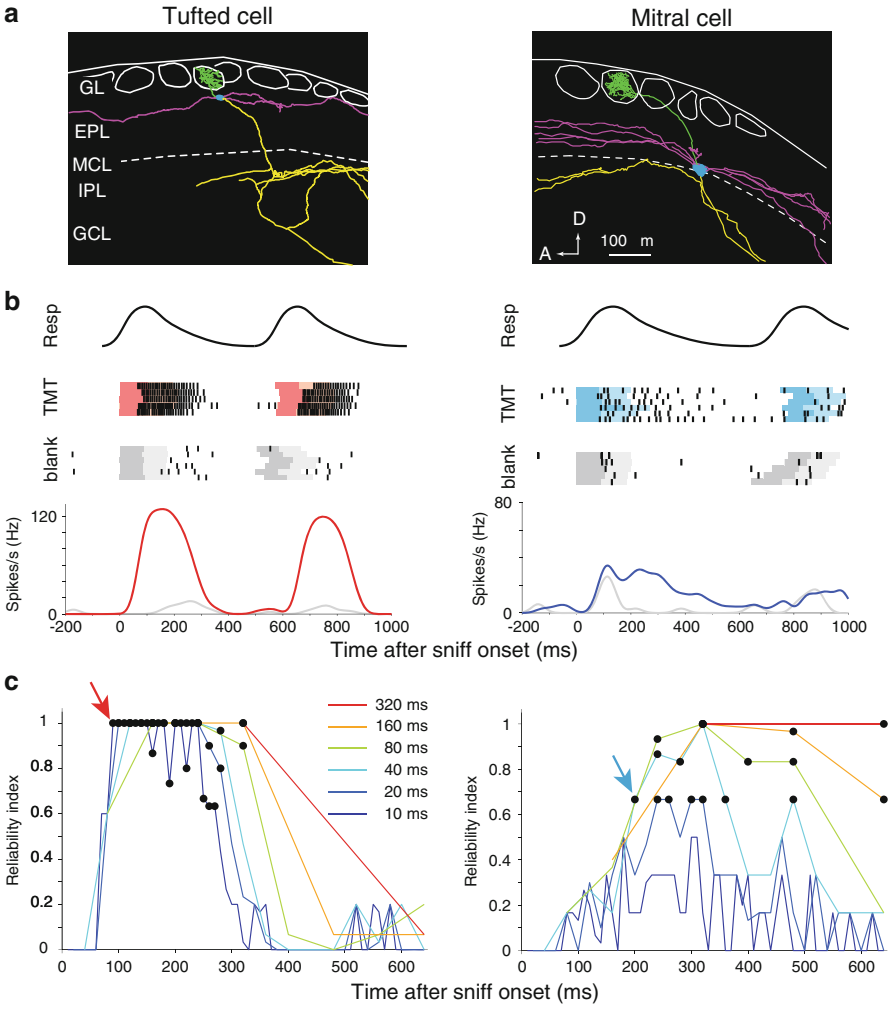

Fig. 7.4 Odor signal timing is faster in tufted cells than mitral cells. (**a**) Morphological reconstruction of an external tufted cell and a mitral cell that responded to fox odor, 2,4,5-trimethylthiazoline (TMT). Cell bodies, axons, primary dendrites, and lateral dendrites are indicated by *blue*, *yellow*, *green*, and *magenta*, respectively. Layer structure is shown as *GL* glomerular layer, *EPL* external plexiform layer, *MCL* mitral cell layer, *IPL* internal plexiform layer, *GCL* granule cell layer. *White circles* in GL indicate glomeruli. *A* anterior, *D* dorsal. (**b**) Timing of spike responses of the cells shown in (**a**). *Top*: Respiration cycles. *Middle*: Raster plots of spike trains evoked by the inhalation of TMT (*red* or *blue*, top plots) or by blank air (*gray*, middle plots). Each row corresponds to a single trial. The *darker* and *lighter colored* shadings behind rasters show respiration inhalation and exhalation, respectively. *Bottom*: Peri-stimulus time histogram of spike response to TMT stimulation (*red* or *blue*) and blank (*gray*). In all analyses, time 0 is shown by aligning at the first onset of odor inhalation. (**c**) Plots of response reliability index of the cells in **a** as a function of time. Reliability index, calculated as an index for reliability of the spike response of a neuron to a stimulus compared to spontaneous activities, was plotted using six different bin widths (10–320 ms; *blue* to *red*). *Black circles* indicate a statistically significant reliability index value of the response of each cell. *Arrows* indicate earliest significant reliability index, indicating the timing when responses of the cell are reliable from spontaneous firings. (Modified from Igarashi et al. 2012)

The slow and long-latency component of depolarization is an indirect feed-forward excitation mediated by intraglomerular dendrodendritic extra-synaptic inputs from sister tufted cells and mitral cells (Carlson et al. 2000; De Saint Jan et al. 2009; Gire and Schoppa 2009). Stronger electrical stimulation of olfactory axons is required to activate the long-latency indirect inputs. These results suggest that the spike output of a subset of tufted cells is shaped mainly by the fast direct synaptic input from olfactory axons, which may reflect instantaneous odor signals from the external world. By contrast, the spike output of mitral cells depends not only on direct input but more heavily on the slow indirect inputs that may reflect the activity state of sister tufted cells and mitral cells. The later-onset responses of mitral cells may be the result of the slow indirect inputs.

In addition, mitral cells are shown to receive inhibitory inputs from periglomerular inhibitory interneurons during the early phase of inhalation (Fukunaga et al. 2012). The early inhibitory inputs during inhalation are also thought to be responsible for the later-onset responses of mitral cells.

7.5 Tufted Cell Circuits and Mitral Cell Circuits Mediate Distinct Gamma Oscillations in the Olfactory Bulb

If you record local field potentials in the mammalian olfactory bulb, you will immediately notice prominent sine wave-like oscillatory potentials that occur in response to each odor inhalation (Fig. 7.5). The frequencies of the main components of these odor inhalation-induced oscillations range from 30 Hz to more than 100 Hz. Oscillation within this frequency range is called gamma-range oscillation.

As early as 1942, Adrian discovered that odor inhalation induces gamma oscillations of local field potentials in the olfactory bulb of the hedgehog brain (Adrian 1942). Since then, a number of studies have demonstrated these odor inhalation-induced gamma oscillations in the mammalian olfactory bulb (Adrian 1942; Bressler 1984; Buonviso et al. 2003; Cenier et al. 2008; Freeman 1975; Mori and Takagi 1977; Neville and Haberly 2003; Rosero and Aylwin 2011). The gamma oscillations accompany synchronized spike discharges of projection neurons, tufted cells, and mitral cells (Figs. 7.6, 7.7) (Kashiwadani et al. 1999; Mori and Takagi 1977). Dendrodendritic reciprocal synaptic interactions between the projection neurons and granule cells participate in the generation of gamma oscillations (Fig. 7.8) (Friedman and Strowbridge 2003; Lagier et al. 2004; Mori and Takagi 1977; Rall and Shepherd 1968; Shepherd et al. 2004).

Mitral cells extend long lateral (secondary) dendrites in the deeper sublamina of the external plexiform layer and form numerous dendrodendritic reciprocal synaptic connections, mainly with mitral cell-targeting granule cells. Each dendrodendritic reciprocal synapse consists of a pair of a mitral-to-granule excitatory synapse and adjacent granule-to-mitral inhibitory synapse (Fig. 7.8). Because individual mitral cell-targeting granule cells have several hundreds of dendrodendritic synaptic

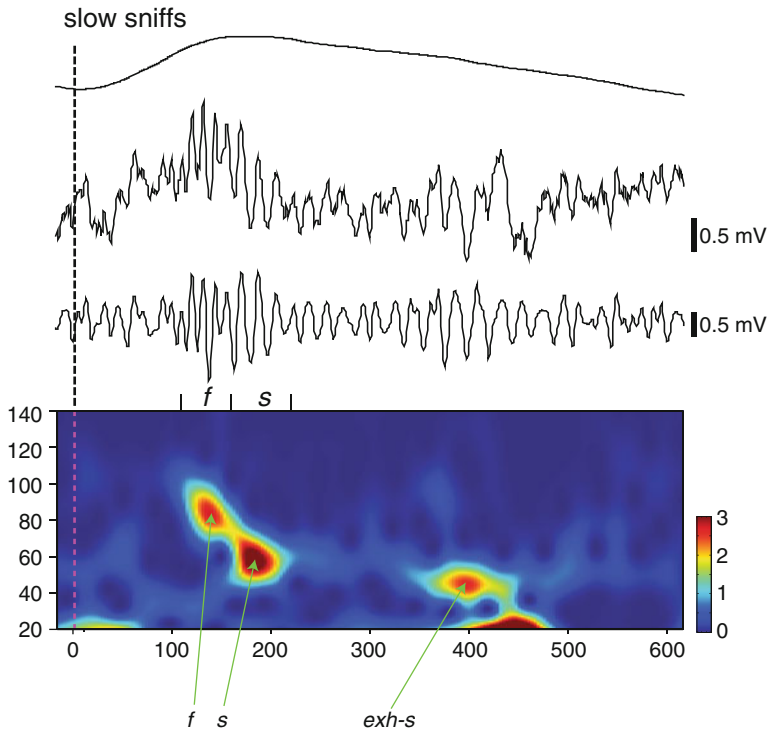

Fig. 7.5 Sniff-rhythm-paced gamma oscillations in the olfactory bulb. Simultaneous recordings of respiration (*topmost trace*; upward swing indicates inhalation and downward swing shows exhalation), local field potential in the granule cell layer of the olfactory bulb (*middle trace*), and gamma oscillations of the local field potential (bandpass filtered, 30–140 Hz; trace). Wavelet power spectrogram of gamma oscillations is shown below the tracings. *Dashed line* indicates inhalation onset. *f* fast gamma oscillations, *s* slow gamma oscillations, *exh-s* exhalation slow gamma oscillations. *Abscissa* indicates the frequency of oscillation (Hz); *ordinate* indicates time (ms). (Modified, with permission, from Manabe and Mori 2013)

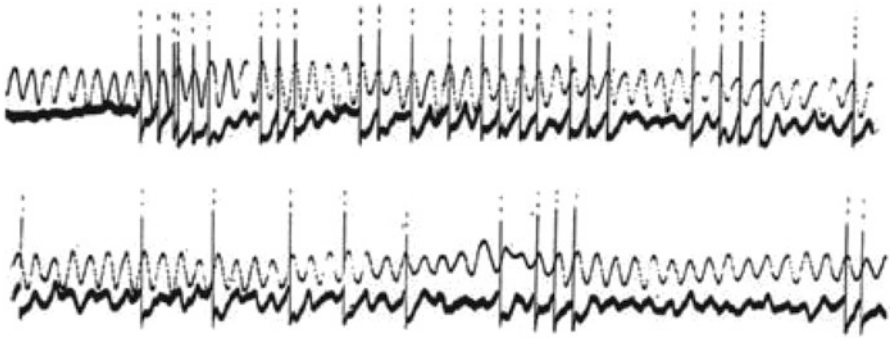

Fig. 7.6 Spike timing of a mitral cell against gamma oscillations. Simultaneous recordings of intracellular potential of a mitral cell (*lower trace* including spikes) and local field potential in the granule cell layer (*upper thin trace* of gamma oscillation) of the olfactory bulb induced by odor stimulation (amyl acetate) with artificial inhalation. *Upper traces* indicate odor-induced initial response of mitral cell; *lower traces* show later part of the response. Note that the spike responses of the mitral cell occurred at the rising phase of each gamma oscillation cycle of the local field potential. The recordings were obtained from the olfactory bulb of a urethane-anesthetized rabbit. (From Mori and Takagi, unpublished data)

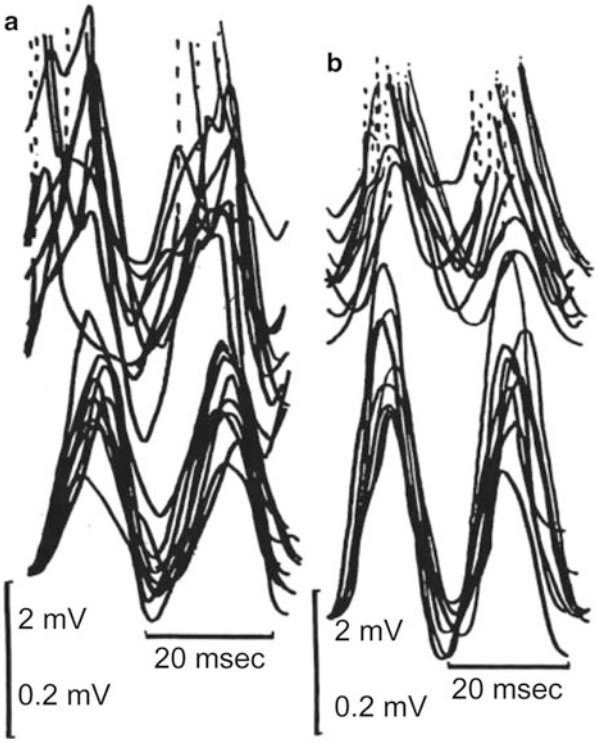

Fig. 7.7 Synchronization of intracellular membrane potentials and gamma oscillations. Superimposed line drawings of odor-induced gamma oscillations (two cycles) of the local field potential in the granule cell layer (*lower traces*) and corresponding intracellular potentials (*upper traces*) recorded from a mitral cell (**a**) and a presumed granule cell (**b**) These potentials were recorded from the olfactory bulb of a urethane-anesthetized rabbit. Note that membrane potentials of the presumed granule cell (**b**) are in phase with the gamma oscillation of the local field potential while membrane potentials of the mitral cell (**a**) precede those of the local field potential gamma oscillation. *Broken lines* indicate action potentials. (From Mori and Takagi 1977)

connections in the deep sublamina of the EPL, each granule cell may form dendrodendritic synapses with many sister mitral cells associated with the parental glomerulus. In other words, approximately 20 sister mitral cells associated with a single parental glomerulus (and thus belonging to a glomerular module) in the mouse olfactory bulb may have numerous dendrodendritic reciprocal synaptic connections with a group of mitral cell-targeting granule cells, forming the mitral cell circuit of the glomerular module (Fig. 7.2b).

If these sister mitral cells are activated by olfactory sensory inputs to the parental glomerulus, they may activate a number of mitral cell-targeting granule cells via the mitral-to-granule dendrodendritic excitatory synapses. Because individual granule cells form granule-to-mitral dendrodendritic inhibitory synapses on many sister mitral cells, the activated granule cells might then synchronously inhibit the sister mitral cells. The inhibition of mitral cell activity diminishes the activity

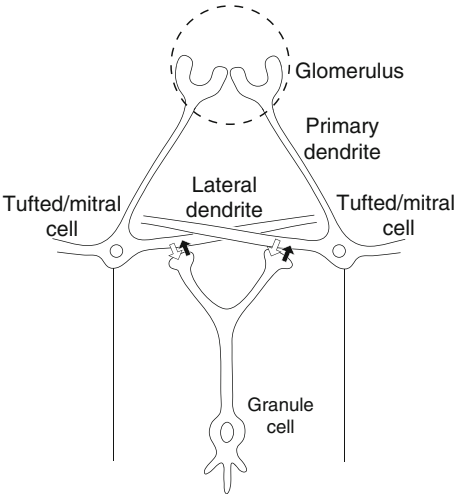

Fig. 7.8 Dendrodendritic synapses between mitral/tufted cells and granule cells. Mitral cells project secondary dendrites tangentially for long distances and make numerous dendrodendritic reciprocal synapses with deep granule cell dendrites in the EPL. The reciprocal synapses consist of a mitral → granule glutamatergic excitatory synapses (*white arrows*) and a granule → mitral GABAergic inhibitory synapses (*black arrows*). Activation of a mitral cell results in feedback inhibition of the cell, as well as lateral inhibition of neighboring mitral cells. Because the EPL contains a great amount of such synapses that serve as current sinks, these synapses serve as a generator of gamma oscillations in the OB. Note that tufted cells make dendrodendritic synapses with superficial granule cells (see Fig. 7.2)

of mitral-to-granule dendrodendritic excitatory synapses, resulting in the decay of granule cell activity and granule-to-mitral inhibition. When the inhibitory synaptic inputs from granule cells have decayed, the sister mitral cells might recover from the hyperpolarization and fire again synchronously either by post-inhibitory rebound activity or by enduring synaptic and extra-synaptic inputs within the glomerulus, and then synchronously activate the mitral cell-targeting granule cells again. In this way the mitral cell circuit has the ability to repeat the cycle and generate gamma oscillatory activity (Figs. 7.6, 7.7).

Because mitral cells associated with a given activated glomerular module project very long lateral dendrites, these mitral cells may have large-scale dendrodendritic interactions and synchronize with mitral cells associated with other coactivated glomerular modules that are distributed over a wide area of the olfactory bulb.

The lateral dendrites of internal and middle tufted cells extend into the superficial half of the EPL. External tufted cells typically extend short dendrites at the most superficial part of the EPL. The tufted cell dendrites form dendrodendritic reciprocal synaptic connections mainly with tufted cell-targeting granule cells (Fig. 7.2a). Each reciprocal synapse is composed of a pair consisting of a tufted-to-granule dendrodendritic excitatory synapse and a granule-to-tufted dendrodendritic inhibitory synapse (Fig. 7.8). We speculate that about 50 sister tufted cells of a glomerular

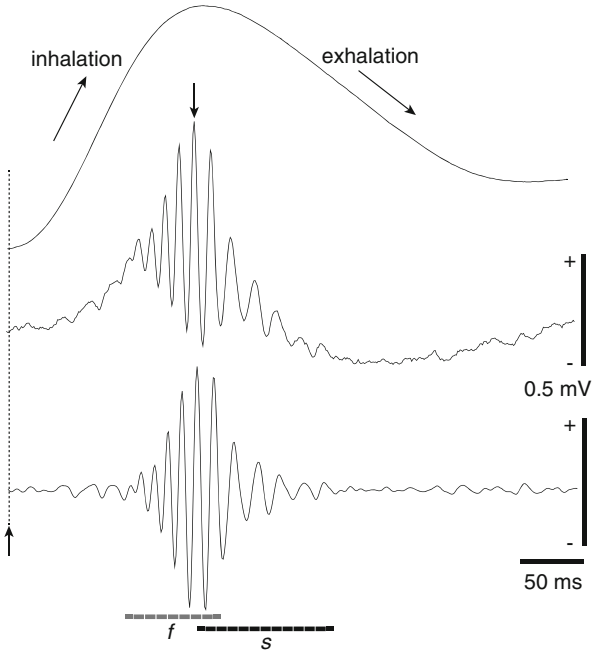

Fig. 7.9 Each sniff induces a fast gamma–slow gamma oscillation sequence. *Uppermost trace* indicates respiration rhythm. *Middle trace* shows sniff rhythm-paced gamma oscillations recorded from the olfactory bulb of a freely behaving rat. This trace was obtained by averaging the sniff-induced local field potentials ($n = 277$ sniffs) of the olfactory bulb in reference to the peak of gamma oscillation (*downward arrow*). *Bottom trace* shows averaged local field potentials were bandpass filtered (30–140 Hz). Sniff onset is indicated by a *vertical broken line* and *upward arrow*. *f* fast gamma oscillations, *s* slow gamma oscillations. (Modified, with permission, from Mori et al. 2013)

module in the mouse olfactory bulb have numerous dendrodendritic synaptic connections with a group of tufted cell-targeting granule cells, forming a tufted cell circuit of the glomerulus module (Fig. 7.2a). As discussed with the mitral cell circuit, the tufted cell circuit also has the potential to generate gamma oscillatory activity. Because of the relatively short lateral dendrites of tufted cells, tufted cells of a given activated glomerular module may show small-scale synchronization with tufted cells belonging to other coactivated glomerular modules in the neighborhood.

Which of the tufted cell circuits or mitral cell circuits generates the odor-induced gamma oscillations in the olfactory bulb? It is possible that both circuits generate these oscillations, and that each circuit generates distinct gamma-range oscillations with a different frequency range. To address these questions, the temporal structure of the sniff-induced gamma oscillations was studied in the olfactory bulb of freely behaving rats (Manabe and Mori 2013). As shown in Figs. 7.5 and 7.9, simultaneous recordings of respiratory rhythm and local field potentials in the olfactory bulb showed that each sniff induces early-onset fast gamma oscillations (65–100 Hz)

that are nested at the inhalation phase, followed by later-onset slow gamma oscillations (40–65 Hz) that are nested at the transition phase from inhalation to exhalation. A similar sequence of fast and slow gamma oscillations is also observed in the mouse olfactory bulb (Lepousez and Lledo 2013).

A close inspection of Fig. 7.5 shows that nested slow gamma oscillations also occur during the long exhalation phase (exh-s in Fig. 7.5). This chapter does not discuss these exhalation-phase slow gamma oscillations but rather concentrates on inhalation-induced fast and slow gamma oscillations.

The time window of the early-onset fast gamma oscillations corresponds well with that of the early-onset high-frequency burst discharges of tufted cells (Fig. 7.9), suggesting that the sniff-paced early-onset fast gamma oscillations are mediated mainly by tufted cell circuits. The late-onset slow gamma oscillations that start at the inhalation–exhalation transition period or early part of exhalation correspond in timing and frequency with the later-onset lower-frequency burst discharges of mitral cells. We therefore speculate that the later-onset slow gamma oscillations are largely caused by the activity of mitral cell circuits. In other words, the tufted cell circuits may function as early-onset fast gamma oscillators and the mitral cell circuits as a later-onset slow gamma oscillators.

Compared with the relatively short lateral dendrites of tufted cells, lateral dendrites of mitral cells extend for longer distances covering a wider area of the olfactory bulb. We therefore suggest that fast gamma synchronization of tufted cell circuits involves neurons in a relatively small area whereas slow gamma synchronization of mitral cell circuits recruits more neurons in a larger area of the olfactory bulb.

Because tufted cells and mitral cells convey odor signals to the olfactory cortex, these results suggest that during the inhalation phase and the inhalation–exhalation transition phase of a sniff cycle:

1. Tufted cells send odor information to the olfactory cortex with early-onset fast gamma synchronization, and
2. Mitral cells send their signals to the olfactory cortex with later-onset slow gamma synchronization.

7.6 Size Principle in the Olfactory Bulb

The onset of sniff-paced fast gamma oscillation in the rat olfactory bulb precedes that of slow gamma oscillation by an average of about 45 ms (Fig. 7.9). During the inhalation phase and inhalation–exhalation transition phase of a sniff cycle, tufted cells are initially activated and mitral cells are subsequently recruited. If the activation timing is compared among three subtypes of tufted cells, nearly 100 % of external tufted cells, 70 % of middle tufted cells, and 40 % of internal tufted cells show only the early-onset response, which corresponds in timing with the early-onset fast gamma oscillations. However, 28 % of middle tufted cells and 60 % of internal tufted cells show both the early-onset response at the rising phase of

inhalation and the later-onset responses during the early part of exhalation. Although simultaneous recordings from the three subtypes of tufted cells belonging to the same glomerulus are lacking, these results suggest that external tufted cells tend to be activated first during a sniff cycle, followed by middle tufted cells and finally internal tufted cells. Forty-five percent of mitral cells show a weak early-onset response and a strong later-onset response, whereas 55 % show only later-onset responses, suggesting that mitral cells may be activated last during a sniff cycle.

Based on these observations, we speculate that during the inhalation phase of a sniff cycle the activated glomerular module may initially recruit only external tufted cells and a subset of middle tufted cells, which have relatively small cell bodies. These tufted cells may have the lowest odor concentration threshold. At a later phase of inhalation, the activated glomerulus then recruits subsets of middle and internal tufted cells, which have middle-sized cell bodies. Finally, at the inhalation–exhalation transition phase, mitral cells and a subset of internal tufted cells (or displaced mitral cells) appear to be recruited. The mitral cells may have the highest odor concentration threshold.

The length and extent of dendritic projection of tufted cells and mitral cells increase according to their soma size. Thus, external tufted cells have the shortest dendrites and middle tufted cells extend relatively short lateral dendrites covering a small area of the olfactory bulb. These small tufted cells may form small-scale dendrodendritic circuits in a restricted area and generate early-onset fast gamma oscillations. Internal tufted cells project long lateral dendrites and mitral cells extend the longest lateral dendrites to wide areas of the olfactory bulb. These large-size projection neurons may form larger-scale dendrodendritic circuits and generate the later-onset slow gamma oscillations.

Such sequential recruitment of tufted and mitral cells according to cell size resembles Henneman's size principle of orderly recruitment of motoneurons (Henneman et al. 1965). During reflex activation, motoneurons with the smallest cell bodies have the lowest threshold and motoneurons with the largest cell bodies have the highest. Motor units are recruited according to their size as a voluntary contraction increases from zero to the maximal voluntary force level. Motoneurons in the spinal cord and principal neurons in the olfactory bulb might have a similar logic of sequential activation according to their size.

7.7 Tufted Cells and Mitral Cells Differ in the Pattern of Axonal Projection to the Olfactory Cortex

Do tufted cells and mitral cells differ in the manner of axonal projection to the olfactory cortex? Gross anatomical studies indicate that tufted cells send axons only to the olfactory peduncle areas (anterior olfactory nucleus and tenia tecta), rostrolateral part of the olfactory tubercle, and the rostroventral part of the anterior piriform cortex. In striking contrast, mitral cells project axons to all areas of the

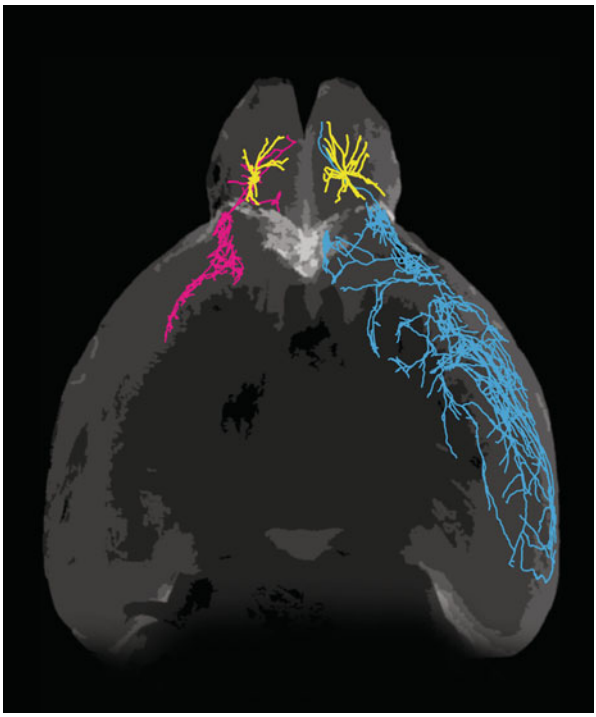

Fig. 7.10 Ventral view of reconstructed mitral and tufted cells. *Left*: Ventral view of a single TMT-responsive middle tufted cell. Axons and dendrites are indicated by *magenta* and *yellow*, respectively, on a transparent view of the brain. *Right*: Ventral view of a single TMT-responsive mitral cell. Axons and dendrites are indicated by *cyan* and *yellow*, respectively. Note that tufted axons cover a confined region whereas mitral axons cover very wide areas in the olfactory cortex

olfactory cortex: in addition to the aforementioned olfactory peduncle areas, mitral cells project to whole parts of the anterior piriform cortex, olfactory tubercle, posterior piriform cortex, anterior cortical amygdaloid nucleus, posterolateral cortical amygdaloid nucleus, nucleus of the lateral olfactory tract, and lateral entorhinal cortex.

Single-cell labeling studies show that individual tufted cells project axons densely to focal targets only in the anterior olfactory nucleus (a major area of the olfactory peduncle), rostrolateral part of the olfactory tubercle, and ventrorostral part of the anterior piriform cortex (Fig. 7.10). Given that tufted cells project axons to focal targets in or near the olfactory peduncle, the early-onset signals of tufted cells might be sent to the focal targets with fast gamma synchronization.

In striking contrast to tufted cells, individual mitral cells project axons in a dispersed manner to nearly all areas of the olfactory cortex, including nearly all parts of the piriform cortex (Fig. 7.10) (Igarashi et al. 2012). Sister mitral cells belonging to a given glomerulus project their axons to the piriform cortex in a highly dispersed pattern, with their terminals distributed throughout the piriform cortex (Ghosh et al. 2011; Nagayama et al. 2010; Sosulski et al. 2011). Given that mitral cell circuits generate later-onset slow gamma oscillatory activity, we speculate that sister mitral cells belonging to an activated glomerulus provide a mechanism for the dispersion of later-onset slow gamma oscillatory activity across whole parts of the piriform cortex and even across many different areas of the olfactory cortex (Mori et al. 2013).

7.8 Gamma Oscillation Coupling Between Olfactory Bulb and Olfactory Cortex

How are the early-onset fast gamma oscillatory signals of tufted cells and later-onset slow gamma oscillatory signals of mitral cells transmitted to the areas of the olfactory cortex? Because sniff-paced burst discharges of tufted cells occur earlier than those of mitral cells during an inhalation–exhalation sniff cycle, it is natural to suppose that tufted cell inputs arrive in the olfactory cortex earlier than mitral cell inputs. Early-onset fast gamma synchrony of tufted cell activity might be transmitted first to the olfactory cortex. After a delay of approximately 45 ms, the later-onset slow gamma synchrony of mitral cell activity would be subsequently transmitted to the olfactory cortex.

To address this question, Manabe and colleagues made simultaneous recordings of local field potentials in the granule cell layer of the olfactory bulb and in layer III of the anterior piriform cortex (Fig. 7.11) (Manabe, unpublished data) (Mori et al. 2013). Manabe found that local field potentials in the anterior piriform cortex show sniff-paced fast and slow gamma oscillations, and that the fast and slow gamma oscillations in the anterior piriform cortex phase-couple those in the olfactory bulb. The early-onset fast gamma oscillations in the anterior piriform cortex correspond in timing and frequency with the early-onset fast gamma oscillations in the olfactory bulb, which are mainly generated by tufted cell circuits. Meanwhile, the later-onset slow gamma oscillations in the anterior piriform cortex correspond in timing and frequency with later-onset slow gamma oscillations in the olfactory bulb, which are mainly generated by mitral cell circuits.

In addition to these sniff-paced fast and slow gamma oscillations during the inhalation and inhalation–exhalation transition phases, the anterior piriform cortex occasionally shows slow gamma oscillations during the long exhalation phase (exh-s in Fig. 7.11). These slow gamma oscillations during the exhalation phase in the anterior piriform cortex typically phase-couple with those in the olfactory bulb, indicating a rich communication between anterior piriform cortex and olfactory bulb during the off-line exhalation phase (see Chap. 1).

7.9 Tufted Cells May Provide Specificity-Projecting Circuits, Whereas Mitral Cells Give Rise to Dispersedly-Projecting "Binding" Circuits

What is the functional role of the tufted cell pathway and mitral cell pathway in odor information processing in the olfactory cortex? Do tufted cell and mitral cell pathways differ in how they convey information to the olfactory cortex? To address these questions, we need first to understand axonal target regions of tufted and mitral cells that belong to specific functionally relevant glomerular modules. For this purpose, we focused on tufted and mitral cells that respond to fox odor, 2,4,5-trimethylthiazoline (TMT).

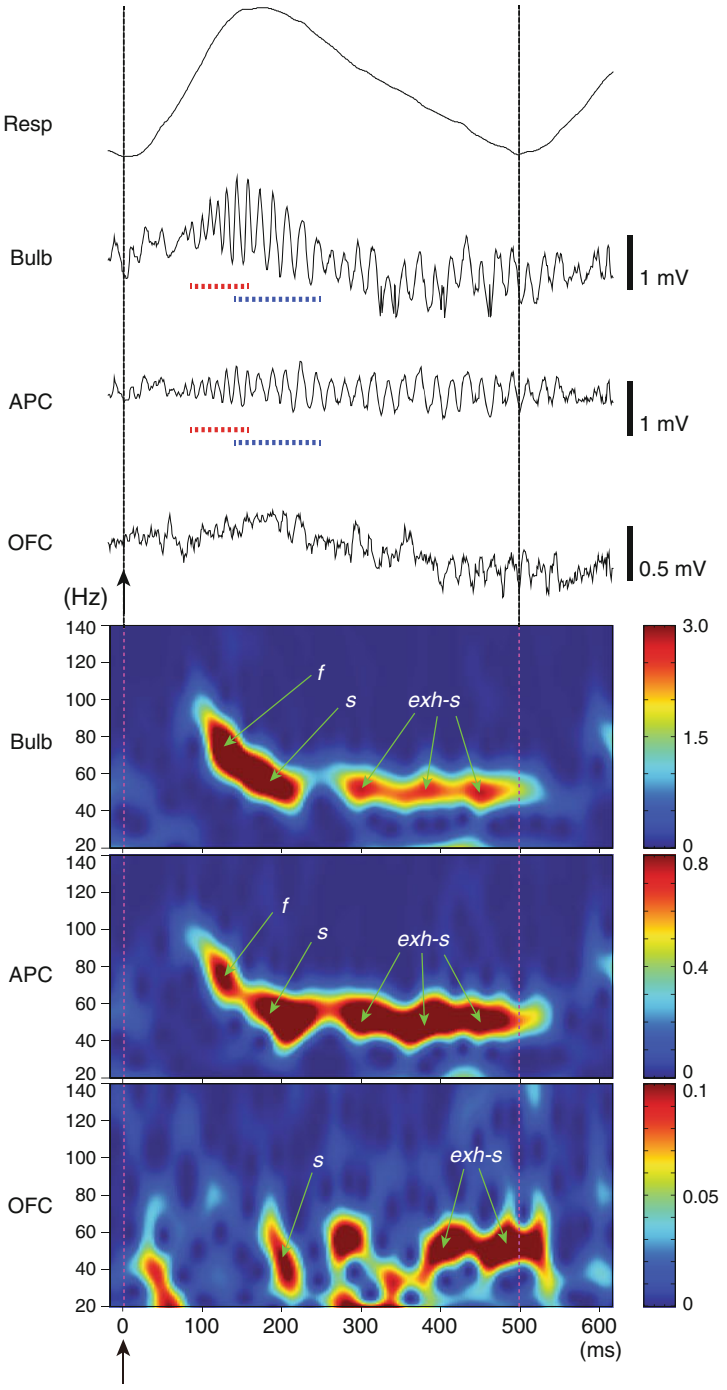

Fig. 7.11 Gamma oscillation couplings across the olfactory bulb, anterior piriform cortex, and orbitofrontal cortex. Simultaneous recordings of respiratory pattern (*Resp*; upward swing indicates inhalation), local field potential in the granule cell layer of the olfactory bulb (*Bulb*), local field

Foxes, cats, and weasels are dangerous predators to mice and rats. To flee unharmed from these predators, rats and mice have innate neuronal circuits that can detect predator odors at a very low concentration. For example, the odor molecule TMT secreted from the anal glands of foxes induces fear responses in rodents. Although TMT-responsive glomeruli are distributed both in the DII domain and V domain of the glomerular map of the rodent olfactory bulb (see Chap. 4), the fear responses themselves are induced only by glomeruli in the DII domain (Kobayakawa et al. 2007). We thus analyzed the spike responses and axonal projection targets of tufted and mitral cells located in the DII domain that respond to the fox odor TMT.

During the early phase of a sniff cycle inhaling the fox odor TMT, the olfactory bulb shows early-onset fast gamma oscillations, and TMT-responsive tufted cells show burst discharges. However, mitral cells do not yet start to discharge at this early phase. To which region of the olfactory cortex do TMT-responsive tufted cells send these early-onset signals? Figure 7.12 shows that these early-onset signals are sent to focal target neurons at specific regions in the anterior olfactory nucleus, olfactory tubercle, and anterior piriform cortex.

One of the focal targets of axons of TMT-responsive tufted cells is the dorsolateral corner of the pars externa of the anterior olfactory nucleus (AONpE) (Figs. 7.12, 7.13). Within the AONpE, axons of TMT-responsive tufted cells form dense terminal bushes (Fig. 7.13). These terminal bushes do not occur in any other part of the AONpE. Previous studies have shown a topographic relationship between the position of tufted cells in the glomerular map of the olfactory bulb and the position of their axon terminals in the AONpE (Schoenfeld and Macrides 1984; Yan et al. 2008). The AONpE has a U-shaped structure, and position within it is thought to represent a specific category of odorants (Kikuta et al. 2008, 2010). It has been shown that individual neurons in the AONpE show sniff-paced burst discharges and can distinguish the right or left position of an odor source by referencing signals from the right and left nostrils. Based on these results, we speculate that at the early phase of a sniff cycle, the tufted cells rapidly send the TMT signal to the topographically fixed position (dorsolateral corner) of the AONpE to compute the right or left localization of the odor source (Kikuta et al. 2008, 2010).

Another example of a focal target of TMT-responsive tufted cells is a relatively small region in the posteroventral subdivision of the anterior olfactory nucleus (AONpv) (Figs. 7.12, 7.13). Pyramidal cells in this region receive inputs from the TMT-responsive tufted cells and project axons (Ib associational axons) to the ventral part of the anterior piriform cortex (APCv), including the most rostroventral

Fig. 7.11 (continued) potential in layer III of the anterior piriform cortex (*APC*), and that in the deep layer of the orbitofrontal cortex (OFC), during micro-arousal. *Red broken line* indicates fast gamma oscillations, *blue broken line* shows slow gamma oscillations, *vertical broken lines* and *arrows* show onset of inhalation. Wavelet power spectrograms of the local field potentials are shown in the lower three figures. *f* fast gamma oscillations, *s* slow gamma oscillations, *exh-s* exhalation slow gamma oscillations. (Modified from Mori et al. 2013)

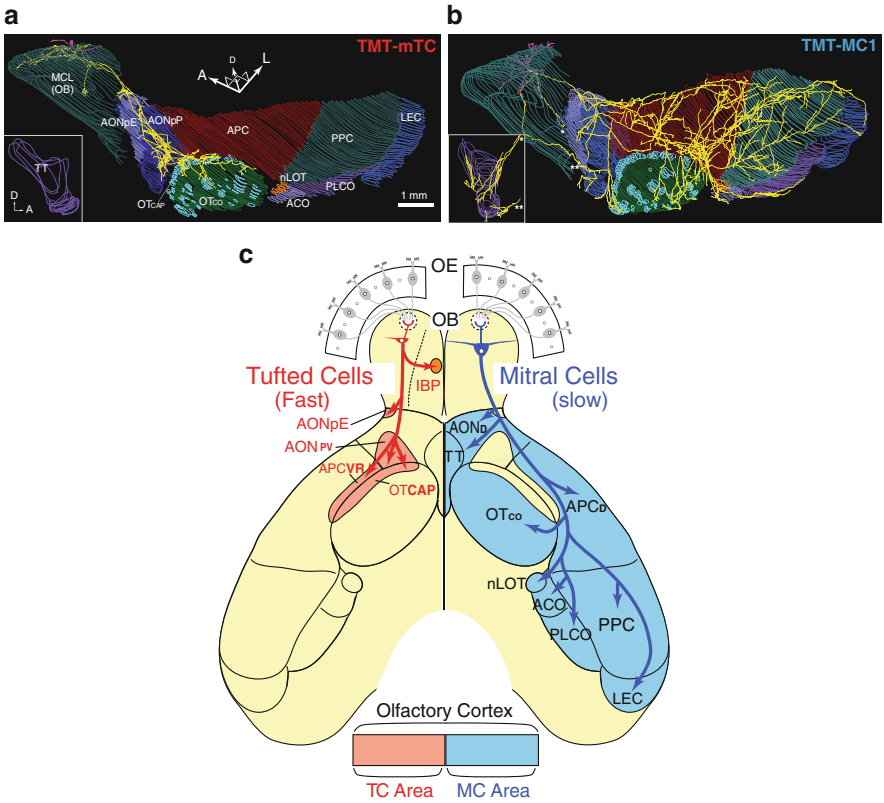

Fig. 7.12 Axonal projection patterns of mitral cells and tufted cells to the olfactory cortex. (**a**) Axonal projection of TMT-responsive middle tufted cell. The 3-D brain reconstruction containing the cell was rotated to a ventrolateral view. Dendrites (*magenta*) and axons (*yellow*) are shown with the mitral cell layer of the olfactory bulb and layer II of each region of the OC. *Inset:* Medial view of axons in the tenia tecta, which is hidden in the ventrolateral view. (**b**) Axonal projection of a TMT-responsive mitral cell. (**c**) A schematic diagram for parallel pathways of mitral cells and tufted cells from the olfactory bulb to the olfactory cortex. The segregated projections of mitral cells and tufted cells suggest the existence of parallel mitral cell (*MC*) and tufted cell (*TC*) pathways in the central olfactory system. The axonal projections of the two cell types are represented on the left (tufted cells, *red*) and right (mitral cells, *blue*) sides of the diagram of the ventral-viewed mouse brain. In the olfactory cortex, tufted cells route fast odor information to the pars externa of anterior olfactory nucleus (*AONpE*), posteroventral part of the anterior olfactory nucleus (AON_{PV}), anterolateral part of the olfactory tubercle that corresponds to the cap part of the olfactory tubercle (OT_{CAP}), and the ventrorostral part of the anterior piriform cortex (APC_{VR}). These regions are represented as tufted cell areas (*pink*). In the olfactory bulb (OB), tufted cells in the lateral map target the intrabulbar projection axons to the confined small area in the intrabulbar projection (*IBP*) area. By contrast, mitral cells route slower odor information widely to the dorsal part of the anterior olfactory nucleus (AON_D), cortical part of the olfactory tubercle (OT_{CO}), dorsal part of the anterior piriform cortex (APC_D), tenia tecta (*TT*), posterior piriform cortex (*PPC*), lateral entorhinal cortex (*LEC*), nucleus of the lateral olfactory tract (*nLOT*), anterior cortical amygdaloid nucleus (*ACO*), and posterolateral cortical amygdaloid nucleus (*PLCO*) (mitral cell area, *cyan*). *OE* olfactory epithelium

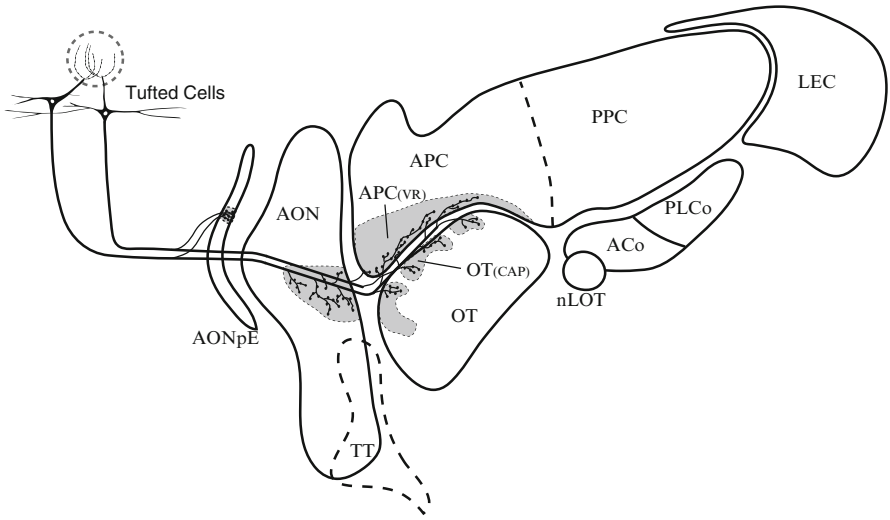

Fig. 7.13 Possible target region of early-onset signals of TMT-responsive tufted cells. Axonal projection pattern of tufted cells was schematized in the unrolled map of the olfactory cortex. Tufted cells route fast odor information to the pars externa of anterior olfactory nucleus (*AONpE*), posteroventral part of the anterior olfactory nucleus (AON_{PV}), anterolateral part of the olfactory tubercle that corresponds to the cap part of the olfactory tubercle (OT_{CAP}), and the ventrorostral part of the anterior piriform cortex (APC_{VR})

part of the anterior piriform cortex (APCvr). Therefore, the early-phase signals of TMT-responsive tufted cells might be relayed by the pyramidal cells in the AONpv and then sent via Ib associational axons to the APCv. TMT-responsive tufted cells also send axons directly to the APCvr. Pyramidal cells in the APCv project axons to the anterior and posterior piriform cortex. Therefore, early-onset TMT signals are presumably conveyed to the piriform cortex via tufted cell axons–Ib associational fiber pathways. Although the connectivity patterns of the di-synaptic or polysynaptic pathways originating from tufted cells are not understood in any detail, we speculate that the tufted axon–Ib associational fiber pathways are the major route of transmitting specific TMT signals to the piriform cortex.

Interestingly, pyramidal cells in the APCvr project axons to the ventrolateral orbital cortex (VLO) (see Chap. 1), which also receive nociceptive inputs (Ekstrand et al. 2001), the information that threatens the life of rodents. These results suggest that tufted cells carrying information about predator odor send the early-onset signal with fast gamma synchronization via the APCvr to the VLO. Early-onset fast-gamma synchronization might be advantageous in rapidly conveying the predator odor information through the tufted cell-APCvr-VLO pathway at the early phase of the sniff cycle.

The TMT-responsive tufted cells also project axons to focal targets in the lateral cap region of the olfactory tubercle (OTcap in Figs. 7.12, 7.13). As explained in Chap. 8, the olfactory tubercle appears to play a role as an interface between

olfactory signals and a variety of motivational behaviors, and is thought to contain motivation modules, including an "appetitive motivation module" and "aversive motivation module." We speculate that the lateral cap region is part of the "alert motivation module" and that specific signals of the predator odor TMT are rapidly sent to the lateral cap region via the early-onset responses of the TMT-responsive tufted cells.

Extrapolating the foregoing results to whole glomerular modules, we speculate that tufted cells provide specificity-projecting circuits, which send information from specific odorant receptors by early-onset fast gamma oscillations to focal targets in the olfactory peduncle areas, the APCv and olfactory tubercle. The idea of specificity-projecting circuits sending specific sensory information is reasonable and of no particular interest, because similar specificity-projecting circuits are present everywhere in the visual, auditory, somatosensory, and gustatory systems. These specificity-projecting circuits seem to be essential for perceiving sensory reality.

However, a major surprise and difficult questions arise when considering the axonal projection targets of TMT-responsive mitral cells. Dye-labeling of TMT-responsive mitral cells showed that individual mitral cells project axons in a dispersed manner to nearly all areas of the olfactory cortex, including nearly all parts of the piriform cortex (Figs. 7.10, 7.12) (Igarashi et al. 2012). In other words, TMT-responsive mitral cells appear to disperse their signal throughout a wide area of the piriform cortex, in striking contrast to the focal projection of TMT-responsive tufted cells. Labeling of sister mitral cells belonging to a single glomerulus also showed that they project axons in a highly distributed fashion throughout the piriform cortex (Ghosh et al. 2011; Nagayama et al. 2010; Sosulski et al. 2011). It appears that sister mitral cells send the odorant receptor information to nearly all pyramidal cells of the piriform cortex. For what functional purpose do sister mitral cells distribute their signals widely throughout the piriform cortex?

Given that mitral cell circuits in the olfactory bulb generate later-onset slow gamma oscillatory activity, we speculate that sister mitral cells belonging to an activated glomerulus provide a mechanism for the dispersion of later-onset slow gamma oscillatory activity across whole parts of the piriform cortex (Fig. 7.14). Because mitral cells extend long lateral dendrites and have extensive dendro-dendritic reciprocal synaptic connections, mitral cells belonging to different glomerular modules are able to synchronize their discharges at the slow gamma frequency when coactivated by an odor inhalation. Therefore, mitral cells that are coactivated by odor inhalation would likely provide later-onset synchronized inputs at slow gamma frequency to pyramidal cells across whole parts of the piriform cortex (Fig. 7.14).

Although individual pyramidal cells receive only weak input from individual mitral cell axons, nearly simultaneous arrival of the synchronized inputs from many mitral cells may effectively summate their excitatory postsynaptic potentials (EPSPs) and thereby strongly modulate pyramidal cell activity in synchrony with the slow gamma oscillatory inputs. We hypothesize that the gamma-synchronized coincident inputs from many mitral cell axons coordinate the response timing of

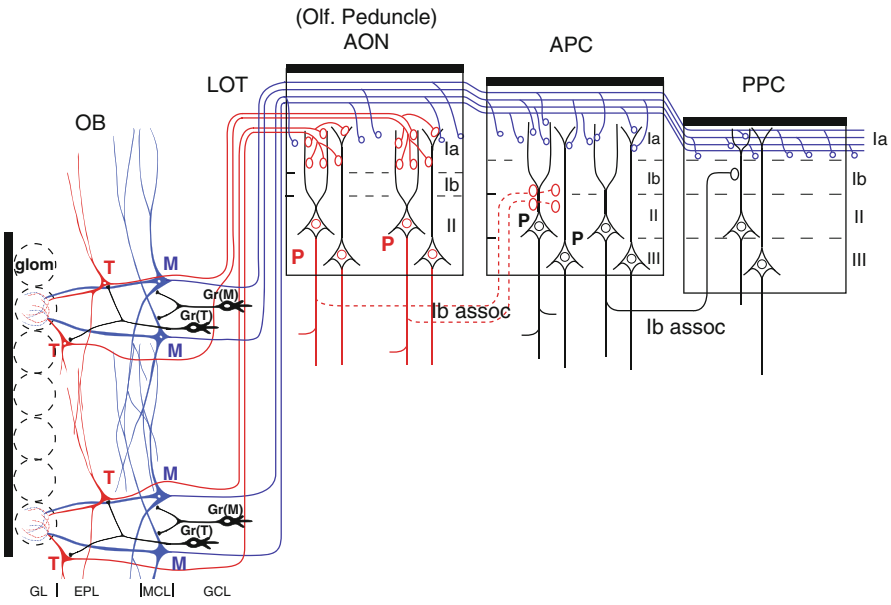

Fig. 7.14 Structural organization of tufted cell circuits and mitral cell circuits in the olfactory bulb and olfactory cortex. In the olfactory bulb (OB), tufted cells (*T*, *red*) extend relatively short lateral dendrites in the superficial sublamina of the EPL and make dendrodendritic reciprocal synaptic connections mainly with tufted cell-targeting granule cells (*Gr(T)*). Mitral cells (*M*, *blue*) extend long lateral dendrites in the deep sublamina of the EPL and form dendrodendritic synapses mainly with mitral cell-targeting granule cells (*Gr(M)*). Tufted cells project axons (*red* and *orange lines*) to focal targets in the olfactory peduncle areas including AON. Mitral cells project axons (*blue lines*) dispersedly to nearly all areas of the olfactory cortex. Layers of the olfactory bulb: *GL* glomerular layer, *EPL* external plexiform layer, *MCL* mitral cell layer, *GCL* granule cell layer. Layers in the olfactory cortex: *Ia* layer Ia, *Ib* layer Ib, *II* layer II, *III* layer III. *LOT* lateral olfactory tract, *Ib* assoc, *Ib* associational axon. *Red P* indicates pyramidal cells in the AON. *Black P* shows pyramidal cells in the APC. *Glom* glomerulus

pyramidal cells that are spatially distributed across whole parts of the piriform cortex over a sustained time window. This mitral cell-induced synchronized activity of pyramidal cells across whole parts of the piriform cortex may have a key role in "binding" together the spike activities of numerous coactivated pyramidal cells with different odor tuning specificity, as described in more detail in Chap. 8. Based on these speculations, we hypothesize that mitral cells provide dispersedly-projecting feed-forward "binding" circuits, sending the response synchronization timing with slow gamma synchrony to pyramidal cells across whole parts of the piriform cortex (Fig. 7.14).

As just described, sniff-paced early-onset fast and later-onset slow gamma oscillatory activity in the anterior piriform cortex (APC) corresponds in timing and frequency with the early-onset fast and later-onset slow gamma oscillatory activity of the olfactory bulb. This observation raises the possibility that the activity

of APC pyramidal cells during early-onset gamma oscillation may be the result of the tufted cell axon–Ib association fiber inputs whereas that during later-onset slow gamma oscillation is induced by the combination of preceding tufted cell axon–Ib associational axon inputs and later-onset synchronized inputs from many mitral cells. If so, the later-onset synchronized inputs from mitral cells may cause profound synchronization of those pyramidal cells that had been depolarized by preceding early-onset inputs from tufted cell axon–Ib association axon inputs, but have little influence on those pyramidal cells that had not been depolarized by the tufted cell axon–Ib association axon inputs.

These scenarios of the possible functional role of tufted cell and mitral cell pathways are preliminary and require development and experimental evaluation. However, they may provide a working hypothesis for a framework of the functional differentiation of tufted and mitral cell pathways in odor information processing in the olfactory system.

7.10 Fast and Slow Gamma Oscillations in the Piriform Cortex and Hippocampus

Sniff-paced gamma oscillatory inputs from tufted cells and mitral cells arrive in the APC at different phases of a sniff cycle. Early-onset fast gamma activity of tufted cells begins to arrive in the piriform cortex (via pyramidal cells in the olfactory peduncle) at the middle of the inhalation phase. Later-onset slow gamma activity of mitral cells may start to arrive in the piriform cortex at a later phase of inhalation or at the transition phase from inhalation to exhalation. As explained previously, the time lag between fast gamma input from specificity-projecting tufted cell–Ib association fiber pathways and slow gamma input from dispersedly-projecting mitral cell pathways can play a critical role in information processing in the piriform cortex.

A similar time lag between fast and slow gamma inputs has been reported in the hippocampus, a structure critical to spatial and episodic memory (Fig. 7.15). The CA1 region of the hippocampus receives direct inputs from the entorhinal cortex and the CA3 region. In this circuit, gamma oscillatory inputs from the medial part of the entorhinal cortex (MEC) and CA3 arrive in CA1 at different phases of the theta cycle (Colgin et al. 2009; Colgin and Moser 2009). Fast gamma oscillations in CA1 are synchronized with fast gamma oscillatory inputs from the MEC, an area that provides specific information about the animal's current position. The fast gamma oscillations normally occur at the trough of theta oscillations. In contrast, slow gamma oscillations in CA1 are coherent with slow gamma oscillatory inputs from CA3, an area essential for storage of positional information. The slow gamma oscillations are maximal near the falling phase of theta oscillations. The fast and slow gamma oscillations usually occur at different theta cycles but sometimes coexist in the same cycle. In these cycles, they are thought to be discriminated by CA1 using

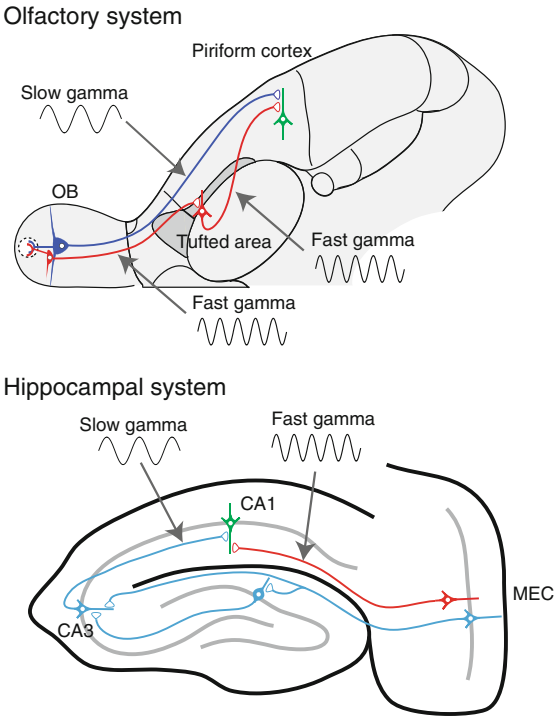

Fig. 7.15 Comparison between the olfactory system and hippocampal system. *Top*: In the olfactory system, odor information is sent from the olfactory bulb (OB) to the olfactory cortex via two pathways. Tufted cells (*red*) send odor information carried on fast gamma oscillations to tufted area. Mitral cells (*blue*) send information riding on slow gamma oscillations to the piriform cortex. In piriform cells, this slow signal may be integrated with fast gamma information sent from tufted area. *Bottom*: In the hippocampal system, fast gamma oscillations from medial entorhinal cortex (MEC) and slow gamma oscillations from hippocampal CA3 region are integrated in neurons in hippocampal CA1 region

phase information. In the piriform cortex, similar phase information in relationship to sniff rhythms (see Chap. 1) might be used by pyramidal cells to discriminate specificity-conveying tufted-related fast gamma input and dispersedly-projecting mitral-related slow gamma input.

In the entorhinal-hippocampal circuit, the frequency of slower "carrier" oscillations, theta oscillations in this case, varies in different animal states and can also be a mechanism for gating input from different brain regions. When rats are performing olfactory-cued association tasks, theta oscillations of around 6–7 Hz are abundant in the CA1-EC circuit while rats are immobile and attending to cues (Igarashi, unpublished data). These theta oscillations (so-called a-theta) are slower than those of 8–12 Hz (so-called t-theta) normally observed when animals are actively running in the environment. In the foregoing experiment, with these slower theta oscillations, 20–40 Hz oscillations emerged in both CA1 and the lateral

entorhinal cortex (LEC) and are synchronized across two regions during the learning of the task. Thus, to discriminate input from the MEC and LEC, CA1 uses subtypes of not only fast oscillations (60–100 Hz gamma vs. 20–40 Hz oscillations, respectively) but also theta oscillations (t-theta vs. a-theta, respectively). The shift in frequency might reflect not only the functional nature of inputs between the MEC and LEC but also different roles of these two regions in different animal states (running vs. attention, respectively).

In the olfactory system, slow "carrier" oscillations correspond to sniff rhythms with frequencies ranging from 2 to 10 Hz in mice. As described in Chap. 1, the behavioral state and degree of attention correlate with sniff rhythm and sniff pattern, raising the possibility that sniff rhythm also contributes to the gating of inputs from different regions. Although the presence of oscillatory activities in the piriform cortex has long been known, their functional properties in terms of information flow remain largely unknown. Future work will elucidate the neuronal circuit mechanisms that generate these oscillations and their functional roles in olfactory information processing and transmission in large-scale networks of the central olfactory system.

References

Adrian ED (1942) Olfactory reactions in the brain of the hedgehog. J Physiol 100:459–473

Allison AC, Warwick RT (1949) Quantitative observations on the olfactory system of the rabbit. Brain 72:186–197

Bressler SL (1984) Spatial organization of EEGs from olfactory bulb and cortex. Electroencephalogr Clin Neurophysiol 57:270–276

Buonviso N, Amat C, Litaudon P, Roux S, Royet JP, Farget V, Sicard G (2003) Rhythm sequence through the olfactory bulb layers during the time window of a respiratory cycle. Eur J Neurosci 17:1811–1819

Cajal SRY (1955) Studies on the cerebral cortex (limbic structures). Lloyd-Luke, London

Carlson GC, Shipley MT, Keller A (2000) Long-lasting depolarizations in mitral cells of the rat olfactory bulb. J Neurosci 20:2011–2021

Cenier T, Amat C, Litaudon P, Garcia S, Lafaye de Micheaux P, Liquet B, Roux S, Buonviso N (2008) Odor vapor pressure and quality modulate local field potential oscillatory patterns in the olfactory bulb of the anesthetized rat. Eur J Neurosci 27:1432–1440

Colgin LL, Moser EI (2009) Hippocampal theta rhythms follow the beat of their own drum. Nat Neurosci 12:1483–1484

Colgin LL, Denninger T, Fyhn M, Hafting T, Bonnevie T, Jensen O, Moser MB, Moser EI (2009) Frequency of gamma oscillations routes flow of information in the hippocampus. Nature (Lond) 462:353–357

De Saint Jan D, Hirnet D, Westbrook GL, Charpak S (2009) External tufted cells drive the output of olfactory bulb glomeruli. J Neurosci 29:2043–2052

Ekstrand JJ, Domroese ME, Johnson DM, Feig SL, Knodel SM, Behan M, Haberly LB (2001) A new subdivision of anterior piriform cortex and associated deep nucleus with novel features of interest for olfaction and epilepsy. J Comp Neurol 434:289–307

Freeman WJ (1975) Mass action in the nervous system. Academic, New York

Friedman D, Strowbridge BW (2003) Both electrical and chemical synapses mediate fast network oscillations in the olfactory bulb. J Neurophysiol 89:2601–2610

Fukunaga I, Berning M, Kollo M, Schmaltz A, Schaefer AT (2012) Two distinct channels of olfactory bulb output. Neuron 75:320–329

Ghosh S, Larson SD, Hefzi H, Marnoy Z, Cutforth T, Dokka K, Baldwin KK (2011) Sensory maps in the olfactory cortex defined by long-range viral tracing of single neurons. Nature (Lond) 472:217–220

Gire DH, Schoppa NE (2009) Control of on/off glomerular signaling by a local GABAergic microcircuit in the olfactory bulb. J Neurosci 29:13454–13464

Golgi C (1875) Sulla fina struttura dei bulbi olfactorii (On the fine structure of the olfactory bulb). Rivista Sperimentale di Freniatria e Medicina Legale 1:405–425

Hayar A, Karnup S, Ennis M, Shipley MT (2004) External tufted cells: a major excitatory element that coordinates glomerular activity. J Neurosci 24:6676–6685

Henneman E, Somjen G, Carpenter DO (1965) Functional significance of cell size in spinal motoneurons. J Neurophysiol 28:560–580

Hinds JW (1968) Autoradiographic study of histogenesis in the mouse olfactory bulb. I. Time of origin of neurons and neuroglia. J Comp Neurol 134:287–304

Igarashi KM, Ieki N, An M, Yamaguchi Y, Nagayama S, Kobayakawa K, Kobayakawa R, Tanifuji M, Sakano H, Chen WR, Mori K (2012) Parallel mitral and tufted cell pathways route distinct odor information to different targets in the olfactory cortex. J Neurosci 32:7970–7985

Imamura F, Greer CA (2013) Pax6 regulates Tbr1 and Tbr2 expressions in olfactory bulb mitral cells. Mol Cell Neurosci 54:58–70

Inaki K, Nishimura S, Nakashiba T, Itohara S, Yoshihara Y (2004) Laminar organization of the developing lateral olfactory tract revealed by different expression of cell recognition molecules. J Comp Neurol 479:243–256

Kashiwadani H, Sasaki YF, Uchida N, Mori K (1999) Synchronized oscillatory discharges of mitral/tufted cells with different molecular receptive ranges in the rabbit olfactory bulb. J Neurophysiol 82:1786–1792

Kikuta S, Kashiwadani H, Mori K (2008) Compensatory rapid switching of binasal inputs in the olfactory cortex. J Neurosci 28:11989–11997

Kikuta S, Sato K, Kashiwadani H, Tsunoda K, Yamasoba T, Mori K (2010) Neurons in the anterior olfactory nucleus pars externa detect right or left localization of odor sources. Proc Natl Acad Sci USA 107:12363–12368

Kikuta S, Fletcher ML, Homma R, Yamasoba T, Nagayama S (2013) Odorant response properties of individual neurons in an olfactory glomerular module. Neuron 77:1122–1135

Kobayakawa K, Kobayakawa R, Matsumoto H, Oka Y, Imai T, Ikawa M, Okabe M, Ikeda T, Itohara S, Kikusui T et al (2007) Innate versus learned odour processing in the mouse olfactory bulb. Nature (Lond) 450:503–508

Lagier S, Carleton A, Lledo PM (2004) Interplay between local GABAergic interneurons and relay neurons generates gamma oscillations in the rat olfactory bulb. J Neurosci 24:4382–4392

Lepousez G, Lledo PM (2013) Odor discrimination requires proper olfactory fast oscillations in awake mice. Neuron 80:1010–1024

Manabe H, Mori K (2013) Sniff rhythm-paced fast and slow gamma-oscillations in the olfactory bulb: relation to tufted and mitral cells and behavioral states. J Neurophysiol 110:1593–1599

Matsumoto H, Kashiwadani H, Nagao H, Aiba A, Mori K (2009) Odor-induced persistent discharge of mitral cells in the mouse olfactory bulb. J Neurophysiol 101:1890–1900

Mori K, Sakano H (2011) How is the olfactory map formed and interpreted in the mammalian brain? Annu Rev Neurosci 34:467–499

Mori K, Takagi SF (1977) Inhibition in the olfactory bulb: dendrodendritic interaction and their relation to the induced waves. In: Katsuki K, Sato M, Takagi S, Oomura Y (eds) Food intake and chemical senses. University of Tokyo Press, Tokyo, pp 33–43

Mori K, Kishi K, Ojima H (1983) Distribution of dendrites of mitral, displaced mitral, tufted, and granule cells in the rabbit olfactory bulb. J Comp Neurol 219:339–355

Mori K, Nagao H, Yoshihara Y (1999) The olfactory bulb: coding and processing of odor molecule information. Science 286:711–715

Mori K, Manabe H, Narikiyo K, Onisawa N (2013) Olfactory consciousness and gamma oscillation couplings across the olfactory bulb, olfactory cortex, and orbitofrontal cortex. Front Psychol 4:743

Nagao H, Yoshihara Y, Mitsui S, Fujisawa H, Mori K (2000) Two mirror-image sensory maps with domain organization in the mouse main olfactory bulb. Neuroreport 11:3023–3027

Nagayama S, Takahashi YK, Yoshihara Y, Mori K (2004) Mitral and tufted cells differ in the decoding manner of odor maps in the rat olfactory bulb. J Neurophysiol 91:2532–2540

Nagayama S, Enerva A, Fletcher ML, Masurkar AV, Igarashi KM, Mori K, Chen WR (2010) Differential axonal projection of mitral and tufted cells in the mouse main olfactory system. Front Neural Circuits 4:120

Najac M, De Saint Jan D, Reguero L, Grandes P, Charpak S (2011) Monosynaptic and polysynaptic feed-forward inputs to mitral cells from olfactory sensory neurons. J Neurosci 31:8722–8729

Neville KR, Haberly LB (2003) Beta and gamma oscillations in the olfactory system of the urethane-anesthetized rat. J Neurophysiol 90:3921–3930

Orona E, Rainer EC, Scott JW (1984) Dendritic and axonal organization of mitral and tufted cells in the rat olfactory bulb. J Comp Neurol 226:346–356

Patterson MA, Lagier S, Carleton A (2013) Odor representations in the olfactory bulb evolve after the first breath and persist as an odor afterimage. Proc Natl Acad Sci USA 110:E3340–E3349

Phillips ME, Sachdev RN, Willhite DC, Shepherd GM (2012) Respiration drives network activity and modulates synaptic and circuit processing of lateral inhibition in the olfactory bulb. J Neurosci 32:85–98

Price JL, Sprich WW (1975) Observations on the lateral olfactory tract of the rat. J Comp Neurol 162:321–336

Rall W, Shepherd GM (1968) Theoretical reconstruction of field potentials and dendrodendritic synaptic interactions in olfactory bulb. J Neurophysiol 31:884–915

Rosero MA, Aylwin ML (2011) Sniffing shapes the dynamics of olfactory bulb gamma oscillations in awake behaving rats. Eur J Neurosci 34:787–799

Royet JP, Souchier C, Jourdan F, Ploye H (1988) Morphometric study of the glomerular population in the mouse olfactory bulb: numerical density and size distribution along the rostrocaudal axis. J Comp Neurol 270:559–568

Royet JP, Distel H, Hudson R, Gervais R (1998) A re-estimation of the number of glomeruli and mitral cells in the olfactory bulb of rabbit. Brain Res 788:35–42

Schoenfeld TA, Macrides F (1984) Topographic organization of connections between the main olfactory bulb and pars externa of the anterior olfactory nucleus in the hamster. J Comp Neurol 227:121–135

Shepherd GM, Chen WR, Greer CA (2004) Olfactory bulb. In: Shepherd GM (ed) The synaptic organization of the brain. Oxford University Press, New York, pp 165–216

Sosulski DL, Bloom ML, Cutforth T, Axel R, Datta SR (2011) Distinct representations of olfactory information in different cortical centres. Nature (Lond) 472:213–216

Yan Z, Tan J, Qin C, Lu Y, Ding C, Luo M (2008) Precise circuitry links bilaterally symmetric olfactory maps. Neuron 58:613–624

Chapter 8
Piriform Cortex and Olfactory Tubercle

Kensaku Mori

Abstract This chapter describes perspectives on the possible functional logic of neuronal circuits in the central olfactory system. The central olfactory system has multiplex pathways and loops that connect the olfactory bulb, olfactory cortex, neocortex, thalamus, ventral striatum, amygdala, hippocampus, and hypothalamus. Among the complex circuits, this chapter focuses on the possible functional differentiation of "olfactory bulb axon–Ib association axon (afferent) circuits" and "deep association axon (recurrent and top-down) circuits" in the piriform cortex. It is hypothesized that the activity of the former circuits is induced mainly by olfactory sensory inputs during the on-line inhalation phase of the sniff cycle, whereas activity of the latter circuits may occur mainly during the off-line exhalation phase. This chapter also discusses the possible function of motivation modules in the neuronal circuits of the olfactory tubercle.

Keywords Deep association axons • Endopiriform nucleus • Ib association axons • Medium-sized spiny neurons • Olfactory bulb • Olfactory tubercle • Orbitofrontal cortex • Piriform cortex • Thalamus • Ventral striatum

8.1 Introduction

Two types of projection neurons in the olfactory bulb, tufted cells and mitral cells, convey odor inhalation-induced signals to the olfactory cortex, which includes the piriform cortex and olfactory tubercle. In Chap. 7, Nagayama et al. described the hypothesis that the two types of projection neurons play distinct roles in sending sniff rhythm-paced odor signals from the olfactory bulb to the olfactory cortex during the inhalation phase. Tufted cells may provide specificity-projecting circuits

K. Mori (✉)
Department of Physiology, Graduate School of Medicine, The University of Tokyo, Bunkyo-ku, Tokyo 113-0033, Japan
e-mail: moriken@m.u-tokyo.ac.jp

K. Mori (ed.), *The Olfactory System: From Odor Molecules to Motivational Behaviors*, DOI 10.1007/978-4-431-54376-3_8,

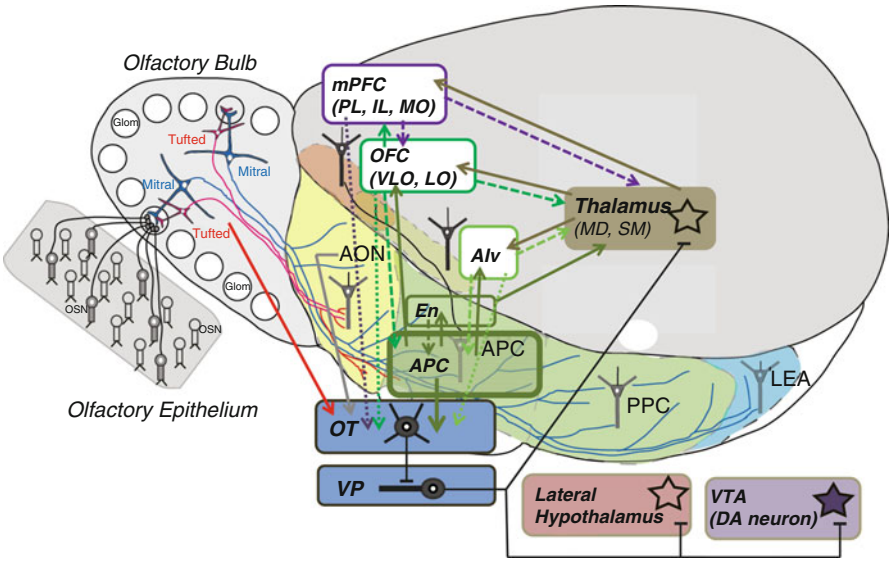

Fig. 8.1 Schematic diagram of central olfactory pathways and loops in the rodent brain. Areas in the olfactory cortex: *AON* anterior olfactory nucleus, *APC* anterior piriform cortex, *PPC* posterior piriform cortex, *LEA* lateral entorhinal area, *OT* olfactory tubercle. *En* endopiriform nucleus. Areas in the orbitofrontal cortex (*OFC*): *VLO* ventrolateral orbital cortex, *LO* lateral orbital cortex. Areas in the medial prefrontal cortex (*mPFC*): *PL* prelimbic cortex, *IL* infralimbic cortex, *MO* medial orbital cortex. *AIv* ventral agranular insular cortex. Thalamic nuclei: *MD* mediodorsal nucleus of thalamus, *SM* submedius nucleus of thalamus. *VP* ventral pallidum, *VTA* ventral tegmental area, *DA neuron* dopaminergic neuron. *Arrows* with *solid lines* indicate afferent excitatory synaptic connections; *arrows* with *broken lines* show top-down excitatory synaptic connections. T-shaped axonal terminals indicate inhibitory synaptic connections. *Glom* glomerulus, *OSN* olfactory sensory neurons. (Modified from Mori et al. 2013)

that send specific odor information to focal targets in the olfactory peduncle areas of the olfactory cortex with early-onset fast gamma synchronization. In contrast, mitral cells may give rise to dispersed-projection feed-forward "binding" circuits that transmit the response synchronization timing via their later-onset slow gamma synchronization to pyramidal cells across all parts of the piriform cortex as well as all areas of the olfactory cortex.

This chapter describes perspectives on the possible functional logic of neuronal circuits in the piriform cortex and olfactory tubercle. For this purpose, I briefly summarize structural organization of afferent pathways in the olfactory cortex and large-scale neuronal pathways and loops that originate from the piriform cortex. The latter pathways include (1) piriform cortex → neocortex → piriform cortex loops, (2) piriform cortex → thalamus → neocortex → piriform cortex loops, and (3) piriform cortex → ventral-striatum (olfactory tubercle) — ventral pallidum — thalamus → neocortex → piriform cortex loops (in which → indicates excitatory synaptic connection and — indicates inhibitory synaptic connection) (Fig. 8.1).

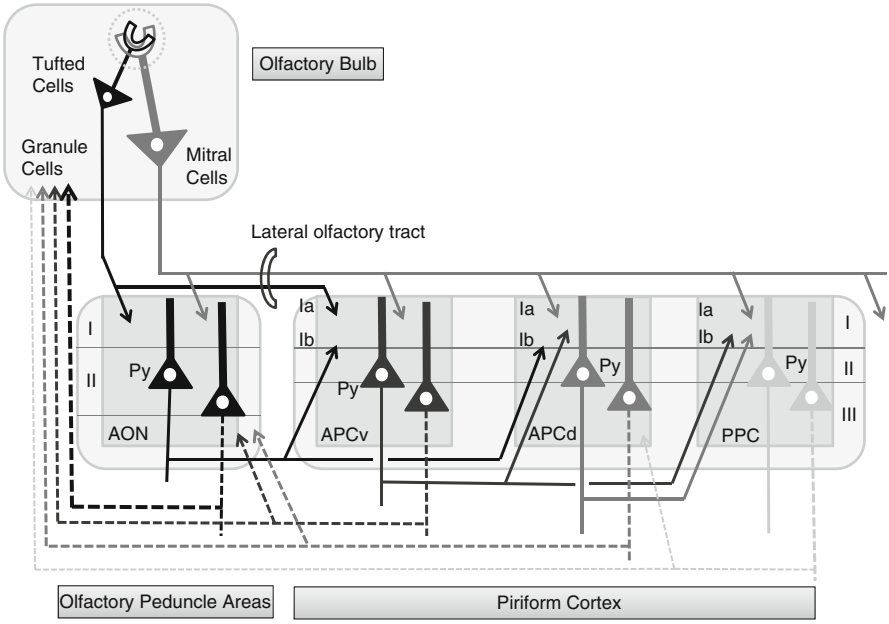

Fig. 8.2 Possible organization of afferent and top-down connections among olfactory bulb, anterior olfactory nucleus (*AON*), ventral subdivision of the anterior piriform cortex (*APCv*), dorsal subdivision of the anterior piriform cortex (*APCd*), and posterior piriform cortex (*PPC*). *Solid lines* with *arrowheads* indicate afferent axons of tufted cells and mitral cells and Ib association axons of pyramidal cells of the olfactory cortex. *Broken lines* with *arrowheads* show top-down collaterals of "deep association axons" of pyramidal cells that project to the deep layers of the olfactory bulb and AON. Layers in the AON: *I* layer I, *II* layer II. Layers in the piriform cortex: *Ia* layer Ia, *Ib* layer Ib, *I* layer I, *II* layer II, *III* layer III. *Py* pyramidal cell

The piriform cortex is the largest area of the olfactory cortex, composed of the anterior piriform cortex (APC) and posterior piriform cortex (PPC), although the definition of the boundary between the APC and PPC varies among researchers (Figs. 8.1, 8.2; see also Fig. 1.5 in Chap. 1) (Haberly 1983; Neville and Haberly 2004; Shipley and Ennis 1996). The anterior piriform cortex is further subdivided into ventral subdivision (APCv) and dorsal subdivision (APCd). Based on the direct afferent inputs from the olfactory bulb and the connectivity pattern of Ib association fibers of pyramidal cells in the olfactory cortex (Fig. 8.2), a major direction of afferent olfactory information flow is suggested as follows (Luskin and Price 1983a, b; Neville and Haberly 2004) : olfactory bulb (OB) → anterior olfactory nucleus (AON) → APCv → APCd → PPC (in which → indicates excitatory synaptic connection). The AON also send direct Ib association axons to the APCd. APCv also directly project Ib association axons to the PPC. In addition, each area of the piriform cortex project Ib and deep recurrent association fibers to its own area and other areas (Fig. 8.3). It should be noted that the bottom-up afferent pathways from the OB are typically associated with top-down feedback axonal projections, forming

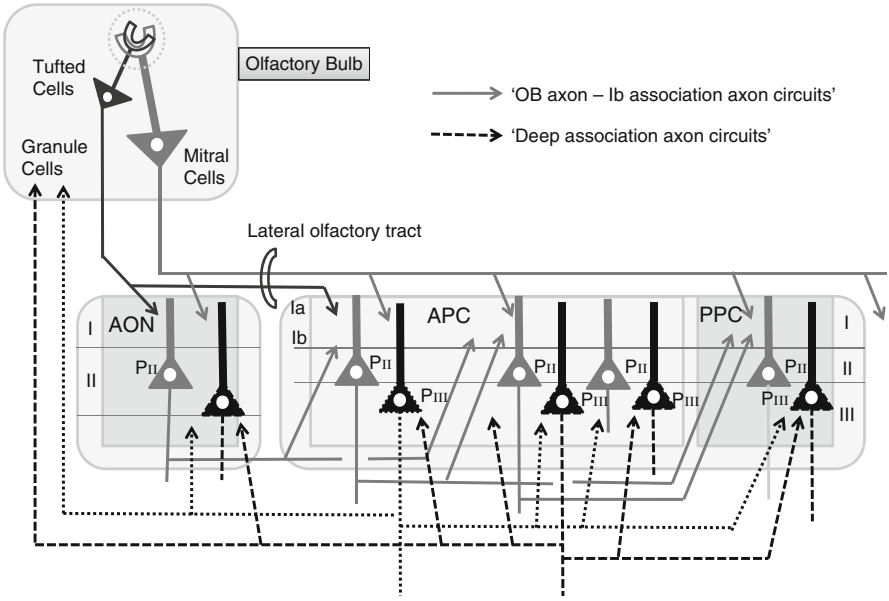

Fig. 8.3 Possible organization of "olfactory bulb (OB) axon–Ib association axon circuits" and "deep association axon circuits" in the olfactory cortex. *AON* anterior olfactory nucleus, *APC* anterior piriform cortex, *PPC* posterior piriform cortex. *PII* layer II pyramidal cells, *PIII* layer III pyramidal cells. "OB axon–Ib association axon circuits" are shown by *solid lines* with *arrowheads*; "deep association axon circuits" are indicated by *broken lines* with *arrowheads*. Endopiriform nucleus (not shown) is involved in the "deep association axon circuits". Layers in the piriform cortex: *Ia* layer Ia, *Ib* layer Ib, *I* layer I, *II* layer II, *III* layer III

neuronal loops, including OB → AON → OB loops and OB → APC → OB loops. The piriform cortex also sends top-down inputs to the AON (Figs. 8.2, 8.3).

The endopiriform nucleus (En) is located deep to the piriform cortex and reciprocally connected with the piriform cortex (Fig. 8.1) (see also Fig. 1.7 in Chap. 1), suggesting that the two regions form piriform cortex → En → piriform cortex loops. Pyramidal cells in the APC or neurons in the En project axons to higher association areas such as orbitofrontal cortex, thalamus, hypothalamus, and ventral striatum, including the olfactory tubercle (Fig. 8.1).

One of the major olfactory afferent streams beyond the APC is the information flow to the orbitofrontal cortex (OFC) and further to the medial prefrontal cortex (mPFC). The OFC receives multimodality sensory inputs including olfactory and gustatory inputs and is thought to be involved in conscious perception of the olfactory image of objects (Li et al. 2010; Plailly et al. 2008). In rodents, the OFC plays a key role in the sensory cue–reward association learning (Schoenbaum et al. 2007), whereas mPFC is important in action–outcome association learning.

The layer II pyramidal cells of the APC project axons directly to the layer I of the OFC. As described in Chap. 1, this projection from the APC to the orbitofrontal cortex is composed of two parallel pathways: APCv projects to the ventrolateral orbital cortex (VLO) and the APCd sends axons to the lateral orbital cortex (LO).

Neurons in the OFC send the information to the mPFC, which includes the prelimbic cortex (PL), infralimbic cortex (IL), and medial orbital cortex (MO).

In addition, the OFC project axons back to the APC. For example, the VLO send top-down axons to the APCv, indicating the presence of APCv → VLO → APCv loops. The LO project back to the APCd, forming the APCd → LO → APCd loops. APCd also directly and reciprocally connects with the ventral agranular insular cortex (AIv), forming the APCd → AIv → APCd loops. The posterior piriform cortex has reciprocal connections with AIv and the posterior agranular insular cortex (AIp) (see Fig. 1.7 in Chap. 1). Thus, the piriform cortex gives rise to piriform cortex → orbitofrontal cortex/agranular insular cortex → piriform cortex loops.

Neurons in the endopiriform nucleus project axons to the thalamus. Pre-endopiriform nucleus neurons (pEn) that are associated with the APCv project axons to the submedius nucleus of thalamus. The thalamocortical neurons in the submedius nucleus reciprocally connect with the VLO, forming thalamocorticothalamic loops. Because VLO project axons back to the APCv, these connections form APCv ↔ pEn → submedius nucleus ↔ VLO ↔ APCv loops (in which ↔ indicates reciprocal excitatory projections).

Endopiriform nucleus neurons that are associated with APCd project to the central segment of the mediodorsal nucleus (MDc) of the thalamus. Thalamocortical neurons in the MDc reciprocally connect with the LO and AIv. These connections thus form APCd ↔ En → MDc ↔ LO/AIv ↔ APCd loops. In summary, the piriform cortex gives rise to piriform cortex ↔ endopiriform nucleus → thalamus ↔ orbitofrontal cortex/agranular insular cortex ↔ piriform cortex loops.

The piriform cortex also projects massively to the olfactory tubercle (Fig. 8.1). However, there is no direct feedback projection from the olfactory tubercle to the piriform cortex. Together with the accumbens nucleus, the olfactory tubercle forms the ventral striatum, which is thought to have a key role as an interface between sensory signals and motivational behaviors (Ikemoto 2007). Principal neurons in the olfactory tubercle are GABAergic medium-sized spiny neurons, and axons of the medium-sized spiny neurons terminate on GABAergic neurons in the rostral part of the ventral pallidum, forming the olfactory tubercle — ventral pallidum pathway (in which — indicates inhibitory synaptic connection).

The neurons in the ventral pallidum send inhibitory output to the lateral hypothalamus, ventral tegmental area, and most notably the MD and SM of thalamus (ventral pallidum — thalamus pathway). Because ventral pallidum neurons tonically inhibit target neurons in the thalamus, hypothalamus, and ventral tegmental area, activation of olfactory tubercle appears to disinhibit the target neurons. Thus the piriform cortex ↔ endopiriform nucleus → thalamus ↔ orbitofrontal cortex/agranular insular cortex ↔ piriform cortex loops are controlled by the piriform cortex → olfactory tubercle — ventral pallidum — thalamus pathways.

Besides these large-scale pathways and loops, the piriform cortex is known to give rise to the piriform cortex (cortical amygdaloid nuclei) → amygdaloid nucleus (including the bed nucleus of stria terminalis) pathways and the piriform cortex → entorhinal cortex → hippocampus pathways.

Looking at these large-scale pathways and loops in the central olfactory system (Fig. 8.1), it is tempting to raise questions of how and when in the sniff (respiration) cycle the olfactory information is transferred along each of these pathways and loops. Another interesting question is for what purpose the olfactory information is transferred along a variety of pathways and loops. Does each pathway or loop play distinct functional roles in the process of the odor input–behavioral output translation? Future studies are needed to answer these questions. In the following sections, I briefly summarize basic knowledge of neuronal circuits of the piriform cortex and olfactory tubercle, hoping that the knowledge is helpful for addressing important questions regarding the workings of the large-scale networks of the central olfactory system.

8.2 Neuronal Circuits in the Piriform Cortex

The piriform cortex is thought to use spatially distributed overlapping ensembles of active pyramidal cells to represent odors (Neville and Haberly 2004; Wilson and Sullivan 2011). At the level of the OB, individual glomeruli represent a single type of odorant receptor and thus respond to particular molecular features of odorants (Kikuta et al. 2013; Mori et al. 1999). On the other hand, individual neurons in the piriform cortex respond not to individual features but to combinations of features (Haberly 2001; Litaudon et al. 2003; Poo and Isaacson 2011; Wilson and Sullivan 2011; Yoshida and Mori 2007).

Piriform cortex neurons that respond to a given odor are dispersedly distributed across the wide space of the piriform cortex without spatial preference (Illig and Haberly 2003; Litaudon et al. 1997; Mitsui et al. 2011; Rennaker et al. 2007; Stettler and Axel 2009). As already stated, excitatory responses of individual neurons in the piriform cortex are tuned to specific combinations of stimulus odorants. The two characteristic properties of the piriform cortex ("sparse distribution of the odor-induced activity" and "selective odor tuning of individual neurons") resemble those of the hippocampus ("sparse distribution of CA1 pyramidal cells (place cells) that fire at a particular place" and "individual pyramidal cells have the property of well-tuned place cell"). Based on these properties and its characteristic anatomical structure, the hippocampus has been proposed to be a giant cortical module (Buzsaki 2006). Similarity between piriform cortex and hippocampus implies that the piriform cortex might also be categorized as a giant cortical module.

Recurrent axon collaterals of pyramidal cells in the piriform cortex form excitatory synaptic connections on dendrites of other pyramidal cells that are distributed widely in the piriform cortex (Fig. 8.3) (Chen et al. 2003; Franks et al. 2011; Haberly and Presto 1986; Johnson et al. 2000; Yang et al. 2004). These recurrent axon collaterals are classified into those that terminate in layer Ib (Ib association axons) and those that terminate in layers II and III (deep association axons). Association axons in the bottom-up afferent pathway tend to be dominated by the

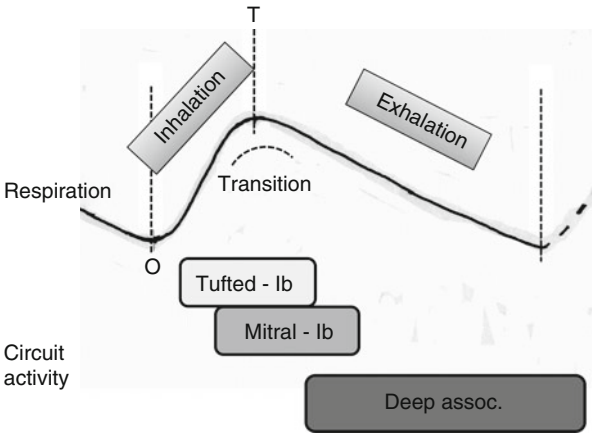

Fig. 8.4 "OB axon–Ib association circuit" activity is induced by olfactory sensory inputs during the inhalation phase (and the transition phase), whereas "deep association axon circuit" activity may occur mainly during the exhalation phase. *Upper trace* indicates the respiration cycle during awake resting state. Upward swing shows inhalation and downward swing indicates exhalation. *Abscissa* shows time (one sniff cycle is about 500 ms). *O* onset of inhalation, *T* period of transition from inhalation to exhalation. *Tufted–Ib*, activities of "tufted cell axon–IB association axon circuits" in the olfactory cortex. *Mitral–Ib*, activities of "mitral cell axon–Ib association axon circuits" in the olfactory cortex. *Deep assoc*, activities of "deep association axon circuits" in the olfactory cortex

Ib association axons, whereas those in the top-down pathway tend to be the deep association axons. For example, recurrent axons collaterals of pyramidal cells in the PPC terminate mostly on basal dendrites of other pyramidal cells in layer III of the whole piriform cortex, and only a small percentage of them terminate on apical dendrites in layer Ib (Haberly 2001).

As described in Fig. 8.2, a major direction of olfactory afferent information flow to the piriform cortex is OB → AON → APCv → APCd → PPC. The afferent stream of odor information is conveyed by axons of tufted and mitral cells in the OB (OB axons) and Ib association axons of pyramidal cells in the AON and piriform cortex. It should be underscored that both the OB axons and Ib association axons form excitatory synaptic terminals on apical dendrites (in layer I) of pyramidal cells in the piriform cortex, forming "OB axon–Ib association axon circuits" (Figs. 8.2, 8.3).

As discussed in Chap. 1, each sniff cycle consists of a sequence of the inhalation phase (or on-line phase) followed by the exhalation phase (or off-line phase). Odor-inhalation activates the OB axon–Ib association axon circuits during the inhalation phase, including the inhalation–exhalation transition phase, as shown in Chap. 7. In other words, OB axon–Ib association axon circuits are active mainly during the on-line inhalation phase of the sniff cycle (Fig. 8.4). Furthermore, the activity of OB axon–Ib association axon circuits during the inhalation phase consists of an early-onset fast gamma oscillation phase (mediated by tufted cell circuits) and a later-onset slow gamma oscillatory phase (mediated by mitral cell circuits) (Fig. 8.4).

Pyramidal cells in the piriform cortex also emit recurrent association axons that terminate in layers II and III of the piriform cortex and on neurons of the endopiriform nucleus. Because pyramidal cells in the piriform cortex extend basal dendrites in layers II and III, the deep association axons form excitatory synaptic terminals mainly on the basal dendrites of other pyramidal cells, forming the "deep association axon circuits" (Fig. 8.3). Hiroyuki Manabe and Kimiya Narikiyo in my laboratory recently found that the deep association axon circuits are active mainly during the later part of the long exhalation phase (off-line phase) of the sniff cycle in freely behaving animals. These results suggest that the OB axon–Ib association axon circuits and the deep association axon circuits in the piriform cortex are activated at different phases of the sniff cycle (Fig. 8.4).

Physiological analysis of the piriform cortex circuits during wakefulness and sleep also suggests the link between the activity of the deep association axon circuits and the off-line processing of olfactory information. During slow-wave sleep (off-line period) in which the OB axon–Ib association axon circuits are suppressed by behavioral state-dependent sensory gating (Murakami et al. 2005), numerous neurons in the APC generate synchronized spike activities that are associated with sharp waves (Manabe et al. 2011). Current source density analysis of the sharp waves indicated that the deep association axon circuits including the endopiriform nucleus are responsible for generating the synchronized spike discharges of APC neurons during slow-wave sleep. The sharp wave-associated synchronized discharges of APC neurons travel also to the deep layer (granule cell layer) of the olfactory bulb (Manabe et al. 2011) and to the deep layer of the olfactory tubercle (Narikiyo et al. 2013), sending synchronized synaptic inputs repeatedly to these regions during slow-wave sleep.

It is not well understood at present how the activity of the OB axon–Ib association axon circuits during the on-line inhalation phase is transmitted to the deep association axon circuits in the piriform cortex and generates the activity of the latter circuits that occurs mainly during the off-line exhalation phase. In addition, it is not clear what types of neurons in the piriform cortex are involved in the OB axon–Ib association axon circuits and the deep association axon circuits in the piriform cortex. For example, semilunar cells whose cell bodies are located in the superficial subdivision of layer II (layer IIa) of the piriform cortex appeas to be associated with the OB axon–Ib association axon circuits because these cells project apical dendrites widely to layer I and lack basal dendrites. Inhibitory interneurons in layer I such as large horizontal cells and layer Ia neuroglial cells (Bekkers 2013) might also be involved in the OB axon–Ib association axon circuits. Fast-spiking large multipolar cells are GABAergic inhibitory neurons whose somata are distributed in layers II and III (Suzuki and Bekkers 2012). Because they receive deep recurrent association axon inputs, they may be involved in the deep-association axon circuits in the piriform cortex. Further studies are needed to elucidate the neuronal substrates for the OB axon–Ib association axon circuits that works mainly during the inhalation phase and those for the deep association axon circuits that are activated during the later part of long exhalation phase.

8.3 Plasticity of Recurrent Association Fiber Synaptic Connections Among Pyramidal Cells in the Piriform Cortex

Piriform cortex networks have been described as containing a combinatorial, auto-associative array capable of content addressable memory (Haberly 2001; Wilson and Sullivan 2011). Both Ib and deep recurrent association axons of pyramidal cells in the piriform cortex form excitatory synaptic connections on dendritic spines of other pyramidal cells that are distributed widely in the piriform cortex (Figs. 8.3, 8.5) (Chen et al. 2003; Haberly and Presto 1986; Johnson et al. 2000; Yang et al. 2004). It has been proposed that Ib and deep association axon synaptic connections among pyramidal cells in the piriform cortex form networks with an iterative recurrent reexcitatory pattern that can store input patterns from the OB by plastically changing their synaptic connections (Barkai et al. 1994; Haberly 2001; Marr 1971; Neville and Haberly 2004; Wilson and Sullivan 2011).

Based on the idea of spike timing-dependent plasticity (Feldman 2012), it can be speculated that during the learning or storage of input patterns the association axon synaptic connections would be strengthened between pyramidal cells with different odorant-tuning specificity that are coactivated by odor inhalation, whereas the association axon synaptic connections would be weakened between activated and nonactivated pyramidal cells (Fig. 8.5). After learning the olfactory input pattern, the strengthened association axon synaptic connections could temporally synchronize the spike activity of those coactivated pyramidal cells with different odorant-tuning specificity when the same or similar input patterns arrive from the olfactory bulb (Neville and Haberly 2004). Computer modeling studies showed that the recurrent association axon networks can store and retrieve multiple input patterns that may include olfactory images of numerous different objects (Barkai et al. 1994). The recurrent association axon connections among pyramidal cells can thus provide a mechanism for feedback binding of coactivated pyramidal cells based on the memory traces of previously stored input patterns.

Based on the foregoing considerations, Mori, Manabe, Narikiyo, and Onisawa hypothesized that the late-onset synchronous gamma oscillatory inputs from mitral cells cause temporal “binding” of the spike activities of numerous pyramidal cells with different tuning specificity that are coactivated via tufted cell axon–Ib association axon pathways during odor inhalation (Mori et al. 2013) (Fig. 8.5). The mitral cell-induced spike synchronization of pyramidal cell activities would facilitate the strengthening of the association axon synaptic connections among the coactivated pyramidal cells during the storage of input patterns that are provided by tufted cell–Ib association axon pathways. In summary, Mori et al. proposed a model in which mitral cell pathways provide feed-forward binding circuits, sending the spike synchronization timing to facilitate the storage of olfactory sensory inputs patterns by causing the spike synchronization of coactivated pyramidal cells at the gamma frequency, and thus strengthening association axon synaptic connections among coactivated pyramidal cells with different tuning specificity.

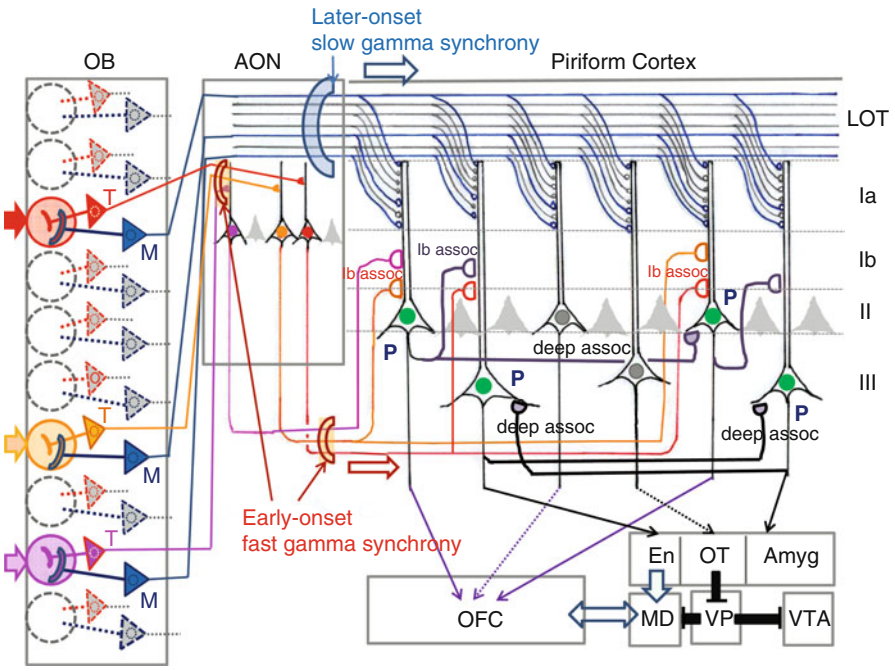

Fig. 8.5 Schematic diagram of possible functional differentiation between the tufted cell pathway and mitral cell pathway in odor information processing in the neuronal circuits of the piriform cortex. In this model, *red*, *yellow*, and *pink* glomeruli are assumed to be activated simultaneously by an odor inhalation. Activated tufted cells (*T*; shown by *red*, *orange*, or *pink*) send the odor information with early-onset fast gamma synchrony to specific target pyramidal cells in the anterior olfactory nucleus (*AON*), which in turn send the information presumably with fast gamma synchrony with specific target pyramidal cells in the piriform cortex. Activated mitral cells (*M*, shown by *blue*) provide dispersedly-projecting feed-forward binding circuits transmitting the spike synchronization timing with later-onset slow gamma synchrony to whole pyramidal cells in the piriform cortex. Pyramidal cells (*P*) in layer II of the anterior piriform cortex project axons directly to the orbitofrontal cortex (*OFC*). Pyramidal cells in the piriform cortex form recurrent association axon synaptic connections (*Ib assoc*. and *deep assoc*.) with other pyramidal cells, forming feedback binding circuits. These pyramidal cells project axons also to the endopiriform nucleus (*En*), olfactory tubercle (*OT*), and amygdaloid nuclei (*Amyg*). Neurons of the endopiriform nucleus send axons to the mediodorsal nucleus (*MD*) of thalamus. The MD provides thalamocortical projections to the OFC, and OFC sends feedback corticothalamic connections to the MD. Neurons in the OT send inhibitory output to the ventral pallidum (*VP*), which sends inhibitory output to the MD and ventral tegmental area (*VTA*). *Ia*, *Ib*, *II*, *III* are layers in the piriform cortex. Pyramidal cells with *green nucleus* in the piriform cortex indicate neurons coactivated by an odor inhalation. Recurrent collateral excitatory synaptic connections (*deep assoc*) among these neurons form feedback binding circuits. (Modified from Mori et al. 2013)

If this scenario is correct, the next question is to which neuronal circuits the coactivated pyramidal cells of the piriform cortex send the synchronized spike outputs. Because the olfactory tubercle receives association fiber inputs from virtually all parts of the piriform cortex, the olfactory tubercle is one of the candidate targets that receive the synchronized inputs from the piriform cortex.

8.4 The Olfactory Tubercle Is Part of the Ventral Striatum and Receives Axonal Projection from the Olfactory Bulb, Piriform Cortex, and Frontal Cortex

The olfactory tubercle is an area of the olfactory cortex and part of the ventral striatum that has a key role in a variety of motivational behaviors (Heimer 2003; Heimer et al. 1987; Ikemoto 2003, 2007; Switzer et al. 1982). The olfactory tubercle has a layered structure that consists of superficial layer I, dense cell layer (layer II), and deep layer (layer III), although these layers have undulations and are interrupted by CAP-like regions and islands of Calleja (Fig. 8.6) (Millhouse 1987; Millhouse and Heimer 1984). Although the olfactory tubercle has a cortex-like layered structure, it has a striatum-like organization consisting of GABAergic medium-sized spiny neurons (MSNs) as major output neurons (Millhouse and Heimer 1984).

The olfactory tubercle contains cortex-like regions and CAP regions (Fig. 8.6). In the cortex-like region, two types of MSNs (dopamine D1 receptor-expressing MSNs and D2 receptor-expressing MSNs) are intermingled. These MSNs extend apical dendrites superficially in layer I and basal dendrites in layers II and III. In the CAP region, smaller MSNs (dwarf cells) are packed in the layer II (dense cell layer). In the CAP region, layer Ib is very thin and apical dendrites of the smaller MSNs are distributed mostly in layer Ia. In both CAP and cortex-like regions of the olfactory tubercle, axons of MSNs make inhibitory synaptic connections on dendrites of neurons in the rostral part of the ventral pallidum (Fig. 8.6) (Heimer et al. 1987; Luskin and Price 1983a; Newman and Winans 1980; Tripathi et al. 2013).

Tufted and mitral cells in the olfactory bulb project axons to layer Ia of the olfactory tubercle and form excitatory synaptic connections on the spines of apical

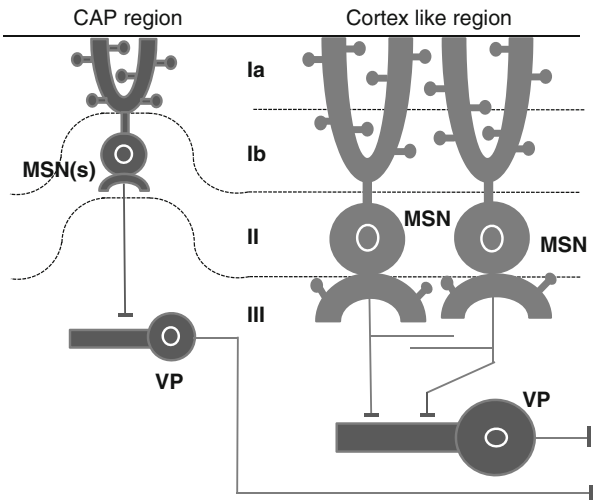

Fig. 8.6 Principal neurons and neuronal circuits in the olfactory tubercle and ventral pallidum (*VP*). Olfactory tubercle can be subdivided into CAP region (*left*) and cortex-like region (*right*). *MSN* medium-sized spiny neuron in the cortex-like region, *MSN*(*s*) smaller MSN (dwarf cells) in the CAP region. Layers in the olfactory tubercle: *Ia* layer Ia, *Ib* layer Ib, *II* layer II (dense cell layer), *III* layer III

dendrites of MSNs (Price 1973). Association axons originated from pyramidal cells in the piriform cortex terminate in layers Ib, II, and III of the olfactory tubercle (Luskin and Price 1983a; Price 1973). Based on the classification of Ib association axons and deep association axons in the piriform cortex, the association axon inputs from the piriform cortex pyramidal cells to the olfactory tubercle can be classified into two subsets: "Ib association axon inputs" and "deep association axon inputs." The Ib association axon inputs may reflect the OB axon–Ib association axon circuit activity and may terminate on apical dendrites (in layer I) of MSNs whereas the deep association axon inputs may be associated with the activity of deep association axon circuits in the piriform cortex and mainly terminate on basal dendrites (layers II and III) of MSNs.

The olfactory tubercle is thought to contain motivation behavior modules that function as gateways for odor information to induce specific motivation behaviors (Ikemoto 2007). In line with this idea, Koshi Murata in my laboratory found, in mice, that the regions or modules within the olfactory tubercle do not represent odors but rather are activated when mice show specific motivational behaviors. Activation of MSNs in a specific motivation behavior module may lead to the expression of the motivational behavioral outputs via the olfactory tubercle — ventral pallidum — thalamus/hypothalamus/ventral tegmental area pathways (Heimer et al. 1987; Zahm and Heimer 1987; Zahm et al. 1987) (Figs. 8.1, 8.6). This observation suggests that the olfactory sensory pathways to the olfactory tubercle provide an excellent model neuronal circuit for analyzing the neuronal mechanism of the odor input–behavioral output translation.

There are multiple neuronal pathways from the olfactory sensory neurons to the olfactory tubercle (Fig. 8.1). First, tufted and mitral cells in the olfactory bulb project axons directly to the olfactory tubercle, forming direct pathways from the olfactory bulb. Second, the olfactory tubercle receives association axon inputs from many areas of the olfactory cortex including the AON, tenia tecta, piriform cortex, cortical amygdaloid nuclei, and entorhinal cortex, forming the OB → olfactory cortex → olfactory tubercle pathways. In these pathways, odor signals are first processed in the neuronal circuits of the olfactory cortex, possibly in reference to olfactory memories, and then the processed results are sent to the motivation behavior modules in the olfactory tubercle.

Third, the olfactory tubercle receives inputs from the amygdaloid nuclei, thus forming the OB → olfactory cortex (including cortical amygdaloid nuclei) → amygdala → olfactory tubercle pathways. Fourth, the olfactory cortex receives inputs from the OFC and mPFC, thus forming OB → olfactory cortex → frontal cortex → olfactory tubercle pathways. Thus, odor signals are processed first in the olfactory cortex and then in the frontal cortex. After the integration of olfactory signals with other sensory and motor signals, the frontal cortex may send the signal to the olfactory tubercle. Therefore, multiplex parallel pathways rather than a single pathway convey olfactory information from the olfactory bulb to the olfactory tubercle (Fig. 8.1).

Furthermore, neurons in the ventral pallidum, which receives inputs from the olfactory tubercle, project axons to the ventral tegmental area. Dopaminergic

neurons in the ventral tegmental area are involved in the expectancy of reward and project axons densely back to the olfactory tubercle.

At present, it is unclear how these multiple olfaction-related pathways to the olfactory tubercle work during the inhalation–exhalation sniff cycle. It is a great challenge of future studies to understand the function and its neuronal mechanism of each pathway as well as those that coordinate the functions of these multiple pathways to the olfactory tubercle.

The foregoing speculations regarding the multiple parallel neuronal pathways to the olfactory tubercle can be extrapolated to many other pathways and loops in the central olfactory system. Intensive research on the piriform cortex, olfactory tubercle, and higher association areas has started only recently, and a number of important questions remain unanswered or even questions themselves remain unknown. Recent studies suggest that there will be a rapid acceleration of the understanding of the structure and function of the large-scale networks in the central olfactory system in the near future. Finally, neuronal circuits in the central olfactory system provide an excellent model system with which to study the functional organization of the cortical, thalamic, and basal ganglia networks for the translation of external sensory information to appropriate motivational and emotional behaviors.

References

Barkai E, Bergman RE, Horwitz G, Hasselmo ME (1994) Modulation of associative memory function in a biophysical simulation of rat piriform cortex. J Neurophysiol 72:659–677

Bekkers JMSN (2013) Neurons and circuits for odor processing in the piriform cortex. Trends Neurosci 36:429–438

Buzsaki G (2006) Rhythms of the brain. Oxford University Press, New York

Chen S, Murakami K, Oda S, Kishi K (2003) Quantitative analysis of axon collaterals of single cells in layer III of the piriform cortex of the guinea pig. J Comp Neurol 465:455–465

Feldman DE (2012) The spike-timing dependence of plasticity. Neuron 75:556–571

Franks KM, Russo MJ, Sosulski DL, Mulligan AA, Siegelbaum SA, Axel R (2011) Recurrent circuitry dynamically shapes the activation of piriform cortex. Neuron 72:49–56

Haberly LB (1983) Structure of the piriform cortex of the opossum. I. Description of neuron types with Golgi methods. J Comp Neurol 213:163–187

Haberly LB (2001) Parallel-distributed processing in olfactory cortex: new insights from morphological and physiological analysis of neuronal circuitry. Chem Senses 26:551–576

Haberly LB, Presto S (1986) Ultrastructural analysis of synaptic relationships of intracellularly stained pyramidal cell axons in piriform cortex. J Comp Neurol 248:464–474

Heimer L (2003) A new anatomical framework for neuropsychiatric disorders and drug abuse. Am J Psychiatry 160:1726–1739

Heimer L, Zaborszky L, Zahm DS, Alheid GF (1987) The ventral striatopallidothalamic projection: I. The striatopallidal link originating in the striatal parts of the olfactory tubercle. J Comp Neurol 255:571–591

Ikemoto S (2003) Involvement of the olfactory tubercle in cocaine reward: intracranial self-administration studies. J Neurosci 23:9305–9311

Ikemoto S (2007) Dopamine reward circuitry: two projection systems from the ventral midbrain to the nucleus accumbens-olfactory tubercle complex. Brain Res Rev 56:27–78

Illig KR, Haberly LB (2003) Odor-evoked activity is spatially distributed in piriform cortex. J Comp Neurol 457:361–373
Johnson DM, Illig KR, Behan M, Haberly LB (2000) New features of connectivity in piriform cortex visualized by intracellular injection of pyramidal cells suggest that "primary" olfactory cortex functions like "association" cortex in other sensory systems. J Neurosci 20:6974–6982
Kikuta S, Fletcher ML, Homma R, Yamasoba T, Nagayama S (2013) Odorant response properties of individual neurons in an olfactory glomerular module. Neuron 77:1122–1135
Li W, Lopez L, Osher J, Howard JD, Parrish TB, Gottfried JA (2010) Right orbitofrontal cortex mediates conscious olfactory perception. Psychol Sci 21:1454–1463
Litaudon P, Datiche F, Cattarelli M (1997) Optical recording of the rat piriform cortex activity. Prog Neurobiol 52:485–510
Litaudon P, Amat C, Bertrand B, Vigouroux M, Buonviso N (2003) Piriform cortex functional heterogeneity revealed by cellular responses to odours. Eur J Neurosci 17:2457–2461
Luskin MB, Price JL (1983a) The laminar distribution of intracortical fibers originating in the olfactory cortex of the rat. J Comp Neurol 216:292–302
Luskin MB, Price JL (1983b) The topographic organization of associational fibers of the olfactory system in the rat, including centrifugal fibers to the olfactory bulb. J Comp Neurol 216:264–291
Manabe H, Kusumoto-Yoshida I, Ota M, Mori K (2011) Olfactory cortex generates synchronized top-down inputs to the olfactory bulb during slow-wave sleep. J Neurosci 31:8123–8133
Marr D (1971) Simple memory: a theory for archicortex. Philos Trans R Soc Lond B Biol Sci 262:23–81
Millhouse OE (1987) Granule cells of the olfactory tubercle and the question of the islands of Calleja. J Comp Neurol 265:1–24
Millhouse OE, Heimer L (1984) Cell configurations in the olfactory tubercle of the rat. J Comp Neurol 228:571–597
Mitsui S, Igarashi KM, Mori K, Yoshihara Y (2011) Genetic visualization of the secondary olfactory pathway in Tbx21 transgenic mice. Neural Syst Circuits 1:5
Mori K, Nagao H, Yoshihara Y (1999) The olfactory bulb: coding and processing of odor molecule information. Science 286:711–715
Mori K, Manabe H, Narikiyo K, Onisawa N (2013) Olfactory consciousness and gamma oscillation couplings across the olfactory bulb, olfactory cortex, and orbitofrontal cortex. Front Psychol 4:743
Murakami M, Kashiwadani H, Kirino Y, Mori K (2005) State-dependent sensory gating in olfactory cortex. Neuron 46:285–296
Narikiyo K, Manabe H, Mori K (2013) Sharp wave-associated synchronized inputs from the piriform cortex activate olfactory tubercle neurons during slow-wave sleep. J Neurophysiol 111:72–81
Neville KR, Haberly LB (2004) Olfactory cortex. In: Shepherd GM (ed) The synaptic organization of the brain. Oxford University Press, New York, pp 415–454
Newman R, Winans SS (1980) An experimental study of the ventral striatum of the golden hamster. II. Neuronal connections of the olfactory tubercle. J Comp Neurol 191:193–212
Plailly J, Howard JD, Gitelman DR, Gottfried JA (2008) Attention to odor modulates thalamocortical connectivity in the human brain. J Neurosci 28:5257–5267
Poo C, Isaacson JS (2011) A major role for intracortical circuits in the strength and tuning of odor-evoked excitation in olfactory cortex. Neuron 72:41–48
Price JL (1973) An autoradiographic study of complementary laminar patterns of termination of afferent fibers to the olfactory cortex. J Comp Neurol 150:87–108
Rennaker RL, Chen CF, Ruyle AM, Sloan AM, Wilson DA (2007) Spatial and temporal distribution of odorant-evoked activity in the piriform cortex. J Neurosci 27:1534–1542
Schoenbaum G, Saddoris MP, Stalnaker TA (2007) Reconciling the roles of orbitofrontal cortex in reversal learning and the encoding of outcome expectancies. Ann N Y Acad Sci 1121:320–335
Shipley MT, Ennis M (1996) Functional organization of olfactory system. J Neurobiol 30:123–176

Stettler DD, Axel R (2009) Representations of odor in the piriform cortex. Neuron 63:854–864
Suzuki N, Bekkers JM (2012) Microcircuits mediating feedforward and feedback synaptic inhibition in the piriform cortex. J Neurosci 32:919–931
Switzer RC 3rd, Hill J, Heimer L (1982) The globus pallidus and its rostroventral extension into the olfactory tubercle of the rat: a cyto- and chemoarchitectural study. Neuroscience 7:1891–1904
Tripathi A, Prensa L, Mengual E (2013) Axonal branching patterns of ventral pallidal neurons in the rat. Brain Struct Funct 218:1133–1157
Wilson DA, Sullivan RM (2011) Cortical processing of odor objects. Neuron 72:506–519
Yang J, Ul Quraish A, Murakami K, Ishikawa Y, Takayanagi M et al (2004) Quantitative analysis of axon collaterals of single neurons in layer IIa of the piriform cortex of the guinea pig. J Comp Neurol 473:30–42
Yoshida I, Mori K (2007) Odorant category profile selectivity of olfactory cortex neurons. J Neurosci 27:9105–9114
Zahm DS, Heimer L (1987) The ventral striatopallidothalamic projection. III. Striatal cells of the olfactory tubercle establish direct synaptic contact with ventral pallidal cells projecting to mediodorsal thalamus. Brain Res 404:327–331
Zahm DS, Zaborszky L, Alheid GF, Heimer L (1987) The ventral striatopallidothalamic projection: II. The ventral pallidothalamic link. J Comp Neurol 255:592–605

Chapter 9
Human Olfaction: A Typical Yet Special Mammalian Olfactory System

Tali Weiss, Lavi Secundo, and Noam Sobel

Abstract In this chapter we concentrate on human olfaction, asking what the study of human olfaction has taught us about mammalian olfaction in general, and what it has shown as uniquely human olfactory structure and function. We first briefly highlight the superb olfactory capabilities of humans, starting with keen detection and discrimination, through unlikely tasks such as scent tracking, and culminating in complex social chemosignaling. We then describe the neural organization of human olfaction subserving these tasks, noting unique human olfactory sampling strategies, apparently unique organizational features of the human olfactory epithelium and bulb, and functional specializations in olfactory cortex. Although these attributes may constitute nuances of sensory system organization, the most unique aspect of human olfaction, and indeed of humans in general, remains coding into language. It is this language-based key that has allowed uncovering a small but significant portion of the rules by which molecular structures transform into olfactory percepts.

Keywords Functional imaging • Human chemosignaling • Human olfaction • Odor space • Olfactory coding • Olfactory space • Sniffing

9.1 Introduction

9.1.1 Humans Have Keen Olfactory Abilities Used for Social Chemosignaling

In contrast to popular notions, behavioral studies have repeatedly found that humans have a superbly keen sense of smell (Shepherd 2004; Zelano and Sobel 2005). Human olfactory performance in terms of *detection thresholds* and

T. Weiss • L. Secundo • N. Sobel (✉)
Department of Neurobiology, Weizmann Institute of Science, Rehovot 76100, Israel
e-mail: noam.sobel@weizmann.ac.il

K. Mori (ed.), *The Olfactory System: From Odor Molecules to Motivational Behaviors*, DOI 10.1007/978-4-431-54376-3_9, © Springer Japan 2014

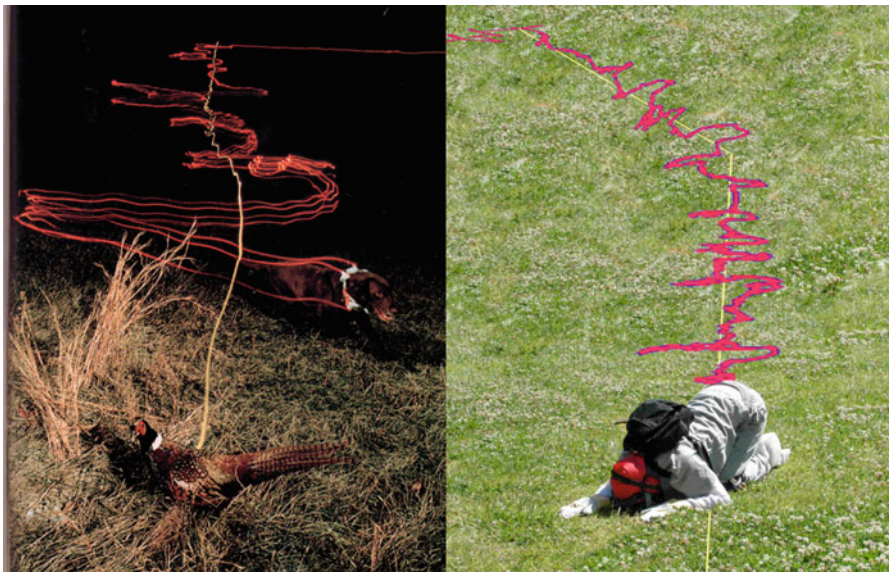

Fig. 9.1 Humans can scent-track. On the *left* is a figure from *National Geographic* depicting scent-tracking strategies in the dog (Gibbons 1986). On the *right* is a depiction of a human subject conducting a similar task (Porter et al. 2007). The *yellow line* denotes the scent track, and the *red line* denotes tracking pattern

discrimination is often close to, or on par with, that of other mammals (Laska and Freyer 1997; Laska et al. 1999a, b). For example, the odorant ethyl mercaptan, which is often added to propane as a warning agent, can be detected at concentrations less than 1 part per billion (ppb) and perhaps as low as 0.2 ppb (Whisman et al. 1978). This concentration is equivalent to approximately three drops of odorant within an Olympic-size swimming pool; given two pools, a human could detect by smell which pool contained the three drops of odorant. Moreover, this performance can improve with practice. For example, men and women who were completely unable to detect the odor of androstenone developed the ability to detect it after repeated exposure (Wysocki et al. 1989; Mainland et al. 2002), and *detection thresholds* for everyday odors improved with repeated exposure, but only in women and not in men (Dalton et al. 2002). Humans not only detect and discriminate odors; they can also act on them in complex ways. For example, as can many microsmatic animals, humans can track a scent trail in a field, and again further improve their performance with practice (Porter et al. 2007) (Fig. 9.1). In fact, after only 4 days of scent-tracking practice, the rate-limiting factor on human performance was their rate of crawling; humans could scent-track as fast as they could crawl.

Finally, similar to all mammals, humans make extensive use of *social chemosignaling* (Wysocki and Preti 2004). Perhaps the best known example of human chemosignaling is the phenomenon of menstrual synchrony, whereby women who live in close proximity, such as roommates in dormitories, synchronize their menstrual cycle over time (McClintock 1971). This effect is mediated by an

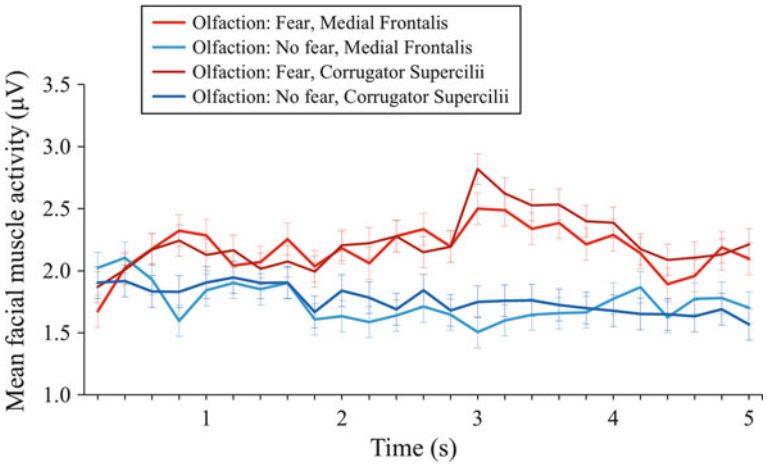

Fig. 9.2 The smell of fear drives fearful facial expressions. Mean impact of the olfactory (fear, no fear) message on EMG from the medial frontalis and corrugator supercilii activity over time. *Error bars* indicate 68 % confidence intervals (de Groot et al. 2013)

odor in sweat. This concept was verified in a series of studies where experimenters obtained underarm sweat extracts from donor women during either the ovulatory or follicular menstrual phase. These extracts were then deposited on the upper lips of recipient women, where follicular sweat accelerated ovulation, and ovulatory sweat delayed it (Russell et al. 1980; Stern and McClintock 1998). Moreover, variation in menstrual timing can be increased by the odor of other lactating women (Jacob et al. 2004), or regulated by the odor of male hormones (Cutler et al. 1986; Wysocki and Preti 2004).

Menstrual synchrony is not the only human behavior regulated or impacted by chemosignals. A second case that has recently been studied extensively is that of the smell of fear. Fear or distress chemosignals are prevalent throughout animal species (Pageat and Gaultier 2003; Hauser et al. 2008). In an initial study in humans, Chen and Haviland-Jones (Chen and Haviland-Jones 2000) collected underarm odors on gauze pads from young women and men after they watched funny or frightening movies. They later asked other women and men to determine, by smell, which was the odor of people when they were "happy" or "afraid." Women correctly identified happiness in men and women and fear in men. Men correctly identified happiness in women and fear in men. A similar result was later obtained in a study that examined women only (Ackerl et al. 2002). Moreover, women had improved performance in a cognitive verbal task after smelling fear sweat versus neutral sweat (Chen et al. 2006), and the smell of fearful sweat biased women toward interpreting ambiguous expressions as more fearful, but had no effect when the facial emotion was more discernible (Zhou and Chen 2009). Moreover, subjects had an increased startle reflex when exposed to anxiety-related sweat versus sports-related sweat (Prehn et al. 2006), and fear-related sweat induced fearful facial expressions as estimated by facial EMG (Groot et al. 2013) (Fig. 9.2). Finally, imaging studies

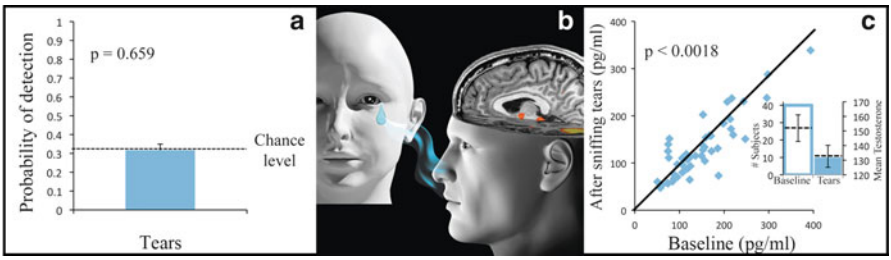

Fig. 9.3 Human emotional tears contain a chemosignal. (**a**) In a three-alternative forced-choice task, 30 subjects could not discriminate tears from saline. (**b**) The odorless tears induced brain activation in the limbic system. (**c**) The odorless tears drove a reduction in salivary testosterone. The *insert* reflects the number of subjects who expressed the effect (*bars*) and the mean values (*dotted line*)

have revealed dissociable brain representations after smelling anxiety sweat versus sports-related sweat (Prehn-Kristensen et al. 2009). These differences are evident in the amygdala, a brain substrate common to olfaction, fear responses, and emotional regulation of behavior (Mujica-Parodi et al. 2009). Taken together, this body of research strongly suggests that humans can discriminate the scent of fear from other body odors and that this chemosignal influences behavior.

Human chemosignals are not limited to sweat alone. Two additional sources that have been examined are vaginal secretions (Doty et al. 1975; Cerda-Molina et al. 2013) and emotional tears (Gelstein et al. 2011; Oh et al. 2012). Sniffing of apparently odorless (Fig. 9.3a) emotional tears drives a host of psychological, physiological, and hormonal responses; these include reductions in autonomic arousal as measured with skin conductance, reductions in neural activity measured with functional magnetic resonance imaging (fMRI) throughout the limbic system including the hypothalamus (Gelstein et al. 2011) (Fig. 9.3b), and reductions in salivary testosterone (Gelstein et al. 2011; Oh et al. 2012) (Fig. 9.3c). These results imply a chemosignaling function for emotional tears similar to that observed in rodents, where lachrymal secretions alter both aggressive (Shanas and Terkel 1997) and sociosexual behavior (Kimoto et al. 2005, 2007). Finally, rather than using the potential signal carriers such as sweat and tears, several candidate signaling molecules have been identified in the signaling media, synthesized, and tested independently. Most of these are androgen-related steroids, the one called androstadienone (4,16-androstadien-3-one, AND) receiving the most attention. AND is found in axillary secretions at levels up to 20 times higher in men than in women, and when smelled, it induces a host of behavioral (Grosser et al. 2000; Jacob et al. 2001a; Bensafi et al. 2003b, 2004; Bensafi 2004; Lundstrom and Olsson 2005; Hummer and McClintock 2009), hormonal (Wyart et al. 2007), and brain (Jacob et al. 2001b) responses that are sex specific (Savic et al. 2001) and sexual orientation specific (Savic et al. 2005).

The foregoing examples highlight how human olfaction is in many ways a typical example of mammalian olfaction. Human olfaction, however, is also unique

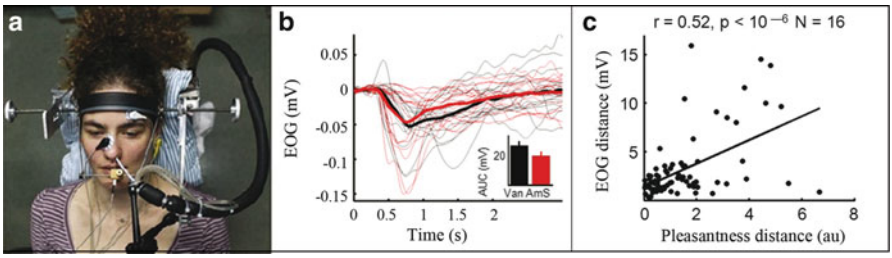

Fig. 9.4 Recording a local field potential (LFP) from the human olfactory epithelium (OE). (**a**) Experimental apparatus. (**b**) Average electro-olfactograms (EOGs) from 16 subjects (*thin lines*), as well as grand average (*thick lines*) for the odorants vanillin (Van, *black*) and ammonium sulfide (AmS, *red*), showing clear separation. (**c**) The difference in EOG response between any two odors was related to the difference in pleasantness between those two odors

and special in several ways, and most critically in its translation into language. Later we detail how this uniqueness has recently advanced our understanding of what is arguably the central question in olfaction research, namely, the triangular relationship between odor structure, neuronal coding, and perception.

9.1.2 We Can Measure Neural Activity in the Human Olfactory System

The study of human olfaction is not limited to behavior and perception alone. Although most studies on the anatomy and physiology of olfaction are conducted in animals, new techniques allow researchers to measure neural responses in human subjects in vivo. At the peripheral level, the accessibility of the olfactory sensory neurons (OSNs) allows researchers to place an electrode on the olfactory epithelium (OE) and measure the combined electrical activity of thousands of OSNs in response to odor stimulation. This response is referred to as an electro-olfactogram (EOG) (Fig. 9.4) (Kobal and Hummel 1991; Knecht and Hummel 2004; Hummel et al. 2006; Lapid et al. 2009, 2011; Lapid and Hummel 2013). An additional promising method for measuring odor-driven activity of human OSNs is by intrinsic optical signal (IOS) imaging. Changes in blood oxygenation, blood flow, and light scattering related to vascular and metabolic activities caused by neuronal activation can be measured using a light source and CCD camera mounted on a nasal endoscope (Ishimaru et al. 2007, 2011). At the cortical level, methodological advances in techniques for functional neuroimaging such as positron emission tomography (PET) and fMRI allow visualizing human brain activity in response to odorant stimulation and olfactory tasks (Gottfried 2010). A critical advantage to making all these measurements in humans rather than in other animals is that they can coincide with simultaneous perceptual estimates provided by the subjects: this may allow formulation of rules linking neural responses and olfactory perception.

9.2 The Study of Humans Uncovers Novel Aspects in Brain Organization of Olfaction

As in other mammals, human olfaction starts with stimulus acquisition or sniffing, which is followed by transduction at OSNs that line the OE in the nose. Information is then transmitted via the olfactory nerve, through the cribriform plate, and to the olfactory bulb (OB) in the brain. OB output is transmitted via the lateral olfactory tract to the primary and secondary olfactory cortices, mainly the piriform and the orbitofrontal cortex (OFC), respectively (Price 1990) (Fig. 9.5). This organization is bilateral and symmetrical, and although structural connectivity appears largely ipsilateral (i.e., from the left epithelium to the left bulb to the left cortex), functional studies in humans have implied that connectivity to the cortex may follow contralateral pathways as well (Savic and Gulyas 2000; Porter et al. 2005).

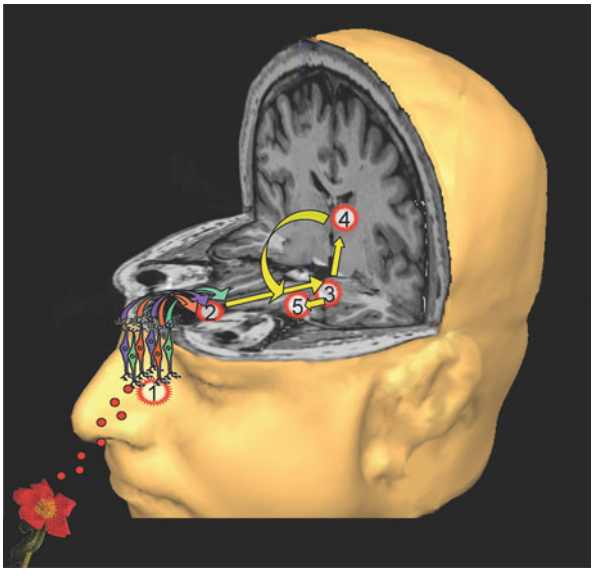

Fig. 9.5 Schematic of the human olfactory system. Odorants are transduced at the olfactory epithelium (OE) (*1*). Different receptor types (three illustrated, ~400 in humans) converge via the olfactory nerve onto common glomeruli at the olfactory bulb (OB) (*2*). From here, information is conveyed via the lateral olfactory tract to the primary olfactory cortex (*3*). From here, information is further relayed throughout the brain, most notably to the orbitofrontal cortex (OFC) (*5*), via a direct and indirect route through the thalamus (*4*)

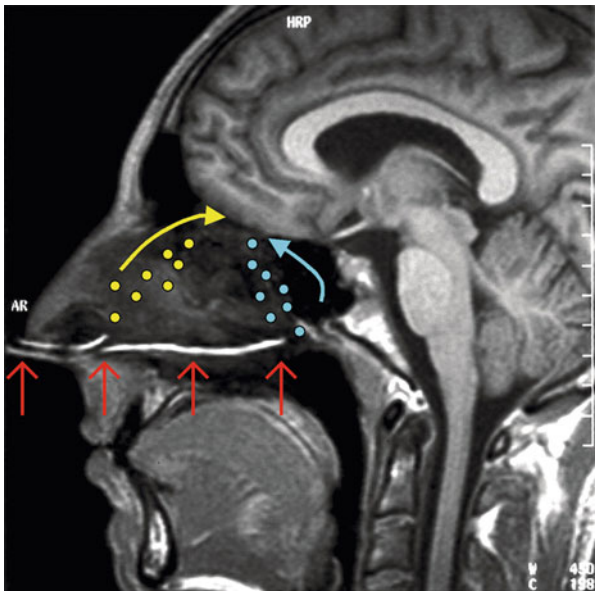

Fig. 9.6 Simultaneous orthonasal and retronasal stimulation. A magnetic resonance image (MRI) from Small et al. (2005) shows placement of the nasal cannulae at the external nares, to achieve orthonasal delivery, and at the retropharynx, to achieve retronasal delivery

9.2.1 Nostril-Specific Sniffs Drive Nostril-Specific Odor Perception

Before air-borne stimuli are processed, they first must be acquired. An odorant molecule may reach the OE primarily through two routes; sniffed through the nose (orthonasal), or whereby an odorant enters the mouth and then propagates back up the throat into the nose (retronasal). Retronasal olfaction may be particularly important for processing the odors of foods. In what was perhaps the most technically challenging human olfaction study published to date, Small and colleagues alternately delivered odorants either orthonasaly or retronasaly through an inserted catheter (Fig. 9.6), and simultaneously measured the brain response with fMRI (Small et al. 2005). They found that a given odor will induce a different pattern of brain activation as a function of method of acquisition (i.e., orthonasal or retronasal). Most strikingly, retronasal delivery induced greater activity than orthonasal delivery in the perigenual cingulate and medial OFC only for the food-related odor of chocolate, but not for the non-food-related odorants of lavender, butanol, or farnesol. This study implies unique brain representation of odors that reflect a food and are perceived retronasaly.

Mechanisms of retronasal acquisition may be common across human and nonhuman mammals, but human orthonasal acquisition is unique. Specifically, although most mammals engage in highly stereotypical olfactory sniffing bouts at 4–12 Hz (Deschenes et al. 2012), humans use much slower and more variable sniffing.

This behavior was extensively characterized by Laing and colleagues, who found that human sniffs are typically ~1.6 s in duration, that they occur either as single sniffs or short bouts of ~0.5 s sniffs, and that an individual's sniffing pattern remains optimal for that individual (Laing 1983). Moreover, although in rodents the relationship between sniffing patterns and perception remains controversial (Rojas-Libano and Kay 2012; Cenier et al. 2013), humans predictably modify their sniff in accordance with odorant properties in what has been termed the sniff response. In the sniff response, humans reduce sniff magnitude for both intense (Laing 1982, 1983; Frank et al. 2003; Mainland et al. 2005) and unpleasant odorants (Bensafi et al. 2003a; Arzi et al. 2012), and they start doing this within ~160 ms of sniff onset (Johnson et al. 2003). This robust phenomenon provides a nonverbal measure of olfactory perception that can serve in a host of investigations on olfactory function in health and disease.

The study of human sniffing behavior also uncovered what may be a central organizational feature of mammalian olfaction. Specifically, as in other mammals, airflow through the human nasal passages is asymmetrical, that is, resistance to airflow is usually greater in one nostril than in the other, resulting in higher airflow in one nostril over the other (the reader can easily sense this difference in nasal airflow by blocking one nostril at a time and inhaling). This difference is a reflection of increased blood flow to one nostril over the other, resulting in increased volume of the nasal turbinates on one side, which then physically block airflow. This asymmetry alternates across left and right nostrils over time in what is referred to as the nasal cycle (Stoksted 1953; Shannahoff-Khalsa 1991). The nasal cycle is regulated by the autonomic nervous system, and its implications for general health and performance remain unclear. For olfaction, however, given the influence of nasal airflow on odorant sorption (Mozell and Jagodowicz 1973; Scott et al. 2014), the implication of this cycle is that each nostril is better tuned to specific odorants as a function of airflow in that nostril. In other words, with each sniff the nose sends the brain two offset images of olfactory content (Sobel et al. 1999). How the brain utilizes this offset in perception remains unclear, although it likely serves a critical function in spatial localization of odors (Porter et al. 2005, 2007; Rajan et al. 2006; Parthasarathy and Bhalla 2013).

9.2.2 The Olfactory Epithelium Is Organized Along Perceptual Axes

Once sniffed, an odorant makes its way up the nasal cavity toward the OE located mainly on the cribriform plate (known as the olfactory cleft). Recent studies suggest that human OE can also be found on the surface of the superior turbinate, middle turbinate, and the upper portion of the nasal septum (Feron et al. 1998; Leopold et al. 2000; Escada et al. 2009). The OE contains four major cell types: bipolar OSNs, supporting cells, basal cells, and duct cells of Bowman's glands.

As in other mammals, olfactory receptors (ORs) expressed by OSNs are mostly seven-transmembrane domain proteins that activate G protein-based signaling cascades when activated by odorants. Although the mammalian genome contains approximately 1,300 OR gene subtypes, with ~1,100 of them functional (Young 2002; Zhang and Firestein 2002), humans have ~400 functional OR genes subtypes and ~600 putative OR pseudogenes (Gilad and Lancet 2003; Mainland et al. 2014). Additionally, the rodent main OE contains a smaller family of trace amine-associated receptors (TAARs), which may be involved in detecting social chemosignals (Liberles and Buck 2006; Zhang et al. 2013). In humans, OMP-positive nasal biopsies scanned for TAAR cDNAs revealed five intact human TAAR genes, although it is still unknown whether they are expressed in OSNs (Carnicelli et al. 2010).

Linking genetic variation in olfactory receptors to olfactory perception has been challenging (Frumin et al. 2013). One of the best characterized cases is that of a receptor named OR7D4, which responds to the previously noted odorant androstenone. Androstenone psychophysics are rather unusual. Most of the population perceives it as a sweaty and rather unpleasant smell, but a proportion of the population perceives it as very mild and pleasant, and an additional proportion cannot smell it at all and are referred to as androstenone anosmic. Such specifically anosmic individuals indeed had particular variants of OR7D4 (Keller et al. 2007). Similarly, the receptors OR11H7P and OR10G4 respond to isovaleric acid and guaiacol respectively, and indeed, polymorphisms in each alter human perception of their respective ligands (Menashe et al. 2007; Mainland et al. 2014). Together, these studies confirm that an individual's OR gene repertoire influences their olfactory perception.

The spatial organization of OSNs expressing different OR subtypes at the OE is unclear. Several expression studies in rodents have suggested that OR subtypes are randomly distributed in each of four topographically distinct zones (Ressler et al. 1993). In contrast, directly measuring epithelial response, both electrically and optically, revealed potential order in the organization of the olfactory receptive surface. As mentioned in the Introduction, OSNs are in direct contact with the environment; therefore, it is possible to record a local field potential (LFP), termed an EOG in vivo in humans. A recent study from our laboratory found that different recording sites along the OE were differently tuned, implying that dispersion of OR subtypes is neither uniform nor random. Furthermore, the same study found that pairwise differences in odorant pleasantness predicted pairwise differences in neuronal response; that is, a location that responded maximally to a pleasant odorant was likely to respond strongly to other pleasant odorants, and a location that responded maximally to an unpleasant odorant was likely to respond strongly to other unpleasant odorants (Lapid et al. 2011) (Fig. 9.4c). These results imply a clear link between OE topography and olfactory perception.

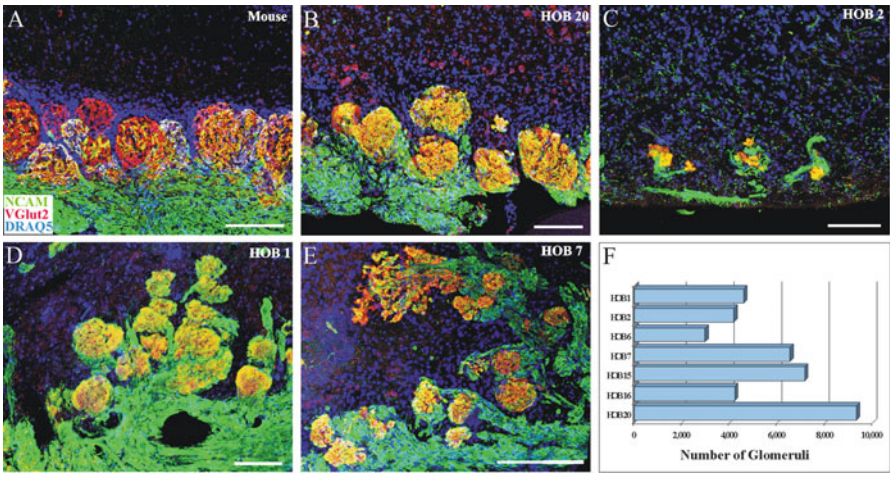

Fig. 9.7 Morphology and variability among human OB glomeruli shown with NCAM (*green*), VGlut2 (*red*), and DRAQ5 (*blue*). (**a**) Mouse glomeruli are spherical and evenly spaced. (**b–e**) Human OB glomeruli show a broader range of morphology and variability. (**f**) The number of human OB glomeruli in seven individuals. *Bars* 100 μm. (From Maresh et al. 2008)

9.2.3 The Human Olfactory Bulb Contains ~5,500 Glomeruli

From the OE signals are transmitted to the OB. The OB is an ovoid shape structure located in the anterior cranial fossa, above the cribriform plate of the ethmoid bone, under the frontal lobe. In healthy subjects, the average OB volume is ~70 mm^3 for men and ~65 mm^3 for women. Although there is large variation between individuals, within-individual variation (i.e., right vs. left) is relatively small. OB volume varies as a function of olfactory sensitivity in healthy subjects and is decreased in patients with olfactory disorders (i.e., post-infectious, post-traumatic, or sinunasal olfactory loss) (Buschhuter et al. 2008).

The OB is perhaps the least accessible component of the human olfactory system. On one hand, its location renders it inaccessible to intranasal recording electrodes. In turn, its proximity to the sinuses renders it a poor source of fMRI signal. It is assumed that the human OB has the same basic laminar organization arranged in six circular layers as in other mammals, yet recent studies questioned the similarity between human and rodent OB regarding both anatomy and physiology. One difference is in the OR subtypes to glomeruli convergence ratio. In rodents, axons of OSNs expressing the same subtype of OR converge on one, or at most, a few glomeruli within the OB, with an average convergence ratio of ~2:1. Recent human postmortem studies revealed an average of ~5,500 glomeruli per bulb (Maresh et al. 2008) (Fig. 9.7f). Given the ~400 human OR subtypes, this implies a convergence ratio of more than ~10:1. The functional significance of this difference between rodents and humans remains unclear, and whether human glomeruli are OR subtype specific as they are in rodents remains unknown.

Another possible difference between human and rodent OB coding follows OB neurogenesis. It has been suggested that adult neurogenesis constitutes an adaptive mechanism to optimally encode olfactory information (Sahay et al. 2011). In rodents, the subventricular zone (SZ) of the lateral ventricles produces neuroblasts that migrate along the rostral migratory stream (RMS) toward the OB where they differentiate into granular and periglomerular interneurons. The existence of human OB neurogenesis is debated; although the SZ maintains the ability to produce neuroblasts (Johansson et al. 1999), there is no clear evidence of migration of neuroblasts from the SZ to the OB (Sanai et al. 2004; Curtis et al. 2007; Wang et al. 2011) (for review, see Huart et al. (2013)). Limited neurogenesis in adult human OB was also implied by a recent study that measured nuclear bomb test-derived ^{14}C concentrations in postmortem OB genomic DNA. In this study, ^{14}C concentration in neuronal cells was very close to that present in the atmosphere at the time of birth of the individuals; thus, the annual turnover was estimated to be negligible, corresponding to <1 % of neurons exchanged after 100 years, whereas in rodents approximately 50 % of the OB neurons are exchanged annually. Together, these studies imply meaningful potential differences between rodent and human OB coding.

9.2.4 Right Orbitofrontal Cortex May Be Responsible for Olfactory Awareness

From the OB, olfactory information is projected via the olfactory tract to primary olfactory cortex (POC). By current definition, POC consists of all brain regions that receive direct input from the mitral and tufted cell axons, including (by order along the olfactory tract) the anterior olfactory nucleus, the ventral tenia tecta, anterior hippocampal continuation and indiusium griseum, the olfactory tubercle, piriform cortex, the anterior cortical nucleus of the amygdala, the periamygdaloid cortex, and the rostral entorhinal cortex (Carmichael et al. 1994). Given that this vast neural architecture is likely responsible for assorted neuronal computations, a stricter application of the term POC is for piriform cortex alone. The piriform cortex is a three-layered allocortex (paleocortex), which lies along the olfactory tract at the junction of the frontal and temporal lobes and continues on to the dorsomedial aspect of the temporal lobe. It may be divided into two different sections: an anterior (frontal) part (APC), and a posterior (temporal) part (PPC). A recent fMRI study found that the two parts are functionally distinct: representations of odorant structure were encoded in the anterior part and representations of odor perceptual quality were encoded in the posterior part (Gottfried et al. 2006). A finer-grained examination of odor quality encoding using multivariate analysis techniques revealed that odor categorical perception was reflected in distributed spatial ensembles in the posterior part (Howard et al. 2009) (Fig. 9.8).

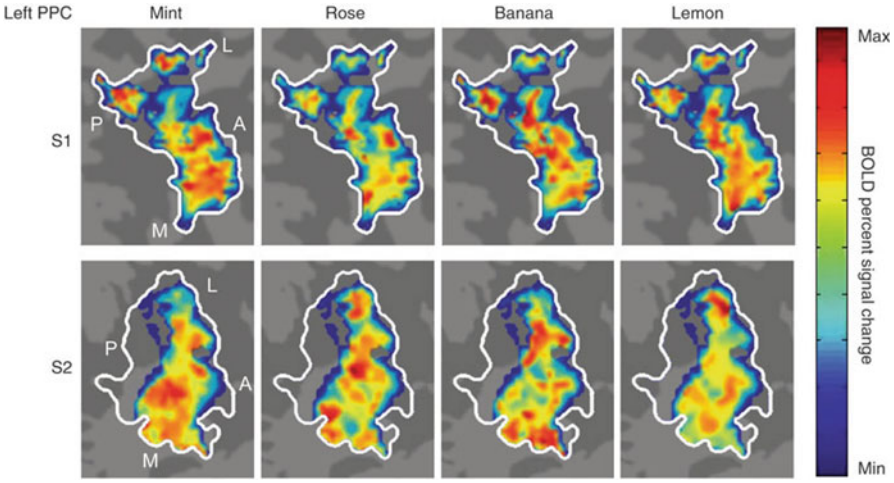

Fig. 9.8 Odorant-specific spatial maps in the posterior piriform cortex (*PPC*). Three-dimensional representations of odorant-evoked activity in the PPC from two subjects were projected onto two-dimensional (flat) maps, allowing visualization of voxel-wise odor patterns within a single plane. Maps depict the odorant-evoked BOLD percent signal change in all odor-active voxels (liberally thresholded at $P < 0.5$), averaged across trials for each of the four odorants. The pseudocolor scale spans the full range of BOLD percent signal change within each map, from minimum (*deep blue*) to maximum (*bright red*). Each odorant elicited a distributed pattern of fMRI activity within the left PPC (*white outline*) that overlapped with, but was distinct from, the other odorants. Unique distributed, overlapping profiles were also observed in the right PPC (not shown). *A* anterior, *L* lateral, *M* medial, *P* posterior. (From Howard et al. 2009)

From the POC, olfactory information is distributed widely throughout the brain, most prominently to the OFC and agranular insula. Projection from the piriform cortex may reach the OFC either directly or indirectly through the mediodorsal nucleus of the thalamus. The functional significance of this thalamic path remains unclear, yet one hypothesis is that it may mediate attention to odors (Plailly et al. 2008; Tham et al. 2009). The OFC participates in a wide variety of higher-level operations related to multisensory integration, reward processing, and associative learning (Gottfried et al. 2006). A notable recent suggestion is that the right OFC plays a major role in conscious olfactory perception: this followed the study of a patient who became completely anosmic after traumatic damage to the right OFC. Despite this anosmia, the patient maintained left OFC odorant-induced activation but not right OFC activation (Fig. 9.9). This observation implied a special role for right OFC in odor awareness (Li et al. 2010).

One should keep in mind that odor representation in the brain is highly plastic, consistent with observed changes in odor perception following experience and learning. Different paradigms have been used to test the behavioral or neural plasticity in odor representation: among these are repeated exposure (Mainland et al. 2002; Wang et al. 2004), aversive conditioning (Li et al. 2008), odor habituation (Li et al. 2006), and, most recently, prolonged odor deprivation

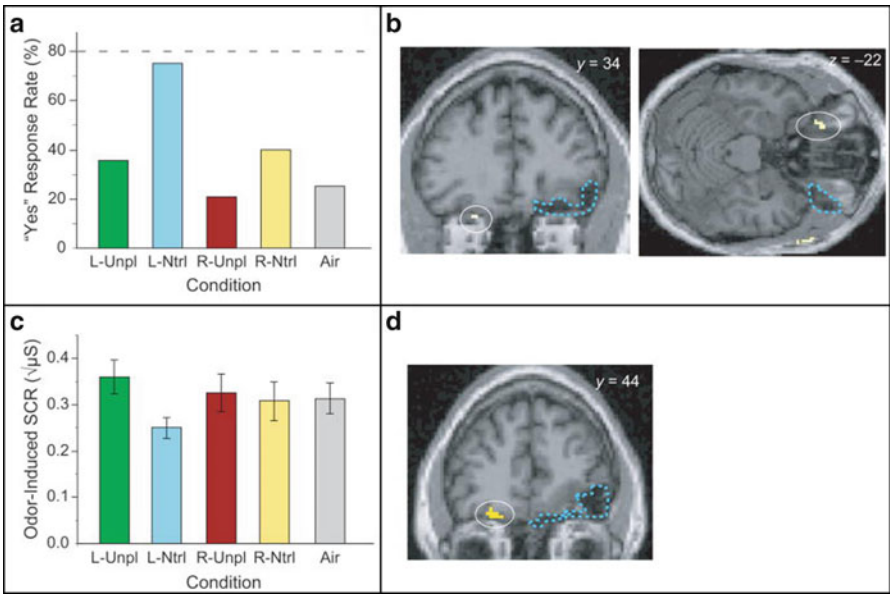

Fig. 9.9 Role of the right OFC in conscious perception of smell.Behavioral, physiological, and imaging evidence of unconscious olfactory processing in patient S. Graph in (**a**) shows the percentage of "yes" responses (indicating that S. detected an odor) in each condition of the odor detection task. Unpleasant odors ("*Unpl*"), neutral odors ("*Ntrl*"), and *air* only were delivered in separate trials to the left nostril (*L*) and the right nostril (*R*). The *dashed line* indicates the chance percentage of "yes" responses (80 %), reflecting the fact that 80 % of trials contained odors. (**b**) Areas in the left OFC showing greater activation in response to odors delivered to the left nostril, in comparison with air only. Cyan curves demarcate the right OFC lesion. Amplitudes of the skin conductance response (*SCR*) to odor presentation are shown in (**c**), and areas showing greater left anterior OFC activity following unpleasant odors, compared with neutral odors, delivered to the left nostril are shown in (**d**). Display threshold for images in (**b**) and (**d**) is $p < 0.005$, uncorrected. *Error bars* in **c** represent standard deviations. (From Li et al. 2010)

(Wu et al. 2012). In this study, occlusion of both nostrils for 7 days induced reversible changes in odor-evoked fMRI activity in piriform cortex and OFC. Moreover, multivariate analysis suggested that deprivation influenced odor quality coding in the OFC, that is, categorical specificity in the OFC was disrupted, and this change in brain activity pattern was correlated with ratings of perceived similarity between odorants.

9.2.5 The Brain Response to Odors Is Extensive

In addition to probing the function of previously recognized olfactory brain structures, functional imaging in humans has identified brain components not previously associated with the olfactory system. Notably, the cerebellum is consistently

activated by odors across imaging studies (Sobel et al. 1998; Ferdon and Murphy 2003; Cerf-Ducastel and Murphy 2006). We had initially hypothesized that the cerebellar role in olfaction was related to sniffing, and this was largely verified in a study of patients with focal cerebellar lesions who failed to modulate their sniffing in accordance with odorant content (Mainland et al. 2005). Moreover, the cerebellum is also involved in cognitive appraisal of odors regardless of sniffing (Qureshy et al. 2000). Although the cerebellar olfactory role has been further investigated, there remain a host of brain structures not previously implicated in olfaction yet routinely activated in imaging studies of olfaction. These structures go well beyond the limbic system and include components of classic higher-order visual and auditory cortices (Royet et al. 2000, 2001; Kjelvik et al. 2012). Whether these structures were activated because of nonolfactory task components, or whether these are odorant-induced activations per se, remains to be investigated. What is clear, however, is that tasks involving odor drive extensive activity well beyond the classic neuroanatomy of olfaction.

9.2.6 Human Have a Vomeronasal Duct That Is Considered Vestigial

All mammals perceive airborne signals in more than the main olfactory system alone. In humans, most odorants activate not only OSNs but also trigeminal nerve endings in the nose. This trigeminal activation provides the cooling sensation associated with odorants such as menthol, or the stinging sensation associated with odorants such as ammonia or onion. Only a few odors may be considered as "pure olfactants," as they activate the olfactory nerve alone (Doty et al. 1978). Trigeminal activation may then interact with pure olfactory activation in complex ways (Hummel and Livermore 2002; Albrecht et al. 2010).

Rodent social chemosignaling is largely, although not exclusively, dependent on an accessory olfactory system, complete with its independent sensory epithelia: the vomeronasal organ (VNO) within a vomeronasal duct (VND) (Keverne 1999). The VNO is lined with dedicated receptors belonging to at least two multigene families, V1R and V2R, which encode seven-transmembrane proteins (Ihara et al. 2013). From the VNO, information is transmitted via the vomeronasal nerve to the accessory olfactory bulb, and from there toward the amygdala and the anterior hypothalamus (Brennan 2001). Given the previously detailed extensive evidence for social chemosignaling in humans, one may ask whether they have an accessory olfactory system? In the human embryo, the VNO is detectable and contains bipolar cells similar to other species; however, no structures other than the VND are detectable at birth (Meredith 2001). In adults, the opening of the VND can be detected in the anterior nasal septum, unilaterally or bilaterally (Trotier et al. 2000; Abolmaali et al. 2001). However, most findings indicate that the human VND is vestigial, especially because there are no nerves connecting to or from the VND

(Witt and Hummel 2006; Trotier 2011). Lack of human VNO functionality is further indicated by several studies: First, there is no apparent difference in response to social chemosignals between adults with and without a visible VND (Knecht et al. 2003; Frasnelli et al. 2011); second, occlusion of the VND did not alter perception or brain activity (Knecht et al. 2003; Frasnelli et al. 2011); and finally, although initial studies reported a chemosignal-induced LFP recorded directly from the VND (Grosser et al. 2000), later studies implied that this may have been a trigeminal artifact (Witt and Hummel 2006). Taken together, the human VNO may be functional in some way in the human fetus, but there is currently little if any evidence for its functionality in the adult.

9.3 Human Language Uncovers Links Between Odorant Structure and Odorant Perception

Olfaction remains an "unsolved" sensory system. The sense in which it is unsolved was elegantly stated 100 years ago by no other than Alexander Graham Bell:

> Can you measure the difference between one kind of smell and another? It is very obvious that we have very many different kinds of smells, all the way from the odor of violets and roses up to asafetida. But until you can measure their likenesses and differences you can have no science of odor (Bell 1914) (Fig. 9.10a).

As noted in the Introduction, the most exceptional aspect of human olfaction is its coding into language: this allows us to collect language descriptors for odors and

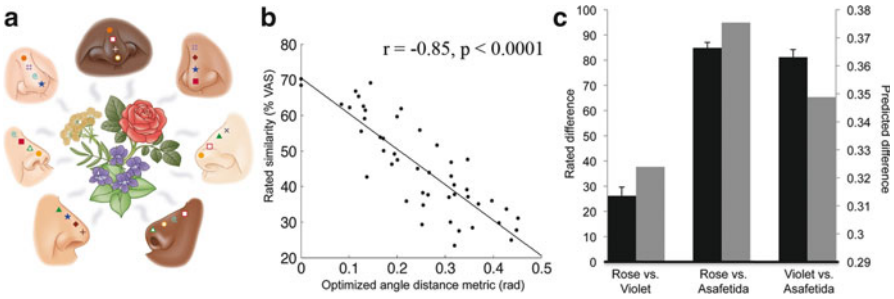

Fig. 9.10 Predicting odorant similarity from odorant structure. (**a**) A schematic depicting Bell's question. (**b**) Performance of the optimized angle distance model. Each *dot* represents a comparison between two mixtures (ranging in size from 4 to 40 components) tested in 24 subjects. The model provided a strong prediction of mixture perceptual similarity from mixture structure alone (Snitz et al. 2013). (**c**) Bell's question answered: Predicting the perceptual difference between rose, violets, and asafetida. We bought rose and violet perfumes from a local perfumer and asafetida at a local spice market. We modeled the odorants based on their primary constituents in the published record (*gray bars*). Ten subjects then rated pairwise similarity (*black bars*). The angle distances between the three odorants were in strong agreement with perception: *rose* and *violet* are similar to each other, and both are dissimilar from asafetida, yet *violet* is closer to asafetida than *rose*

use these in an effort to generate a "measure" or "metric" of the type Bell implied. Several groups have recently set out on this path (Madany Mamlouk et al. 2003; Khan et al. 2007; Haddad et al. 2008a, b; Zarzo 2008, 2011; Koulakov et al. 2009; Kermen et al. 2011; Castro et al. 2013; Gabler et al. 2013; Snitz et al. 2013), and here we describe our own efforts in this direction. This work started with reanalysis of a previously collected dataset, namely the "Atlas of Odor Character Profiles" amassed by Andrew Dravnieks and colleagues in the 1980s (Dravnieks 1985). This text contains numerical ratings provided by about 150 experts who rated 138 monomolecular odorants along 146 verbal descriptors (e.g., "flowery," "tar like," "almond like," "sickening"). We hypothesized that the functional dimensionality of this data is lower than its apparent dimensionality of 146, and therefore applied principal components analysis (PCA). PCA takes data consisting of *N* points in an M-dimensional space (e.g., 138 odorants in the 146-dimensional odor descriptor space) and finds a rotation matrix that rotates the *N* points onto a new M-dimensional space such that the new dimensions, called principal components (PCs), successively explain a maximal portion of the variance. Thus, PC1 explains the most variance of any linear transform applied to the original data space, PC2 explains the largest amount of the remaining variance, and so on. The application of PCA to the "Atlas of Odor Character Profiles" uncovered two important facts. First, a small number of PCs explained the majority of variance in the data, with ~30 % of the variance explained by the first PC (PC1) alone. In other words, in contrast to the notion of a high-dimensional percept, this implied a low-dimensional olfactory percept dominated by one perceptual axis. Second, and consistent with numerous previous studies (Yeshurun and Sobel 2010), the primary dimension of olfactory perception (PC1) reflected odorant pleasantness, that is, an axis ranging from very unpleasant to very pleasant (Khan et al. 2007). The primacy of this perceptual axis is further borne out in its mapping onto activity patterns in the human OE (Lapid et al. 2011). Moreover, it is likely not limited to human olfaction alone, as evidenced in the identification of receptors that are specific for aversive odors in rodents (Dewan et al. 2013), identification of aspects on the rodent olfactory bulb that are innately tuned to aversive odorants (Kobayakawa et al. 2007), and identification of valence as a coding axis in the fly brain (Knaden et al. 2012).

Next, we used modern analytical chemistry software to obtain ~1,600 chemical descriptors for each of ~1,500 odorant molecules. Again, hypothesizing that the functional dimensionality of this data is lower than its apparent dimensionality of ~1,600, we applied PCA, and again characterized a small number of PCs that explained a large proportion of the variance in the data. Moreover, PC1 of the odorant structure, which also explained ~30 % of the variance, was strongly influenced by molecular size and compression, and we tentatively refer to it as compactness. We next asked whether any of the PCs of perception were correlated with any of the PCs of structure. Strikingly, we identified such a privileged correlation between PC1 of perception (pleasantness) and PC1 of structure (compactness) (Khan et al. 2007). In other words, the primary dimension of olfactory perception is linked to a fundamental physical regularity in nature (Khan et al. 2007; Zarzo 2011). This link allowed us to develop an algorithm that

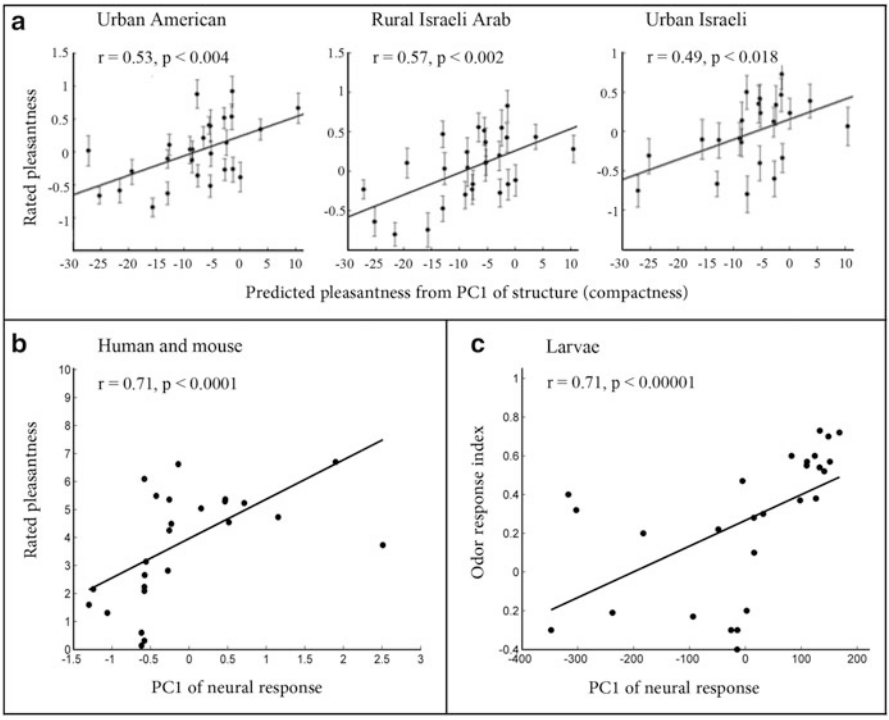

Fig. 9.11 A metric for olfaction. In all panels, each dot represents an odor. (**a**) The metric predicts odorant pleasantness across cultures. (**b**, **c**) Although **a** shows that principal component 1 (*PC1*) of perception (pleasantness) is linked to PC1 of structure, in the following panels we see that the same PC1 of perception is linked to PC1 of the responses of human and mouse ORs to odorants in vitro (**b**). (**c**) An animal analogue for PC1 of perception, namely, the behavior of approach or withdrawal, is also linked to PC1 of neural response in *Drosophila* larvae

cross-culturally successfully predicts a modest but significant portion of odorant pleasantness from odorant structure alone (Khan et al. 2007) (Fig. 9.11a).

Given that PC1 of odorant structure also predicted behavior in mice (Mandairon et al. 2009), we next asked whether it is reflected in animal neural activity. We collected neural response data from 12 published data sets using seven species (Haddad et al. 2010). Neural recordings are multidimensional in space and time, and again assuming that functional dimensionality is lower than apparent dimensionality, we applied PCA. Again, we found that a small number of PCs explained the majority of the variance in neural activity. Moreover, we found that PC1 of neural activity, which explained ~25 % of the variance, reflected overall neural response magnitude. In other words, in contrast to the notion of a high-dimensional combinatorial neural code underlying olfaction, this implied that a simple neural code may underlie much of olfactory computation. We next asked whether this axis of neural activity is related to olfactory perception. We found that PC1 of neural activity was related to PC1 of odorant perception, which we recall is related to PC1

of odorant structure (Haddad et al. 2010). In other words, the primary dimension of odorant structure (compactness) is coded in the primary dimension of odorant-induced neural activity (total neural response) that is reflected in the primary dimension of olfactory perception (pleasantness). These relationships allowed us to generate modest but significant predictions across odorant structure, odorant-induced neural activity, and odorant-induced perception (Fig. 9.11).

In the foregoing analyses we represented each odorant with a single value reflecting its structure. We arrived at this value by first generating a multidimensional representation of the odorant across ~1,600 structural features and then reducing this to a single value with PCA. This single value, namely projection on PC1, or compactness, proved to be a reasonably useful olfactory metric in that it allowed us to compare between odorants and their induced perception and neural activity. PCA, however, is not the only way to represent a multidimensional odorant structure. For example, the single chemical variable of "molecular complexity" successfully predicted the number of discreet olfactory notes, or perceptual complexity attributed to an odorant (Kermen et al. 2011). Alternatively, a single value reflecting the vibrational spectra of a molecule predicted responses in olfactory receptors of flies (Gabler et al. 2013). Another alternative is to continue representing each odor using many structural features (e.g., ~1,600), and then computing the distance between any two odorants by the square root of the sum of squares of the differences between the descriptors: this is referred to as Euclidean distance. We found that Euclidean distance effectively predicted the difference in neural response induced by any two odorants (Haddad et al. 2008b). Moreover, using this approach one can optimize the number of features needed, that is, ask which of the ~1,600 physicochemical features we modeled are most important in the olfactory response. This approach allowed derivation of various optimized descriptor lists that further improved predictions, albeit in a species-specific manner (Haddad et al. 2008b; Saito et al. 2009).

All the foregoing description constitutes an initial effort to generate a metric space for olfaction, but has this brought us any closer to answering Bell's question posed at the outset? Although these efforts were all using monomolecular odorants, the real olfactory world that contains rose, violet, and asafetida is made up of mixtures often containing hundreds of components. How can one apply a single metric value to such mixtures? We tested two alternatives: one was comparing between mixtures by conducting all the pairwise Euclidian comparisons between all molecular components in both mixtures (Fig. 9.12a), and the other was to first generate a single vector reflecting the mixture (e.g., by normalized summation), and then compare the single vectors (Fig. 9.12b).

We compared the single vectors by measuring the angle between them, generating what we refer to as the "angle distance metric." We found that only the latter approach provided valid predictions of odorant mixture perceptual similarity based on odorant mixture structure (Snitz et al. 2013) (Fig. 9.10b). This finding is consistent with the view of how the mammalian brain treats odors: synthesizing a singular odor percept for an odorant mixture rather than analytically extracting individual odorant features reflecting mixture components

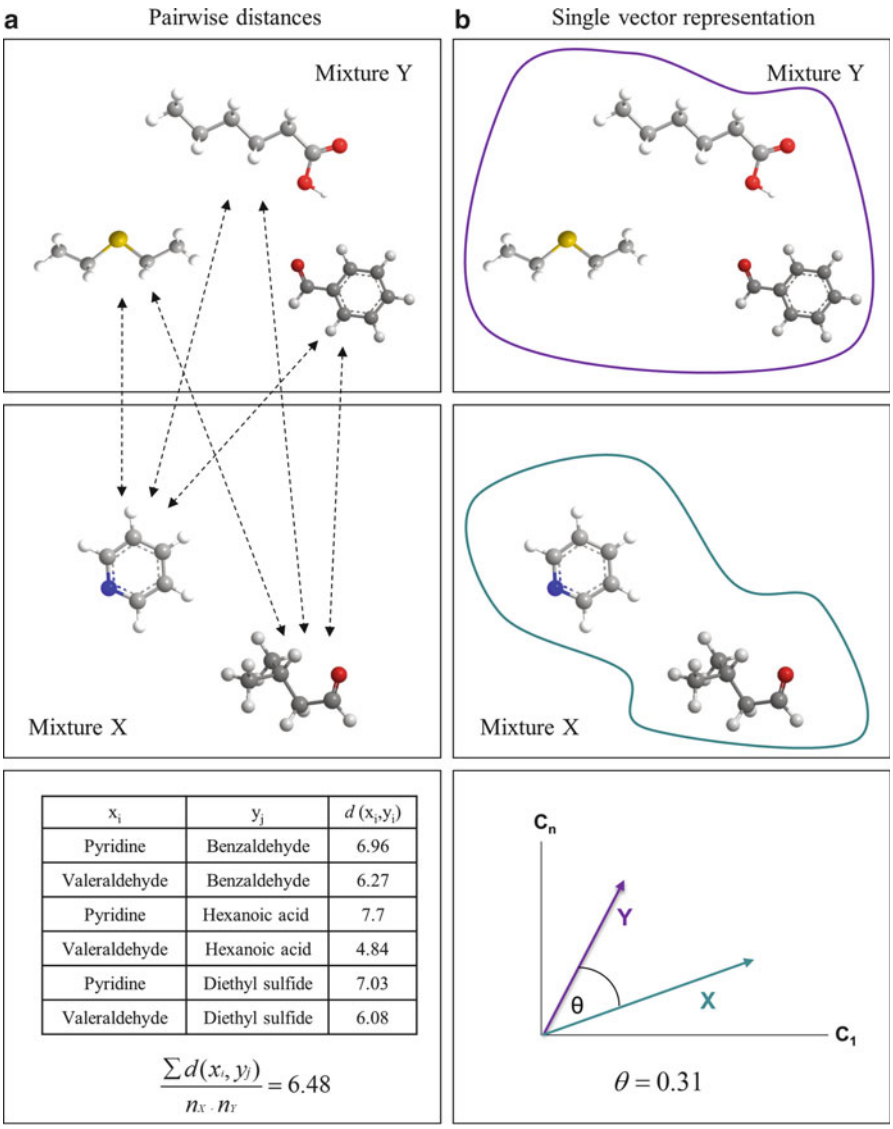

x_i	y_j	$d(x_i,y_j)$
Pyridine	Benzaldehyde	6.96
Valeraldehyde	Benzaldehyde	6.27
Pyridine	Hexanoic acid	7.7
Valeraldehyde	Hexanoic acid	4.84
Pyridine	Diethyl sulfide	7.03
Valeraldehyde	Diethyl sulfide	6.08

Fig. 9.12 Modeling odorant mixtures as singular objects rather than component amalgamations. The top panels represent one mixture (Y) made of three monomolecular components and the bottom panels represent a different mixture (X) made of two monomolecular components. The distance between X and Y can be calculated as the mean of all pairwise distances between all the components of X and Y (**a**). (**b**) Alternatively, one can represent both X and Y as single vectors reflecting the sum of their components, and define the distance between them as the angle between these two vectors within a physicochemical space of n dimensions. Only the latter approach predicted mixture perceptual similarity (Snitz et al. 2013)

(Wilson and Sullivan 2011). This outcome had two implications. First, the averaging involved in the metric calculation implied that as one adds more and more components that span olfactory space to each of two mixtures, these mixtures should smell more and more similar to each other, despite sharing no components in common. This trend continues to a point where all mixtures are predicted to smell the same. We called this point *olfactory white*, and obtained experimental data to support its existence (Weiss et al. 2012). A second implication of this result is that it allowed answering Bell's question. We computed the distances between rose, violet, and asafetida, and per Bell's challenge, accurately predicted their "likenesses and differences" (Fig. 9.10c). To conclude this path, we used perception to generate physicochemical metrics for smell. These metrics predicted modest but significant portions of perception and neural activity. The current best-performing metric is the one we refer to as the angle distance metric (Snitz et al. 2013), yet this is likely not the final step in the evolution of these metrics. For example, the current metric does not account for component concentrations and intensities within a mixture, and this remains a critical necessary step for olfactory metrics in the future.

9.4 Conclusions

Studying human olfaction has served to verify many findings initially made in rodents, yet it has also uncovered novel aspects of structural and functional systems-level mammalian neurobiology. Some structural findings, primarily altered receptor-to-glomeruli ratio, may be unique to the human olfactory system. That said, we consider them unique because they differ from the heavily studied rodents. However, it is not beyond consideration that the human example may be as equally representative of mammalians as the lab rat or mouse. Notable functional findings first made in humans include finding that each nostril provides the brain with a different image of the olfactory world, that the cerebellum takes part in odor processing, and that brain representation is different for orthonasal versus retronasal olfactory perception. However, although the foregoing could have equally been discovered in rodents, other key discoveries could not. Notable among these are that the right OFC may be a key for odor awareness. Finally, it is only with the help of human verbal reports that we have made initial progress in systematically linking odorant structure to odorant perception, a task that remains the primary target of olfaction research.

References

Abolmaali ND, Kuhnau D, Knecht M, Kohler K, Huttenbrink KB, Hummel T (2001) Imaging of the human vomeronasal duct. Chem Senses 26:35–39

Ackerl K, Atzmueller M, Grammer K (2002) The scent of fear. Neuro Endocrinol Lett 23:79–84

Albrecht J, Kopietz R, Frasnelli J, Wiesmann M, Hummel T, Lundstrom JN (2010) The neuronal correlates of intranasal trigeminal function: an ALE meta-analysis of human functional brain imaging data. Brain Res Rev 62:183–196

Arzi A, Shedlesky L, Ben-Shaul M, Nasser K, Oksenberg A, Hairston IS, Sobel N (2012) Humans can learn new information during sleep. Nat Neurosci 15:1460–1465

Bell A (1914) Discovery and invention. Nat Geogr 25:649

Bensafi M (2004) Sniffing a human sex-steroid derived compound affects mood and autonomic arousal in a dose-dependent manner. Psychoneuroendocrinology 29:1290–1299

Bensafi M, Porter J, Pouliot S, Mainland J, Johnson B, Zelano C, Young N, Bremner E, Aframian D, Khan R (2003a) Olfactomotor activity during imagery mimics that during perception. Nat Neurosci 6:1142–1144

Bensafi M, Brown WM, Tsutsui T, Mainland JD, Johnson BN, Bremner EA, Young N, Mauss I, Ray B, Gross J, Richards J, Stappen I, Levenson RW, Sobel N (2003b) Sex-steroid derived compounds induce sex-specific effects on autonomic nervous system function in humans. Behav Neurosci 117:1125–1134

Bensafi M, Brown WM, Khan R, Levenson B, Sobel N (2004) Sniffing human sex-steroid derived compounds modulates mood, memory and autonomic nervous system function in specific behavioral contexts. Behav Brain Res 152:11–22

Brennan PA (2001) The vomeronasal system. Cell Mol Life Sci 58:546–555

Buschhuter D, Smitka M, Puschmann S, Gerber JC, Witt M, Abolmaali ND, Hummel T (2008) Correlation between olfactory bulb volume and olfactory function. Neuroimage 42:498–502

Carmichael ST, Clugnet MC, Price JL (1994) Central olfactory connections in the macaque monkey. J Comp Neurol 346:403–434

Carnicelli V, Santoro A, Sellari-Franceschini S, Berrettini S, Zucchi R (2010) Expression of trace amine-associated receptors in human nasal mucosa. Chemosens Percept 3:99–107

Castro JB, Ramanathan A, Chennubhotla CS (2013) Categorical dimensions of human odor descriptor space revealed by non-negative matrix factorization. PLoS One 8:e73289

Cenier T, McGann JP, Tsuno Y, Verhagen JV, Wachowiak M (2013) Testing the sorption hypothesis in olfaction: a limited role for sniff strength in shaping primary odor representations during behavior. J Neurosci 33:79–92

Cerda-Molina AL, Hernandez-Lopez L, de la OC, Chavira-Ramirez R, Mondragon-Ceballos R (2013) Changes in men's salivary testosterone and cortisol levels, and in sexual desire after smelling female axillary and vulvar scents. Front Endocrinol (Lausanne) 4:159

Cerf-Ducastel B, Murphy C (2006) Neural substrates of cross-modal olfactory recognition memory: an fMRI study. Neuroimage 31:386–396

Chen D, Haviland-Jones J (2000) Human olfactory communication of emotion. Percept Motor Skills 91:771

Chen D, Katdare A, Lucas N (2006) Chemosignals of fear enhance cognitive performance in humans. Chem Senses 31:415

Curtis MA, Kam M, Nannmark U, Anderson MF, Axell MZ, Wikkelso C, Holtas S, van Roon-Mom WMC, Bjork-Eriksson T, Nordborg C, Frisen J, Dragunow M, Faull RLM, Eriksson PS (2007) Human neuroblasts migrate to the olfactory bulb via a lateral ventricular extension. Science 315:1243–1249

Cutler WB, Preti G, Krieger A, Huggins GR, Garcia CR, Lawley HJ (1986) Human axillary secretions influence women's menstrual cycles: the role of donor extract from men. Horm Behav 20:463–473

Dalton P, Doolittle N, Breslin PA (2002) Gender-specific induction of enhanced sensitivity to odors. Nat Neurosci 5:199–200

de Groot JH, Semin GR, Smeets MA (2013) I can see, hear, and smell your fear: comparing olfactory and audiovisual media in fear communication. J Exp Psychol Gen 143:825–834

Deschenes M, Moore J, Kleinfeld D (2012) Sniffing and whisking in rodents. Curr Opin Neurobiol 22:243–250

Dewan A, Pacifico R, Zhan R, Rinberg D, Bozza T (2013) Non-redundant coding of aversive odours in the main olfactory pathway. Nature (Lond) 497:486–489

Doty RL, Ford M, Preti G, Huggins GR (1975) Changes in the intensity and pleasantness of human vaginal odors during the menstrual cycle. Science 190:1316–1318

Doty RL, Brugger WE, Jurs PC, Orndorff MA, Snyder PJ, Lowry LD (1978) Intranasal trigeminal stimulation from odorous volatiles: psychometric responses from anosmic and normal humans. Physiol Behav 20:175–185

Dravnieks A (1985) Atlas of odor character profiles. ASTM Press, West Conshohocken

Escada PA, Lima C, da Silva JM (2009) The human olfactory mucosa. Eur Arch Otorhinolaryngol 266:1675–1680

Ferdon S, Murphy C (2003) The cerebellum and olfaction in the aging brain: a functional magnetic resonance imaging study. Neuroimage 20:12–21

Feron F, Perry C, McGrath JJ, Mackay-Sim A (1998) New techniques for biopsy and culture of human olfactory epithelial neurons. Arch Otolaryngol Head Neck Surg 124:861–866

Frank RA, Dulay MF, Gesteland RC (2003) Assessment of the sniff magnitude test as a clinical test of olfactory function. Physiol Behav 78:195–204

Frasnelli J, Lundstrom JN, Boyle JA, Katsarkas A, Jones-Gotman M (2011) The vomeronasal organ is not involved in the perception of endogenous odors. Hum Brain Mapp 32:450–460

Frumin I, Sobel N, Gilad Y (2013) Does a unique olfactory genome imply a unique olfactory world? Nat Neurosci 17:6–8

Gabler S, Soelter J, Hussain T, Sachse S, Schmuker M (2013) Physicochemical vs. vibrational descriptors for prediction of odor receptor responses. Mol Inform 32:855–865

Gelstein S, Yeshurun Y, Rozenkrantz L, Shushan S, Frumin I, Roth Y, Sobel N (2011) Human tears contain a chemosignal. Science 331:226–230

Gibbons B (1986) The intimate sense of smell. Nat Geogr 170:324–361

Gilad Y, Lancet D (2003) Population differences in the human functional olfactory repertoire. Mol Biol Evol 20:307–314

Gottfried JA (2010) Central mechanisms of odour object perception. Nat Rev Neurosci 11:628–641

Gottfried JA, Winston JS, Dolan RJ (2006) Dissociable codes of odor quality and odorant structure in human piriform cortex. Neuron 49:467–479

Grosser BI, Monti-Bloch L, Jennings-White C, Berliner DL (2000) Behavioral and electrophysiological effects of androstadienone, a human pheromone. Psychoneuroendocrinology 25:289–299

Haddad R, Lapid H, Harel D, Sobel N (2008a) Measuring smells. Curr Opin Neurobiol 18:438–444

Haddad R, Khan R, Takahashi YK, Mori K, Harel D, Sobel N (2008b) A metric for odorant comparison. Nat Methods 5:425–429

Haddad R, Weiss T, Khan R, Nadler B, Mandairon N, Bensafi M, Schneidman E, Sobel N (2010) Global features of neural activity in the olfactory system form a parallel code that predicts olfactory behavior and perception. J Neurosci 30:9017–9026

Hauser R, Marczak M, Karaszewski B, Wiergowski M, Kaliszan M, Penkowski M, Kernbach-Wighton G, Jankowski Z, Namiesnik J (2008) A preliminary study for identifying olfactory markers of fear in the rat. Lab Anim (NY) 37:76–80

Howard JD, Plailly J, Grueschow M, Haynes JD, Gottfried JA (2009) Odor quality coding and categorization in human posterior piriform cortex. Nat Neurosci 12:932–938

Huart C, Rombaux P, Hummel T (2013) Plasticity of the human olfactory system: the olfactory bulb. Molecules 18:11586–11600

Hummel T, Livermore A (2002) Intranasal chemosensory function of the trigeminal nerve and aspects of its relation to olfaction. Int Arch Occup Environ Health 75:305–313

Hummel T, Mojet J, Kobal G (2006) Electro-olfactograms are present when odorous stimuli have not been perceived. Neurosci Lett 397:224–228

Hummer TA, McClintock MK (2009) Putative human pheromone androstadienone attunes the mind specifically to emotional information. Horm Behav 55:548–559

Ihara S, Yoshikawa K, Touhara K (2013) Chemosensory signals and their receptors in the olfactory neural system. Neuroscience 254:45–60

Ishimaru T, Reden J, Krone F, Scheibe M (2007) Optical recordings from the human nasal mucosa in response to olfactory stimulation. Neurosci Lett 423:231–235
Ishimaru T, Reden J, Krone F, Scheibe M (2011) Topographical differences in the sensitivity of the human nasal mucosa to olfactory and trigeminal stimuli. Neurosci Lett 493:136–139
Jacob S, Hayreh DJ, McClintock MK (2001a) Context-dependent effects of steroid chemosignals on human physiology and mood. Physiol Behav 74:15–27
Jacob S, Kinnunen LH, Metz J, Cooper M, McClintock MK (2001b) Sustained human chemosignal unconsciously alters brain function. Neuroreport 12:2391–2394
Jacob S, Spencer NA, Bullivant SB, Sellergren SA, Mennella JA, McClintock MK (2004) Effects of breastfeeding chemosignals on the human menstrual cycle. Hum Reprod 19:422–429
Johansson CB, Svensson M, Wallstedt L, Janson AM, Frisen J (1999) Neural stem cells in the adult human brain. Exp Cell Res 253:733–736
Johnson BN, Mainland JD, Sobel N (2003) Rapid olfactory processing implicates subcortical control of an olfactomotor system. J Neurophysiol 90:1084–1094
Keller A, Zhuang H, Chi Q, Vosshall LB, Matsunami H (2007) Genetic variation in a human odorant receptor alters odour perception. Nature (Lond) 449:468–472
Kermen F, Chakirian A, Sezille C, Joussain P, Le Goff G, Ziessel A, Chastrette M, Mandairon N, Didier A, Rouby C, Bensafi M (2011) Molecular complexity determines the number of olfactory notes and the pleasantness of smells. Sci Rep 1:206
Keverne EB (1999) The vomeronasal organ. Science 286:716–720
Khan R, Luk C, Flinker A, Aggarwal A, Lapid H, Haddad R, Sobel N (2007) Predicting odor pleasantness from odorant structure: pleasantness as a reflection of the physical world. J Neurosci 27:10015–10023
Kimoto H, Haga S, Sato K, Touhara K (2005) Sex-specific peptides from exocrine glands stimulate mouse vomeronasal sensory neurons. Nature (Lond) 437:898–901
Kimoto H, Sato K, Nodari F, Haga S, Holy TE, Touhara K (2007) Sex- and strain-specific expression and vomeronasal activity of mouse ESP family peptides. Curr Biol 17:1879–1884
Kjelvik G, Evensmoen HR, Brezova V, Haberg AK (2012) The human brain representation of odor identification. J Neurophysiol 108:645–657
Knaden M, Strutz A, Ahsan J, Sachse S, Hansson BS (2012) Spatial representation of odorant valence in an insect brain. Cell Rep 1:392–399
Knecht M, Hummel T (2004) Recording of the human electro-olfactogram. Physiol Behav 83:13–19
Knecht M, Lundstrom JN, Witt M, Huttenbrink KB, Heilmann S, Hummel T (2003) Assessment of olfactory function and androstenone odor thresholds in humans with or without functional occlusion of the vomeronasal duct. Behav Neurosci 117:1135–1141
Kobal G, Hummel T (1991) Human electro-olfactograms and brain responses to olfactory stimulation. In: Laing DG, Doty RL, Breipohl W (eds) The human sense of smell. Springer, Berlin
Kobayakawa K, Kobayakawa R, Matsumoto H, Oka Y, Imai T, Ikawa M, Okabe M, Ikeda T, Itohara S, Kikusui T, Mori K, Sakano H (2007) Innate versus learned odour processing in the mouse olfactory bulb. Nature (Lond) 450:503–508
Koulakov AA, Enikolopov AG, Rinberg D (2009) The structure of human olfactory space. Arxiv preprint arXiv:09073964
Laing DG (1982) Characterisation of human behaviour during odour perception. Perception 11:221–230
Laing DG (1983) Natural sniffing gives optimum odour perception for humans. Perception 12:99–117
Lapid H, Hummel T (2013) Recording odor-evoked response potentials at the human olfactory epithelium. Chem Senses 38:3–17
Lapid H, Seo HS, Schuster B, Schneidman E, Roth Y, Harel D, Sobel N, Hummel T (2009) Odorant concentration dependence in electroolfactograms recorded from the human olfactory epithelium. J Neurophysiol 102:2121–2130

Lapid H, Shushan S, Plotkin A, Voet H, Roth Y, Hummel T, Schneidman E, Sobel N (2011) Neural activity at the human olfactory epithelium reflects olfactory perception. Nat Neurosci 14:1455–1461

Laska M, Freyer D (1997) Olfactory discrimination ability for aliphatic esters in squirrel monkeys and humans. Chem Senses 22:457–465

Laska M, Liesen A, Teubner P (1999a) Enantioselectivity of odor perception in squirrel monkeys and humans. Am J Physiol 277:R1098–R1103

Laska M, Trolp S, Teubner P (1999b) Odor structure-activity relationships compared in human and nonhuman primates. Behav Neurosci 113:998–1007

Leopold DA, Hummel T, Schwob JE, Hong SC, Knecht M, Kobal G (2000) Anterior distribution of human olfactory epithelium. Laryngoscope 110:417–421

Li W, Luxenberg E, Parrish T, Gottfried JA (2006) Learning to smell the roses: experience-dependent neural plasticity in human piriform and orbitofrontal cortices. Neuron 52:1097–1108

Li W, Howard JD, Parrish TB, Gottfried JA (2008) Aversive learning enhances perceptual and cortical discrimination of indiscriminable odor cues. Science 319:1842–1845

Li W, Lopez L, Osher J, Howard JD, Parrish TB, Gottfried JA (2010) Right orbitofrontal cortex mediates conscious olfactory perception. Psychol Sci 21:1454–1463

Liberles SD, Buck LB (2006) A second class of chemosensory receptors in the olfactory epithelium. Nature (Lond) 442:645–650

Lundstrom JN, Olsson MJ (2005) Subthreshold amounts of social odorant affect mood, but not behavior, in heterosexual women when tested by a male, but not a female, experimenter. Biol Psychol 70:197–204

Madany Mamlouk A, Chee-Ruiter C, Hofmann UG, Bower JM (2003) Quantifying olfactory perception: mapping olfactory perception space by using multidimensional scaling and self-organizing maps. Neurocomputing 52:591–597

Mainland JD, Bremner EA, Young N, Johnson BN, Khan RM, Bensafi M, Sobel N (2002) Olfactory plasticity: one nostril knows what the other learns. Nature (Lond) 419:802

Mainland J, Johnson BN, Khan R, Ivry RB, Sobel N (2005) Olfactory impairments in patients with unilateral cerebellar lesions are selective to inputs from the contralesion nostril. J Neurosci 25:6362–6371

Mainland J, Keller A, Li Y, Zhou T, Trimmer C, Snyder L, Moberly A, Adipietro K, Liu W, Zhuang H, Zhan S, Lee S, Lin A, Matsunami H (2014) The missense of smell: functional variability in the human odorant receptor repertoire. Nat Neurosci 17:114–120

Mandairon N, Poncelet J, Bensafi M, Didier A (2009) Humans and mice express similar olfactory preferences. PLoS One 4:e4209

Maresh A, Rodriguez Gil D, Whitman MC, Greer CA (2008) Principles of glomerular organization in the human olfactory bulb: implications for odor processing. PLoS One 3:e2640

McClintock MK (1971) Menstrual synchrony and suppression. Nature (Lond) 229:244–245

Menashe I, Abaffy T, Hasin Y, Goshen S, Yahalom V, Luetje CW, Lancet D (2007) Genetic elucidation of human hyperosmia to isovaleric acid. PLoS Biol 5:e284

Meredith M (2001) Human vomeronasal organ function: a critical review of best and worst cases. Chem Senses 26:433–445

Mozell MM, Jagodowicz M (1973) Chromatographic separation of odorants by the nose: retention times measured across in vivo olfactory mucosa. Science 181:1247–1249

Mujica-Parodi LR, Strey HH, Frederick B, Savoy R, Cox D, Botanov Y, Tolkunov D, Rubin D, Weber J (2009) Chemosensory cues to conspecific emotional stress activate amygdala in humans. PLoS One 4:113–123

Oh TJ, Kim MY, Park KS, Cho YM (2012) Effects of chemosignals from sad tears and postprandial plasma on appetite and food intake in humans. PLoS One 7:e42352

Pageat P, Gaultier E (2003) Current research in canine and feline pheromones. Vet Clin N Am Small Anim Pract 33:187–211

Parthasarathy K, Bhalla US (2013) Laterality and symmetry in rat olfactory behavior and in physiology of olfactory input. J Neurosci 33:5750–5760
Plailly J, Howard JD, Gitelman DR, Gottfried JA (2008) Attention to odor modulates thalamocortical connectivity in the human brain. J Neurosci 28:5257–5267
Porter J, Anand T, Johnson B, Khan RM, Sobel N (2005) Brain mechanisms for extracting spatial information from smell. Neuron 47:581–592
Porter J, Craven B, Khan RM, Chang SJ, Kang I, Judkewitz B, Volpe J, Settles G, Sobel N (2007) Mechanisms of scent-tracking in humans. Nat Neurosci 10:27–29
Prehn A, Ohrt A, Sojka B, Ferstl R, Pause BM (2006) Chemosensory anxiety signals augment the startle reflex in humans. Neurosci Lett 394:127–130
Prehn-Kristensen A, Wiesner C, Bergmann TO, Wolff S, Jansen O, Mehdorn HM, Ferstl R, Pause BM (2009) Induction of empathy by the smell of anxiety. PLoS One 4:e5987
Price JL (1990) Olfactory system. In: Paxinos G (ed) The human nervous system. Academic Press, San Diego, pp 979–1001
Qureshy A, Kawashima R, Imran MB, Sugiura M, Goto R, Okada K, Inoue K, Itoh M, Schormann T, Zilles K, Fukuda H (2000) Functional mapping of human brain in olfactory processing: a PET study. J Neurophysiol 84:1656–1666
Rajan R, Clement JP, Bhalla US (2006) Rats smell in stereo. Science 311:666–670
Ressler KJ, Sullivan SL, Buck LB (1993) A zonal organization of odorant receptor gene expression in the olfactory epithelium. Cell 73:597–609
Rojas-Libano D, Kay LM (2012) Interplay between sniffing and odorant sorptive properties in the rat. J Neurosci 32:15577–15589
Royet JP, Zald D, Versace R, Costes N, Lavenne F, Koenig O, Gervais R (2000) Emotional responses to pleasant and unpleasant olfactory, visual, and auditory stimuli: a positron emission tomography study. J Neurosci 20:7752–7759
Royet JP, Hudry J, Zald DH, Godinot D, Gregoire MC, Lavenne F, Costes N, Holley A (2001) Functional neuroanatomy of different olfactory judgments. Neuroimage 13:506–519
Russell MJ, Switz GM, Thompson K (1980) Olfactory influences on the human menstrual cycle. Pharmacol Biochem Behav 13:737–738
Sahay A, Wilson DA, Hen R (2011) Pattern separation: a common function for new neurons in hippocampus and olfactory bulb. Neuron 70:582–588
Saito H, Chi Q, Zhuang H, Matsunami H, Mainland JD (2009) Odor coding by a mammalian receptor repertoire. Sci Signal 2:ra9
Sanai N, Tramontin AD, Quinones-Hinojosa A, Barbaro NM, Gupta N, Kunwar S, Lawton MT, McDermott MW, Parsa AT, Manuel-Garcia Verdugo J, Berger MS, Alvarez-Buylla A (2004) Unique astrocyte ribbon in adult human brain contains neural stem cells but lacks chain migration. Nature (Lond) 427:740–744
Savic I, Gulyas B (2000) PET shows that odors are processed both ipsilaterally and contralaterally to the stimulated nostril. Neuroreport 11:2861–2866
Savic I, Berglund H, Gulyas B, Roland P (2001) Smelling of odorous sex hormone-like compounds causes sex-differentiated hypothalamic activations in humans. Neuron 31:661–668
Savic I, Berglund H, Lindstrom P (2005) Brain responses to putative pheromones in homosexual men. Proc Natl Acad Sci USA 102:7356–7361
Scott J, Sherrill L, Jiang J, Zhao K (2014) Tuning to odor solubility and sorption pattern in olfactory epithelial responses. J Neurosci 34:2025–2036
Shanas U, Terkel J (1997) Mole-rat Harderian gland secretions inhibit aggression. Anim Behav 54:1255–1263
Shannahoff-Khalsa D (1991) Lateralized rhythms of the central and autonomic nervous systems. Int J Psychophysiol 11:225–251
Shepherd GM (2004) The human sense of smell: are we better than we think? PLoS Biol 2:E146
Small DM, Gerber JC, Mak YE, Hummel T (2005) Differential neural responses evoked by orthonasal versus retronasal odorant perception in humans. Neuron 47:593–605

Snitz K, Yablonka A, Weiss T, Frumin I, Khan RM, Sobel N (2013) Predicting odor perceptual similarity from odor structure. PLoS Comput Biol 9:e1003184
Sobel N, Prabhakaran V, Hartley CA, Desmond JE, Zhao Z, Glover GH, Gabrieli JD, Sullivan EV (1998) Odorant-induced and sniff-induced activation in the cerebellum of the human. J Neurosci 18:8990–9001
Sobel N, Khan RM, Saltman A, Sullivan EV, Gabrieli JD (1999) The world smells different to each nostril. Nature (Lond) 402:35
Stern K, McClintock MK (1998) Regulation of ovulation by human pheromones. Nature (Lond) 392:177–179
Stoksted P (1953) Rhinometric measurements for determination of the nasal cycle. Acta Otolaryngol Suppl 109:159–175
Tham WW, Stevenson RJ, Miller LA (2009) The functional role of the mediodorsal thalamic nucleus in olfaction. Brain Res Rev 62:109–126
Trotier D (2011) Vomeronasal organ and human pheromones. Eur Ann Otorhinolaryngol Head Neck Dis 128:184–190
Trotier D, Eloit C, Wassef M, Talmain G, Bensimon JL, Doving KB, Ferrand J (2000) The vomeronasal cavity in adult humans. Chem Senses 25:369–380
Wang L, Chen L, Jacob T (2004) Evidence for peripheral plasticity in human odour response. J Physiol 554:236–244
Wang C, Liu F, Liu YY, Zhao CH, You Y, Wang L, Zhang J, Wei B, Ma T, Zhang Q, Zhang Y, Chen R, Song H, Yang Z (2011) Identification and characterization of neuroblasts in the subventricular zone and rostral migratory stream of the adult human brain. Cell Res 21:1534–1550
Weiss T, Snitz K, Yablonka A, Khan RM, Gafsou D, Schneidman E, Sobel N (2012) Perceptual convergence of multi-component mixtures in olfaction implies an olfactory white. Proc Natl Acad Sci USA 109:19959–19964
Wilson DA, Sullivan RM (2011) Cortical processing of odor objects. Neuron 72:506–519
Witt M, Hummel T (2006) Vomeronasal versus olfactory epithelium: is there a cellular basis for human vomeronasal perception? Int Rev Cytol 248:209–259
Wu KN, Tan BK, Howard JD, Conley DB, Gottfried JA (2012) Olfactory input is critical for sustaining odor quality codes in human orbitofrontal cortex. Nat Neurosci 15:1313–1319
Wyart C, Webster WW, Chen JH, Wilson SR, McClary A, Khan RM, Sobel N (2007) Smelling a single component of male sweat alters levels of cortisol in women. J Neurosci 27:1261–1265
Wysocki CJ, Preti G (2004) Facts, fallacies, fears, and frustrations with human pheromones. Anat Rec A Discov Mol Cell Evol Biol 281:1201–1211
Wysocki CJ, Dorries KM, Beauchamp GK (1989) Ability to perceive androstenone can be acquired by ostensibly anosmic people. Proc Natl Acad Sci USA 86:7976–7978
Yeshurun Y, Sobel N (2010) An odor is not worth a thousand words: from multidimensional odors to unidimensional odor objects. Annu Rev Psychol 61:219–241
Young JM (2002) Different evolutionary processes shaped the mouse and human olfactory receptor gene families. Hum Mol Genet 11:535–546
Zarzo M (2008) Psychologic dimensions in the perception of everyday odors: pleasantness and edibility. J Sens Stud 23:354–376
Zarzo M (2011) Hedonic judgments of chemical compounds are correlated with molecular size. Sensors (Basel) 11:3667–3686
Zelano C, Sobel N (2005) Humans as an animal model for systems-level organization of olfaction. Neuron 48:431–454
Zhang X, Firestein S (2002) The olfactory receptor gene superfamily of the mouse. Nat Neurosci 5:124–133
Zhang J, Pacifico R, Cawley D, Feinstein P, Bozza T (2013) Ultrasensitive detection of amines by a trace amine-associated receptor. J Neurosci 33:3228–3239
Zhou W, Chen D (2009) Fear-related chemosignals modulate recognition of fear in ambiguous facial expressions. Psychol Sci 20:177

Index

K. Mori (ed.), *The Olfactory System: From Odor Molecules to Motivational Behaviors*,
DOI 10.1007/978-4-431-54376-3, © Springer Japan 2014